IN-1376

IN-1376
NASA-CR-72681
May 1970

CRITICAL EXPERIMENTS ON A MODULAR CAVITY REACTOR

J F Kunze and P L Chase

Prepared for

NATIONAL AERONAUTICS AND SPACE ADMINISTRATION

Contract C-67747-A

IDAHO NUCLEAR CORPORATION
National Reactor Testing Station
Idaho Falls, Idaho

IN-1376
NASA CR-72681
Issued May 1970
Limited Distribution

C R I T I C A L E X P E R I M E N T S
O N A
M O D U L A R C A V I T Y R E A C T O R

by

J F Kunze and P. L. Chase

Prepared for

NATIONAL AERONAUTICS AND SPACE ADMINISTRATION
Contract C-67747-A

Technical Management
NASA-Lewis Research Center
Cleveland, Ohio

Nuclear Systems Division
Robert E Hyland, Project Manager

Space Nuclear Propulsion Office
Capt C E Franklin, USAF

IDAHO NUCLEAR CORPORATION

A Jointly Owned Subsidiary of

AEROJET GENERAL CORPORATION
ALLIED CHEMICAL CORPORATION
PHILLIPS PETROLEUM COMPANY

U S Atomic Energy Commission Scientific and Technical Report
Issued Under Contract AT(10-1)-1230
Idaho Operations Office

ABSTRACT

Two fundamental design concepts have been under consideration for the cavity nuclear rocket reactor One of these is the open-fuel-cycle concept, in which the fuel is partially contained in the cavity by hydrodynamic forces of the surrounding propellant The other is the closed-fuel-cycle concept, in which the fuel is contained by a wall transparent to radiation. In the latter concept, the modular design of several small cavities with moderator in the interstices has been employed. This report describes the results of reactor physics measurements on the modular concept, and compares the results with previously reported data on the single large cavity design of the open-fuel-cycle concept.

ACKNOWLEDGEMENTS

The authors wish to acknowledge the work of G D. Pincock, C. G. Cooper, D H. Suckling, and R. R Jones in obtaining the data and performing much of the preliminary analysis.

CONTENTS

TABLES

FIGURES

1.0 SUMMARY

Critical experiments have been conducted to measure the reactor physics parameters in a modular cavity reactor system. Reactors containing three modules and seven modules in a core volume of 183 cm (6 ft) diameter by 122 cm (4 ft) length were constructed. Each of these systems had a 89 cm (3 ft) reflector. Both moderator and reflector were heavy water, with 0.25% H_2O impurity. All fuel was highly enriched uranium (93.2% U-235). The modules consisted of a central cylindrical fuel region within a cavity containing simulated hydrogen. For the seven module core the fuel to cavity radius ratio was varied from 0.38 to 0.72. For the three module core only a radius ratio of 0.55 was studied. Hydrogen coolant, simulated by low density polystyrene, surrounded the fuel on four of the configurations. One configuration was examined without any hydrogen in its cavities.

The modular concept places moderator between each fuel cell creating a benefit of additional moderation that cannot be obtained in the single cavity configurations. However, the nature of the modular design makes it extremely difficult to perform nuclear calculations of reasonable reliability, unless one has a base experiment with which to make a comparison. Both three module and seven module configurations were measured, the latter with three different fuel radii. The 0.55 fuel to cavity radius ratio was measured both with and without hydrogen in the cavity. No variations were made on the amount of moderation between the modules, e.g., by varying module size and spacing.

Measured critical masses varied from 8 to 11.5 kg of uranium. These are significantly lower than critical masses obtained in the single large cavity system. Also, these multiple cavities did not exhibit the large percentage increase in critical mass as was experienced in large single cavities as the fuel to cavity radius ratio became smaller. However, the pressure of the uranium, measured by its atom density, is the more fundamental characteristic for the design of cavity reactors. The pressure for criticality in the 7-module configuration would be 2/3 to 3/4 the pressure in the nominally "equivalent sized" single cavity system. However, this "equivalent" single cavity system had 2 1/2 times the hydrogen coolant-propellant volume, and hence a higher thrust level capability.

2.0 INTRODUCTION

The gas core nuclear rocket has been under investigation for over ten years as a propulsion engine for space applications Such an engine would have a specific impulse of about 1600 sec, approximately four times that obtainable with chemical rockets and twice that obtainable with the solid core nuclear rockets (NERVA). The fuel is allowed to vaporize in the cavity, thus imposing no fuel element temperature limitations as exist in the solid core nuclear reactor systems. However, the gaseous fuel of the gas core rocket must be at least partially contained for economic reasons. One cannot afford to allow nuclear fuel and propellant to flow with mass rates of the same order of magnitude, not only because it would be poor economics but also because the specific impulse advantage would be lost. Therefore, some containment of the fuel must occur. Two approaches are being investigated. One is the open-fuel-cycle, which confines the fuel hydrodynamically through variable flow velocities and directions. The second, commonly referred to as the light bulb concept, is the closed-fuel-cycle which uses a radiation-transparent wall to confine the fuel. The open cycle, in order to be economically acceptable, should have a propellant-to-fuel mass-flow-rate ratio greater than 35 to 1. The closed-fuel-cycle eliminates all fuel loss, providing the transparency and integrity of the thin walls can be maintained.

The cavity nuclear reactor concept utilizes an external moderator and reflector in order to achieve criticality with the low density gaseous fuel. Many passes across the fueled region are required before a thermal neutron is likely to be absorbed in the fuel. The surrounding reflector must, therefore, have a long thermal migration length so as not to adversely affect the thermal neutron population before they are absorbed in the fuel. Under conditions of relatively long absorption mean free paths in both the fuel and moderator-reflector, the neutronics of the cavity reactor becomes one of geometric competition between the fuel volume and moderator volume. The effectiveness of the fuel volume can be enhanced by raising its density (reducing its absorption mean free path). But eventually increases in density involve diminishing returns because the fuel becomes self-shielded. The pressure of the fuel gas, however, continues to increase nominally proportional to the density, and eventually one may reach such high fuel densities for criticality that pressures are beyond the feasibility of engineering construction.

The alternative to increasing fuel density is to increase geometrically the fuel effectiveness with respect to the moderator. This can be done by dispersing a number of small fuel-containing modules throughout the moderator, rather than to use only a single large cavity. This approach involves smaller cavities with smaller fuel volumes in each. Oscillations (or waves) in the effective fuel boundary will now more significantly affect the fuel to cavity volume ratio and adversely affect the stability of the open cycle concept In practice it will probably be necessary to provide a "glass" wall containment for a modular concept that employs modular cavities much smaller than 30 cm radius. Figure 2.1 schematically shows the concept of the two designs

Thus, the closed-cycle "light bulb" concept offers two principal advantages over the open cycle concept The closed cycle does not lose fuel and it allows a design utilizing small modules with interstitial moderator However, it does have disadvantages in addition to the problem of maintaining the integrity of the transparent walls An inert gas (neon)[1] must be circulated around the transparent walls of the fuel chambers to keep them cool The continual circulation removes some fuel from the core region to the downstream flow plenum. This fuel must then be separated from the neon before being recycled Also, the fission products are contained in the closed cycle rocket system, whereas they are lost in outer space in the open cycle system

The "glass" wall or "light bulb", closed cycle cavity concept has been under investigation at United Aircraft Research Laboratories and at the National Aeronautics and Space Administration The use of the closed cycle modular concept is discussed in Reference 1, and a conceptual design from that reference is shown in Figure 2.2. The design shown uses graphite and BeO as the moderator-reflector material, primarily for engineering convenience Heavy water is far superior, nuclearly, resulting in significantly lower critical masses and hence lower operating cavity pressures Heavy water was the reflector-moderator used in the critical experiments described in this report

Criticality calculations on the modular concept are more difficult than on the single cavity concept because of lack of symmetry in the polar angle direction Single cavity calculations are difficult enough (see Reference 5) without adding this additional complication For this reason, experiments are necessary to provide the base from which a workable calculational scheme can be developed This is the commonly employed "benchmark" measurement technique, and is especially necessary for the modular cavity reactor concept design considerations

Critical experiments on the single cavity concept were first conducted about ten years ago at Los Alamos on a small cavity, 40 cm in diameter.[9] Since 1966, experiments on a 183 cm (6-ft) diameter by 122 cm (4-ft) long cavity have been conducted in Idaho[2,3,4] on a variety of different configurations These included variations from the very basic, simple designs amenable to reactor physics calculations to complex designs that incorporate details of engineering construction and thermodynamic performance of the operating cavity reactor system[11,12]

This same reflector-moderator tank (366 cm diameter by 305 cm length) has been used for the critical experiments described in this report on the modular, "light bulb" reactor concept. The cavity (183 cm diameter by 122 cm long) of the reflector tank contained the module tank, thus making the single cavity and the modular experiment equivalent in at least one respect, all had the same "reflector" thickness They did, however, differ in "equivalent" core diameters.

The experiments described in this report had the principal purpose of establishing reasonably simple geometric models of the modular cavity reactor that could be used as "benchmarks" for design calculations. Of secondary interest were measurements of some engineering design effects that can not conveniently be included in calculational models

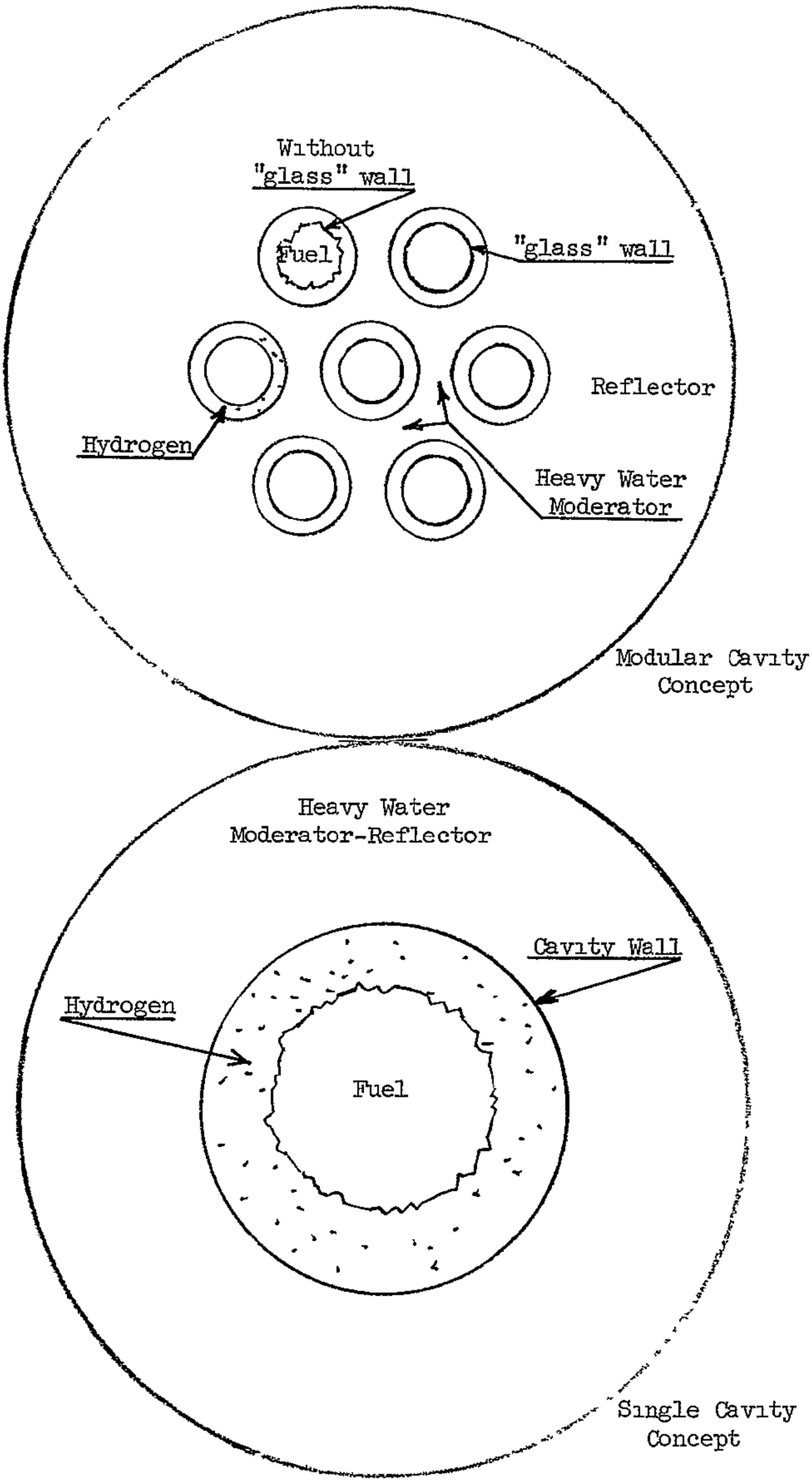

Figure 2.1 Modular and Single Cavity Concepts

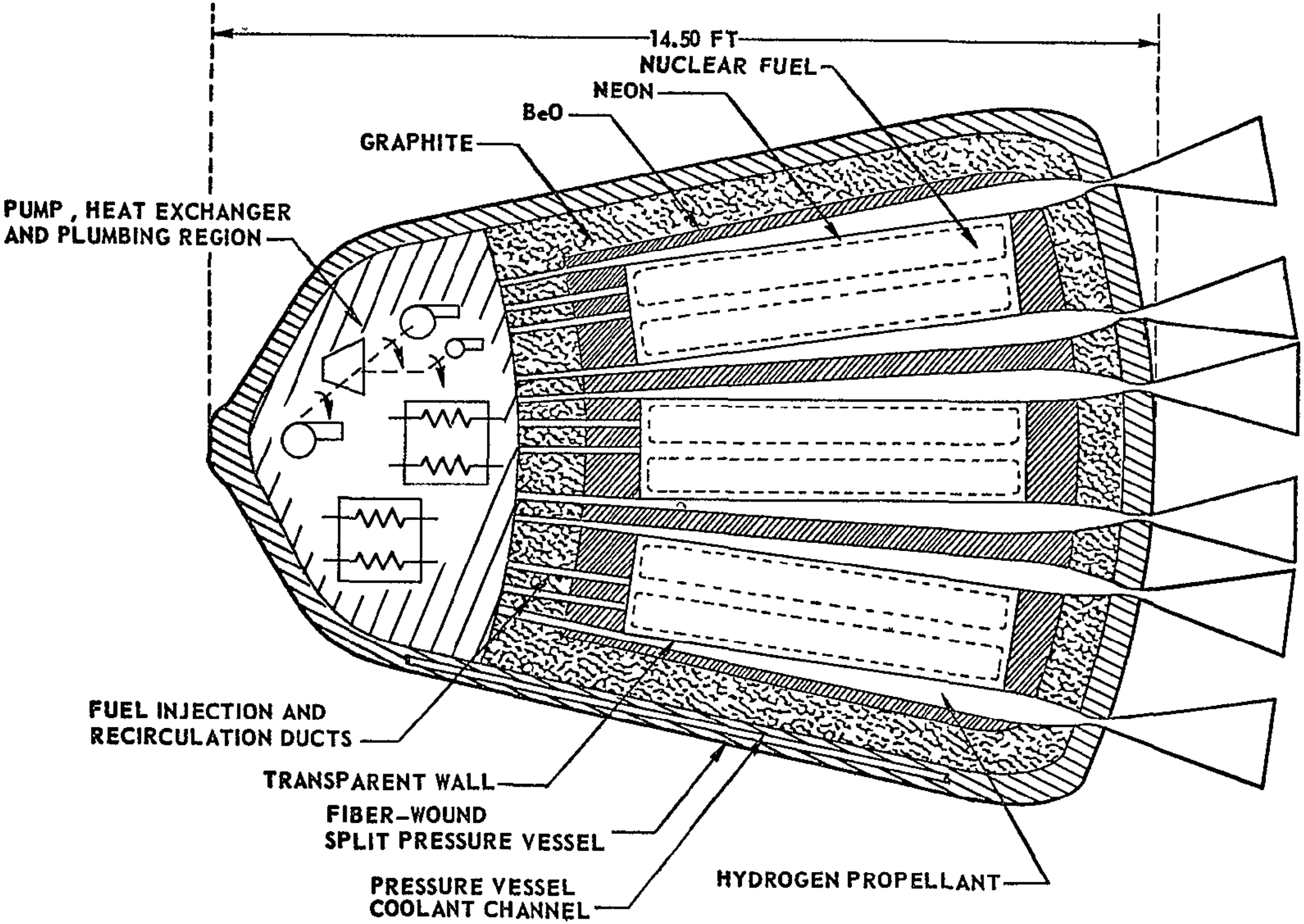

Figure 2.2 Schematic Diagram of Reference Nuclear Light Bulb Engine (from Reference 1, United Aircraft report, G-910375-3)

3.0 REACTOR DESCRIPTION

The main reactor tank was the same as that used for the cylindrical cavity critical experiments of the co-axial flow concept using a single large cavity. The outside dimensions of the heavy water in the tank were 363 8 cm in diameter by 300.8 cm long. The structure of the tank was aluminum, and included structural supports and stiffeners as well as the walls, which were 0.95 to 1 27 cm thick. The details of this structure are shown in Figure 3.1, with a two dimensional (cylindrical) nuclear model shown in Figure 3.2. As shown on this figure, the internal walls of the tank were 1.27 cm thick on the ends and 0 95 cm thick on the circumference. The entire reflector consisted of two tanks that were brought together to achieve criticality. Where the tanks met, the heavy water was interrupted by the aluminum tank walls, 1 27 cm thick each The tanks were not allowed to contact each other, a safety precaution to prevent flooding of the core in the event that an inner wall should leak. The gap was nominally 1.22 cm thick, and all results are quoted with the gap. Its worth was nominally 0 58%Δk, and if it is desired to not include the gap in a calculational model, this amount of reactivity should be added.

The movable tank was essentially one of the end reflectors. It also contained a central hole 30.7 cm in diameter, which was used to simulate the effect of an exhaust nozzle. For some of the experiments this hole was plugged with a tank of heavy water, referred to as the "end plug" or nozzle plug This plug tank had 0.95 cm thick walls

The fixed reflector tank formed the main body and one end of the reflector It was this end that contained the control rods for the experiment. The control was provided by between 8 and 12 actuators driving groups of three boron-carbide control rods with outer diameters of 1.9 cm. These slid in aluminum guide tubes The net effect of the aluminum and the empty tubes was to add 0.684% aluminum (by volume) and 1.0% void to this region of the reflector, Region #14 of Figure 3.2.

Inside the single large cavity of the reflector tank was placed the module tank for the particular experiment. The seven-module tank had a mass of 216.8 kg, and the three-module tank 180 kg. The radial tank walls and module walls were 0.318 cm (1/8-inch) thick, and the end plates were 0.635 (1/4-inch) thick. The dimensions of these tanks are shown in Figures 5.1 and 9.1, respectively. It was difficult to assure that the module tank was completely filled with heavy water, the possibility existing of the top few millimeters containing void (entrapped air). The seven module tank was filled with 1913 kg of heavy water, and the three module tank with 1884 kg Their internal volumes were 1742 liters and 1714 liters, respectively, giving an effective heavy water density of 1.099 gm/cm^3

The heavy water was nominally at a temperature of 22°C throughout the experiment (±1°C variations) Its density at this temperature is 1.105 gm/cc. The H_2O impurity content was measured once during the experiment, and had been measured a number of times before and since these module experiments. During these experiments the H_2O content was (0.25 ± 0.02) molecular percent of the total water.

The fuel used in the experiment was thin sheet metallic uranium, nominally 0 0025 cm thick. All masses quoted throughout the report are uranium masses only. These sheets also contained impurities which were approximately 3 5% of the uranium mass. The impurities were a fluorocarbon coating material and some oxygen from surface oxidation (about 1.3% of the total mass was oxygen, 2% fluorocarbon). The uranium material is that usually referred to as "oralloy", with an isotopic composition of

93.2%	U-235
1.0%	U-234
0.4%	U-236
5.4%	U-238

The aluminum used in the reflector tanks was all type 6061 The module tanks were constructed of type 1100-H14 for the curved (radial and module) walls and type 5052 for the end walls. Note, the 1.27 cm thick outside reflector tank walls are not included in the nuclear model of Figure 3.2 because of their negligible effect on reactivity

Details as to the fuel and hydrogen locations within the modules will be found in the sections on the individual experimental configurations. The hydrogen was simulated with styrofoam, having a nominal density of 0.028 gm/cc. In some cases, the hydrogen atom density was increased by inserting thin sheets of polyethylene between the styrofoam blocks The inner radius of the hydrogen annulus in these experiments was not varied, being 0.72 of the cavity radius for the seven-module configurations and 0.69 for the three-module configurations.

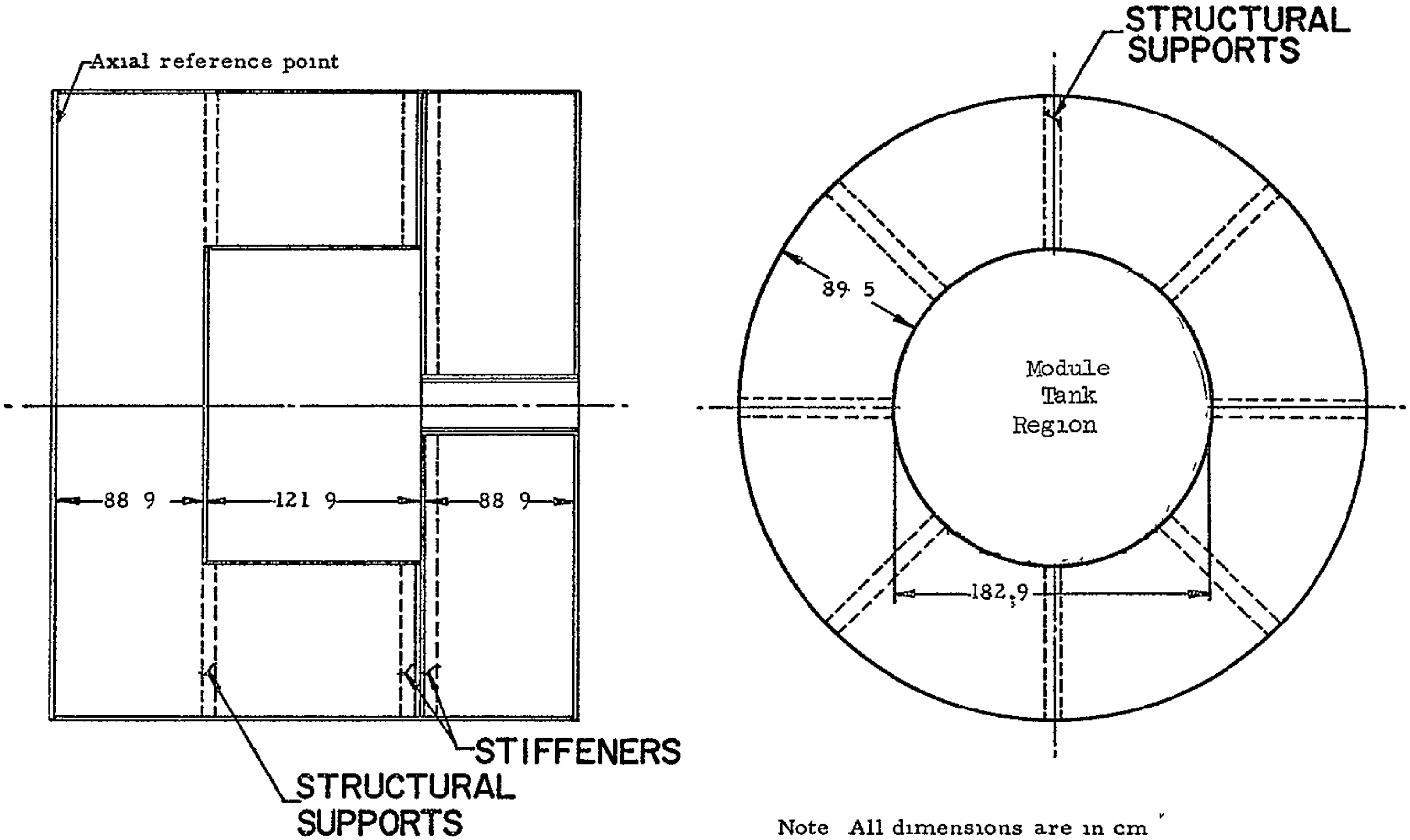

Fig. 3.1 Cavity reactor reflector tank

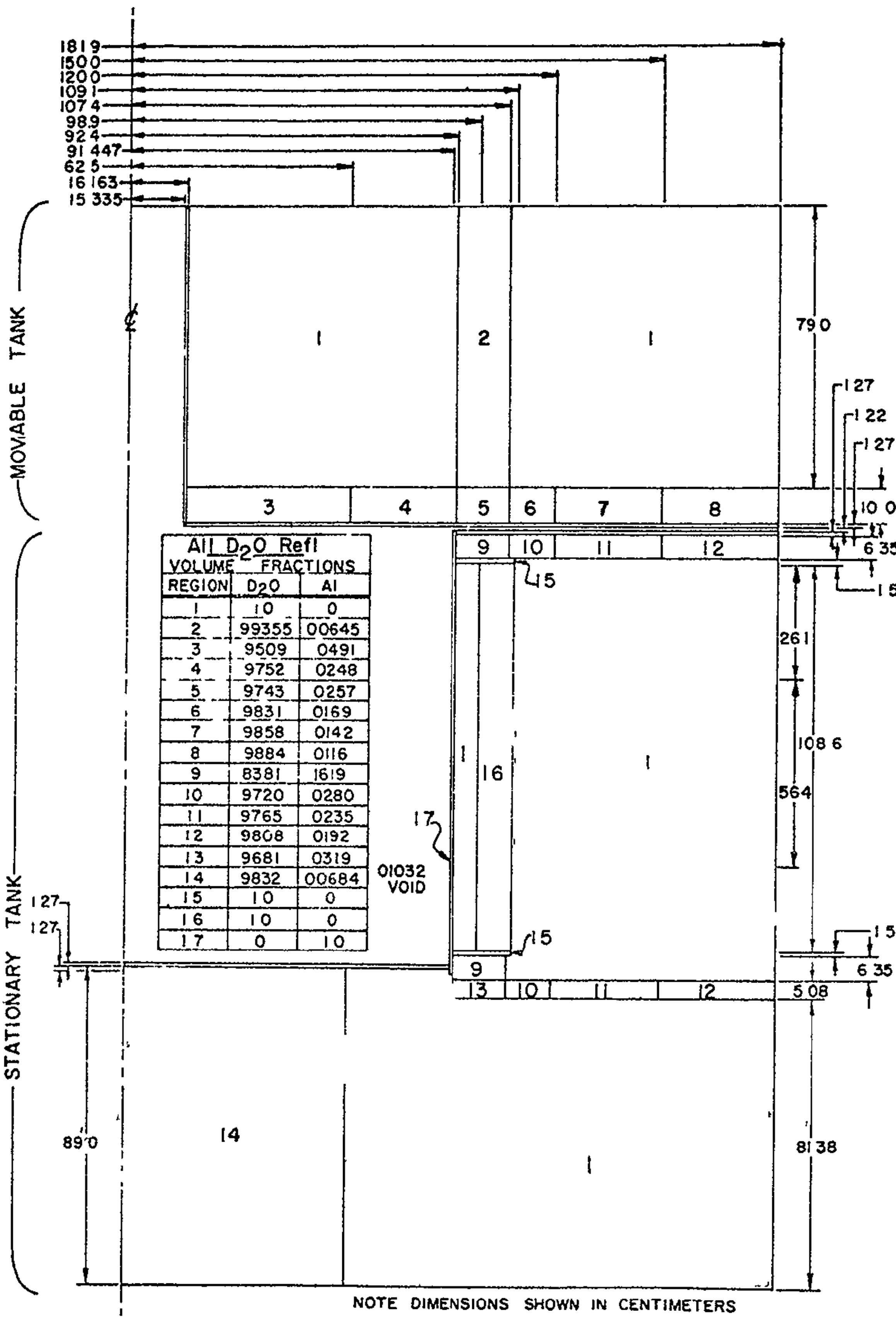

All D2O Refl VOLUME FRACTIONS

REGION	D2O	Al
1	10	0
2	99355	00645
3	9509	0491
4	9752	0248
5	9743	0257
6	9831	0169
7	9858	0142
8	9884	0116
9	8381	1619
10	9720	0280
11	9765	0235
12	9808	0192
13	9681	0319
14	9832	00684
15	10	0
16	10	0
17	0	10

Figure 3 2 Two-dimensional reflector model

4.0 TEST PROCEDURES

The principal measurements made on these critical experiments were reactivity, power distributions and flux distribution The achieving of criticality is considered to be only an intermediate step, and though subcritical data can yield information on reactivity, those results are usually less reliable than the measurements made from the critical configuration When feasible, the measurements were made with the control rods nearly fully withdrawn so as to limit the amount of perturbation of the end reflector flux caused by the control rods.

Reactivity measurements were made using the delayed neutron parameters, either by means of asymptotic positive period measurements and the inhour equation or by means of the inverse kinetics method of computing reactivity from a flux trace Base conditions were established by measuring the asymptotic period rather than by establishing a level power position. The long-lived (γ-n) reactions in the D_2O created a strong enough spurious neutron source that level power conditions were always subcritical, and by differing amounts depending on the past operating history and hence the strength of the source. Period measurements could be made over several decades, thus making possible a reliable extrapolation to the asymptotic, no-source value. The relatively small integrated power of a period measurement also minimized the spurious (γ-n) source buildup. The delayed neutron parameters used for this reactor are given in Table 4.1, and include eight groups of neutrons from (γ-n) reactions in the heavy water The total delayed fraction (one dollar) was 0 765%* All results are reported in %Δk instead of dollars and cents. Without considering uncertainties in the delayed neutron fraction, most period measurements of reactivity have associated with them an uncertainty of approximately ±0.0005%Δk. Table closure positions were reproducible to approximately ±0.02 cm, and control rod positions to ±0.01 cm The temperature coefficient of the system was approximately 0 01%Δk/C°, but the large heat capacity precluded temperature drifts larger than a few tenths of a degree during any eight-hour period Measurements of fuel worth or other material worths usually required opening the table to position the material to be measured into the core. The base measurement always included the effect of any structural material needed to secure the material being measured. Because such measurements involve not only the possibility of disturbing other materials in the reactor, but also an opening and closing of the table, a measurement of a reactivity difference probably involved a net uncertainty of ±0 001%Δk

*Leakage from this reactor gives β/β_{eff}=0.985. This 1 1/2% correction was not included because of the larger uncertainty in the (γ-n) contributions and even in the value of β-direct (data of Keepin et al)

Power distribution measurements were routinely made using aluminum fission-product-catcher foils on cleaned uranium metal sheet. Reproducibility of results is better than ±2%, and there is no detectable spectral dependence of this technique in the thermal or near thermal range. Decay of the foils was automatically included by counting all foils vs a normalizer foil from the same exposure. Absolute power levels were determined with a 2Π beta counter (3.8 cm radius chamber) precalibrated with absolute fission chambers and gold foils. This counter (an NMC type PC-3) gives 56 fiss/gm of U-235 per count per minute 50 minutes after shutdown from a constant 20 minute exposure. Absolute power levels are believed to be accurate to ±3% standard deviation.

Thermal fluxes were determined by use of bare and cadmium covered gold foils. The gold was nominally 0.0012 cm thick, with an effective resonance integral of 680 barns (vs 1555 barns infinitely dilute) In computing cadmium ratios, each foil was corrected for its effective resonance integral (6) by its mass to give the infinitely dilute value. Thermal flux perturbation was negligible, nominally 2% (7). The cadmium covers employed were 0.05 cm thick, giving an effective cadmium cutoff energy of 0.55 ev (8).

Reference positions have been established for defining locations of flux measurements. The longitudinal "0" reference location is at the outside of the end reflector in the control-rod end (fixed table) of the reactor. The radial reference position is either the axis of the reactor or the axis of the fuel module, and the distinction is obvious depending on which portion of the reactor was being measured. When defining positions within a module, the angular positions refer to clockwise rotation from the vertical (12 o'clock) position, when viewing the module tank from the movable table Sketches of the module tanks are shown looking from the movable table, end-reflector tank

TABLE 4.1

Effective Delayed Neutron Parameters

Group	β_1	λ_1
1	0.000210	0 012400
2	0 001410	0 030500
3	0 00127	0 111000
4	0 002550	0 301000
5	0 000740	1 100000
6	0 000270	3 000000
7	0.000780	0 277000
8	0.000240	0 016900
9	0 000084	0 004810
10	0.000040	0.001500
11	0.000025	0 000428
12	0 000028	0 000117
13	0 000004	0 000044
14	0 000001	0 000004
	0 007652	

5.0 0 55 RADIUS RATIO CORE - 7 MODULE

The seven module tank, which was placed in the central cavity region of the existing cavity reactor, is shown in Figure 5 1 The tank walls and module walls were made of 0 3175 cm (1/8 inch) thick, type 1100-H14 aluminum The end plates were 0 635 cm (1/4 inch) thick, type 5052 aluminum The empty tank weighed 216 8 kg

In order to measure the flux through the D_2O between the modules, two aluminum tubes were welded into the tank at the axial center of the core between modules 1 and 3 and from module 1 to the outer tank wall passing between modules 5 and 6 Foils could then be placed in these tubes at desired locations to record flux and power distributions

The fuel elements consisted of 17 spacer discs (fueled), up to eight fuel rings (depending on radius ratio), and four tie rods which clamped the pieces together Figure 5 2 shows an end view of the fuel element with the hardware to hold the fuel rings (spacer tabs) and the slots in the disc through which foils could be inserted A side view of the assembled fuel element is seen in Figure 5 3. As noted here, there were 16 stages of fuel with each stage being 7 46 cm long There were 9 25 kg of aluminum in each fuel element

The fuel rings were made by folding a strip of 0 0127 cm thick aluminum together and sandwiching the fuel inside The fuel was equally spaced around the rings and the gaps on the rings were staggered Fuel sheets were also placed on each fuel stage spacer disc as shown in Figure 5 4 These sheets were numbered as shown Sheets 3 to 8 were full size sheets, being 7 30 cm on a side by 0 00254 cm thick Sheets 1,2,9, and 10 were 1/2 size sheets (3 65 x 7 30 cm^2) This fuel arrangement placed fuel sheets normal to the radial and axial coordinates, thus reducing to a minimum neutron streaming along zero or very low absorption paths in the fuel elements The fuel rings were loaded as follows

Ring Number	Number of Size 1 0 Fuel Sheets	Ring Diameter (cm)
1	1	6 1
2	2	9 9
3	3	13 7
4	5	17.5
5	6	21 3
6	7	25 1

Because of the dilute fuel loading, not all positions specified on the fuel stage spacer discs (Figure 5 4) were used Those positions which did contain fuel are as follows for each disc of the element.

Disc Number	Positions Containing Fuel	Number of Fuel Sheets Whole Sheets	Half Sheets
1	1,2,3,4,7,8,9,10	4	4
2	1,2,4,5,6,7,9,10	4	4
3	1,2,3,5,6,7,8	5	2
4	3,4,5,6,8,9,10	5	2
5	1,2,3,4,7,8,9,10	4	4
6	1,2,4,5,6,7,9,10	4	4
7	1,2,3,5,6,7,8	5	2
8	3,4,5,6,8,9,10	5	2
9	1,2,3,4,7,8,9,10	4	4
10	1,2,4,5,6,7,9,10	4	4
11	1,2,3,5,6,7,8	5	2
12	3,4,5,6,8,9,10	5	2
13	1,2,3,4,7,8,9,10	4	4
14	1,2,4,5,6,7,9,10	4	4
15	1,2,3,5,6,7,8	5	2
16	3,4,5,6,8,9,10	5	2
17	1,2,3,4,7,8,9,10	4	4

The total fuel loading was thus 486 equivalent size 1 0 (full size) fuel sheets per fuel element, or a total of 3402 fuel sheets with a mass of 8.91 kg of U in the seven modules of the reactor core.

Each fuel element contained an annulus of foamed polystyrene (CH) from a radius of 16.4 cm to 22 5 cm. The CH weighed 2411 grams. This gives a hydrogen density within the annulus of 1.23×10^{21} atoms/cc.

5.1 Initial Loading

Initial loading of the seven module reactor began with no D_2O in the module tank, but with the outer, main tank filled. The fuel elements were loaded in the core one at a time and multiplication data were taken each time an element was added. The D_2O was then transferred into the module tank in several increments and multiplication taken for each increment The data results are contained in Table 5.1 and Figure 5.5.

The reactor was loaded with the exhaust-nozzle plug-tank, full of D_2O, in the end reflector The reactor was first critical with 7.359 barrels of D_2O in the tank and k-excess was 0 85%Δk A full 8 0 barrels were then added and k-excess was 1 89%Δk or an increase of 1 04%Δk. At this point, it was necessary to add three more actuators, 12 control rods, in order to maintain the two dollar shutdown requirement while loading was continued It was also decided to increase the hydrogen density by adding some thin strips of polyethylene

(CH_2) between the fuel stage spacer discs and the polystyrene over the annular region of hydrogen. There were 770 grams added to the reactor which increased the hydrogen density to 1 96 x 10^{21} atoms/cc within the annulus (from its initial value of 1.23 x 10^{21} atoms/cc). The increase in hydrogen reduced k-excess 0 312±0.075%Δk thus giving a specific worth of 0.405±0 097%Δk/kg for polyethylene. This was effectively the average worth throughout the propellant region. Previous measurements on other configurations have shown the carbon component is less than 2% of the total worth (ie. p.251 of Vol 1, p.45 of Vol 3)

An additional ten gallons, 42.07 kg of D_2O were added to the module tank and k-excess increased 0 435±0.078%Δk Excess reactivity was 1.896±0.062%Δk and higher than desired for the experiments so the exhaust nozzle plug was removed reducing k-excess to 0.745±0.066%Δk, thus giving a plug worth of 1 150±0.091%Δk

The remaining D_2O was then added to fill the module tank. It took 58.06 kg and it increased k-excess to 1.012±0.033%Δk which was the base excess reactivity for this reactor with the exhaust nozzle tank (end plug) removed from the reactor As will be shown later, the average fuel worth in the modules was 3 928%Δk with an estimated error of less than 5%. If this is applied to the above k-excess of 1 012±0 033%Δk, the critical mass would be 8.64 kg of uranium, with the exhaust nozzle open The total mass of D_2O in the seven-module tank was 1913 kg

5.2 Reactivity Measurements

5.2.1 Rod Worth

Rod worth curves were measured early in the experiment both before and after adding three additional actuators. Inverse kinetics were used to perform the measurements after reducing K to 1.00 by separating the table and withdrawing all actuators to their full out position. The rod worth curve thus obtained for 7 actuators (21 rods) is shown in Figure 5 6, and this was reduced to tabular form, the results of which are given in Table 5 2. The same data for the ten actuators (30 rods) are given in Figure 5.7 and Table 5 3 There was not a large difference between the two curves, but enough to measure These curves were used throughout the seven-module experiments

Rod worth measurements were minimal. A single measurement of seven actuators containing 21 rods gave a total worth of -2.801%Δk. Four separate measurements of ten actuators (30 rods) gave an average worth of -3 927±0.129%Δk. This standard deviation is 3.3% which is about normal for this type of measurement. The inverse kinetics calculations gave -2.907%Δk and -4.111%Δk for the worth of the seven actuator and ten actuator combination of rods, respectively. Both of these values are four to five percent above bump-period measurements, but this difference is considered to be of no real significance (within the expected accuracy of the measurements)

5.2.2 Material Worths

The worth of uranium was measured in Modules 1 and 3 to determine a core average worth as well as produce the radial profile across the fuel elements. A full core-length strip of uranium weighing 7.28 gm sandwiched between two aluminum straps was used to make the measurements. This sandwich was inserted into the measurement tubes or slots on the fuel elements (Figure 5.2) The base measurement contained the aluminum straps with no fuel. Period differences were used in all cases thus reducing the estimated error per measurement to about ±0.003%Δk Table 5 4 and Figure 5.8 show the results. The data are relatively sparse from which to calculate an average fuel worth But, assuming that the fuel worth distribution in Module 1 is constant around the element and that half of Module 3 is typical of the 90° value and the other half is typical of the 270° value, the core average fuel worth is 3.93%Δk/kg of uranium.

Two measurements made during the initial loading and reported in Section 5.1 are the worth of polyethylene (CH_2) and the worth of the exhaust nozzle tank. The values measured are shown in Table 5 5. Although these were measured during the initial loading prior to having all the D_2O in the module tank, the results are considered to be generally applicable. The exhaust nozzle tank was worth more than earlier measurements, (Reference 2, p. 162) on the regular cylindrical cavity reactor. Conceptually the reason for the higher worth is evasive, but is considered to be caused by the internal moderation between the modules that creates a higher flux over the center module than over the outer modules, whereas the opposite was true at the center of the normal cavity reactor.

The worth for polyethylene and polystyrene shows a large difference, -0.405±0 097%Δk/kg for polyethylene (a relatively small perturbation) compared to -0.111±0.019%Δk/kg for polystyrene (measured for entire quantity that was in a single module). One would expect a nominal factor of two difference between these two materials if most of the reactivity penalty were due to the effects of hydrogen without consideration of molecular-binding-energy effects. (Carbon is worth only a few percent of the worth of hydrogen) Part of the difference is undoubtedly caused by the fact that the polyethylene measurement was a small perturbation (the addition of 110 grams per fuel element or six percent in the hydrogen mass) after all of the polystyrene was in the reactor; whereas the polystyrene measurement was a major perturbation (100% removal from one of the modules). For a proper relative comparison, equal hydrogen mass should be used in identical positions in the reactor.

Aluminum worth measurements were made by placing core-length strips of aluminum in the measurement slots in the fuel elements. The mass of the aluminum varied proportional to the radius squared in order to obtain a fuel element structure average worth in a single measurement and so as to place sufficient mass in the reactor to obtain a meaningful measurement The values thus measured are given in Table 5.5. The aluminum was type 1100.

5 2 3 Simulated Exhaust Nozzle Measurements for the Module System

Reactivity measurements were also made in the exhaust nozzle hole and in the end reflector (30.5 cm diameter) to evaluate possible exhaust nozzle configurations for the "light bulb" reactor. Two tanks were assembled for the measurement as shown in Figure 5.9*. Each tank configuration was measured in three steps as shown in Table 5 6 All materials were worth more with the annular tank configuration than with the central tank. Hydrogen at 4 1 x 10^{20} atoms/cc in the form of polystyrene (foamed) has a positive effect on reactivity in the nozzle, indicating that its scattering cross section reduces neutron leakage through the nozzle opening and more than counteracts the absorptions

5.3 Power Mapping (Catcher Foil Data)

Power mapping was done in modules 1 and 3 at different angles As will be noted from Figure 5.2, there were four foil exposure tubes or slots in the measurement fuel elements into which foils could be inserted without disassembling the fuel element These slots extended the full length of the fuel element. The foils were placed on aluminum straps and then the straps were inserted into the slots.

The catcher foil data are given in Table 5.7. The data were first normalized to the point nearest the center of the core and then the axial plots were plotted as shown in Figures 5 10 to 5.14. Each of these axial plots were then averaged using a planimeter and the averages plotted to show the radial profile as presented in Figure 5.15. It will be noted that the core center has the highest power and that the lowest power in the outer modules is on that part of their circumference nearest the radial reflector.

To further identify the detailed circumferential power distribution on the outside of the fuel elements, a strip of catcher foils was placed near the axial center of the core (stage 8) on the outer fuel ring of the fuel element in modules 1 and 4. The resulting profiles are shown in Figure 5 16 Module 4 had a rather smooth profile, with a 17% spread from the maximum to the minimum around the fuel element.

---

*Note: Unrelated to the experiment but of documentary interest, an unidentified chemical reaction occurred with the annular tank, creating sufficient gas pressure inside to buckle the inner wall This event occurred during a prolonged storage period of three weeks at room temperature. Significant chemical reaction or decomposition products were not found in the remaining D_2O. Duplication of suspected conditions such as: 1) dis-similar types of Al; 2) residual machining flux; 3) residue from acetone wash; and 4) "perfectly" clean walls were made in separate experiments. All four experiments eventually developed 2 psi over-pressure in essentially full cans. The residual machining-flux experiment developed the overpressure most rapidly ($\sim$3 weeks vs $\sim$2 months for the others). The cause is believed to be normal aluminum corrosion, which evidently occurs for neutral or slightly basic water conditions, but is allegedly inhibited by slightly acidic conditions (pH = 5 to 6).

Module 1, however, gave a very scattered profile which was hard to define so a second set of data were taken on module 1 with finer resolution (closer foil spacing) and with special attention given to the exact location of the fuel sheets on the outer fuel ring. These are shown in Figure 5.16 and it will be noted that flux peaks occur where there are gaps in the fuel and depressions result where the fuel sheets are The variation amounts to nominally 6%, which is equivalent to the self shielding factor for 0 0025 cm thick uranium metal The second exposure was on stage 11 of module 1 so a direct comparison with the first set of data was not made Module 4 did not show as large a fluctuation as was observed for module 1 In both cases, the catcher foils were mounted on the outside of the outer layer of fuel

Some U^{235}-fission cadmium ratios were also measured in modules 1 and 3 These are shown in Figure 5 17 The system is highly thermal and the center module is generally a little less thermal than the outer module. At the end of the core where the exhaust nozzle hole exists, the thermal component of the flux was significantly enhanced This effect has been noted on previous cavity reactor experiments, and is the result of inward streaming of neutrons from the peak flux regions of the surrounding reflector. The reflector flux peaks about 20 cm from the inner cavity wall

5.4 Flux Mapping (Gold Foil Data)

5.4.1 Bare Gold Data

The gold data were concentrated in the D_2O regions and areas outside the fuel although some data were obtained within the fuel Both bare and cadmium covered foils were exposed and the data are found in Table 5.8 All foils were from 0 001016 to 0 00127 cm thick and nominally 1.43 cm in diameter The cadmium covers were 0 0508 cm thick

Each foil exposure run contained power normalizer foils which were used to correct the gold data to the same reactor power The normalization foils consisted of seven catcher foils mounted between the two tables on the reflector tank. These data are given in Table 5 9

The bare gold data were normalized to the same physical location as the catcher foils as will be noted from Table 5 8 The normalized values were then plotted to show various distributions Figure 5.18 shows the relative distribution in modules 1 and 3 for the inner and outer measurement slot of the fuel elements Gold foils were also exposed on the inner and outer surfaces of the polystyrene in module 7 and the relative distribution is given in Figure 5 19 As with the catcher foils, the peak occurs over the region pointing toward the center of the core and the low point is next to the radial reflector

Bare gold was also exposed in the two special exposure tubes, one running from module 1 to module 3 and the other from module 1 to the module wall between modules 5 and 6. The data are plotted in Figure 5.20. The data from module 1 to module 3 were repeated as it was noted that the foil positions on the first run may have been altered because of displacement of the aluminum strap containing the foils as the element was slid into place. This counts at least in part for the differences in the two sets of data. As would be expected, the peak flux occurs midway between the modules.

A strip of gold foils was also placed along the separation plane over modules 1 and 3 as shown in Figure 5.21. There was no apparent peak at the center of the exhaust nozzle as was observed with the large single cavity configurations, but the catcher foil cadmium ratio was somewhat higher at the exhaust nozzle than elsewhere out to the edge of the outer modules.

The relative distribution in the reflector regions is shown in Figures 5.22 and 5.23. Three sets of data are given and in general the last two runs show good agreement with Run 1168 being the odd set of data. Excess reactivity was high on this run, requiring the rods to be quite a ways in the reactor. On Run 1168 actuators 1,2,3, and 10 were fully withdrawn while actuators 4 to 9 were equally withdrawn 12.6 cm. Run 1173 was the same rod pattern but the six actuators which were equally withdrawn were out 15.2 cm. The same rods on Run 1174 were withdrawn 13.3 cm. These variations are caused by the foils placed in the reactor and slight changes in D_2O temperature. The rods were actually further in on Run 1168 which could account for at least part of the differences. However, control rod effects would not normally be expected to exist in the radial reflector, other than as affected by an overall shift in the average core power distribution.

5.4.2 Cadmium Ratios

Cadmium ratios were calculated for all points where both bare and cadmium covered foils were available. These data are given in Table 5.10. Infinitely dilute activities were calculated for gold. (Refer to Reference 5, p. 69, or to Reference 6, on resonance self-shielding of gold and indium, for the procedure used in reducing the data. For catcher foils, the cadmium ratio is essentially the infinitely dilute value, since only the surface activity of U-235 is seen.) Some of these data are shown graphically in Figures 5.24 to 5.27. A peak cadmium ratio occurs about midway between the modules as noted from Figure 5.24 with the highest value where the D_2O thickness is the largest, the traverse from module 1 between modules 5 and 6.

Module 1 shows a sizable increase in gold cadmium ratio at the end of the core next to the exhaust nozzle opening as observed from Figure 5 25 A similar increase was noted with catcher foils (Figure 5 17) This increase had been observed in previous measurements on the single large cavity over this region with the exhaust nozzle tank removed The extra high thermal flux component originates 10 to 20 cm inside the reflector and streams down the empty exhaust nozzle toward the core

The separation between the gold cadmium ratio plots in the end and radial reflectors (Figure 5.27) was larger than observed from other cavity reactor configurations. One cause for this is probably the position of the control rods in the end reflector, creating a thermal flux depression in the end of the reactor The radial reflector is not affected as much as the end reflector thus the cadmium ratios in the radial reflector are higher than in the end reflector Furthermore, in this module configuration, the effective thickness of the radial reflector is greater than it was in the single large cavity configuration, resulting in a higher thermal to epi-thermal flux ratio

5 4.3 <u>Thermal Neutron Flux</u>

At the same positions where gold cadmium ratio were obtained, thermal (equivalent 2200 m/sec) neutron fluxes were calculated These data are given in Table 5 11 normalized to a watt of reactor power Figure 5.28 shows the distribution in modules 1 and 3 and Figure 5.29 presents the circumferential distribution around module 7 on the inner and outer surfaces of the polystyrene. There was not much of a variation in flux around the outer modules, except for a slight peaking next to the center module with the minimum next to the radial reflector

Sufficient data were obtained to plot the thermal flux distribution at the axial centerline starting at the core center and progressing to the outside of the reflector Traverses were made from the center of module 1 through module 3 and into the radial reflector and from module 1 through the D_2O between modules 5 and 6 The resulting distributions are seen in Figures 5 31 and 5 32 The peak flux in the reactor appears to have occurred in the D_2O between module 1 and the six surrounding modules An unusual dip in flux is evident in the region of the walls of the module and reflector tanks The total thickness of these two walls is 1 27 cm, and this amount of aluminum can be expected to create a flux perturbation in the D_2O The flux dips that appear at the edge of the fuel and at the cavity wall of module 1 are unexpected, and are attributed to spurious experimental error

TABLE 5 1

Initial Loading

7-Module Reactor

0 55 Radius Ratio

Increment	Fuel in Reactor (kg)	Channel No 1 CPM	Channel No 1 CRo/CR	Channel No 2 CPM	Channel No 2 CRo/CR	Channel No 3 CPM	Channel No 3 CRo/CR	Average	Rod Positions
0	0	638	1 000	531	1 000	494	1 000	1 000	In
0	0	886	1 000	755	1 000	687	1 000	1 000	Out
1	1 273	801	0 797	647	0 821	587	0 842	0 820	In
1	1 273	1170	0 757	923	0 818	844	0 814	0 796	Out
2	2 546	1041	0 613	824	0 644	752	0 657	0 638	In
2	2 546	1477	0 600	1189	0 635	1067	0.644	0 626	Out
3	3 819	1256	0 508	1022	0 520	979	0 505	0 511	In
3	3.819	1519	0 583	1271	0 594	1192	0 576	0 584	Out
4	5.092	1539	0 415	1317	0 403	1223	0 404	0 407	In
4	5 092	2397	0 370	1979	0 382	1853	0.371	0 374	Out
5	6 365	1940	0 329	1620	0 328	1449	0 341	0 333	In
5	6 365	3135	0 283	2524	0 299	2270	0.303	0 295	Out
6	7 638	2406	0 265	2006	0 265	1840	0 268	0 266	In
6	7 638	3904	0 227	3224	0 234	2904	0 237	0 233	Out
7	8 911	3089	0 207	2536	0 209	2308	0 214	0 210	In
7	8 911	5168	0 171	4230	0 178	3862	0 178	0 176	Out

TABLE 5 1

(Continued)

Increment	Fuel in Reactor (kg)	Channel No 1 CPM	Channel No 1 CRo/CR	Channel No 2 CPM	Channel No 2 CRo/CR	Channel No 3 CPM	Channel No 3 CRo/CR	Average	Rod Positions
		Addition of D_2O to Central Tank							
	Barrels								
8	1	3051	0 209	2168	0 245	2247	0 220	0 225	In
8	1	4047	0 218	2823	0 267	2905	0 236	0 240	Out
9	2	3142	0 203	2348	0 226	2337	0 211	0 213	In
9	2	5604	0 158	4145	0 182	4149	0 166	0 169	Out
10	3	3543	0 180	2658	0 200	2575	0 192	0 191	In
10	3	6447	0 137	5027	0 150	4709	0 146	0 144	Out
11	5	5313	0 120	4159	0 128	3843	0 129	0 126	In
11	5	11869	0 075	9608	0 079	7731	0 089	0 081	Out
12	6	8569	0 074	6870	0 077	6305	0 078	0 076	In
12	6	33378	0 027	27020	0 028	23867	0 029	0 028	Out
13	6 694	12733	0 050	10235	0 052	9155	0 054	0 052	In
13	6 694	193154	0 0046	150866	0 0050	125062	0 0055	0 0050	Out
14	7 359	18515	0 0346	14830	0 0358	13401	0 0369	0 0357	In

TABLE 5 2

All Rods Worth Curve Data

7 Actuators - 21 Rods

7-Module Reactor

Rods In - 117

Rods Out - 9784

% Worth Inserted

	0	100	200	300	400	500	600	700	800	900
00	100 00	100 00	96 80	93 63	90 49	87.40	84.34	81 32	78 35	75 42
1000	72 54	69 71	66 94	64 22	61 56	58 95	56 42	53 97	51 60	49 31
2000	47 10	44 97	42 91	40 93	39 02	37 18	35 40	33 69	32 04	30 45
3000	28 92	27 45	26 04	24 68	23 38	22 14	20 95	19 81	18 73	17 70
4000	16 72	15 79	14 91	14 07	13 28	12 54	11 84	11 17	10 53	9 92
5000	9 34	8 78	8 24	7 73	7 24	6 77	6 32	5 88	5 46	5 06
6000	4 68	4 32	3 98	3 66	3 35	3 06	2 78	2 52	2 28	2 05
7000	1 84	1 64	1 45	1 28	1 13	1 00	0 89	0 79	0 69	0 60
8000	0 51	0 43	0 35	0 28	0 21	0 15	0.10	0 06	0 03	0 02
9000	0 01	0 00								

Difference

	0	100	200	300	400	500	600	700	800	900
00	0 00	0 00	3 20	3 17	3 14	3 09	3 06	3 02	2 97	2 93
1000	2 88	2 83	2 77	2 72	2 66	2 61	2 53	2 45	2 37	2 29
2000	2 21	2 13	2 06	1 98	1 91	1 84	1 78	1 71	1 65	1 59
3000	1 53	1 47	1 41	1 36	1 30	1 24	1 19	1 14	1 08	1 03
4000	0 98	0 93	0 88	0 84	0 79	0 74	0 70	0 67	0 64	0 61
5000	0 58	0 56	0 54	0 51	0 49	0 47	0 45	0 44	0 42	0 40
6000	0 38	0 36	0 34	0 32	0 31	0 29	0 28	0 26	0 24	0 23
7000	0 21	0 20	0 19	0 17	0 15	0 13	0 11	0 10	0 09	0 09
8000	0 08	0 08	0 07	0 07	0 06	0 05	0 04	0 03	0 02	0 01
9000	0 00									

TABLE 5.3

All Rods Worth Curve Data

10 Actuators - 30 Rods

Exhaust Nozzle Tank in Reactor

7-Module Reactor

% Worth Inserted

	0	100	200	300	400	500	600	700	800	900
00	100 00	100 00	97 20	93 10	89 14	85 32	81 63	78 08	74 67	71 39
1000	68 23	65 20	62 30	59 52	56 86	54 31	51 86	49 53	47 29	45 16
2000	43 12	41 17	39 31	37 53	35 82	34 20	32 63	31 13	29 69	28 30
3000	26 96	25 67	24 43	23 23	22 08	20 98	19 92	18 90	17 91	16 96
4000	16 05	15 17	14 33	13 52	12 74	12 00	11 29	10 61	9 96	9 34
5000	8 75	8 19	7 66	7 16	6 68	6 22	5 78	5 37	4 98	4 61
6000	4 26	3 93	3 62	3 32	3 04	2 78	2 53	2 30	2 08	1 88
7000	1 69	1 51	1 34	1 18	1 03	0 89	0 76	0 64	0 54	0 45
8000	0 37	0 30	0 24	0 19	0 14	0 10	0 07	0 04	0 02	0 01

	0	100	200	300	400	500	600	700	800	900
00	0	0	2 80	4 10	3 96	3 82	3 69	3 55	3 41	3 28
1000	3 16	3 03	2 90	2 78	2 66	2 55	2 45	2 33	2 24	2 13
2000	2 04	1 95	1 86	1 78	1 70	1 63	1 57	1 50	1 44	1 39
3000	1 34	1 29	1 24	1 20	1 15	1 10	1 06	1 02	0 99	0 95
4000	0 91	0 88	0 84	0 81	0 78	0 74	0 71	0 68	0 65	0 62
5000	0 59	0 56	0 53	0 50	0 48	0 46	0 44	0 41	0 39	0 37
6000	0 35	0 33	0 31	0 30	0 28	0 26	0 25	0 23	0 22	0 20
7000	0 19	0 18	0 17	0 16	0 15	0 14	0 13	0 12	0 10	0 09
8000	0 08	0 07	0 06	0 05	0 05	0 04	0 03	0 03	0 02	0 01
9000	0 00									

TABLE 5 4

Fuel Worth Measurements

7-Module Reactor - 0.55 Radius Ratio

Location				
Module	Angle from Centerline (°cw)	Radius (cm)	Reactivity Worth of 7.28g (%Δk)	Specific Worth (%Δk/kg)
3	90	4 0	0.0202±0 003	2 78±0 41
3	90	7 8	0.0208±0 003	2 86±0 41
3	90	11.6	0 0228±0 003	3 13±0 41
3	270	4 0	0 0213±0 003	2 93±0 41
3	270	7 8	0 0231±0.003	3 17±0 41
3	270	11 6	0.0283±0 003	3 89±0 41
1	90	4 0	0 0362±0 003	4 97±0 41
1	90	7 8	0.0377±0 003	5 18±0 41
1	90	11.6	0 0442±0 003	6 07±0 41

TABLE 5 5

Miscellaneous Reactivity Measurements

7-Module Reactor - 0 55 Radius Ratio

Material	Location	Mass (g)	Reactivity Change (%Δk)	Specific Worth (%Δk/kg)
Polyethylene	Hydrogen annulus	770	-0 312 ±0 075	-0 405±0 097
Exhaust Nozzle	End reflector	-----	1 150 ±0 066	---
Polystyrene	Module 5	2411	-0 266 ±0 045	-0 111±0 019
Aluminum	Module 1, 90°[1]	540	-0 0422±0 003	-0 078±0 006
Aluminum	Module 4, 150°	540	-0 0065±0 003	-0 012±0 006
Aluminum	Module 4, 330°	540	-0 0176±0 003	-0 033±0 006

1. Angles are clockwise from core centerline

TABLE 5 6

Reactivity Measurements of Exhaust Nozzle Configurations

Material	Weight (gm)	Total Worth (%Δk)	Worth per kg (%Δk/kg)
21 3 cm O D tank (Aluminum)	4027	-0' 0113±0 003	$-(2.81\pm0\ 74) \times 10^{-3}$
D_2O	34587	+0 608 ±0 074	0 0176±0 0021
Polystyrene (CH)	280*	+0 0268±0 003	0.0957±0 0107
Annular Tank 21 3 cm I D 29 8 cm O D (Aluminum)	7303	-0 0513±0 003	$-(7\ 02\pm0\ 41) \times 10^{-3}$
D_2O	33000	+0 667 ±0 066	0 0202±0 0020
Polystyrene (CH)	280*	+0 0407±0 003	0 145 ±0 011

*Approximate hydrogen atom density was $4\ 1 \times 10^{20}$ atoms/cc

TABLE 5 7

Catcher Foil Data

7-Module Reactor - 0 55 Radius Ratio

Run 1168

Foil Number	Foil Type	Module Number	Location: Angle (°cw)	Location: Radial (cm)	Location: Axial (cm)	Normalized Counts	Local to Foil (X)
1	Bare	1	90°	4 0	92 5	199359	0 977
2	Bare	1	90°	4 0	105 8	204783	1 003
3	Bare	1	90°	4 0	121 0	198881	0 975
4	Bare	1	90°	4 0	136 3	209585	1 027
5	Bare	1	90°	4 0	151 5	204007	1 000 (X)
6	Bare	1	90°	4 0	166 8	196146	0 961
7	Bare	1	90°	4 0	182 0	192109	0 941
8	Bare	1	90°	4 0	197 2	180404	0 884
9	Bare	1	90°	4 0	210 5	194350	0 952
10	Bare	1	90°	7 8	92 5	204182	1 000
11	Bare	1	90°	7 8	105 8	198871	0 974
12	Bare	1	90°	7 8	121 0	211748	1 038
13	Bare	1	90°	7 8	136 3	210262	1 030
14	Bare	1	90°	7 8	151 5	210274	1 030
15	Bare	1	90°	7 8	166 8	201064	0 985
16	Bare	1	90°	7 8	182 0	194713	0 954
17	Bare	1	90°	7 8	197 2	184216	0 903
18	Bare	1	90°	7 8	210 5	187474	0 919
19	Bare	1	90°	11 6	92 5	220544	1 081
20	Bare	1	90°	11 6	105 8	220552	1 081
21	Bare	1	90°	11 6	121 0	231184	1 133
22	Bare	1	90°	11 6	136 3	232027	1 137
23	Bare	1	90°	11 6	151 5	229153	1 123
24	Bare	1	90°	11 6	166 8	229802	1 126
25	Bare	1	90°	11 6	182 0	220739	1 082
26	Bare	1	90°	11 6	197 2	210128	1 030
27	Bare	1	90°	11 6	210 5	202533	0 992
28	Bare	1	90°	15 4	92 5	248729	1 219
29	Bare	1	90°	15 4	105 8	252601	1 238
30	Bare	1	90°	15 4	121 0	262577	1 287
31	Bare	1	90°	15 4	136 3	260240	1 275
32	Bare	1	90°	15 4	151 5	260122	1 275
33	Bare	1	90°	15 4	166 8	252475	1 237
34	Bare	1	90°	15 4	182 0	244783	1 199
35	Bare	1	90°	15 4	197 2	225509	1 105
36	Bare	1	90°	15 4	210 5	220056	1 078
37	Bare	3	90°	4 0	92 5	145113	0 711
38	Bare	3	90°	4 0	105 8	142166	0 697
39	Bare	3	90°	4 0	121 0	148993	0 730
40	Bare	3	90°	4 0	136 3	149483	0 732

TABLE 5 7

(Continued)

Run 1168

Foil Number	Foil Type	Module Number	Location: Angle [1] (°cw)	Location: Radial (cm)	Location: Axial (cm)	Normalized Counts	Local to Foil (X)
41	Bare	3	90°	4.0	151 5	147853	0 724
42	Bare	3	90°	4 0	166 8	146933	0 720
43	Bare	3	90°	4 0	182 0	138596	0 679
44	Bare	3	90°	4 0	197 2	135222	0 663
45	Bare	3	90°	4 0	210 5	143518	0 703
46	Bare	3	90°	7 8	92 5	148070	0 726
47	Bare	3	90°	7 8	105 8	142007	0 696
48	Bare	3	90°	7 8	121 0	152603	0 748
49	Bare	3	90°	7 8	136 3	148342	0 727
50	Bare	3	90°	7 8	151 5	153320	0 751
51	Bare	3	90°	7 8	166 8	145260	0 712
52	Bare	3	90°	7 8	182 0	142950	0 700
53	Bare	3	90°	7 8	197 2	135089	0 662
54	Bare	3	90°	7 8	210.5	145970	0 715
55	Bare	3	90°	11 6	92 5	154993	0 759
56	Bare	3	90°	11 6	105 8	161344	0 791
57	Bare	3	90°	11 6	121 0	165848	0 813
58	Bare	3	90°	11 6	136 3	166192	0 814
59	Bare	3	90°	11 6	151 5	165872	0 813
60	Bare	3	90°	11 6	166 8	152682	0 748
61	Bare	3	90°	11 6	182 0	157619	0 772
62	Bare	3	90°	11 6	197 2	145998	0 715
63	Bare	3	90°	11 6	210 5	153556	0 757
64	Bare	3	90°	15 4	92 5	172307	0 844
65	Bare	3	90°	15 4	105 8	174870	0 857
66	Bare	3	90°	15 4	121 0	181538	0 890
67	Bare	3	90°	15 4	136 3	183857	0 901
68	Bare	3	90°	15 4	151 5	183164	0 898
69	Bare	3	90°	15 4	166 8	180429	0 884
70	Bare	3	90°	15 4	182 0	173053	0 848
71	Bare	3	90°	15 4	197 2	164330	0 805
72	Bare	3	90°	15 4	210 5	161451	0 791

Run 1169

Foil Number	Foil Type	Module Number	Angle (°cw)	Radial (cm)	Axial (cm)	Normalized Counts	Cd Ratio
1	Cd	1	90°	4 0	92 5	5788	34 4
2	Cd	1	90°	4 0	151 5	6482	31 5
3	Cd	1	90°	4 0	210 5	4450	43 7
4	Cd	1	90°	15 4	92 5	5737	43 4
5	Cd	1	90°	15 4	151 5	6681	38 9
6	Cd	1	90°	15 4	210 5	4669	47 1

1 Angle is clockwise from the core centerline

TABLE 5 7

(Continued)

Run 1170

Foil Number	Foil Type	Module Number	Angle (°cw)	Location Radial (cm)	Location Axial (cm)	Normalized Counts	Local to Foil (X)
1	Bare	1	0	4 0	92 5	197853	0 969
2	Bare	1	0	4 0	105 8	204919	1 004
3	Bare	1	0	4 0	121 0	206210	1 010
4	Bare	1	0	4 0	136 3	206017	1 009
5	Bare	1	0	4 0	151 5	209197	1 025
6	Bare	1	0	4 0	166 8	197195	0 966
7	Bare	1	0	4 0	182 0	194307	0 952
8	Bare	1	0	4 0	197 2	183171	0.898
9	Bare	1	0	4 0	210 5	191370	0 938
10	Bare	1	0	7 8	92 5	213804	1 048
11	Bare	1	0	7 8	105 8	200724	0 984
12	Bare	1	0	7 8	121 0	216560	1 061
13	Bare	1	0	7 8	136 3	216189	1 059
14	Bare	1	0	7 8	151 5	214002	1 049
15	Bare	1	0	7 8	166 8	203720	0 998
16	Bare	1	0	7 8	182 0	196101	0 961
17	Bare	1	0	7 8	197 2	184684	0 905
18	Bare	1	0	7 8	210 5	192661	0 944
19	Bare	1	0	11 6	92 5	229124	1 123
20	Bare	1	0	11 6	105 8	225467	1 105
21	Bare	1	0	11 6	121 0	235788	1 155
22	Bare	1	0	11 6	136 3	235116	1 152
23	Bare	1	0	11 6	151 5	233825	1 146
24	Bare	1	0	11 6	166 8	235591	1 154
25	Bare	1	0	11 6	182 0	224315	1 099
26	Bare	1	0	11 6	197 2	208158	1 020
27	Bare	1	0	11 6	210 5	210047	1 029
28	Bare	1	0	15 4	92 5	251161	1 231
29	Bare	1	0	15 4	105 8	256189	1 255
30	Bare	1	0	15 4	121 0	263006	1 289
31	Bare	1	0	15 4	136 3	266484	1 306
32	Bare	1	0	15 4	151 5	268895	1 318
33	Bare	1	0	15 4	166 8	256482	1 257
34	Bare	1	0	15 4	182 0	229735	1 126
35	Bare	1	0	15 4	197 2	233650	1 145
36	Bare	1	0	15 4	210 5	226913	1 112
37	Bare	3	0	4 0	92 5	158746	0 778
38	Bare	3	0	4 0	105 8	149850	0 734
39	Bare	3	0	4 0	121 0	157506	0 772
40	Bare	3	0	4 0	136 3	154933	0 759

TABLE 5 7

(Continued)

Run 1170

Foil Number	Foil Type	Module Number	Location			Normalized Counts	Local to Foil (X)
			Angle (°cw)	Radial (cm)	Axial (cm)		
41	Bare	3	0	4 0	151 5	157703	0 773
42	Bare	3	0	4 0	166 8	145570	0 713
43	Bare	3	0	4 0	182 0	145414	0 713
44	Bare	3	0	4 0	197 2	143335	0 702
45	Bare	3	0	4 0	210 5	154602	0 758
46	Bare	3	0	7 8	92.5	158974	0 779
47	Bare	3	0	7 8	105 8	151312	0 741
48	Bare	3	0	7 8	121 0	161004	0 789
49	Bare	3	0	7 8	136 3	155542	0 762
50	Bare	3	0	7 8	151 5	159497	0 782
51	Bare	3	0	7 8	166 8	152183	0.746
52	Bare	3	0	7 8	182.0	152361	0 747
53	Bare	3	0	7 8	197 2	145662	0 714
54	Bare	3	0	7 8	210 5	161657	0 792
55	Bare	3	0	11 6	92 5	173962	0 852
56	Bare	3	0	11 6	105 8	175618	0 861
57	Bare	3	0	11 6	121 0	179454	0 879
58	Bare	3	0	11 6	136 3	180558	0 885
59	Bare	3	0	11 6	151 5	180610	0.885
60	Bare	3	0	11 6	166 8	172365	0 846
61	Bare	3	0	11 6	182 0	171542	0 841
62	Bare	3	0	11 6	197 2	161275	0 790
63	Bare	3	0	11 6	210 5	171579	0 841
64	Bare	3	0	15 4	92 5	177589	0 870
65	Bare	3	0	15 4	105 8	194924	0 955
66	Bare	3	0	15 4	121.0	198712	0.974
67	Bare	3	0	15 4	136 3	203295	0 996
68	Bare	3	0	15 4	151 5	204366	1 001
69	Bare	3	0	15 4	166 8	196155	0 961
70	Bare	3	0	15.4	182 0	191447	0 938
71	Bare	3	0	15.4	197 2	181130	0 888
72	Bare	3	0	15 4	210 5	183812	0.901

Run 1171

Foil Number	Foil Type	Module Number	Angle (°cw)	Radial (cm)	Axial (cm)	Normalized Counts	Local to Foil (X)
1	Bare	3	270°	4 0	92 5	159617	0 782
2	Bare	3	270°	4 0	105 8	148451	0 727
3	Bare	3	270°	4 0	121 0	157258	0 771
4	Bare	3	270°	4 0	136 3	161261	0 790
5	Bare	3	270°	4 0	151 5	155084	0 760
6	Bare	3	270°	4 0	166 8	149372	0 732
7	Bare	3	270°	4 0	182 0	143803	0 705
8	Bare	3	270°	4 0	197 2	145242	0 712
9	Bare	3	270°	4 0	210 5	156729	0 768

TABLE 5 7

(Continued)

Run 1171

Foil Number	Foil Type	Module Number	Location Angle (°cw)	Location Radial (cm)	Location Axial (cm)	Normalized Counts	Local to Foil (X)
10	Bare	3	270°	7 8	92 5	165328	0 810
11	Bare	3	270°	7 8	105 8	158001	0 774
12	Bare	3	270°	7 8	121 0	162589	0 797
13	Bare	3	270°	7 8	136 3	165690	0 812
14	Bare	3	270°	7 8	151 5	165615	0 812
15	Bare	3	270°	7 8	166 8	156614	0 767
16	Bare	3	270°	7 8	182 0	154010	0 755
17	Bare	3	270°	7 8	197 2	151034	0 740
18	Bare	3	270°	7 8	210 5	167173	0 819
19	Bare	3	270°	11 6	92 5	181206	0 888
20	Bare	3	270°	11 6	105 8	179944	0 882
21	Bare	3	270°	11 6	121 0	185734	0 910
22	Bare	3	270°	11 6	136 3	185658	0 910
23	Bare	3	270°	11 6	151 5	185652	0 910
24	Bare	3	270°	11.6	166 8	175341	0 859
25	Bare	3	270°	11 6	182 0	179268	0 878
26	Bare	3	270°	11 6	197 2	166358	0 815
27	Bare	3	270°	11 6	210 5	177860	0 872
28	Bare	3	270°	15 4	92 5	204198	1 001
29	Bare	3	270°	15 4	105 8	210040	1 029
30	Bare	3	270°	15 4	121 0	212972	1 044
31	Bare	3	270°	15 4	136 3	213506	1 046
32	Bare	3	270°	15 4	151 5	213272	1 045
33	Bare	3	270°	15 4	166 8	182388	0 894
34	Bare	3	270°	15 4	182 0	189415	0 928
35	Bare	3	270°	15 4	197 2	174374	0 854
36	Bare	3	270°	15 4	210 5	174139	0 853

Run 1172

Foil Number	Foil Type	Module Number	Angle (°cw)	Radial (cm)	Axial (cm)	Normalized Counts	Cd Ratio
1	Cd	3	90°	4 0	92 5	4109	35 3
2	Cd	3	90°	4 0	151 5	4645	31 8
3	Cd	3	90°	4 0	210 5	3787	37 9
4	Cd	3	90°	15 4	92 5	3918	44 0
5	Cd	3	90°	15 4	151 5	4635	39 5
6	Cd	3	90°	15 4	210 5	3521	45 9
7	Bare	1	0	12 6	152 0	236142	1 157
8	Bare	1	22 5°	12 6	152 0	231941	1 137
9	Bare	1	45 0°	12 6	152 0	245812	1 204
10	Bare	1	67 5°	12 6	152 0	237453	1 164
11	Bare	1	90 0°	12 6	152 0	245415	1 203
12	Bare	1	112 5°	12 6	152 0	233623	1 145
13	Bare	1	135 0°	12 6	152 0	246769	1 209
14	Bare	1	157 5°	12 6	152 0	229931	1 127

TABLE 5 7

(Continued)

Run 1172

Foil Number	Foil Type	Module Number	Location: Angle (°cw)	Location: Radial (cm)	Location: Axial (cm)	Normalized Counts	Local to Foil (X)
15	Bare	1	180 0°	12 6	152 0	235231	1 153
16	Bare	1	202 5°	12 6	152 0	248795	1 219
17	Bare	1	225 0°	12.6	152 0	243443	1 193
18	Bare	1	247 5°	12 6	152.0	254023	1 245
19	Bare	1	270 0°	12 6	152 0	238120	1 167
20	Bare	1	292 5°	12 6	152 0	250091	1 225
21	Bare	1	315 0°	12 6	152 0	234388	1 149
22	Bare	1	337 5°	12 6	152 0	240837	1 180
23	Bare	4	0	12 6	152 0	187237	0 917
24	Bare	4	22 5°	12 6	152.0	187929	0 921
25	Bare	4	45 0°	12 6	152 0	184109	0 902
26	Bare	4	67 5°	12 6	152 0	174959	0 857
27	Bare	4	90 0°	12 6	152 0	169232	0 829
28	Bare	4	112 5°	12 6	152 0	170488	0 835
29	Bare	4	135 0°	12 6	152 0	168750	0 827
30	Bare	4	157 5°	12 6	152.0	174000	0 853
31	Bare	4	180 0°	12 6	152 0	166432	0 816
32	Bare	4	202 5°	12 6	152 0	171165	0 839
33	Bare	4	225 0°	12 6	152 0	178351	0 874
34	Bare	4	247 5°	12 6	152 0	179960	0 882
35	Bare	4	270 0°	12 6	152 0	192916	0 945
36	Bare	4	292 5°	12 6	152 0	190843	0.935
37	Bare	4	315.0°	12 6	152 0	199133	0 976
38	Bare	4	337 5°	12 6	152 0	190597	0 934

Run 1174

Foil Number	Foil Type	Module Number	Location: Angle (°cw)	Location: Radial (cm)	Location: Axial (cm)	Normalized Counts	Local to Foil (X)
1	Bare	1	0	12 6	168 5	231684	1 136
2	Bare	1	15.0°	12 6	168 5	230561	1 130
3	Bare	1	30 0°	12 6	168 5	243574	1 194
4	Bare	1	45 0°	12 6	168 5	229355	1 124
5	Bare	1	60 0°	12 6	168 5	234583	1 150
6	Bare	1	75 0°	12 6	168 5	238825	1 171
7	Bare	1	90 0°	12.6	168 5	229782	1 126
8	Bare	1	105 0°	12 6	168.5	231636	1 135
9	Bare	1	120 0°	12 6	168 5	238236	1 168
10	Bare	1	135 0°	12 6	168 5	230883	1 131
11	Bare	1	150 0°	12 6	168 5	227121	1 113
12	Bare	1	165 0°	12.6	168.5	233746	1 146
13	Bare	1	180 0°	12.6	168 5	241459	1 184
14	Bare	1	195 0°	12 6	168 5	234050	1 147
15	Bare	1	210 0°	12 6	168 5	226287	1 109

TABLE 5 7

(Continued)

Run 1174

Foil Number	Foil Type	Module Number	Location Angle (°cw)	Location Radial (cm)	Location Axial (cm)	Normalized Counts	Local to Foil (X)
16	Bare	1	225 0°	12 6	168 5	227838	1 117
17	Bare	1	240 0°	12 6	168 5	241909	1 186
18	Bare	1	255 0°	12 6	168 5	228115	1 118
19	Bare	1	270 0°	12 6	168 5	234872	1 151
20	Bare	1	285 0°	12 6	168 5	218792	1 072
21	Bare	1	300 0°	12 6	168 5	230348	1 129
22	Bare	1	315 0°	12 6	168 5	232827	1 141
23	Bare	1	330 0°	12 6	168 5	243157	1 192
24	Bare	1	345 0°	12 6	168 5	241349	1 183

TABLE 5 8

Gold Foil Data

7-Module Reactor - Exhaust Nozzle Removed

0.55 Radius Ratio

Run 1168

Foil Number	Foil Type	Location Radial (cm)	Location Axial (cm)	Foil Weight (g)	Specific Activity d/m-g x 10^{-6}	Local to Foil (X)
1	Bare	0	89 4	0 0354	7 825	0 948
2	Bare	0	74 9	0 0381	9 824	1 190
3	Bare	0	59 6	0 0280	6 800	0 824
4	Bare	0	44 4	0 0380	4 609	0 558
5	Bare	0	29 1	0 0410	2 600	0 315
6	Bare	0	13 9	0 0379	1 244	0 151
7	Bare	0	0	0 0322	0 170	0 021
8	Bare	93 2	151 1	0 0389	8 204	0 994
9	Bare	107 7	151 1	0 0402	6 621	0 802
10	Bare	123 0	151 1	0 0333	4 756	0 576
11	Bare	138 2	151 1	0 0398	3 289	0 398
12	Bare	153 4	151 1	0 0408	1 887	0 229
13	Bare	168 7	151 1	0 0330	0 861	0 104
14	Bare	183 9	151 1	0 0350	0 130	0 016
15	Bare	23 6[1]	151 1	0 0415	10 475	1 269
16	Bare	30 5	151 1	0 0335	13 514	1.637
17	Bare	38 1	151 1	0 0322	13 876	1.681
18	Bare	45 7	151 1	0 0400	12 785	1 549
19	Bare	53 3	151 1	0 0366	12 110	1 467
20	Bare	61 0	151 1	0 0414	10 357	1 255
21	Bare	68 6	151 1	0 0417	10 522	1 275
22	Bare	76 2	151.1	0 0384	9 697	1 175
23	Bare	83 8	151 1	0 0358	8 138	0 986
24	Bare	90 7	151 1	0 0354	7 023	0 851
25	Bare	44 4[2]	151 1	0 0376	7 630	0 924
26	Bare	39 4	151 1	0 0338	10 694	1 296
27	Bare	34 0	151 1	0 0384	13 500	1 636
28	Bare	28 7	151 1	0 0341	12 354	1 497
29	Bare	23 6	151 1	0 0335	9 009	1 092

Run 1169

Foil Number	Foil Type	Location Radial (cm)	Location Axial (cm)	Foil Weight (g)	Specific Activity d/m-g x 10^{-6}	Local to Foil (X)
1	Cd	0	89 4	0 0343	2 038	
2	Cd	0	59 6	0 0363	0 241	
3	Cd	0	29 1	0 0371	0 0077	
4	Cd	93 2	151 1	0 0312	0 640	
5	Cd	123 0	151 1	0 0273	0.025	
6	Cd	153 4	151 1	0 0385	0 0030	

TABLE 5 8

(Continued)

Run 1169

		Location				
Foil Number	Foil Type	Radial (cm)	Axial (cm)	Foil Weight (g)	Specific Activity d/m-g x 10^{-6}	Local to Foil (X)
	Module 3 at 90°					
7	Bare	4 0	92 5	0 0399	5 350	0 648
8	Bare	4 0	121 0	0 0302	5 497	0 666
9	Bare	4 0	151 5	0 0385	5 533	0 670
10	Bare	4 0	182 0	0 0333	5 109	0 619
11	Bare	4 0	210 5	0 0373	5 085	0 616
12	Bare	15 4	92 5	0 0352	5 883	0.713
13	Bare	15 4	121.0	0 0374	6 323	0 766
14	Bare	15 4	151 5	0 0388	6 594	0 799
15	Bare	15.4	182 0	0 0385	6 183	0 749
16	Bare	15 4	210 5	0 0392	5 392	0 653
17	Cd	30 5	151 1	0 0390	2 271	
18	Cd	53 3	151 1	0 0397	1 901	
19	Cd	76 2	151 1	0 0418	1 327	
Run 1170						
1	Bare	0	82 5	0 0369	10 005	1 212
2	Bare	0	67 2	0 0410	8 563	1 037
3	Bare	0	52 0	0 0432	5 832	0 707
4	Bare	100 1	151 1	0 0323	7 938	0 962
5	Bare	115 4	151 1	0 0386	5 959	0 722
6	Bare	130 6	151 1	0 0402	4 118	0 499
7	Bare	0	212 0	0 0357	6 915	0 838
8	Bare	15 2	212 0	0 0411	7 249	0 878
9	Bare	30 5	212 0	0 0379	8 385	1 016
10	Bare	45 7	212 0	0 0360	7 063	0 856
11	Bare	61 0	212 0	0 0381	5 622	0 681
12	Bare	76 2	212 0	0 0404	5 358	0 649
13	Bare	91 4	212 0	0 0399	5 010	0 607
14	Cd	30 5	212 0	0 0392	2 765	
15	Cd	61 0	212 0	0 0414	0 978	
16	Cd	91 4	212 0	0 0368	1 444	
	Module 7 on Inner Surface of Polystyrene					
17	Bare	17 5[3]	153 6	0 0390	6 485	0 786
18	Bare	17 5	153 6	0 0367	6 709	0 813
19	Bare	17 5	153 6	0 0376	7 229	0 876
20	Bare	17 5	153 6	0 0361	7 273	0 881
21	Bare	17 5	153 6	0 0356	7 246	0 878
22	Bare	17 5	153 6	0 0418	6 802	0 824
23	Bare	17 5	153 6	0 0380	6 644	0 805
24	Bare	17 5	153 6	0 0420	6 339	0 768

TABLE 5 8

(Continued)

Run 1170

Foil Number	Foil Type	Location Radial (cm)	Location Axial (cm)	Foil Weight (g)	Specific Activity d/m-g x 10^{-6}	Local to Foil (X)
	Module 7 on Outer Surface of Polystyrene					
25	Bare	22 5[3]	153 6	0.0475	6 726	0.815
26	Bare	22 5	153 6	0 0425	7 416	0 947
27	Bare	22.5	153 6	0 0307	8 030	0.973
28	Bare	22 5	153 6	0 0417	8 115	0 983
29	Bare	22 5	153 6	0 0318	8 298	1 005
30	Bare	22 5	153 6	0 0421	7 714	0 935
31	Bare	22 5	153 6	0 0335	7 328	0.888
32	Bare	22 5	153 6	0 0350	6 902	0 836
	Module 4 on Inner Surface of Polystyrene					
33	Cd	17 5[4]	153 6	0 0337	1 829	
34	Cd	17 5	153 6	0 0416	1 566	
35	Cd	17 5	153 6	0 0348	1 674	
36	Cd	17 5	153 6	0 0339	1 758	
Run 1171						
1	Cd	0	74 9	0 0338	1 151	
2	Cd	0	44 4	0 0357	0 0433	
3	Cd	107 7	151 1	0 0282	0 167	
4	Cd	138 0		0 0338	0 0069	
	Module 1 at 90°					
5	Bare	4 0	92 5	0 0298	7 746	0 939
6	Bare	4 0	121 0	0 0328	8 049	0 975
7	Bare	4 0	151 5	0 0302	8 253	1 000 (X)
8	Bare	4 0	182 0	0 0483	7 111	0 862
9	Bare	4 0	210 5	0 0409	6 873	0 833
10	Bare	15 4	92 5	0 0426	8 738	1 059
11	Bare	15 4	121 0	0 0364	9 391	1 138
12	Bare	15 4	151 5	0 0325	9 806	1 188
13	Bare	15 4	182 0	0 0319	8 951	1 085
14	Bare	15 4	210 5	0 0308	7 943	0 962
	Module 4 on Outer Surface of Polystyrene					
15	Cd	22 5[4]	153 6	0 0348	1 844	
16	Cd	22 5	153 6	0 0421	1 614	
17	Cd	22 5	153 6	0 0345	1 754	
18	Cd	22 5	153 6	0 0391	1 780	

TABLE 5 8

(Continued)

Run 1172

Foil Number	Foil Type	Location Radial (cm)	Location Axial (cm)	Foil Weight (g)	Specific Activity d/m-g x 10^{-6}	Local to Foil (X)
	Module 1 at 90°					
1	Cd	4 0	92 5	0 0370	1 987	
2	Cd	4 0	151 5	0 0367	2 241	
3	Cd	4 0	210 5	0.0361	1 585	
4	Cd	15 4	92 5	0 0368	1 985	
5	Cd	15 4	151 5	0 0359	2 352	
6	Cd	15.4	210 5	0 0396	1 586	
7	Cd	0	74 9	0 0360	1 144	
8	Cd	0	44 4	0 0401	0 0338	
9	Cd	107 7	151 1	0 0428	0 134	
10	Cd	138 0	151 1	0 0357	0 0064	
Run 1173						
1	Bare	0	89 4	0 0350	8 602	1 042
2	Bare	0	74.9	0 0355	10 769	1 305
3	Bare	0	59 6	0 0346	8 547	1 036
4	Bare	0	44 4	0 0347	4 744	0 575
5	Bare	0	29 1	0 0352	3 131	0 379
6	Bare	0	13 9	0 0349	1 450	0 176
7	Bare	0	0	0 0347	0 116	0 014
8	Bare	93 2	151 1	0 0356	9 356	1 134
9	Bare	107 7	151 1	0 0350	7 438	0 901
10	Bare	123 0	151 1	0 0357	5 379	0 652
11	Bare	138 2	151 1	0 0361	2 821	0 342
12	Bare	153 4	151 1	0 0353	1 505	0 182
13	Bare	168 7	151 1	0 0352	0 408	0 049
14	Bare	183 9	151 1	0 0354	0 115	0 014
	Module 3 at 90°					
15	Cd	4 0	92 5	0 0347	1 640	
16	Cd	4 0	151 5	0 0374	1 749	
17	Cd	4 0	210 5	0 0379	1 486	
18	Cd	15 4	92 5	0 0343	1 515	
19	Cd	15 4	151 5	0 0348	1 826	
20	Cd	15 4	210 5	0 0350	1 380	
21	Cd	0	212 0	0 0350	1 667	
22	Cd	23 6[1]	151 1	0 0354	2 682	
23	Cd	45 7	151 1	0 0351	2.295	
24	Cd	68 6	151 1	0 0344	2 185	
25	Cd	90 7	151 1	0 0358	0 700	
26	Cd	44 4[2]	151 1	0 0350	2 131	
27	Cd	34 0	151 1	0 0360	2 552	
28	Cd	23 6	151 1	0 0350	2 664	

TABLE 5.8

(Continued)

Run 1174

Foil Number	Foil Type	Location Radial (cm)	Location Axial (cm)	Foil Weight (g)	Specific Activity d/m-g x 10^{-6}	Local to Foil (X)
1	Bare	0	89 4	0 0349	7 970	1 041
2	Bare	0	74 9	0 0349	9 795	1 280
3	Bare	0	59 6	0.0349	7 146	0 933
4	Bare	0	44 4	0 0350	4 617	0 603
5	Bare	0	29 1	0 0350	2 767	0.361
6	Bare	0	13 0	0 0348	1 336	0.175
7	Bare	0	0	0 0349	0 174	0 023
8	Bare	93 2	151 1	0 0350	8.536	1 115
9	Bare	107 7	151 1	0 0350	6 793	0.887
10	Bare	123 0	151 1	0 0349	4 916	0 642
11	Bare	138 2	151 1	0 0352	2 615	0 342
12	Bare	153 4	151 1	0 0354	1 922	0 251
13	Bare	168 7	151 1	0 0352	0 898	0 117
14	Bare	183 9	151 1	0 0351	0 122	0 016
	Module 1, 90°					
15	Bare	4 0	151 1	0 0350	7 655	1 000 (X)
16	Bare	7 8	151 1	0 0348	7 951	1 039
17	Bare	11 6	151 1	0 0350	8 591	1 122
18	Bare	15 4	151 1	0 0353	9.366	1 223
19	Bare	17 5	151 1	0 0362	9 188	1.200
20	Bare	22 5	151 1	0 0353	11 703	1 529
	Module 3, 270°					
21	Bare	15 4	151 1	0 0356	7 364	0 962
22	Bare	11 6	151 1	0 0351	6 725	0.878
23	Bare	7 8	151 1	0 0352	6 159	0 805
24	Bare	4 0	151 1	0 0358	5 866	0 766
	Module 1, Equivalent 90°					
25	Cd	17 5	151 1	0 0351	2 372	-----
26	Cd	22 5	151 1	0 0349	2 370	-----
	Traverse from Module 1 to Module 3					
27	Bare	23 6	151 1	0 0351	10 891	1 423
28	Bare	28 7	151 1	0 0350	12 676	1 656
29	Bare	34 0	151 1	0 0350	13 073	1.708
30	Bare	39 4	151 1	0 0349	11 686	1 527
31	Bare	44 4	151 1	0 0351	8 947	1 169

1 Traverse in D_2O between modules 5 and 6 (foils 15 to 24)

2 Traverse in D_2O from module 1 to module 3 (foils 25 to 29)

3 Circumferential traverse at 45° intervals going clockwise starting at 0°

4 Circumferential traverse at 90° intervals going clockwise starting at 0°

TABLE 5 9

Power Normalization Factors

7-Module Reactor - 0 55 Radius Ratio

Run	Count Time	Decay Time (min)	Correction Factor	CPM	Corrected CPM	Normalization Factor
1168	------[1]	58 5	1 207	355273	428815	
	------	60 0	1 245	343880	428131	
	------	62 5	1 311	326521	428069	
					428338	1 000
1169	------	25 5	0 496	882600	437770	
	------	27 0	0 523	837570	438049	
	------	29 0	0 559	781968	437120	
					437646	0 979
1170	------	67 0	1 420	307320	436394	
	------	69 0	1 473	296811	437203	
	------	71 0	1 527	286463	437429	
					437009	0 980
1171	------	34 5	0 665	649851	432151	
	------	36 0	0 695	620744	431417	
	------	37 5	0 725	595017	431387	
					431652	0 992
1172	1205 52	60 5	1 258	346652	436088	
	1207 02	62 0	1 285	337089	433159	
	1208 52	63 5	1 326	326996	433597	
					434281	0 986
1173	1541 72	37 48	0 725	550736	399284	
	1544 22	39 98	0 777	515822	400794	
	1546 22	41 98	0 820	489914	401729	
					400602	1 069
1174	1250 42	68 50	1 460	298028	435121	
	1252 42	70 50	1 514	287488	435257	
	1254 42	72 50	1 567	277596	434993	
					435124	0 984

1 Digital clock not operating Decay time determined from stop watch

TABLE 5 10

Gold Foil Cadmium Ratios

7-Module Reactor - Exhaust Nozzle Removed

0 55 Radius Ratio

Location				Infinitely Dilute Foil Activity d/m-g x 10^{-6}		
Radial (cm)	Axial (cm)	Module Number	Angle (°cw)	Cd Covered Foil	Bare Foil	Cadmium Ratio
0	89 4			4 700	10 90	2 32
0	74 9			2 639	11 82	4 48
0	59 6			0 569	7 986	14 04
0	44 4			0 1015	4 735	46 7
0	29 1			0 0183	2 876	157
93 2	151 1			1 421	9 605	6 76
107 7	151 1			0 356	7 237	20 3
123 0	151 1			0 0527	5 100	96 8
138 2	151 1			0 0158	3 079	195
153 4	151 1			0 00725	1 700	235
	Traverse Between Modules 5 & 6					
23 6	151 1			6 266	14 23	2 27
30 5	151 1			5 521	16 62	3 01
45 7	151 1			5 343	15 95	2 99
53 3	151 1			4 656	14 80	3 18
68 6	151 1			5 043	13 55	2 69
76 2	151 1			3 321	11 64	3 51
90 7	151 1			1 643	7 963	4 85
	Traverse from Module 1 to 3					
23 6	151 1			6 195	12 49	2 02
34 0	151 1			6 003	17 02	2 83
44 4	151 1			4 955	10 52	2 12
	Inside CH on Module 7					
17 5	151 1	7	0	3 884	8 771	2 26
17 5	151 1	7	90	4 035	9 579	2 37
17 5	151 1	7	180	4 188	9 646	2 30
17 5	151 1	7	270	3 911	8 929	2 28
	Outside CH on Module 7					
22 5	151 1	7	0	4 055	9 246	2 28
22 5	151 1	7	90	4 332	10 40	2 40
22 5	151 1	7	180	4 278	10 66	2 49
22 5	151 1	7	270	4 051	9 584	2 37
4 0	92 0	1	90	4 727	10 30	2 18
4 0	151 5	1	90	5 313	11 14	2 10
4 0	210 5	1	90	3 733	9 100	2 44
15 4	92 0	1	90	4 712	11 58	2 46
15 4	151 5	1	90	5 526	12 88	2 33
15 4	210 5	1	90	3 880	10 07	2 59

TABLE 5 10

(Continued)

Location				Infinitely Dilute Foil Activity d/m-g x 10^{-6}		
Radial (cm)	Axial (cm)	Module Number	Angle (°cw)	Cd Covered Foil	Bare Foil	Cadmium Ratio
4 0	92 0	3	90	3 800	7 602	2 00
4 0	151 5	3	90	4 179	7 984	1 91
4 0	210 5	3	90	3 570	7 159	2 01
15 4	92 0	3	90	3 494	7 878	2 25
15 4	151 5	3	90	4 236	9 084	2 14
15 4	210 5	3	90	3 209	7 284	2 27
	Traverse at Separation Plane Across Modules 1 & 3					
0	212 0			3 876	9 138	2 36
30 5	212 0			6 736	12 32	1 83
61 0	212 0			2 438	7 047	2 89
91 4	212 0			3 427	7 041	2 05

TABLE 5 11

Thermal Neutron Flux

7-Module Reactor - Exhaust Nozzle Removed

0 55 Radius Ratio

Location Radial (cm)	Location Axial (cm)	Additional Explanation of Location	Thermal Neutron Flux n/cm^2-sec-watt x 10^{-6}
0	89 4	End Reflector	3 763
0	74 9	(Bare foil data from Run 1168)	5 650
0	59 6	(Bare foil data from Run 1168)	4 229
0	44 4	(Bare foil data from Run 1168)	2 956
0	29 1	(Bare foil data from Run 1168)	1 678
0	89 4	End Reflector	4 260
0	74 9	(Bare foil data from Run 1173)	6 241
0	59 6	(Bare foil data from Run 1173)	5 374
0	44 4	(Bare foil data from Run 1173)	3 043
0	29 1	(Bare foil data from Run 1173)	2 022
0	89 4	End Reflector	3 848
0	74 9	(Bare foil data from Run 1174)	5 604
0	59 6	(Bare foil data from Run 1174)	4 466
0	44 4	(Bare foil data from Run 1174)	2 960
0	29 1	(Bare foil data from Run 1174)	1 786
93 2	151 1	Radial Reflector	4 932
107 7	151 1	(Bare foil data from Run 1168)	4 192
123 0	151 1	(Bare foil data from Run 1168)	3 064
138 2	151 1	(Bare foil data from Run 1168)	2 125
153 4	151 1	(Bare foil data from Run 1168)	1 220
93 2	151 1	Radial Reflector	5 664
107 7	151 1	(Bare foil data from Run 1173)	4 716
123 0	151 1	(Bare foil data from Run 1173)	3 466
138 2	151 1	(Bare foil data from Run 1173)	1.822
153 4	151 1	(Bare foil data from Run 1173)	0 972
93 2	151 1	Radial Reflector	5 129
107 7	151 1	(Bare foil data from Run 1174)	4 297
123 0	151 1	(Bare foil data from Run 1174)	3 167
138 2	151 1	(Bare foil data from Run 1174)	1 688
153 4	151 1	(Bare foil data from Run 1174)	1 242
23 6	151 1	Between Modules 5 & 6	5 145
30 5	151 1	Between Modules 5 & 6	7 184
38 1	151 1	Between Modules 5 & 6	7 354[1]
45 7	151 1	Between Modules 5 & 6	6 869
53 3	151 1	Between Modules 5 & 6	6 578
61 0	151 1	Between Modules 5 & 6	5 483[1]
68 6	151 1	Between Modules 5 & 6	5.506
76 2	151 1	Between Modules 5 & 6	5 387
83 8	151 1	Between Modules 5 & 6	4 591[1]
90 7	151 1	Between Modules 5 & 6	4 091

TABLE 5 11

(Continued)

Location Radial (cm)	Axial (cm)	Additional Explanation of Location	Thermal Neutron Flux n/cm^2-sec-watt x 10^{-6}
23 6	151 1	From Module 1 to Module 3	4 076
28 7	151 1	(Bare foil data from Run 1168)	6 274[1]
34 0	151 1	(Bare foil data from Run 1168)	7 130
39 4	151 1	(Bare foil data from Run 1168)	5 312[1]
44 4	151 1	(Bare foil data from Run 1168)	3 600
23 6	151 1	From Module 1 to Module 3	5 236
28 7	151 1	(Bare foil data from Run 1174)	6 501[1]
34 0	151 1	(Bare foil data from Run 1174)	6 778
39 4	151 1	(Bare foil data from Run 1174)	5 975[1]
44 4	151 1	(Bare foil data from Run 1174)	4 413
17 5	153 6	Inner Surface of CH, Module 1 at 90°	4 430
22.5	153 6	Outer Surface of CH, Module 1 at 90°	6 047
17 5	153 6	Module 7, 0° cw	3 164
17 5	153 6	Module 7, 90° cw	3 589
17 5	153 6	Module 7, 180° cw	3 533
17 5	153 6	Module 7, 270° cw	3 248
22 5	153 6	Module 7, 0° cw	3 361
22 5	153 6	Module 7, 90° cw	3 927
22 5	153 6	Module 7, 180° cw	4 134
22 5	153 6	Module 7, 270° cw	3 577
4 0	92 5	Module 1, 90° cw	3 611
4 0	151 5	Module 1, 90° cw	3 773
4 0	210 5	Module 1, 90° cw	3 475
15 4	92 5	Module 1, 90° cw	4 447
15 4	151 5	Module 1, 90° cw	4 763
15 4	210 5	Module 1, 90° cw	4 005
4 0	92 5	Module 3, 90° cw	2 461
4 0	151 5	Module 3, 90° cw	2 463
4 0	210 5	Module 3, 90° cw	2 323
15 4	92 5	Module 3, 90° cw	2 838
15 4	151 5	Module 3, 90° cw	3 138
15 4	210 5	Module 3, 90° cw	2 638
0	212 0	Separation Plane from Module 1 to Module 3	3 406
30 5	212 0	Separation Plane from Module 1 to Module 3	3 613
61 0	212 0	Separation Plane from Module 1 to Module 3	2 984
91 4	212 0	Separation Plane from Module 1 to Module 3	2 339
4 0	151 1	Module 1 at 90° cw	3 466[1]
15 4	151 1	(Bare foil data from Run 1174)	4 519[1]
4 0	151 1	Module 3 at 270° cw	2 640[1]
15 4	151 1	(Bare foil data from Run 1174)	3 652[1]

1 Thermal flux calculation based on extrapolated cadmium covered foil activity

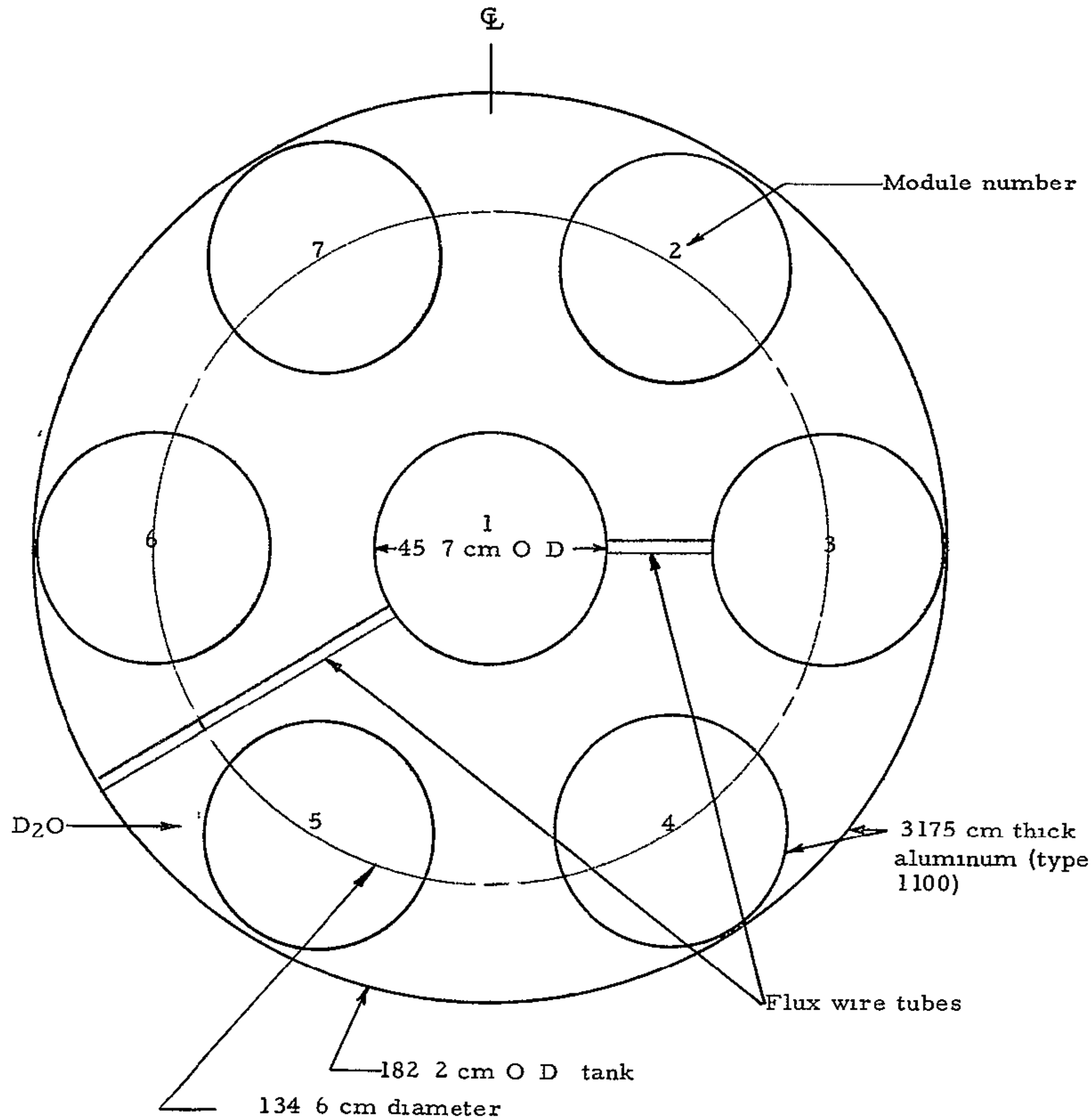

Figure 5.1 End view of seven module tank

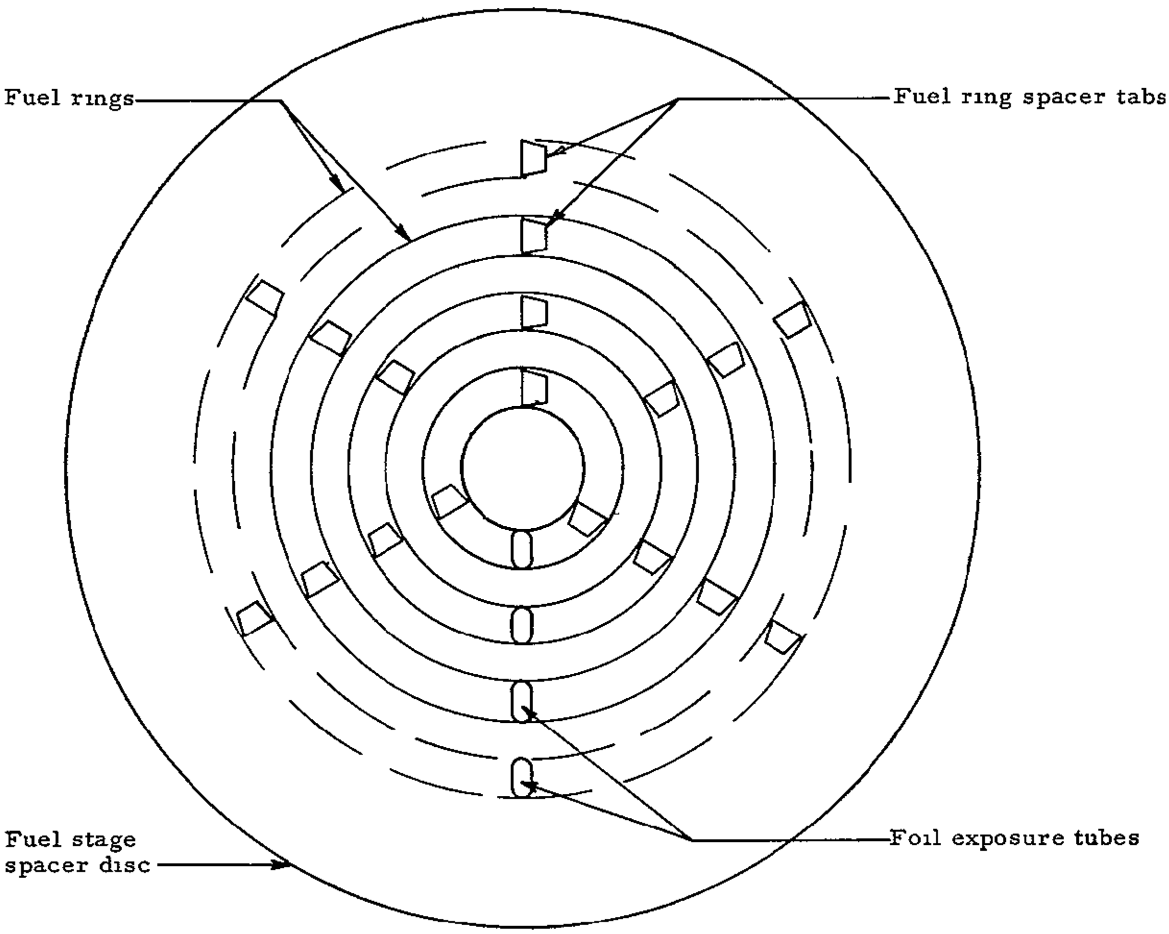

There are 6 fuel rings for the 55 radius ratio and 8 rings for the 72 radius ratio, and 4 rings for the 38 radius ratio

Figure 5 2 End view of fuel element

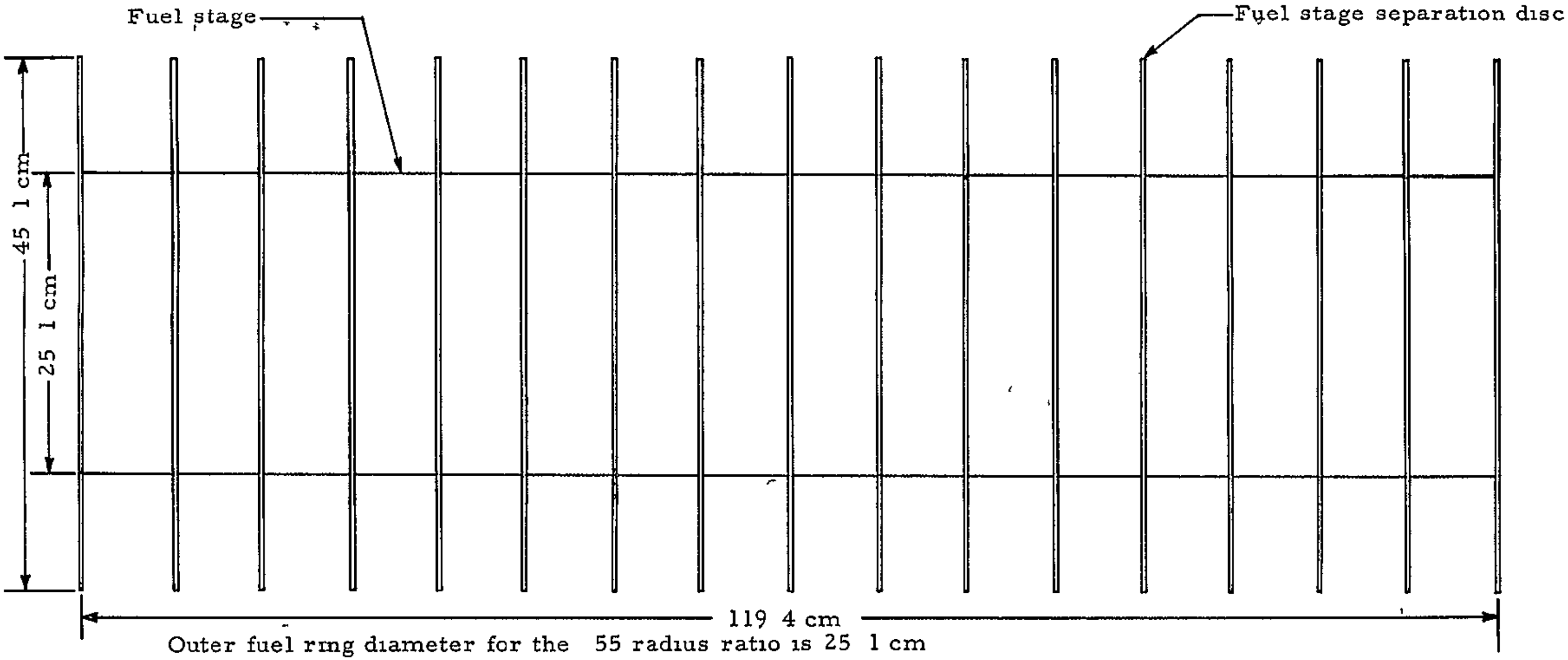

Outer fuel ring diameter for the 55 radius ratio is 25 1 cm

Outer fuel ring diameter for the 72 radius ratio is 32 8 cm

Figure 5 3 Side view of fuel element

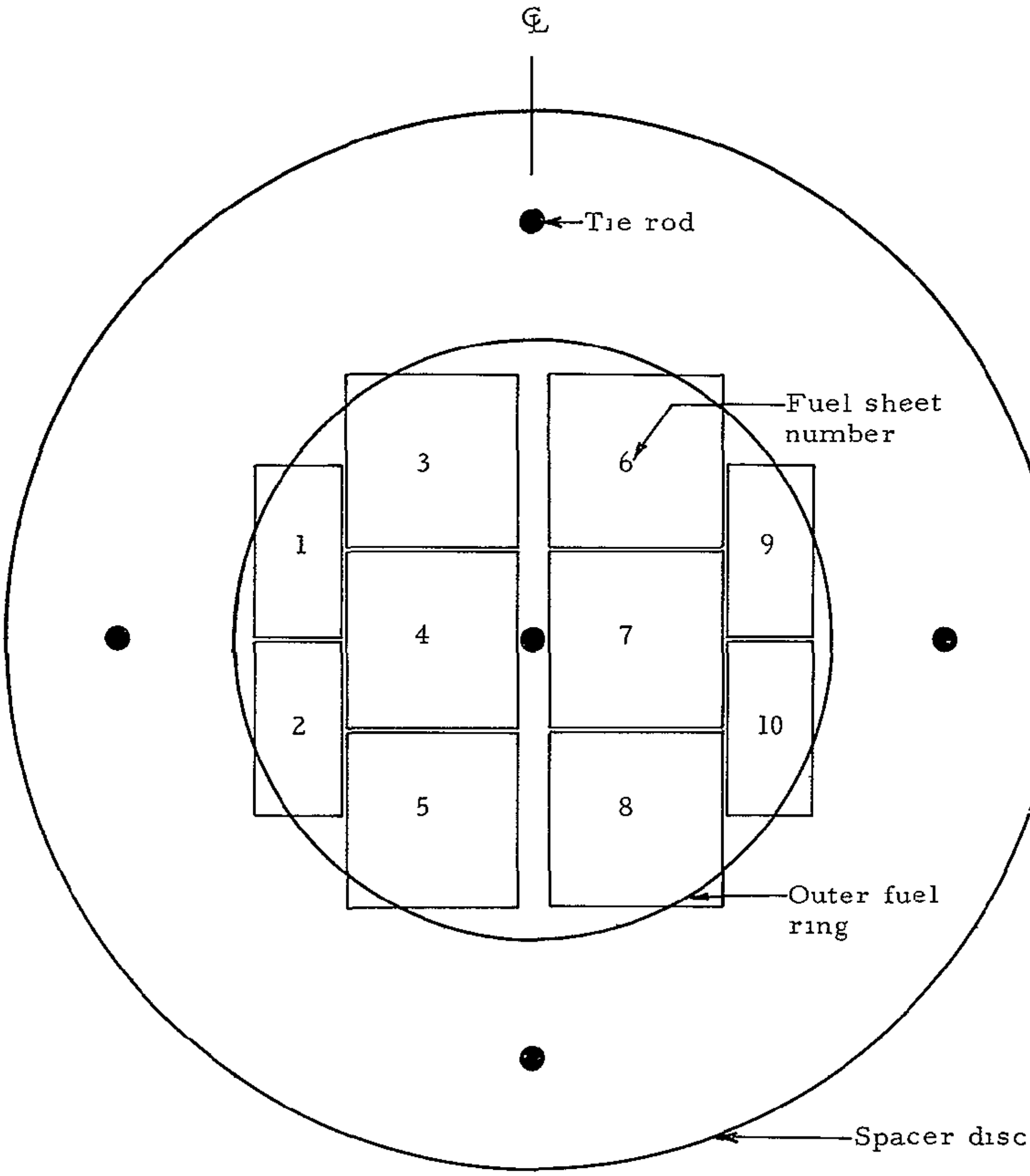

Figure 5 4 Layout of fuel sheets on fuel stage separation disc on the 7 module reactor fuel element with the 0 55 radius ratio loading

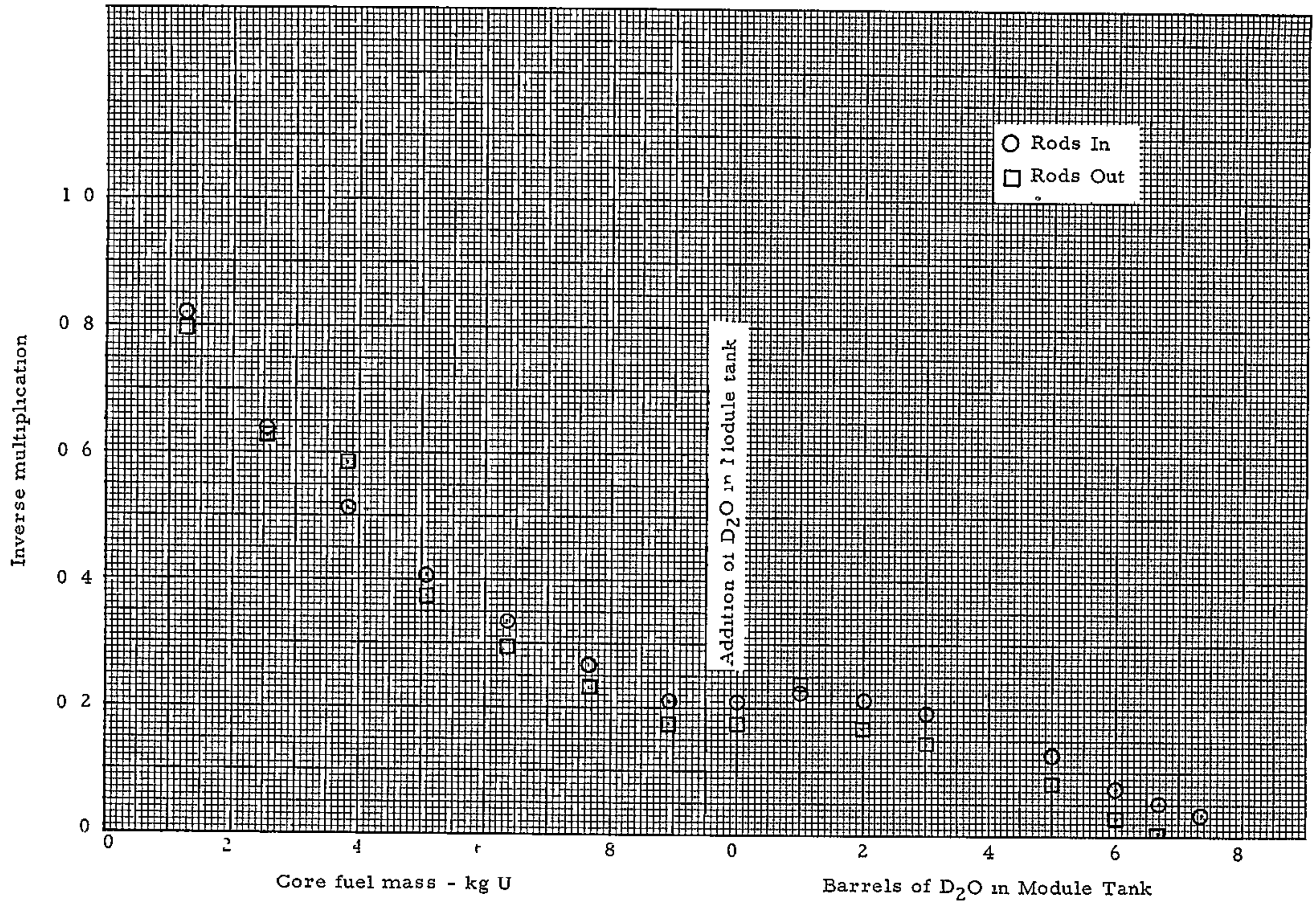

Figure 5.5 Inverse multiplication curve for seven module reactor

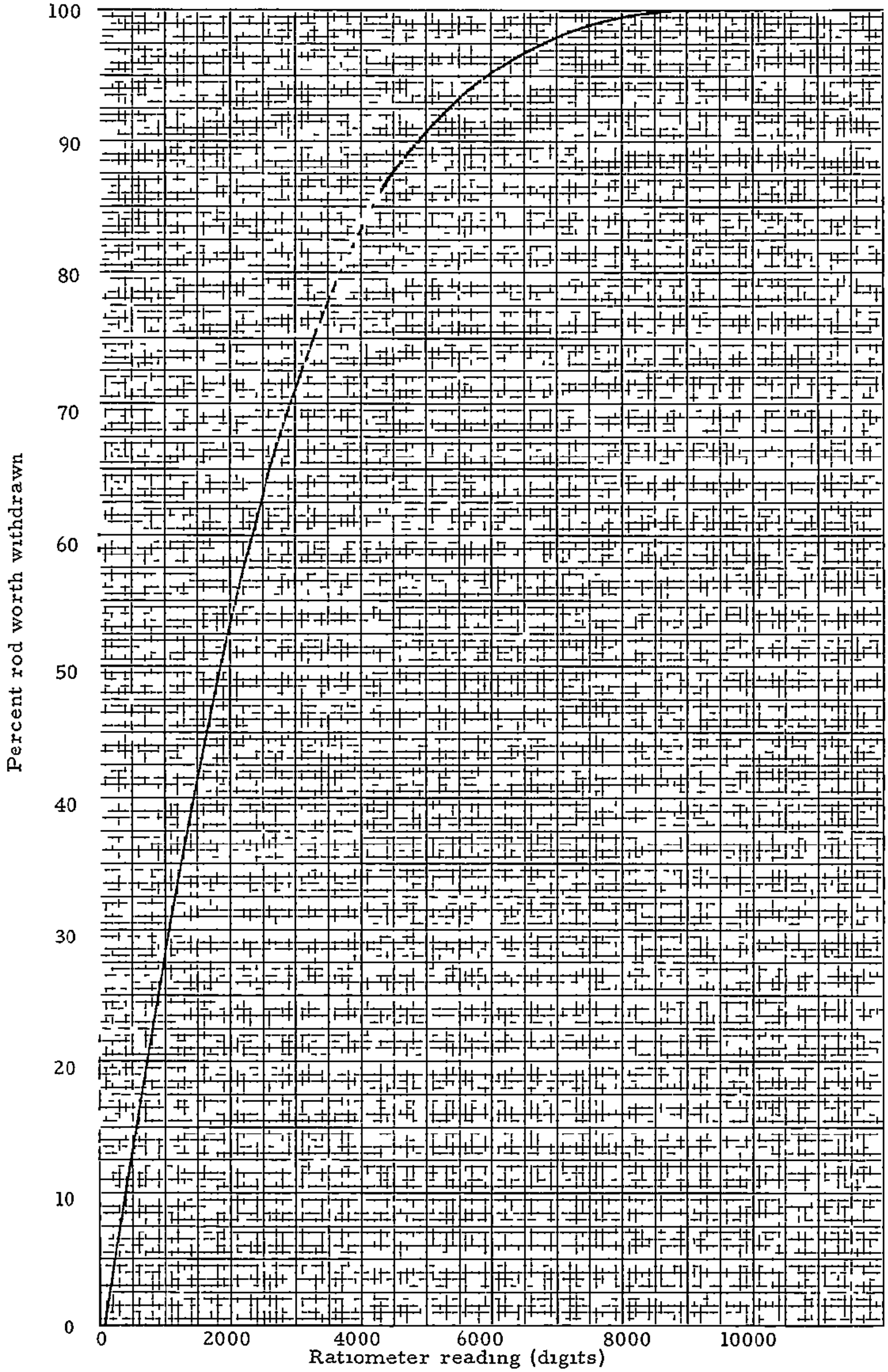

Figure 5 6 Control Rod Shape Curve - seven actuators (21 rods)

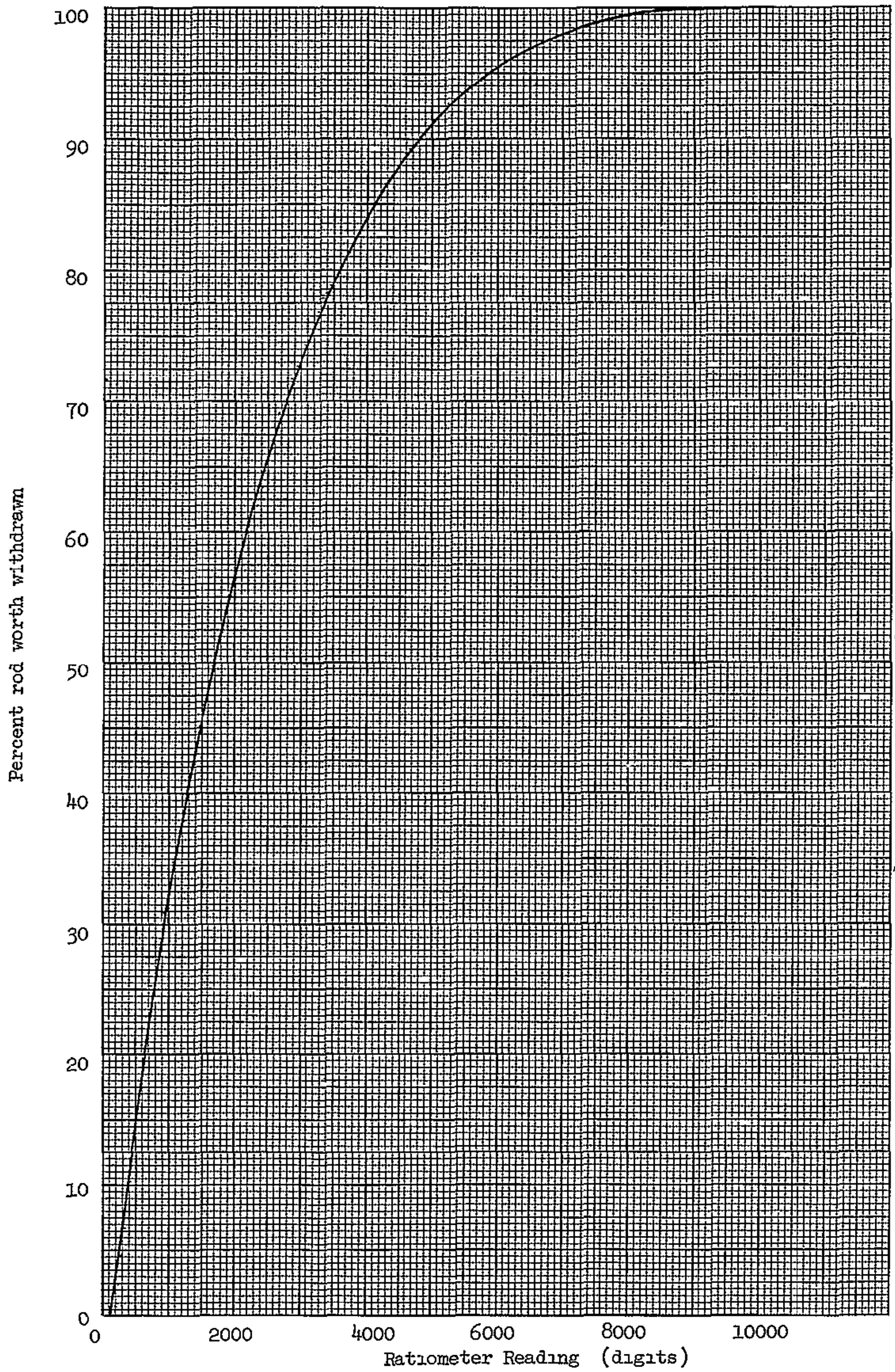

Figure 5.7 Control Rod Shape Curve - All Actuators (30 rods)

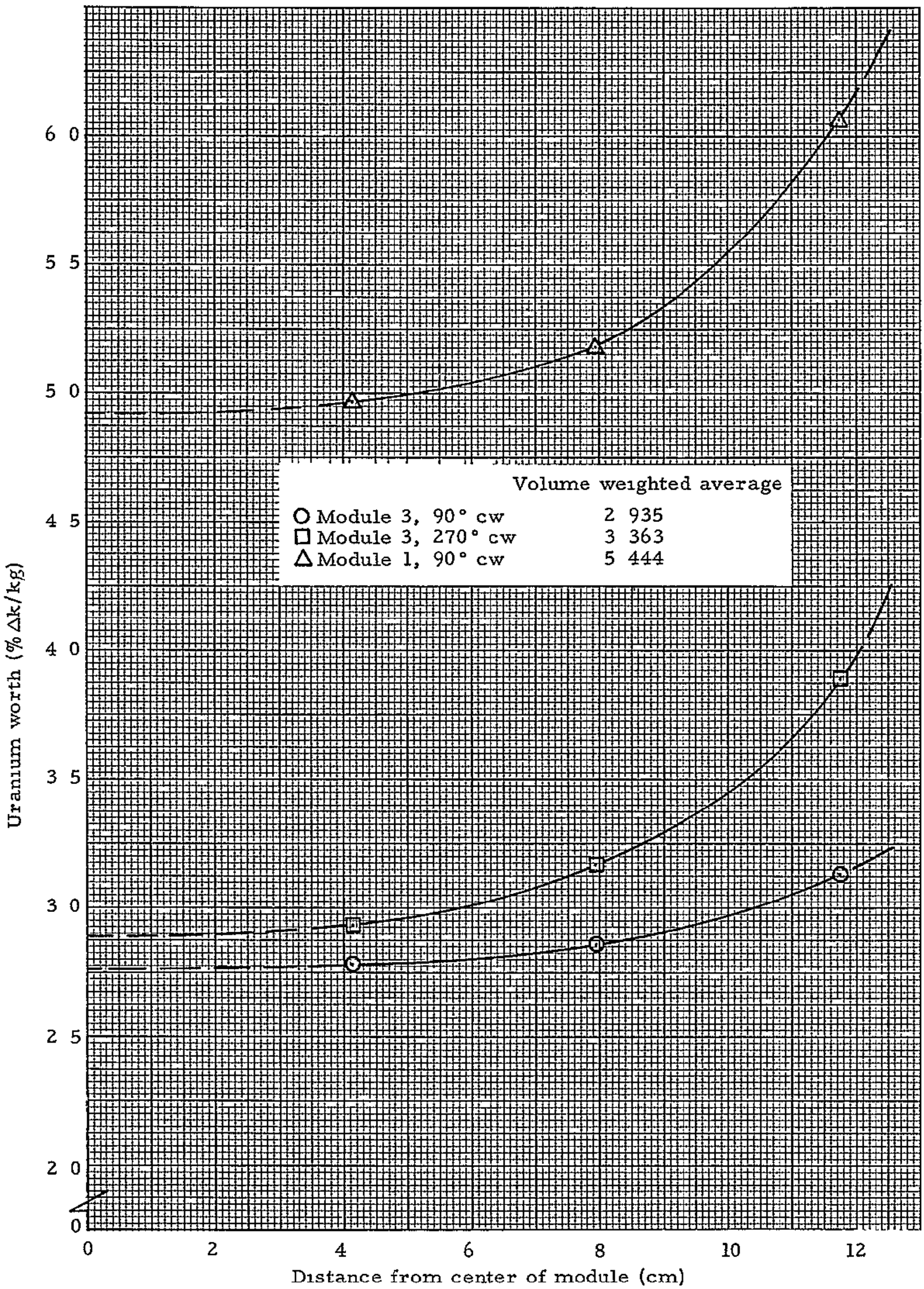

Figure 5 8 Uranium worth measurements - 7 module reactor with 0 55 fuel to module radius ratio

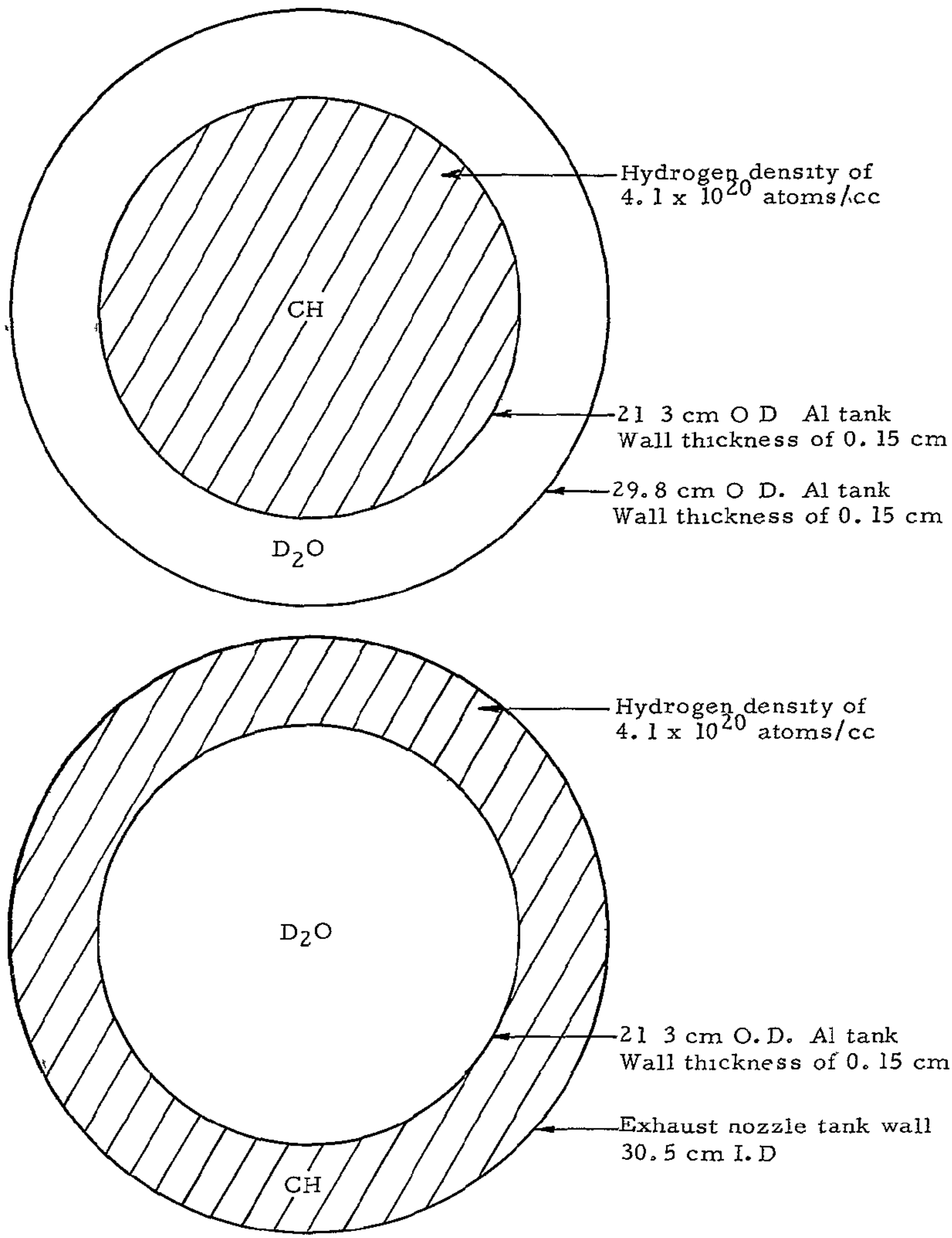

Figure 5 9 Exhaust nozzle configurations for the 7 module reactor

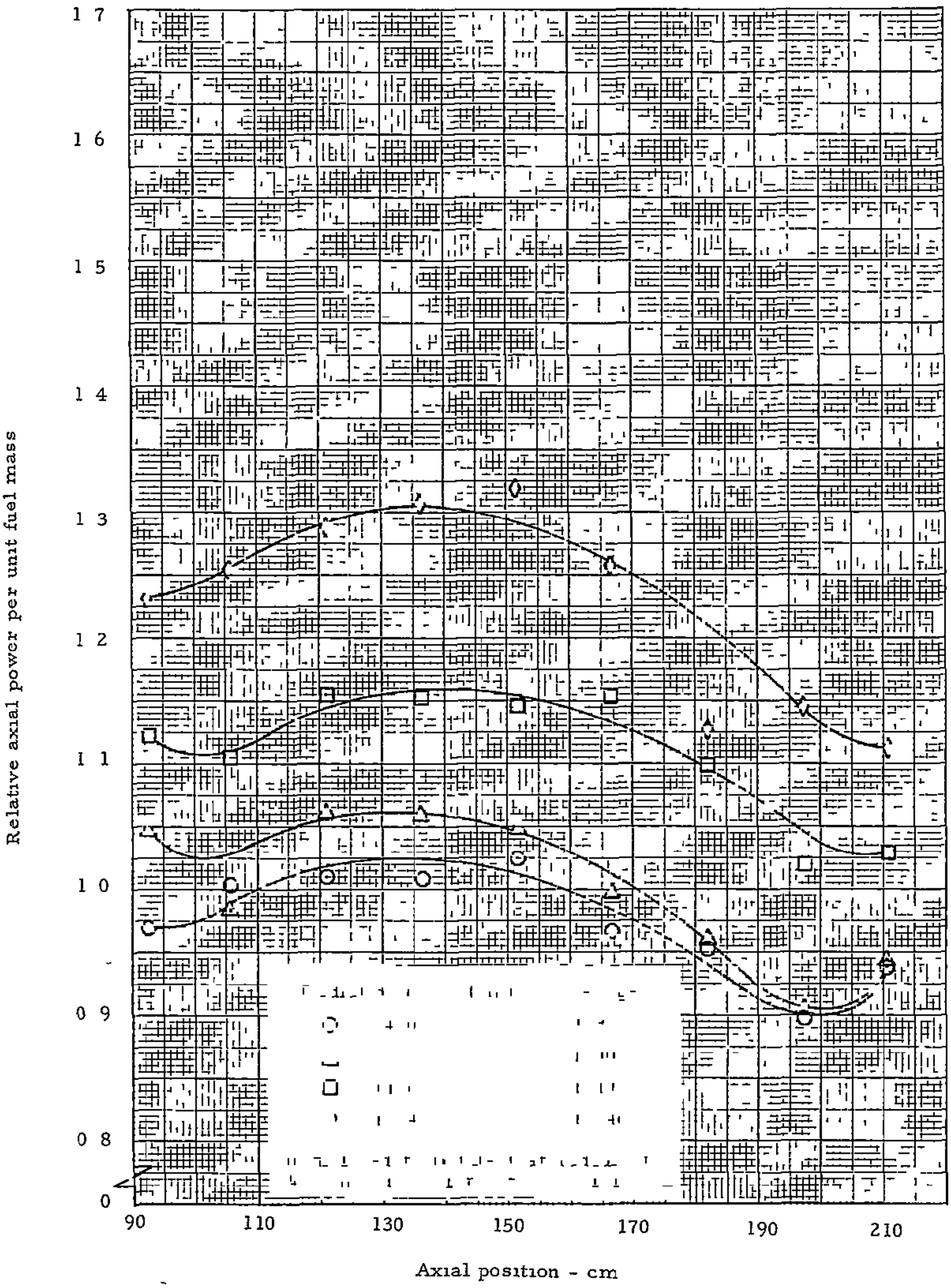

Figure 5.10 Relative axial power distribution in module 1, 0° at the core centerline, 7 module reactor with 0 55 fuel to module radius ratio

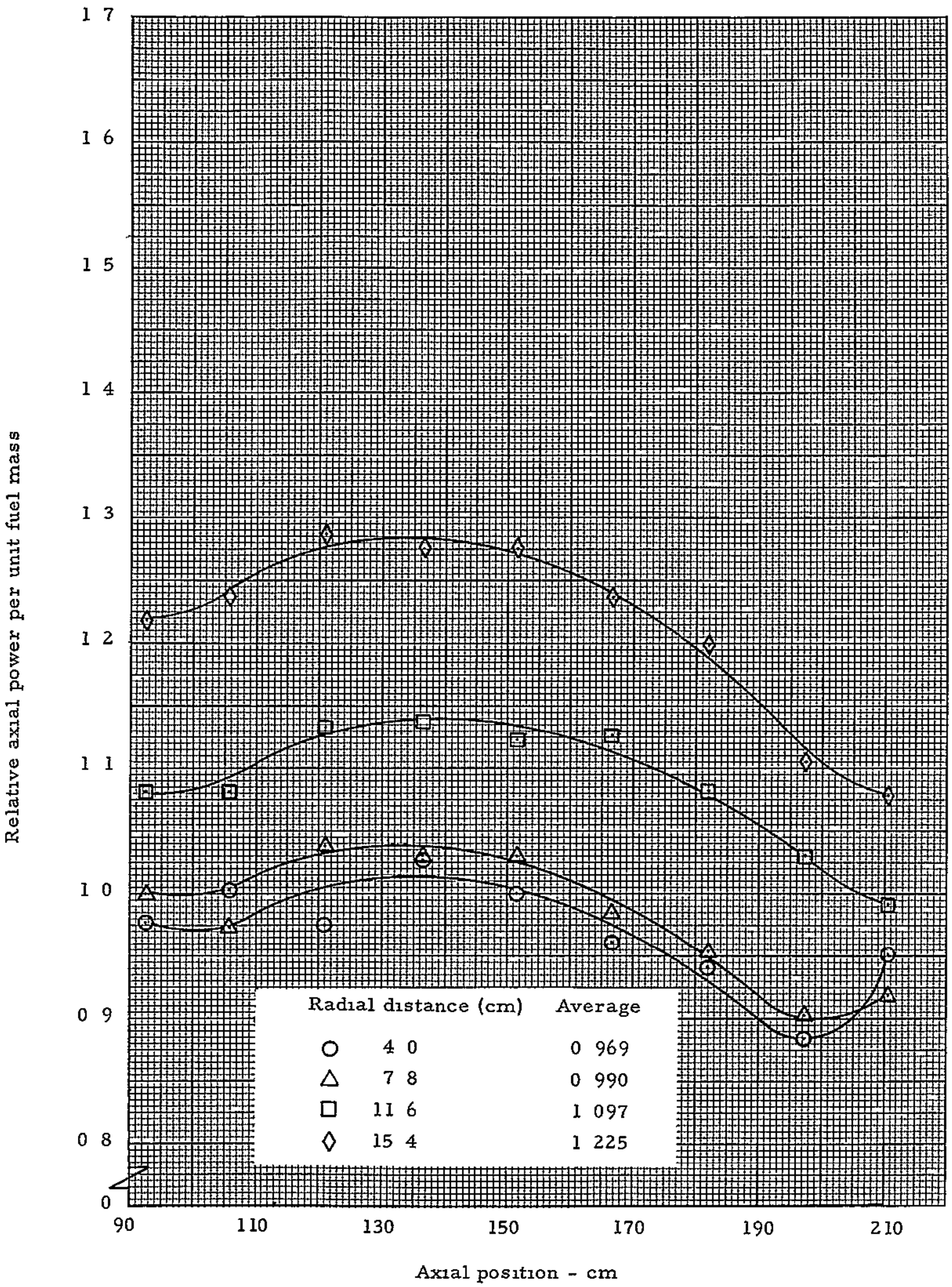

Figure 5 11 Relative axial power distribution in module 1, 90° at the core centerline, 7 module reactor with 0 55 fuel to module radius ratio

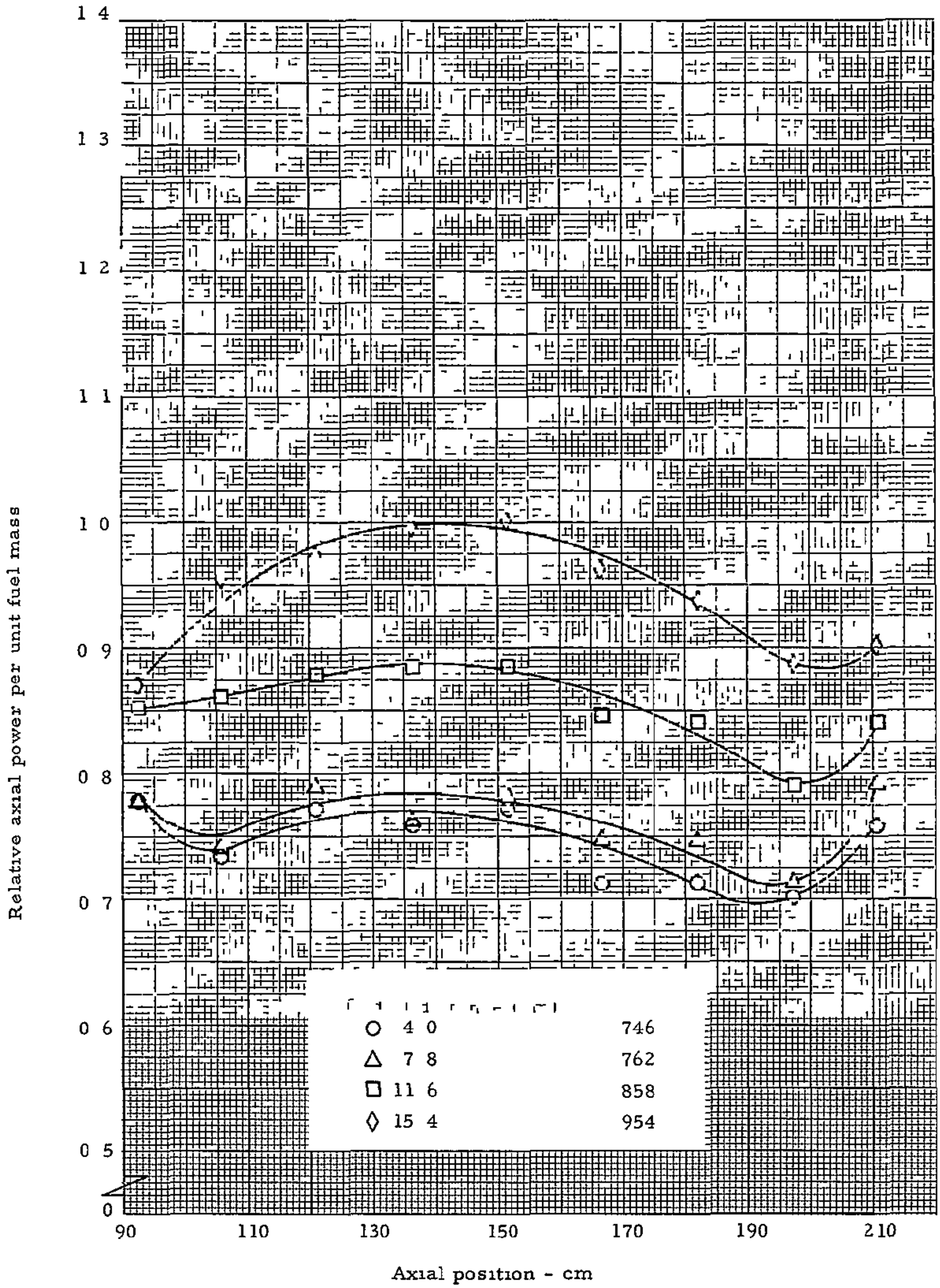

Figure 5 12 Relative axial power distribution in module 3, 0° at the core centerline, 7 module reactor with 0.55 fuel to module radius ratio

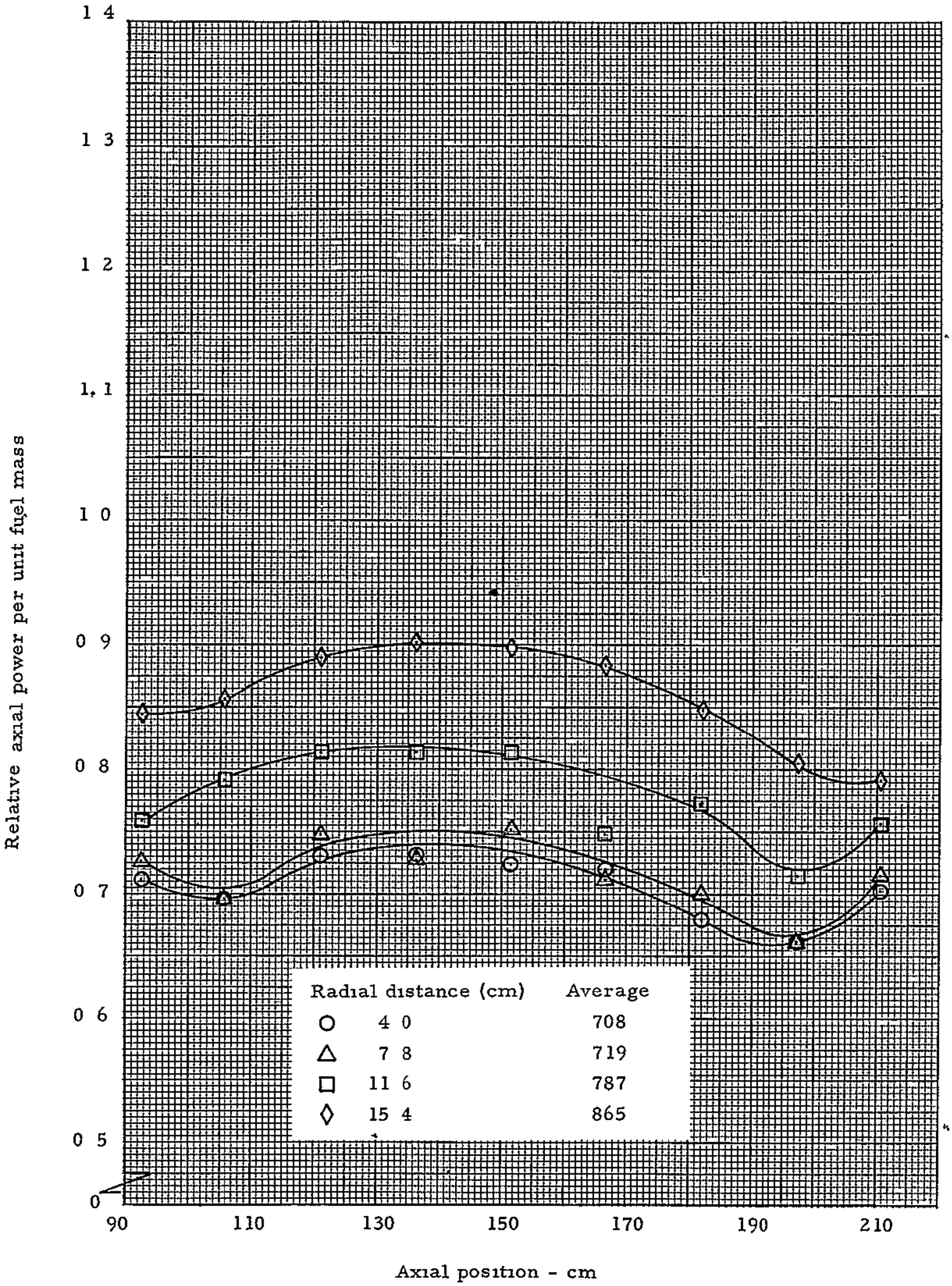

Figure 5 13 Relative axial power distribution in module 3, 90° at the core centerline, 7 module reactor with 0.55 fuel to module radius ratio

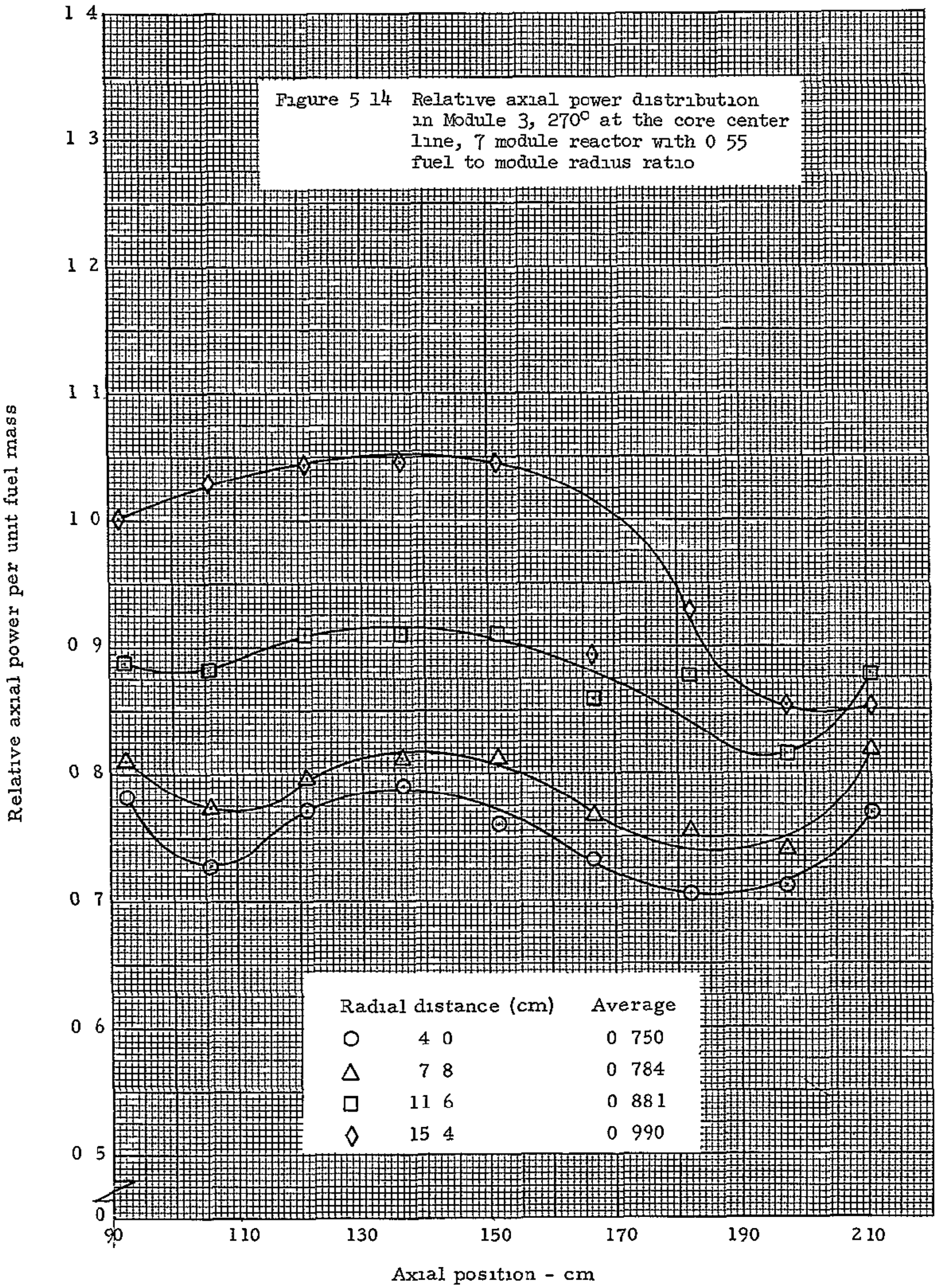

Figure 5.14 Relative axial power distribution in module 3, 270° at the core center line, 7 module reactor with 0 55 fuel to module radius ratio

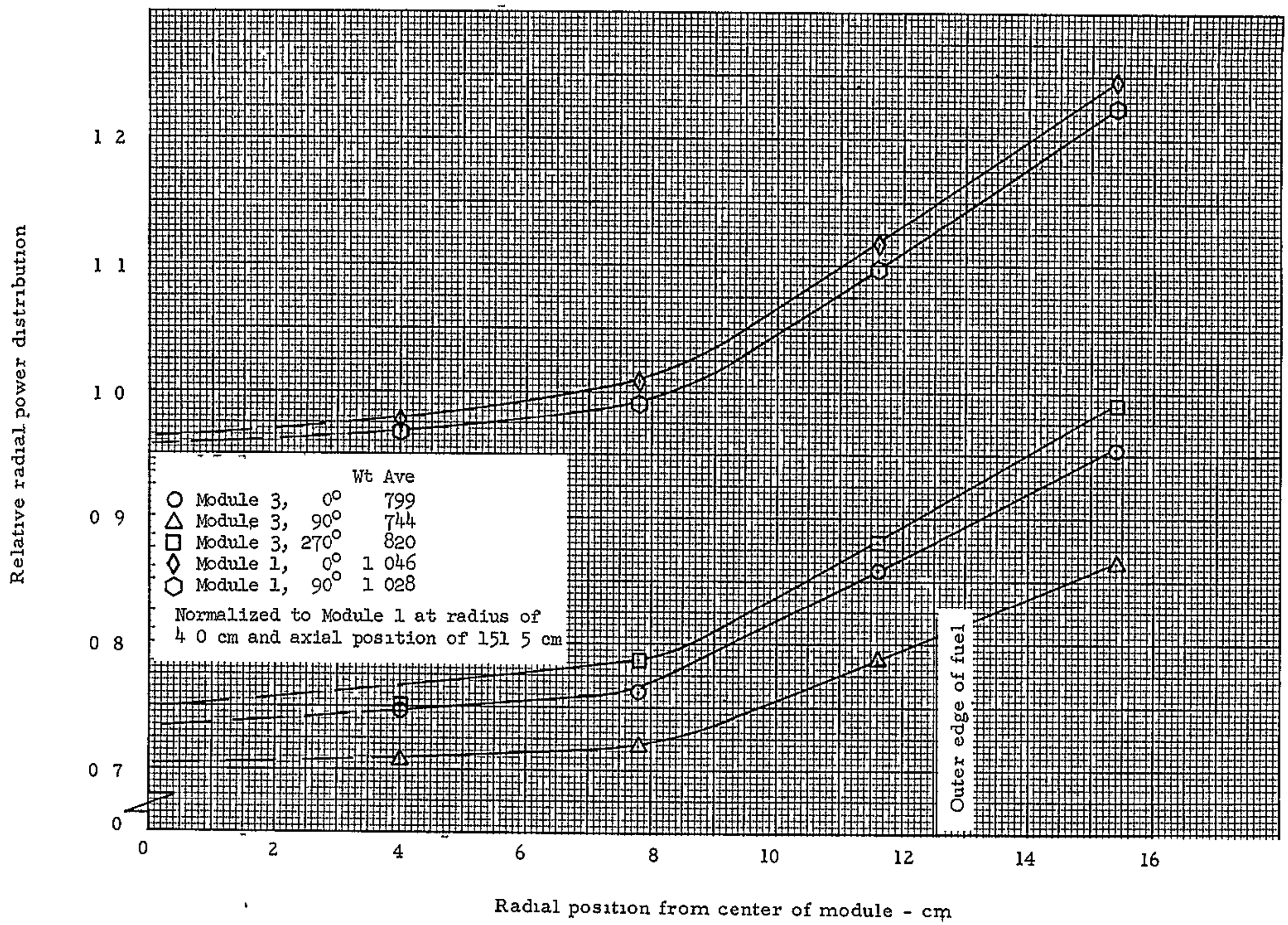

Figure 5.15 Relative radial power distribution in modules 1 and 3 based on axial average power distributions, 7 module reactor with 0 55 fuel to module radius ratio

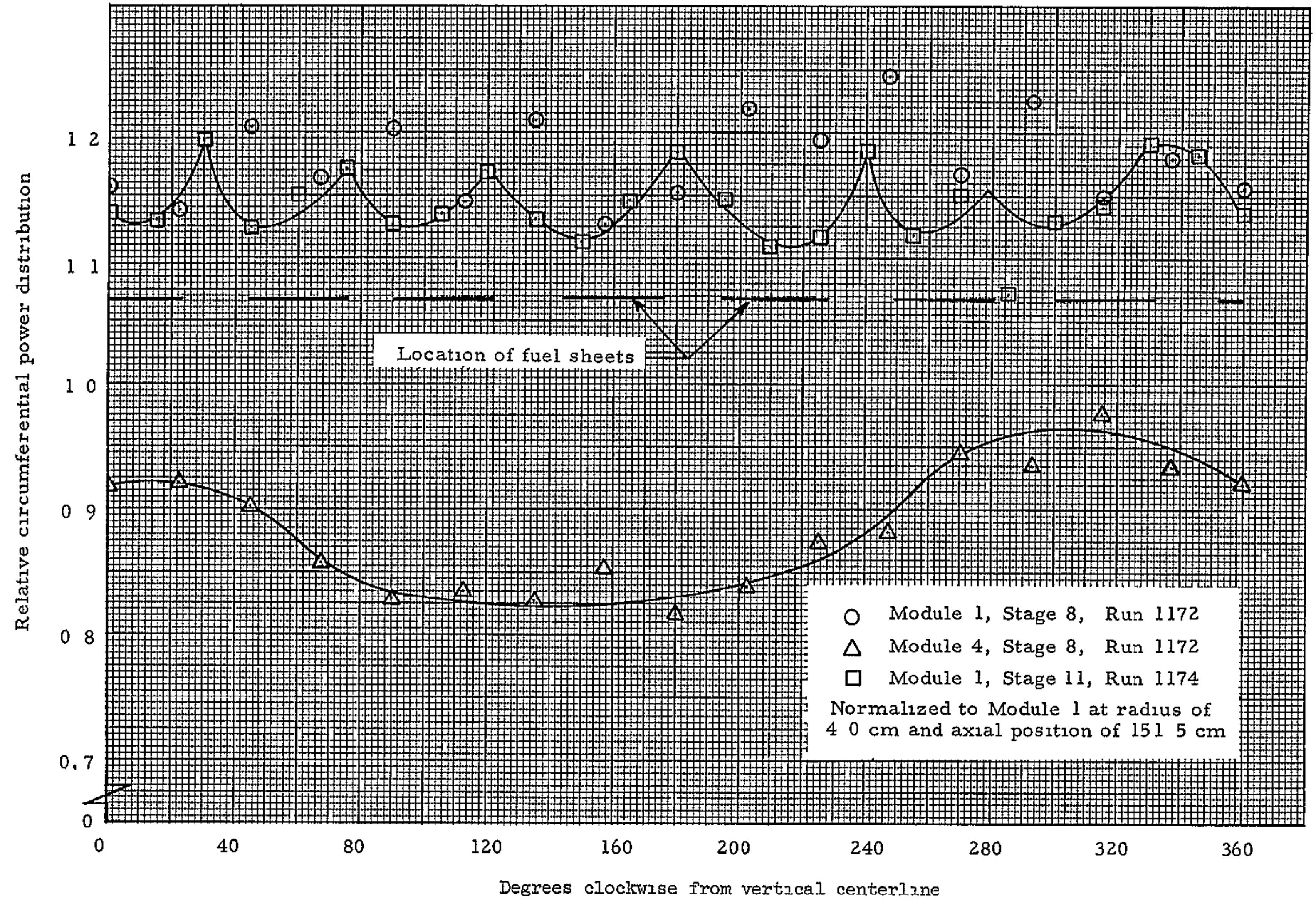

Figure 5 16 Circumferential power distribution on outside fuel ring, 0 55 radius ratio, 7 module configuration

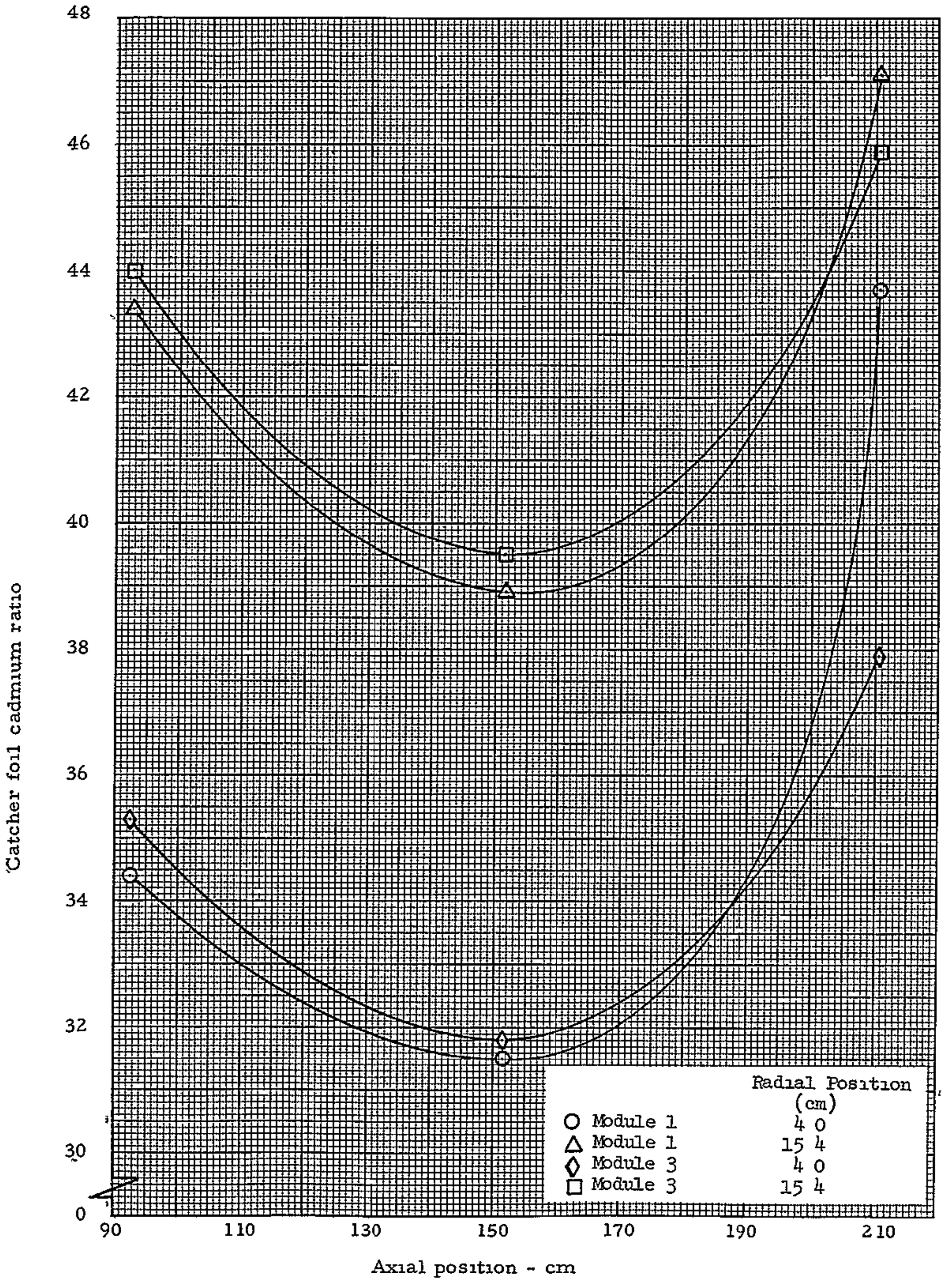

Figure 5.17 Axial distribution of catcher foil cadmium ratios in modules 1 and 3, 7 module reactor with 0 55 fuel to module radius ratio

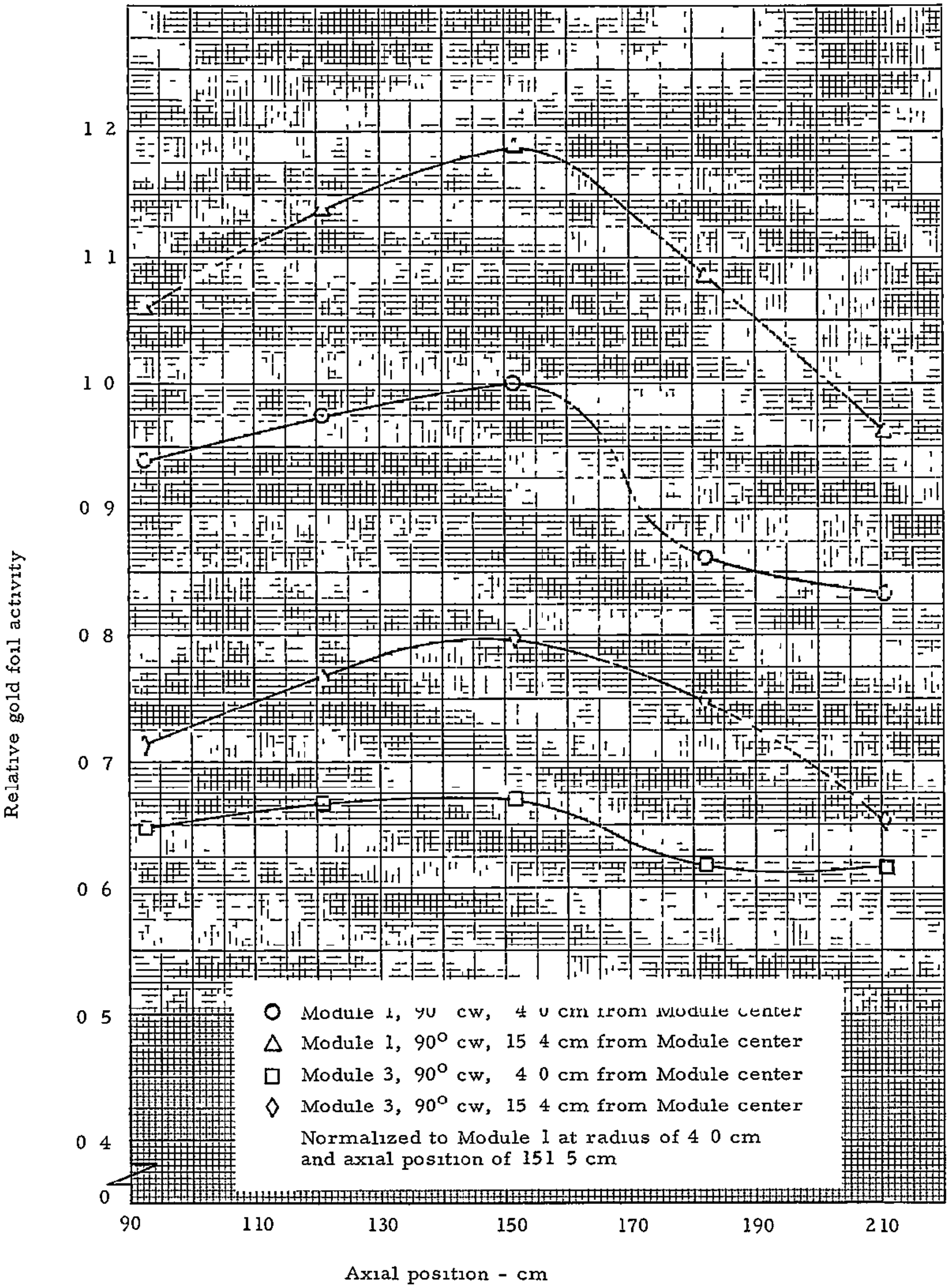

Figure 5 18 Relative bare gold foil activity axial distribution in modules 1 and 3, 7 module reactor with 0 55 fuel to module radius ratio

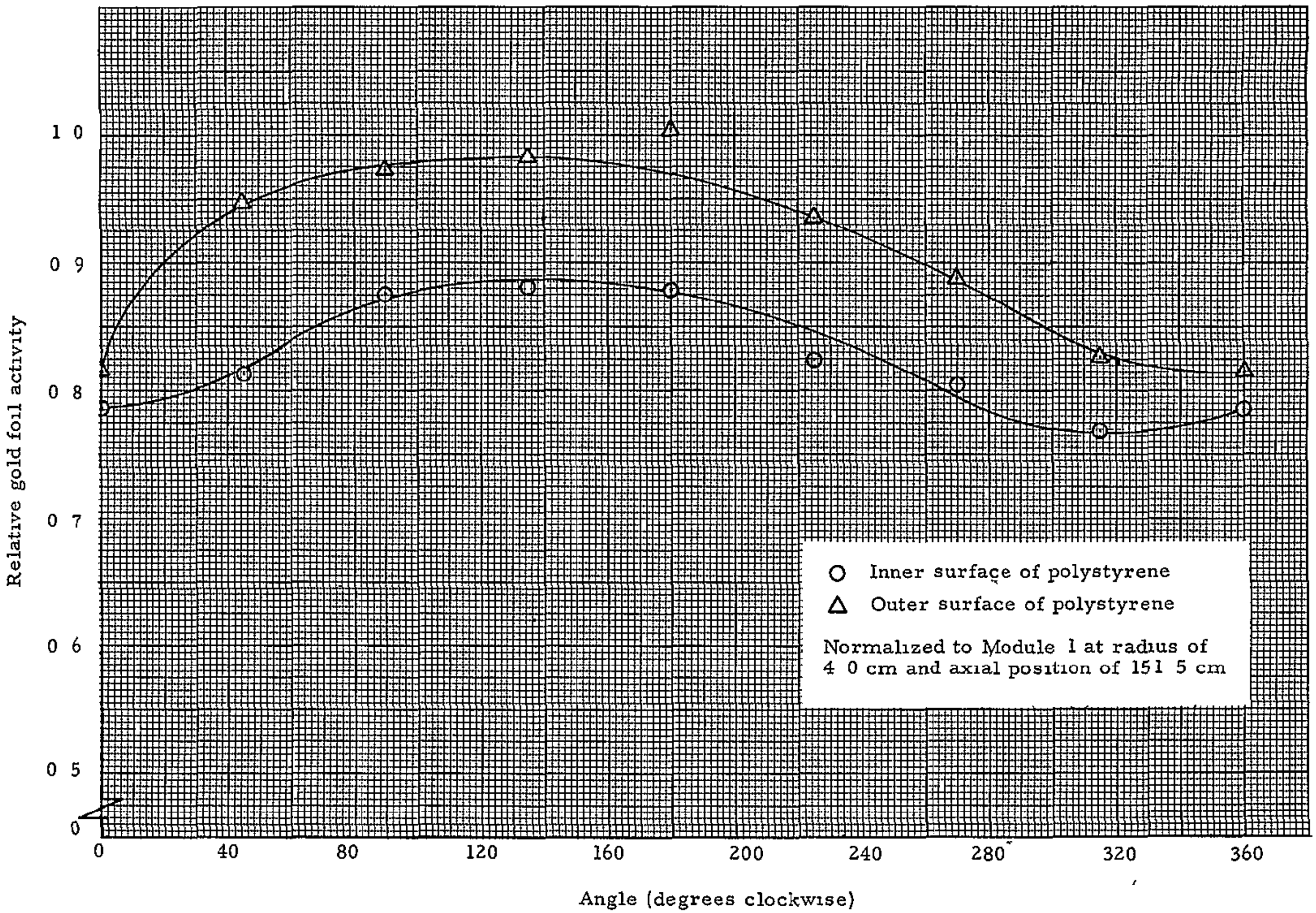

Figure 5 19 Relative bare gold foil activity circumferential distribution on inner and outer surfaces of the polystyrene in module 7, 7 module reactor with 0 55 fuel to module radius ratio

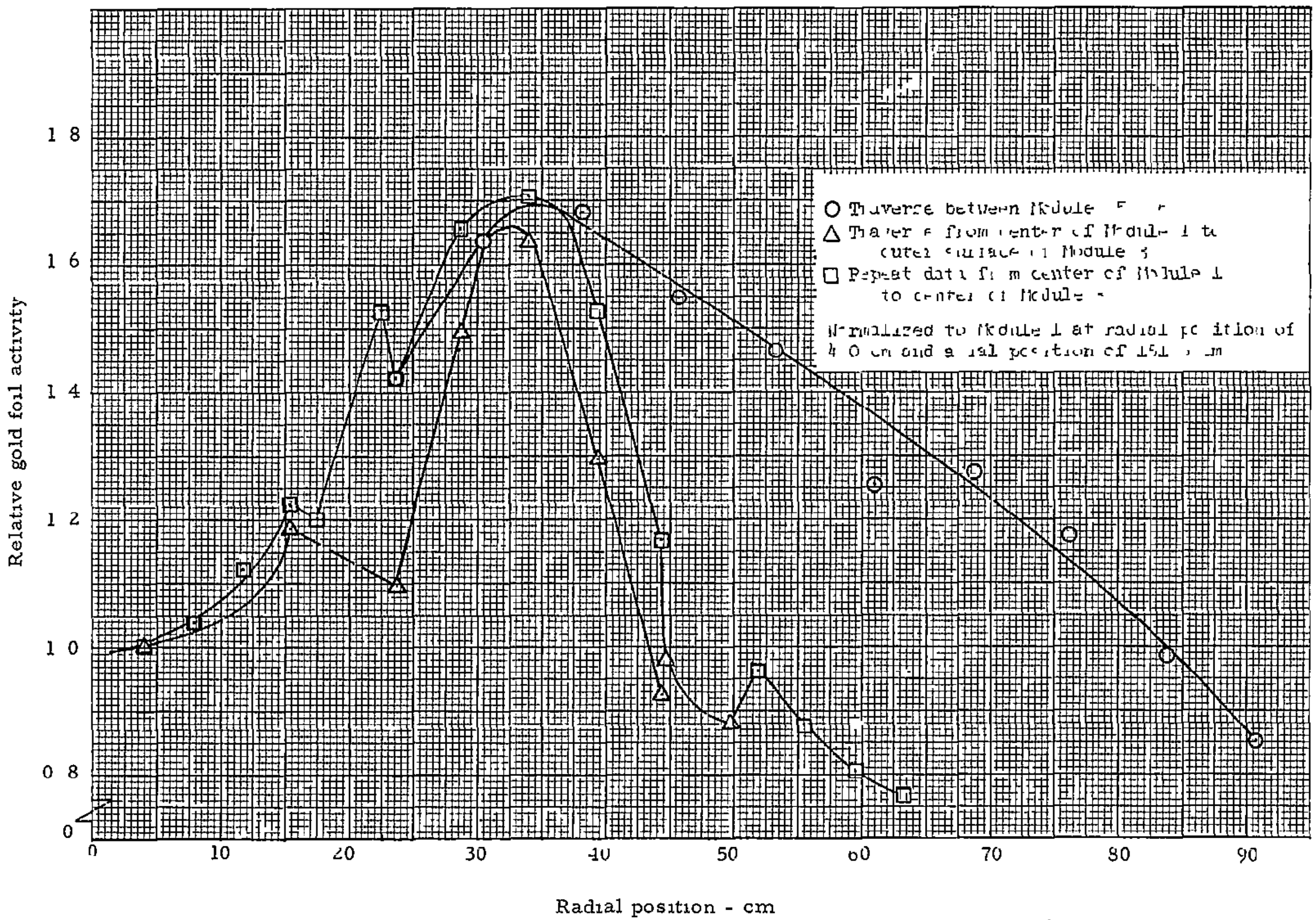

Figure 5.20 Relative bare gold foil activity distribution in the regions between modules

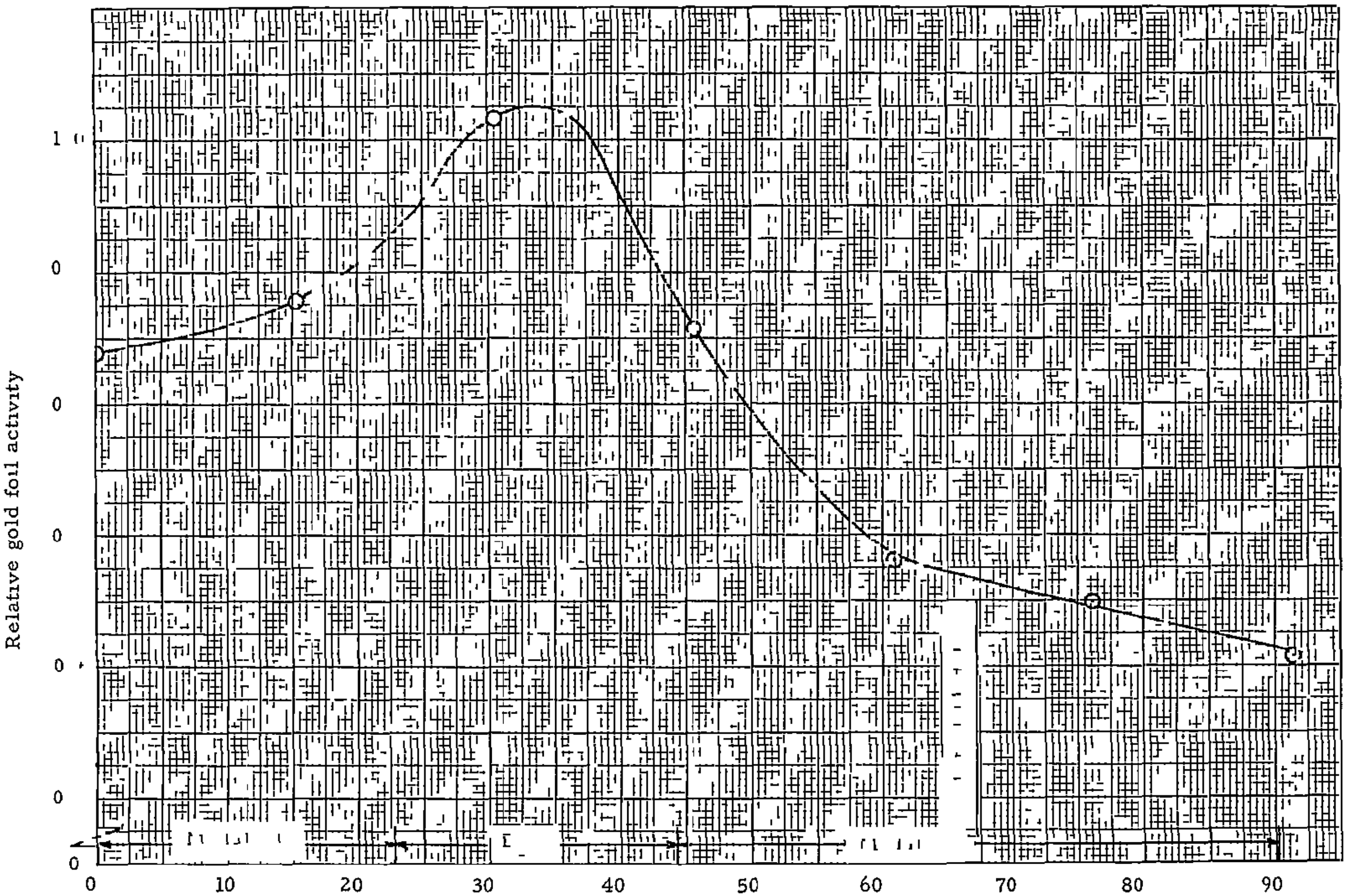

Figure 5 21 Relative bare gold foil activity distribution across the end of the core at the separation plane from the center of module 1 across module 3, 7 module reactor with 0.55 fuel to module radius ratio

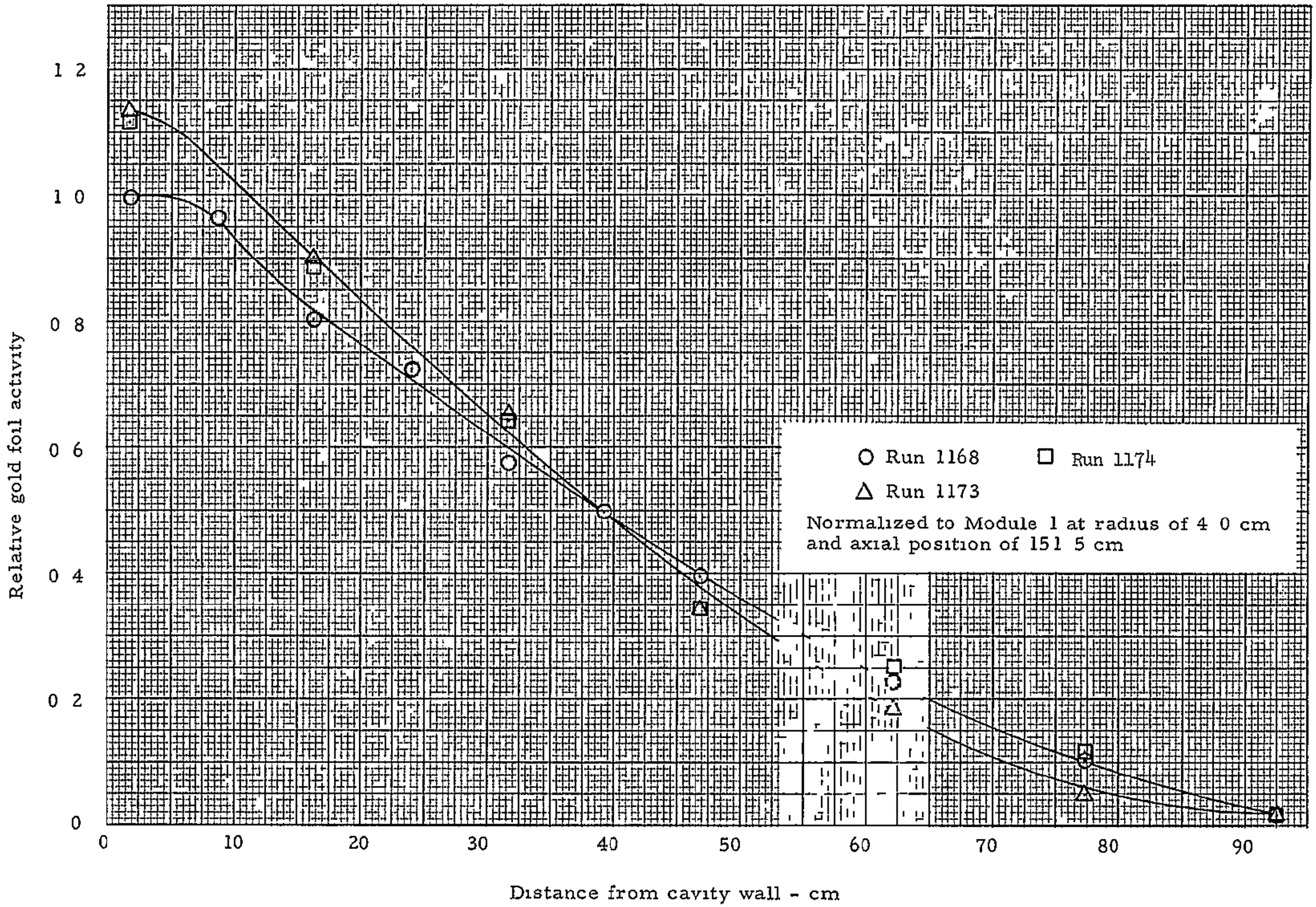

Figure 5 22 Relative bare gold foil activity distribution in the radial reflector, 7 module reactor with 0 55 fuel to module radius ratio

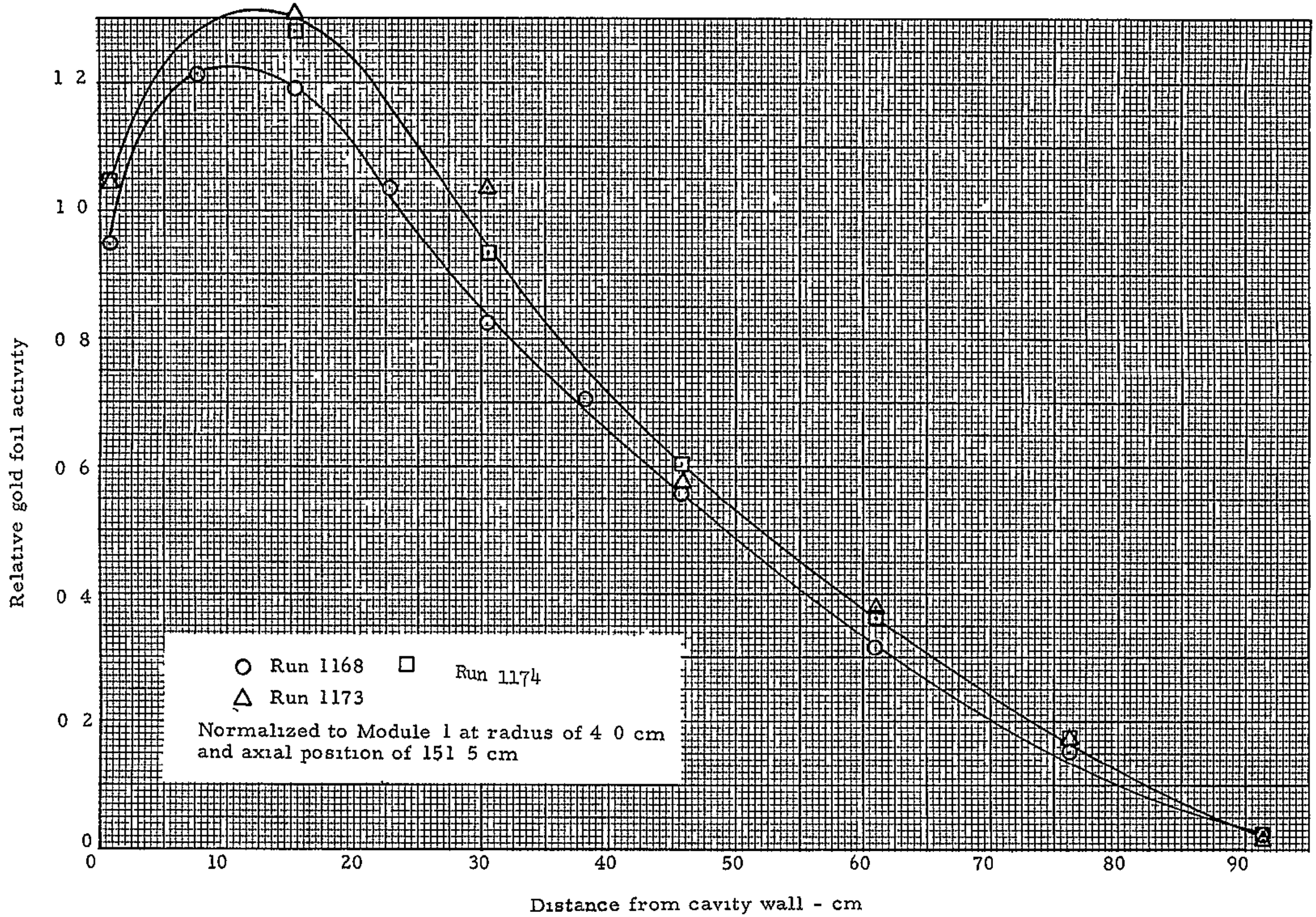

Figure 5.23 Relative bare gold foil activity distribution in the end reflector, 7 module reactor with 0 55 fuel to module radius ratio

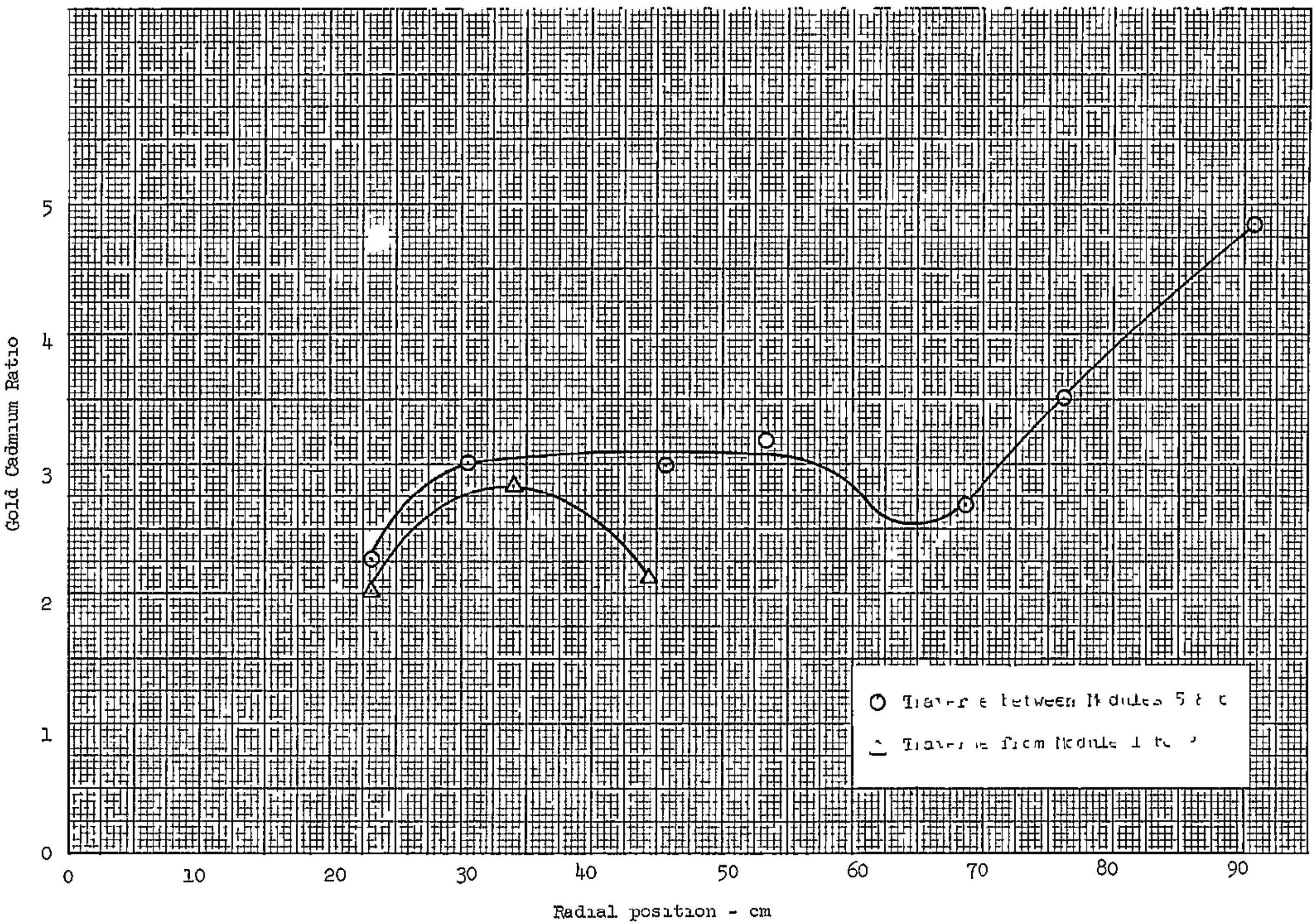

Figure 5 24 Infinitely dilute gold cadmium ratio in region between fuel modules

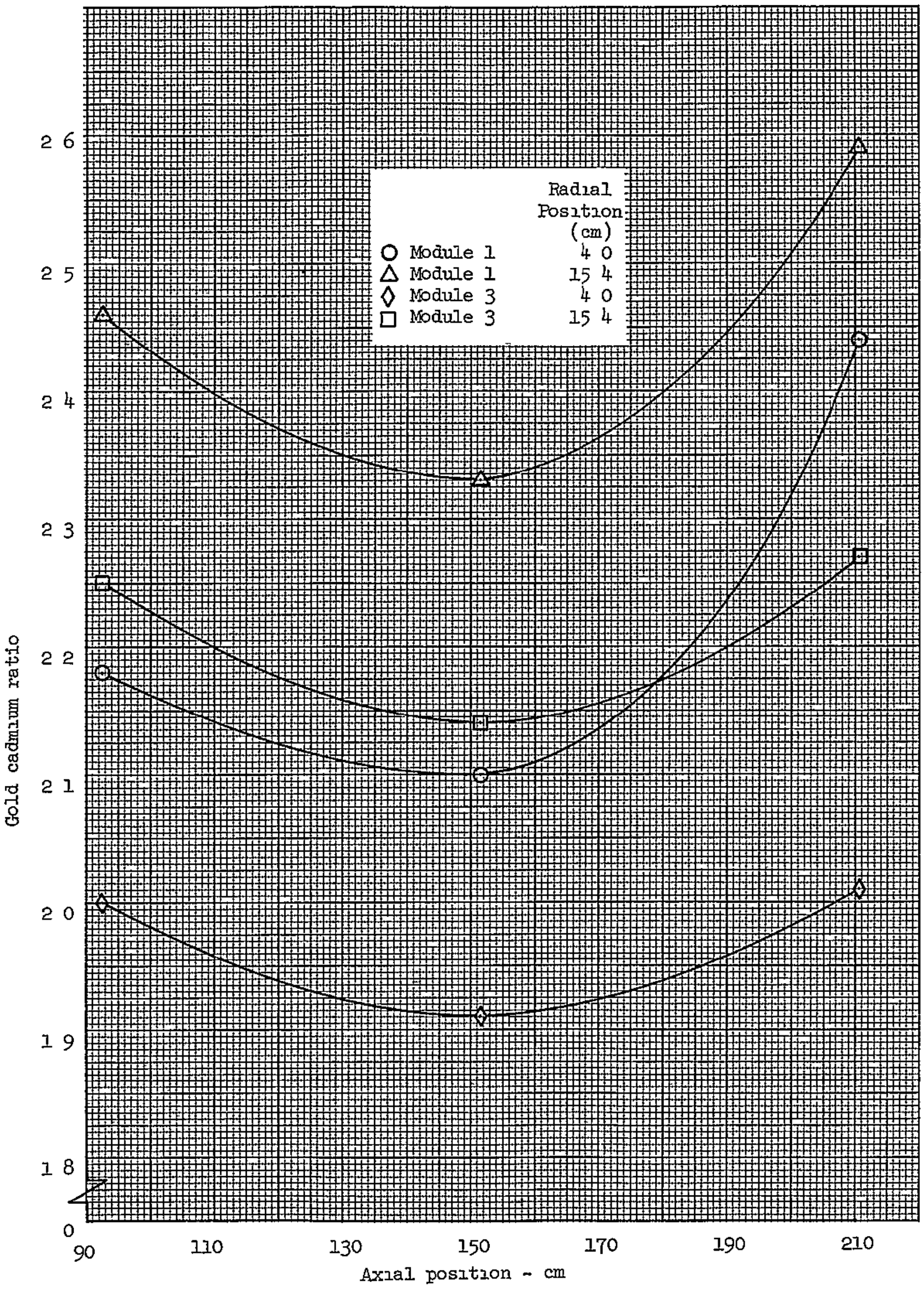

Figure 5 25 Axial distribution of gold foil cadmium ratios in modules 1 and 3 at an angle of 90° cw from core centerline

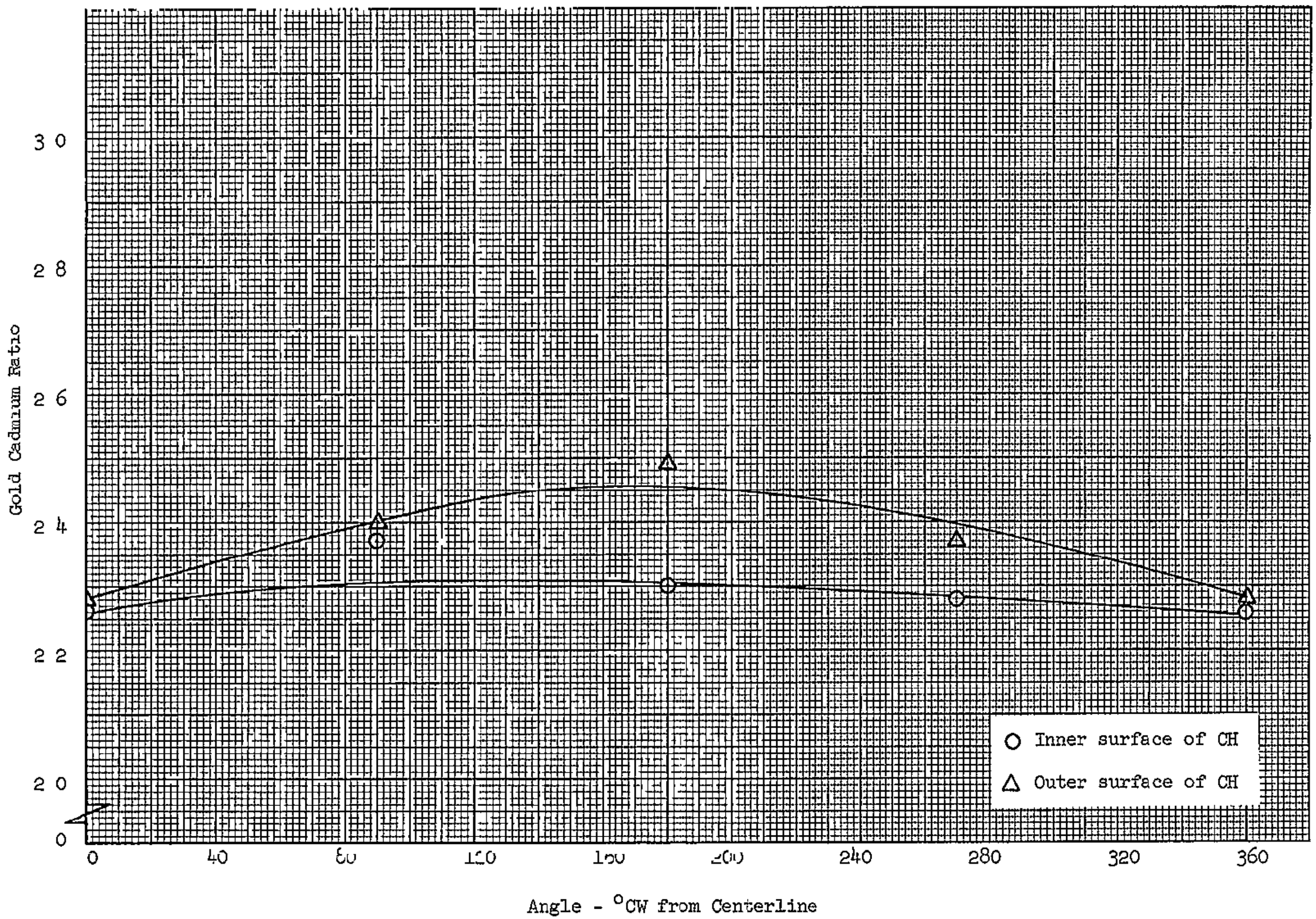

Figure 5.26 Circumferential distribution of gold foil cadmium ratio on inner and outer surface of CH in module 7

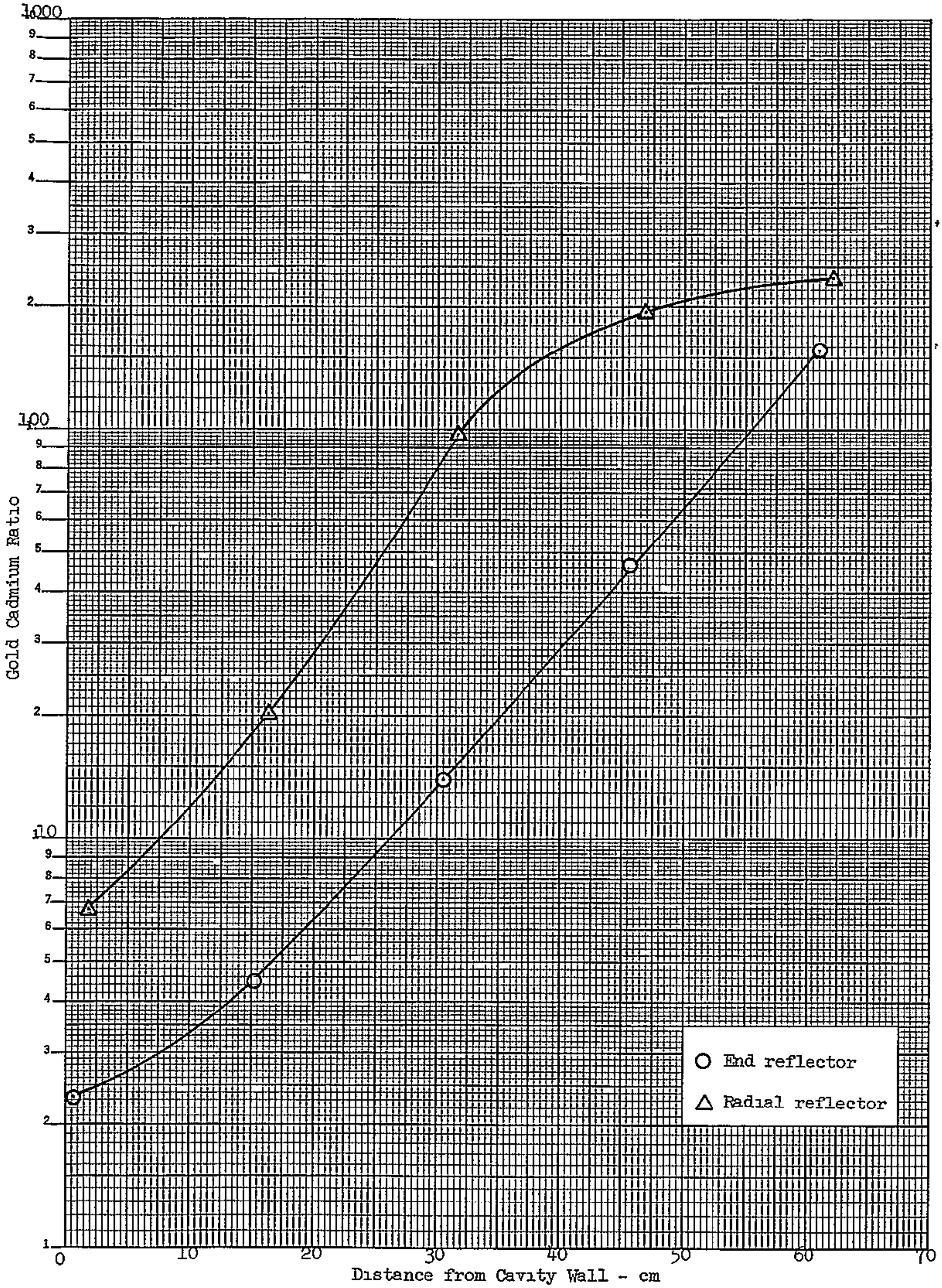

Figure 5.27 Infinitely dilute gold cadmium ratios along center-lines of end and radial reflectors

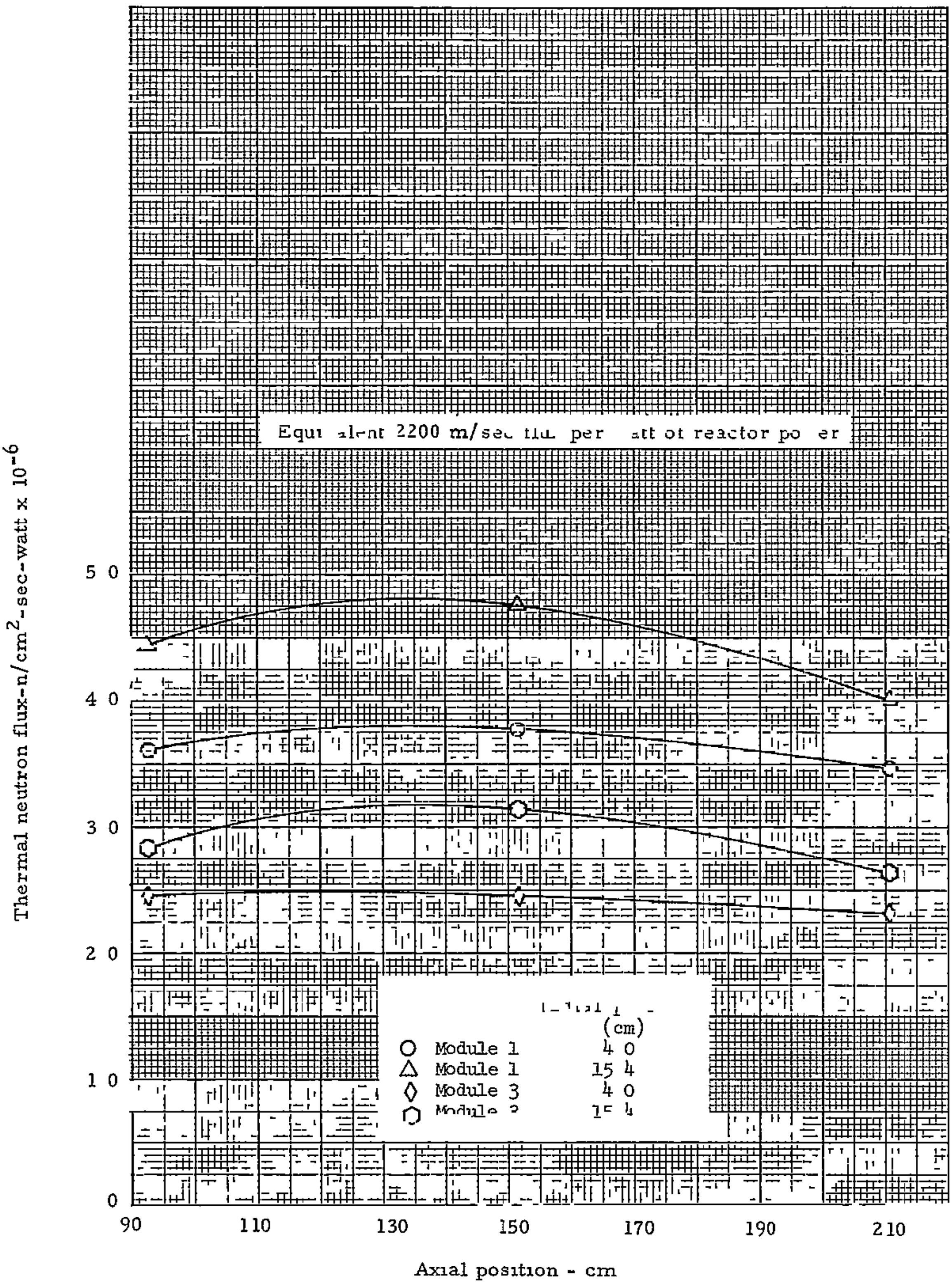

Figure 5 28 Axial distribution of thermal neutron flux in modules 1 and 3 at 90° clockwise from core vertical centerline

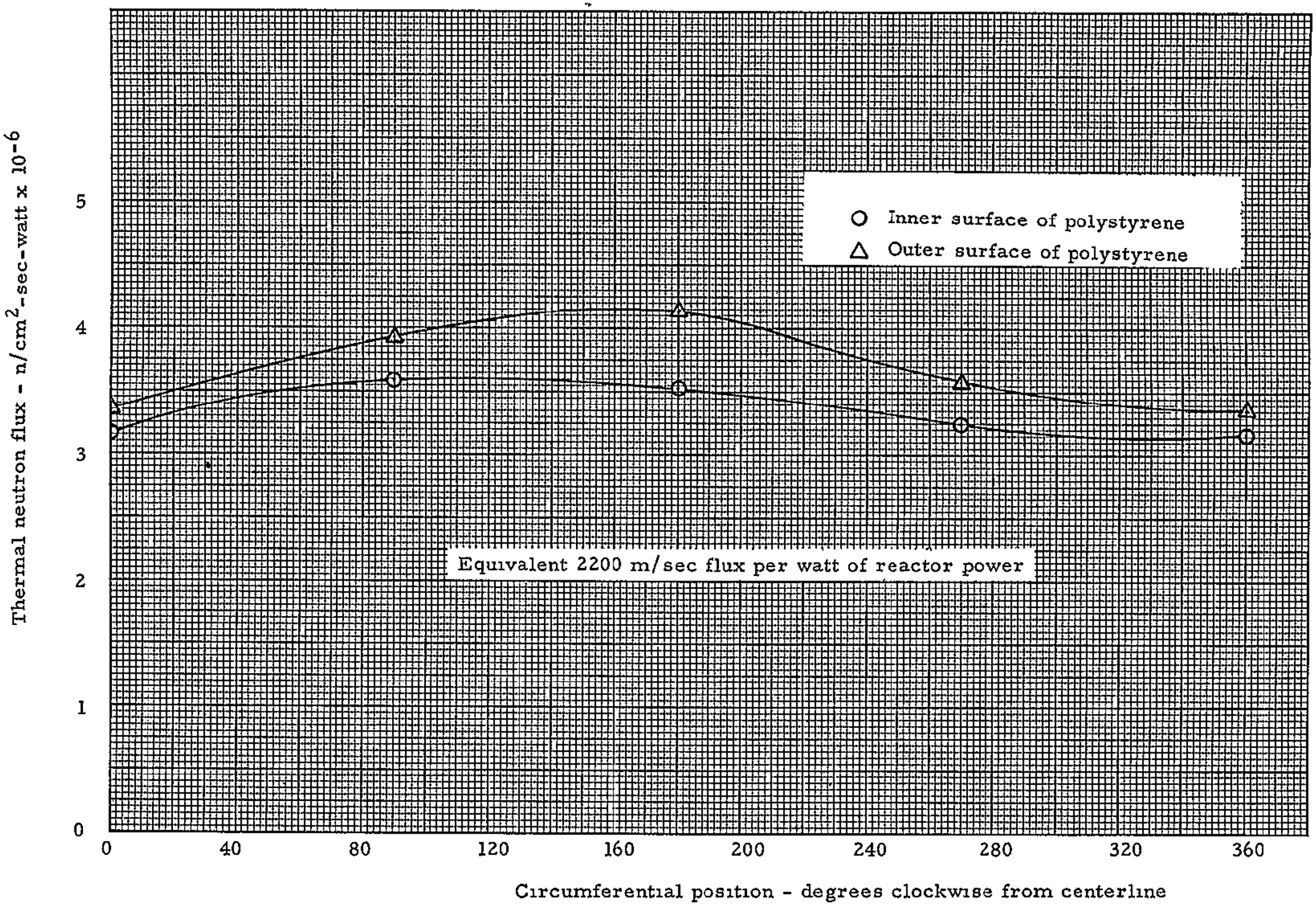

Figure 5 29 Circumferential distribution of thermal neutron flux on the inner and outer surfaces of the polystyrene in module 7

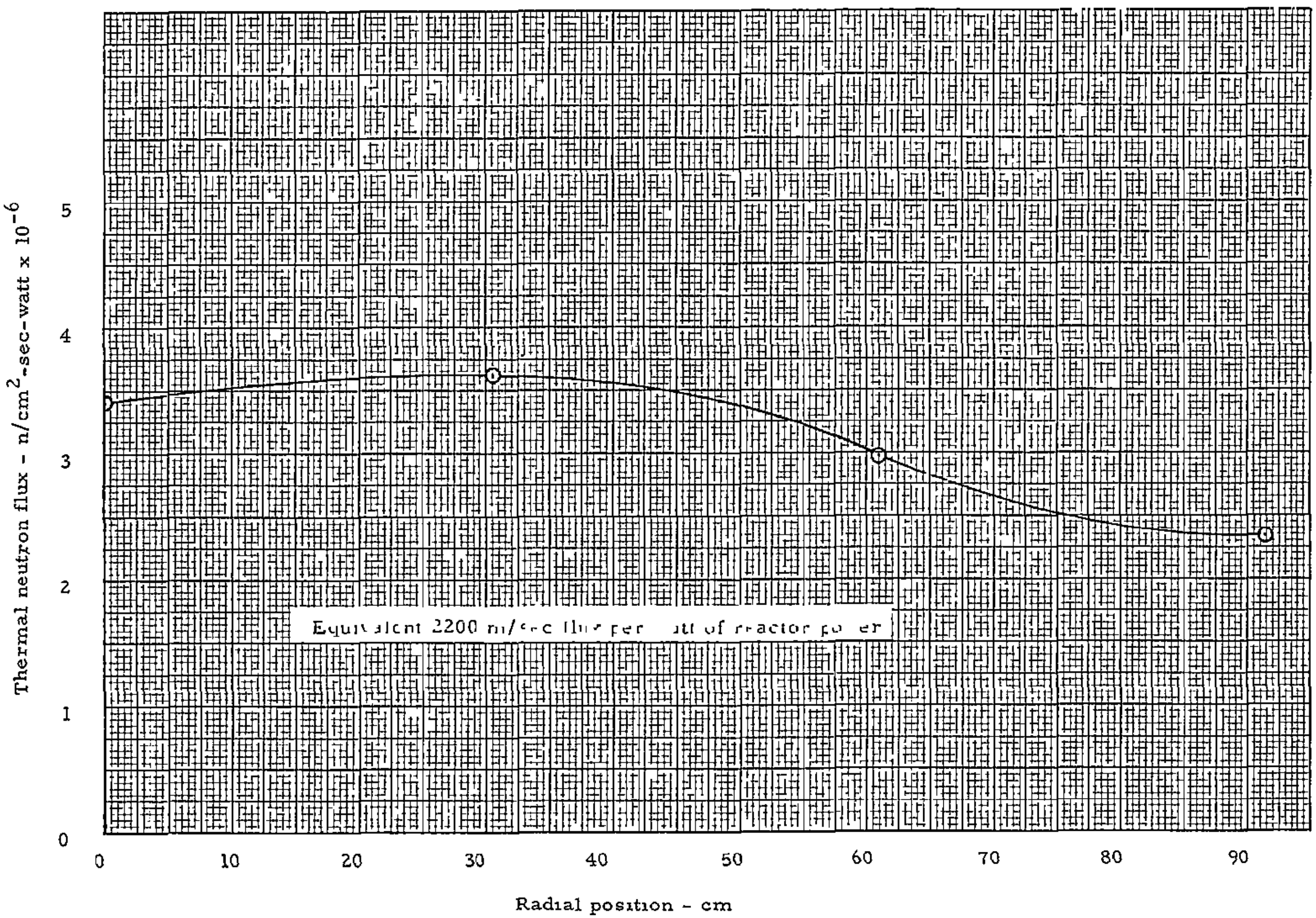

Figure 5.30 Thermal neutron flux distribution across the core at the separation plane from module 1 across module 3

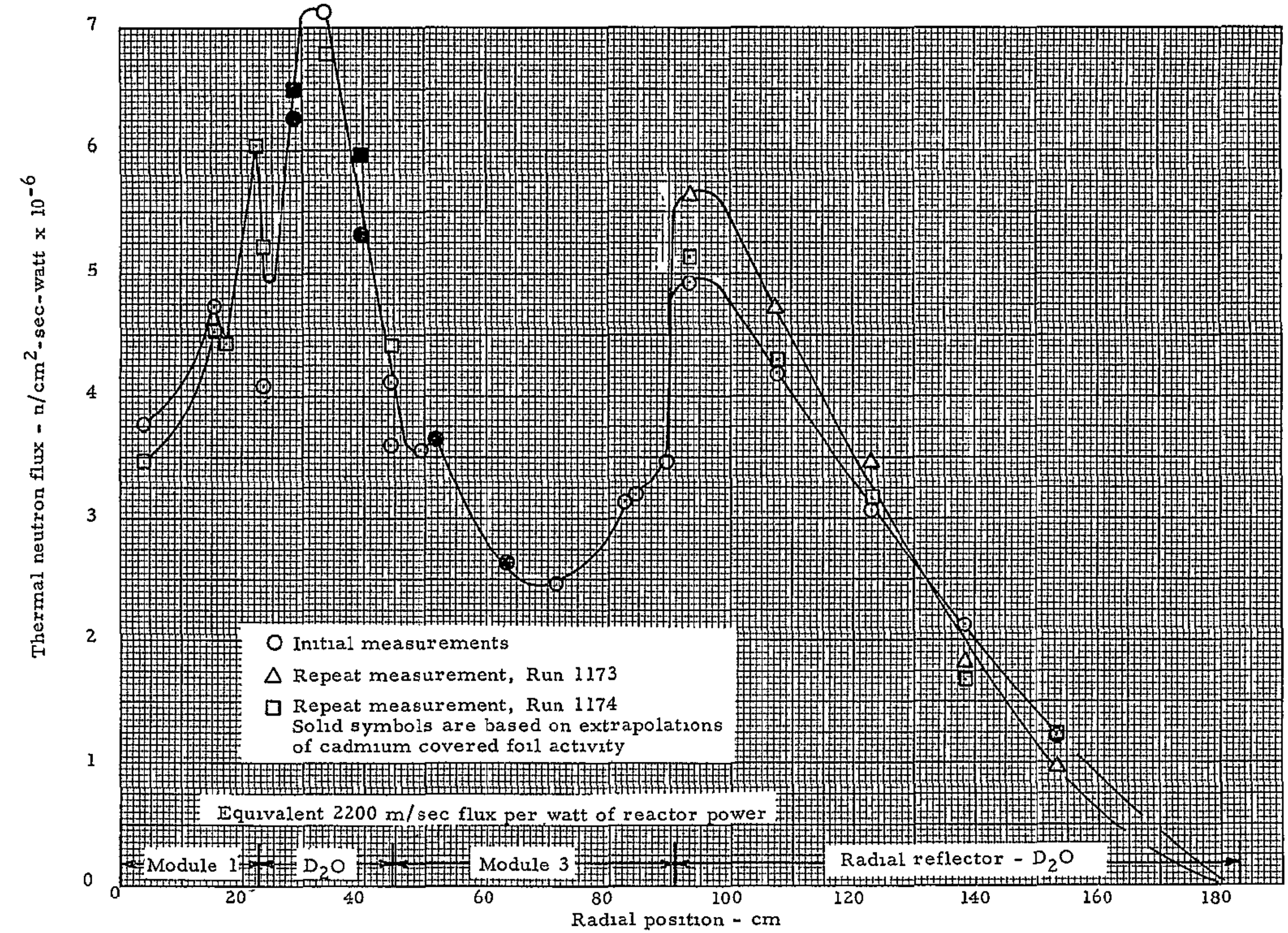

Figure 5 31 Radial distribution of thermal neutron flux from the center of the reactor across module 3 and into the radial reflector, 7-module reactor with 0 55 fuel to module radius ratio

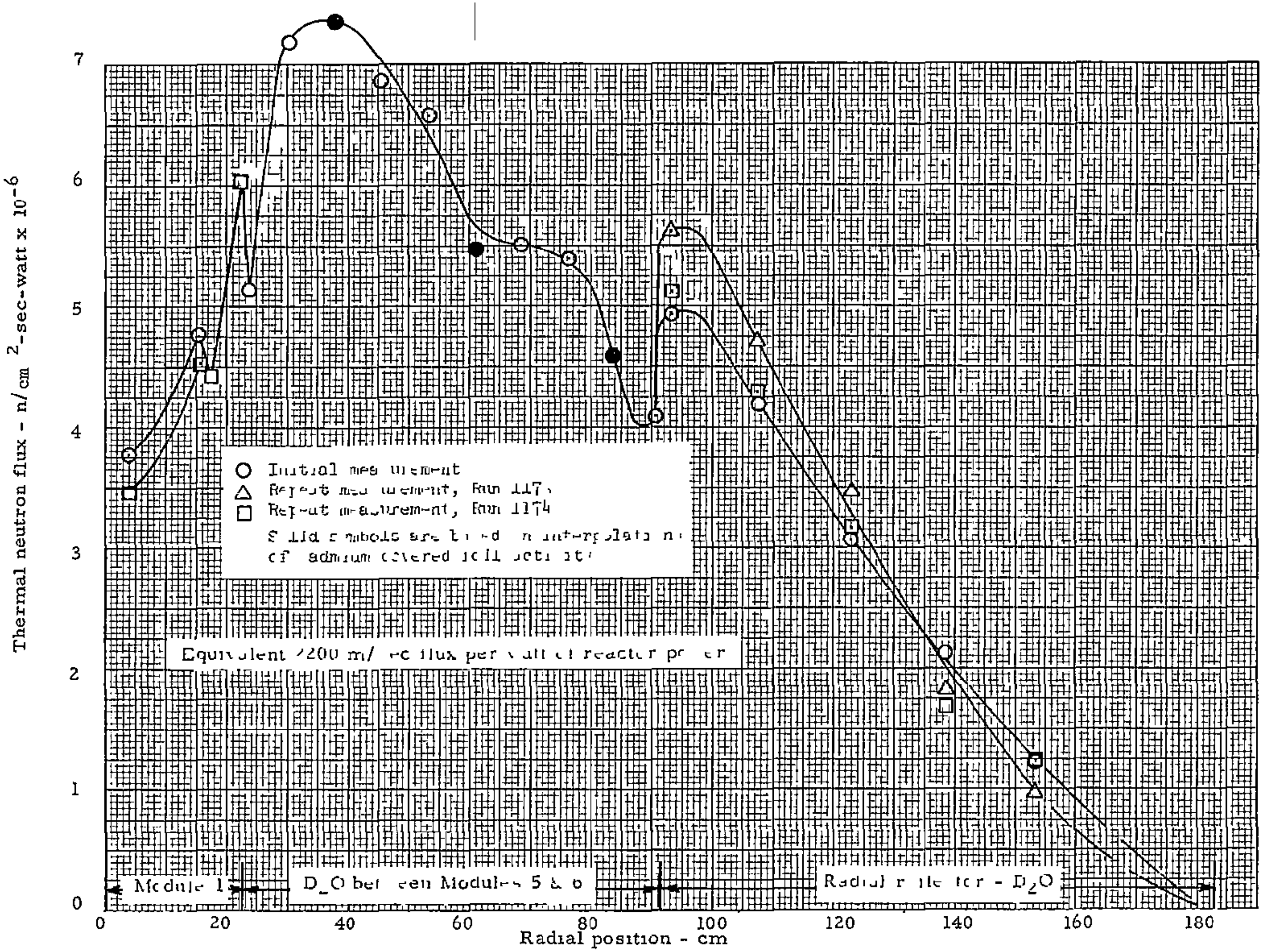

Figure 5 32 Radial distribution of thermal neutron flux from module 1 through the D_2O between modules 5 and 6 and into the radial reflector, 7-module reactor with 0 55 radius ratio

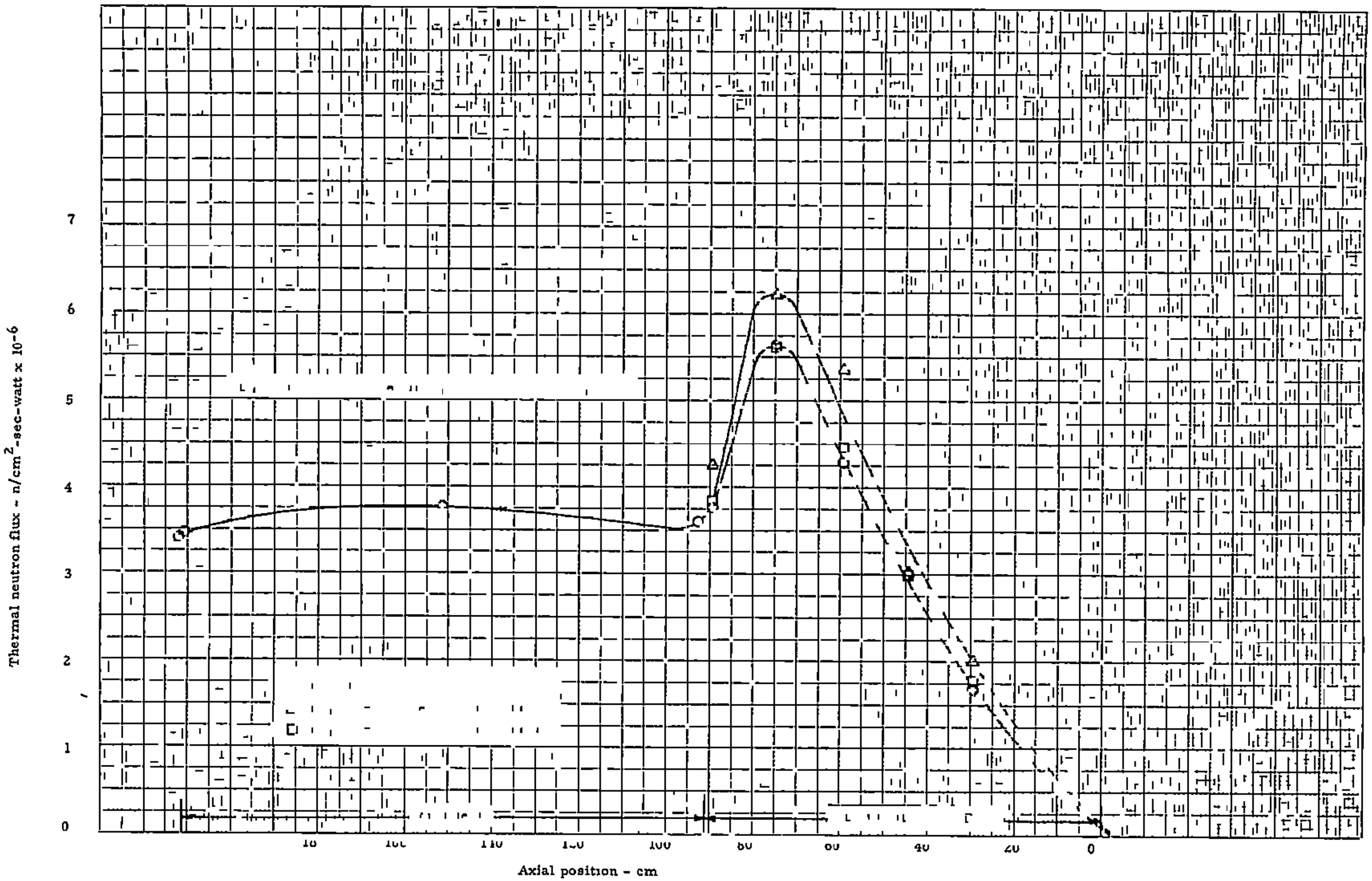

Figure 5 33 Axial distribution of thermal neutron flux through module 1 and into the reflector, 7-module reactor with 0 55 fuel to module radius ratio

6 0 0 72 RADIUS RATIO CORE - 7 MODULE

The change from the 0 55 to 0 72 radius ratio core was made by adding two more rings of fuel, as shown in Figure 5.2 The fuel sheet loading was adjusted on the rings to give a lower average fuel density. It was initially expected that slightly over 7 kg of uranium would be the critical mass but as the change from 0 55 to 0 72 radius ratio was gradually made, a heavier loading was needed The fuel stage separation discs were each loaded with four equivalent "size-one" sheets as shown in Figure 6.1 and specified in Table 6 1 Twenty sheets of fuel were placed on the fuel rings for each stage. The changes which followed as the initial loading progressed are explained in the following section

6.1 Initial Loading

Rather than completely unload the reactor and start with an empty core, the fuel elements were changed one at a time and after each change a k-excess measurement was made. The fuel element in Module 2 was changed first and k-excess decreased about 1 4%Δk It was obvious of course, that the pre-selected 7 kg fuel loading was significantly deficient. No change was made to the separation discs but one extra sheet was placed on the sixth and seventh rings and two sheets were added to the eighth ring of fuel. The loading on the rings then was as follows

Ring Number	Number of Size 1 0 Fuel Sheets	Ring Diameter (cm)
1	1	6 1
2	1	9 9
3	2	13 7
4	2	17 5
5	3	21.3
6	4	25 1
7	5	28.9
8	6	32 7
TOTAL	24	

On this basis, each fuel element would contain 452 equivalent size 1.0 fuel sheets or 1 18 kg of uranium based on 2 62 grams per sheet

Prior to making any further changes, 48 sheets of fuel (126 grams) were placed on the outer ring of fuel in Module 2, making a total of 436 full size sheets in this module K-excess increased 0.532±0.29%Δk, which gives a fuel worth at this outer radius ring of 4.23±0.23%Δk/kg.

Module 5 fuel element was then changed so that it contained 452 equivalent full size fuel sheets at a radius ratio of 0 72 and k-excess decreased only 0.06%Δk. The remaining fuel element changes showed similar decreases in reactivity. Finally, with six elements having 452 and one having 436 equivalent size one sheets, excess reactivity was 0 627%Δk with the exhaust nozzle tank removed from the reactor The total fuel loading was 3148 equivalent full-size sheets, or 8 24 kg of uranium

6.2 Reactivity Measurements

The worth of uranium was measured with the 0 72 radius ratio by using the same procedure as explained in Section 5.2 2 The data are given in Table 6.2 and Figure 6 2 The core volume-weighted average uranium worth was 4.08%Δk/kg This compares to 3.93%Δk/kg for the 0.55 radius ratio. The difference between these two numbers is of the order of the experimental error, and therefore is not considered significant

The worth of aluminum was also measured and the same procedure was used as for the 0.55 radius ratio core. The data are shown in Table 6.2. The same aluminum and the same locations were used as for the 0.55 radius ratio core but a comparison of the two sets of data shows quite large variations as follows:

Module	Angle (degrees cw)	Ratio of Al worth for 0 55 to 0.72 Radius Ratio Core
1	90	0 65
4	150	1.58
4	330	0 67

It appears that the value measured at 150 degrees on module 4 may have been in error, or that the aluminum worth measurements have a 30% uncertainty

Increasing the radius ratio required the addition of two fuel rings. This in turn increased the mass of aluminum 12 2 kg If it is assumed that the aluminum was worth 0 026%Δk/kg, the additional aluminum would have been worth 0.317%Δk or equivalent to about 78 grams of uranium (aluminum negative, uranium positive)

As noted earlier, each fuel element contained 452 equivalent size 1.0 fuel sheets except for Module 2 fuel element which contained 436 sheets. The amount of fuel on the separation discs was the same for all fuel elements. The fuel rings on Module 2 fuel element, however, contained the following fuel:

Ring No.	Number of Fuel Sheets
1	1
2	1
3	2
4	2
5	3
6	3
7	4
8	7

Thus the total equivalent size 1 0 fuel sheets on this fuel element amounted to 436 or 16 less than the other seven. Although the fuel mass on this element was slightly less than the other seven, the equivalent worth of the fuel element should have been about the same as the other six because the outer fuel ring was loaded heavier and the fuel at that location is worth more than it could have been had it been distributed over fuel rings nearer the center of the fuel element The total mass of uranium in the core was 8 24 kg and k-excess was 0 627. Uranium was worth 4.08%Δk/kg, and hence the critical mass was 8 09 kg This result includes no correction for the additional 12 2 kg of aluminum compared to the 0 55 radius ratio core This correction, based on 1 kg of Al being worth 0 025%Δk, is small, amounting to the equivalent of 78 grams of uranium. Thus, the critical mass with the same structure and hydrogen that existed in the 0 55 R/R_o reactor was 8.01 kg The 0 55 R/R_o reactor had a critical mass of 8.64 kg Both of these results are with the exhaust nozzle open.

6.3 Power Mapping - Catcher Foils

The catcher foil data obtained in this configuration are given in Table 6 3 It will be noted that mostly bare foils were used Only four cadmium covered catcher foils were measured The axial profiles in Modules 1 and 3 are given in Figures 6 3 to 6 5 along with the averages for each profile These averages were then plotted to give the radial profile shown in Figure 6.6. Each of these radial power distribution profiles was then volume averaged and these values are given in the figure. These volume weighted averages represent the average axial power at the given axial position, relative to a power of 1 0 at the axial center of the core, 4 0 cm from the radial centerline of the core.

The four cadmium ratios given at the end of Table 6 3 were also from Modules 1 and 3. Although duplicate positions were not available from the 0.55 radius ratio core, comparison with Table 5 7 indicates that the relative ratio of thermal to epi-thermal (epi-Cd) fissions was essentially the same in both cores

6.4 Flux Mapping - Gold Foils

6.4.1 Bare Gold Data

As explained earlier in this report, power normalization foils were exposed on each run so that the gold data could be normalized to a common power level. These data are shown in Table 6 4 There was a scram on Run 1175 so some gold foils were repeated on the subsequent run and the normalization factor was determined by comparing the two sets of data.

The gold results are given in Table 6.5 and include both bare and cadmium covered foils. The bare activities were normalized to a point near the center of Module 7 and these relative values were plotted to show the distributions within the reactor as seen from Figures 6.7 to 6.10. Everything appeared to be normal, following closely a smooth curve through the points. The dip in flux observed at the outer edge of Module 1 on the 0.55 radius ratio core (Figure 5.20) was barely evident here (Figure 6.8) but was more pronounced at the outer edge of module 3

6.4.2 Cadmium Ratios

Gold cadmium ratios (infinitely dilute) were obtained at several locations in the modules and the end and radial reflectors. The radial distributions from near the center of the core through modules 1 and 3 and through module 1 and across the tank between modules 5 and 6 are given in Table 6.6 and plotted in Figures 6.11 and 6.12. The last point in each figure was just inside the radial reflector. The cadmium ratios in the reflector regions are shown in Figure 6.13 and compare very well with the same data from the 0.55 radius ratio core (Figure 5.27)

6.4.3 Thermal Neutron Flux

The thermal neutron flux obtained from the gold foil data are given in Table 6.7. Of primary interest were the radial profiles through the module region and into the radial reflector. These are plotted in Figures 6.14 and 6.15. A flux dip occurs between the outer edge of the fuel and the inner surface of the polystyrene as was noted for the 0.55 radius ratio core (Figure 5.31). However, there was no observed dip at the outer surface of the polystyrene as was the case for the 0.55 radius ratio. The thermal flux in the reflector was generally lower per watt of power throughout the core for the 0.72 radius ratio compared to the 0.55 radius ratio. This appears paradoxical from customary fundamental considerations, since the fuel loading was less in the 0.72 radius ratio. However, between the modules, the 0.72 radius ratio had the higher thermal flux

TABLE 6 1

Fuel Sheets on Fuel Stage Separation Disc

7-Module Reactor - 0 72 Radius Ratio Loading

Disc Number	Positions Containing Fuel		Number of Fuel Whole Sheets	Sheets 1/2 Sheets
1	1,2,9,10		4	
2	3,4,7,8,11,12		2	4
3	5,6,13,14		4	
4	1,2,9,10		4	
5	3,4,7,8,11,12		2	4
6	5,6,13,14		4	
7	1,2,9,10		4	
8	3,4,7,8,11,12		2	4
9	5,6,13,14		4	
10	1,2,9,10		4	
11	3,4,7,8,11,12		2	4
12	5,6,13,14		4	
13	1,2,9,10		4	
14	3,4,7,8,11,12		2	4
15	5,6,13,14		4	
16	1,2,9,10		4	
17	3,4,7,8,11,12		2	4
		Total	56	24

TABLE 6 2

Fuel Worth Measurements

7-Module Reactor - 0 72 Radius Ratio

Location: Module	Location: Angle (degrees clockwise)	Radius (cm)	U Mass (g)	Reactivity Change (%Δk)	Uranium Worth (%Δk/kg)
1	90	4 0	7 28	0 0405±0 003	5 56±0 41
1	90	7 8	7 28	0 0433±0.003	5 95±0 41
1	90	11 6	7 28	0 0440±0 003	6 04±0 41
1	90	15 4	7 28	0 0507±0 003	6 96±0 41
3	90	4 0	7 28	0 0242±0 003	3 32±0 41
3	90	7 8	7 28	0 0247±0 003	3 39±0 41
3	90	11 6	7 28	0 0248±0 003	3 41±0 41
3	90	15 4	7 28	0 0258±0 003	3 54±0 41
3	270	7 8	7 28	0 0272±0 003	3 74±0 41
3	270	15 4	7 28	0 0313±0 003	4 30±0 41
			Al Mass (g)		Aluminum Worth (%Δk/kg)
1	90	Avg	540	0 0278±0 003	0 051±0 006
4	150		540	0 0105±0 003	0 019±0 006
4	330		540	0 0121±0 003	0 022±0 006

TABLE 6 3

Catcher Foil Data

7-Module Reactor - 0 72 Radius Ratio Core

Run 1175

Foil Number	Foil Type	Module Number	Location: Angle (°cw)	Location: Radial (cm)	Location: Axial (cm)	Normalized Counts	Local to Foil (X)
1	Bare	1	90	4 0	92 5	226334	1 007
2	Bare	1	90	4 0	105 8	219714	0 978
3	Bare	1	90	4 0	121 0	227949	1 014
4	Bare	1	90	4 0	151 5	224649	1 000 (X)
5	Bare	1	90	4 0	182 0	205035	0 912
6	Bare	1	90	4 0	197 2	197305	0 878
7	Bare	1	90	4 0	210 5	203469	0 906
8	Bare	1	90	7 8	92 5	226600	1 008
9	Bare	1	90	7 8	105 8	227671	1 013
10	Bare	1	90	7 8	121 0	227779	1 014
11	Bare	1	90	7 8	151 5	242290	1 078
12	Bare	1	90	7 8	182 0	214449	0 954
13	Bare	1	90	7 8	197 2	202414	0 901
14	Bare	1	90	7 8	210 5	202240	0 900
15	Bare	1	90	11 6	92 5	234076	1 042
16	Bare	1	90	11 6	105 8	232481	1 035
17	Bare	1	90	11 6	121 0	237486	1 057
18	Bare	1	90	11 6	151 5	244226	1 087
19	Bare	1	90	11 6	182 0	218231	0 971
20	Bare	1	90	11 6	197 2	212359	0 945
21	Bare	1	90	11 6	210 5	202000	0 899
22	Bare	1	90	15 4	92 5	243441	1 083
23	Bare	1	90	15 4	105 8	244753	1 089
24	Bare	1	90	15 4	121 0	256822	1 143
25	Bare	1	90	15.4	151 5	250966	1 117
26	Bare	1	90	15.4	182 0	236877	1 054
27	Bare	1	90	15 4	197 2	227759	1 014
28	Bare	1	90	15 4	210 5	215024	0 957
29	Bare	3	90	4 0	92 5	168345	0 749
30	Bare	3	90	4 0	105 8	165033	0 734
31	Bare	3	90	4.0	121 0	162244	0 722
32	Bare	3	90	4 0	151 5	169324	0 753
33	Bare	3	90	4 0	182 0	163460	0 727
34	Bare	3	90	4 0	197 2	155842	0.693
35	Bare	3	90	4 0	210 5	158866	0 707
36	Bare	3	90	7 8	92 5	158030	0 703
37	Bare	3	90	7 8	105 8	170390	0 758
38	Bare	3	90	7 8	121 0	164175	0 731
39	Bare	3	90	7 8	151 5	172809	0 769
40	Bare	3	90	7 8	182 0	159689	0 711

TABLE 6 3

(Continued)

Run 1175

Foil Number	Foil Type	Module Number	Angle (°cw)	Location Radial (cm)	Location Axial (cm)	Normalized Counts	Local to Foil (X)
41	Bare	3	90	7 8	197 2	157429	0 701
42	Bare	3	90	7 8	210 5	158046	0 703
43	Bare	3	90	11.6	92 5	169913	0 756
44	Bare	3	90	11 6	105 8	170430	0 758
45	Bare	3	90	11 6	121 0	168733	0 751
46	Bare	3	90	11 6	151 5	171289	0 762
47	Bare	3	90	11 6	182 0	161984	0 721
48	Bare	3	90	11 6	197 2	155039	0 690
49	Bare	3	90	11 6	210 5	152414	0 678
50	Bare	3	90	15 4	92 5	176127	0 784
51	Bare	3	90	15 4	105 8	162904	0 725
52	Bare	3	90	15 4	121 0	182217	0.811
53	Bare	3	90	15 4	151 5	186512	0 830
54	Bare	3	90	15 4	182 0	169581	0 755
55	Bare	3	90	15 4	197 2	158910	0 707
56	Bare	3	90	15 4	210.5	151581	0 675

Run 1176

Foil Number	Foil Type	Module Number	Angle (°cw)	Location Radial (cm)	Location Axial (cm)	Normalized Counts	Local to Foil (X)
1	Bare	3	270	15 4	92 5	207646	0 924
2	Bare	3	270	15 4	105 8	186690	0 861
3	Bare	3	270	15 4	121 0	202542	0 901
4	Bare	3	270	15 4	151 5	205524	0 915
5	Bare	3	270	15 4	182 0	191865	0 854
6	Bare	3	270	15 4	197 2	179356	0 798
7	Bare	3	270	15 4	210 5	184518	0 821
8	Bare	3	270	11 6	92 5	187196	0 833
9	Bare	3	270	11 6	105 8	193520	0.831
10	Bare	3	270	11 6	121 0	184803	0 822
11	Bare	3	270	11 6	151 5	182879	0 814
12	Bare	3	270	11 6	182 0	176486	0 785
13	Bare	3	270	11 6	197 2	171025	0 761
14	Bare	3	270	11 6	210 5	171823	0 765
15	Bare	3	270	7 8	92.5	180427	0.803
16	Bare	3	270	7 8	105 8	180012	0 801
17	Bare	3	270	7 8	121 0	173652	0 773
18	Bare	3	270	7 8	151 5	177323	0 789
19	Bare	3	270	7 8	182 0	171411	0.763
20	Bare	3	270	7 8	197 2	166390	0 740
21	Bare	3	270	7 8	210 5	170880	0 760

TABLE 6 3

(Continued)

Foil Number	Foil Type	Module Number	Angle (°cw)	Location Radial (cm)	Location Axial (cm)	Normalized Counts	Local to Foil (X)
Run 1176							
22	Bare	3	270	4 0	92 5	174455	0 776
23	Bare	3	270	4 0	105 8	170722	0 760
24	Bare	3	270	4 0	121 0	170162	0 757
25	Bare	3	270	4 0	151 5	172971	0 770
26	Bare	3	270	4 0	182 0	163387	0 727
27	Bare	3	270	4.0	197 2	163064	0 726
28	Bare	3	270	4 0	210 5	167506	0 745
Run 1177							
1	Cd	1	90	4 0	182 0	5797	35 4
2	Cd	1	90	15 4	182 0	5781	41 0
3	Cd	3	90	4 0	182 0	4420	37 0
4	Cd	3	90	15 4	182 0	4291	39 5

TABLE 6 4

Power Normalization

7-Module Reactor - 0 72 Radius Ratio

Run	Time of Count	Decay Time	Correction Factor	Counts	Corrected Average Counts/min	Normalization Factor
1175	1158 08	66 00	1 393	287979	401155	
	1200 08	68 00	1 447	277810	401991	
	1201 58	69 50	1.487	266871	396837	
		Scrammed after 6 min			399994	0 996[1]
1176	1114 85	43 50	0 852	501489	427269	
	1116 85	45 50	0 897	475391	426426	
	1118 85	47 50	0 942	452915	426646	
					426780	1 000
1177	1500 82	55 00	1 120	377551	422857	
	1503 32	57 50	1 182	358516	423766	
	1505 32	59 50	1 232	343986	423791	
					423471	0 992

1 Based on gold foil repeat data on Run 1176

TABLE 6 5

Gold Foil Data

7-Module Reactor - 0 72 Radius Ratio

Run 1175

Foil Number	Foil Type	Location Radial (cm)	Location Axial (cm)	Foil Weight (g)	Specific Activity d/m-g x 10^{-6}	Local to Foil (X)*
1	Bare	0	89 4	0 0343	8 318	1 019
2	Bare	0	74 9	0 0343	10 024	1 228
3	Bare	0	59 6	0 0343	7 430	0 910
4	Bare	0	44 4	0 0340	4 995	0 612
5	Bare	0	29 1	0 0340	3 061	0 375
6	Bare	0	13 9	0 0339	1 543	0 189
7	Bare	0	0	0 0340	0 196	0 024
8	Bare	93 2	151 1	0 0337	8.317	1 019
9	Bare	107 7	151 1	0 0338	6 772	0 830
10	Bare	123 0	151 1	0 0338	4 744	0 581
11	Bare	138 2	151 1	0 0339	3 201	0 392
12	Bare	153 4	151 1	0 0337	1 930	0 237
13	Bare	168 7	151 1	0 0338	0 871	0 107
14	Bare	183 7	151 1	0 0338	0 120	0 015
	Module 1, 90°					
15	Bare	4 0	136 3	0 0337	8 278	1 014 (X)*
16	Bare	7 8	136 3	0 0338	8 452	1 036
17	Bare	11 6	136 3	0 0338	8 684	1 064
18	Bare	15 4	136 3	0 0338	9 111	1 116
19	Bare	4 0	166 8	0 0338	8 042	0 985 (X)*
20	Bare	7 8	166 8	0 0339	7 883	0 966
21	Bare	11 6	166 8	0 0338	8 032	0 984
22	Bare	15 4	166 8	0 0338	8 324	1 020
	Module 3, 90°					
23	Bare	4 0	136 3	0 0338	6 020	0 738
24	Bare	7 8	136 3	0 0338	5 985	0 733
25	Bare	11 6	136 3	0 0338	5 963	0 731
26	Bare	15 4	136 3	0 0338	6 386	0 783
27	Bare	4 0	166 8	0 0338	6 020	0 738
28	Bare	7 8	166 8	0 0338	5 805	0 711
29	Bare	11 6	166 8	0 0338	5 700	0 698
30	Bare	15 4	166 8	0 0338	6 138	0 752
	Traverse from Module 1 to 3					
31	Bare	23 6	151 1	0 0338	10 878	1 333
32	Bare	28 7	151 1	0 0338	12 979	1 590
33	Bare	34 0	151 1	0 0338	13 266	1 626
34	Bare	39 4	151 1	0 0338	11 896	1 458
35	Bare	44 4	151 1	0 0338	8 973	1 100

*Note: The standard normalizer location is at 151 5 cm axial position, midway between the two "Foil X's" shown

TABLE 6 5

(Continued)

Run 1175

Foil Number	Foil Type	Location Radial (cm)	Location Axial (cm)	Foil Weight (g)	Specific Activity d/m-g x 10^{-6}	Local to Foil (X)
	Traverse Betwen Modules 5 & 6					
36	Bare	90 7	151 1	0 0338	8 688	1 065
37	Bare	83 8	151 1	0.0338	9.768	1 197
38	Bare	76 2	151 1	0 0338	10.752	1 318
39	Bare	68 6	151 1	0 0339	11 150	1 366
40	Bare	61 0	151 1	0 0339	11 488	1 408
41	Bare	53 3	151 1	0 0338	12 183	1 493
42	Bare	45 7	151 1	0 0338	13 241	1 623
43	Bare	38 1	151 1	0 0338	14 003	1 716
44	Bare	30 5	151 1	0 0337	13 484	1 652
45	Bare	23 6	151 1	0 0337	11 117	1 362
	Outer Surface of CH in Module 3					
46	Bare	22 4 (270°)	165 3	0 0337	8 133	0 997
47	Bare	22 4 (315°)	165 3	0 0337	8 038	0 985
48	Bare	22 4 (0°)	165 3	0 0337	7 741	0 949
49	Bare	22 4 (45°)	165 3	0 0337	7 117	0 872
50	Bare	22 4 (90°)	165 3	0 0337	6 783	0 831
	Inner Surface of CH in Module 3					
51	Bare	17 5 (270°)	165 3	0 0338	6 812	0 835
52	Bare	17 5 (315°)	165 3	0 0338	6 867	0 841
53	Bare	17 5 (0°)	165 3	0 0338	6 534	0 801
54	Bare	17 5 (45°)	165 3	0 0338	6 539	0 801
55	Bare	17 5 (90°)	165 3	Lost	-----	-----
	Outer Surface of CH in Module 1					
56	Bare	22 4 (270°)	165 3	0 0339	9 984	1 223
57	Bare	22 4 (315°)	165 3	0 0337	10 058	1 233
58	Bare	22 4 (0°)	165 3	0 0337	9 945	1 219
	Inner Surface of CH in Module 1					
59	Bare	17 5 (270°)	165 3	0 0337	8 659	1 061
60	Bare	17 5 (315°)	165 3	0 0337	8 736	1 071
61	Bare	17 5 (0°)	165 3	0 0337	8 891	1 090
Run 1176						
1	Cd	0	89 4	0 0332	2.113	
2	Cd	0	59 6	0 0333	0 245	
3	Cd	0	29 1	0 0353	0 00829	
4	Cd	93 2	151 1	0 0341	0 627	
5	Cd	123 0	151 1	0 0345	0 0221	
6	Cd	153 4	151 1	0 0340	0 00333	

TABLE 6 5

(Continued)

Run 1176

Foil Number	Foil Type	Location Radial (cm)	Location Axial (cm)	Foil Weight (g)	Specific Activity d/m-g x 10^{-6}	Local to Foil (X)
	Module 3, 270°					
7	Bare	15 4	136 3	0 0293	7 061	0 865
8	Bare	11 6	136 3	0 0312	6 669	0 817
9	Bare	7 8	136 3	0 0350	6 274	0 769
10	Bare	4 0	136 3	0 0340	6 138	0 752
11	Cd	15 4	166 8	0 0339	1 764	
12	Cd	4 0	166 8	0 0340	1 699	
	Traverse from Module 1 to 3					
13	Cd	23 6	151 1	0 0338	2 520	
14	Cd	34 0	151 1	0.0340	2 302	
15	Cd	44 4	151 1	0 0340	1 754	
	Traverse Between Modules 5 & 6					
16	Cd	23 6	151.1	0 0337	2 532	
17	Cd	53 3	151.1	0 0339	2 183	
18	Cd	83 8	151 1	0 0331	1 009	
	Outer Surface of CH in Module 1					
19	Cd	22 4 (270°)	165 3	0 0334	2 345	
20	Cd	22 4 (0°)	165 3	0 0336	2 351	
	Inner Surface of CH in Module 3					
21	Cd	17 5 (270°)	165 3	0 0338	1 638	
22	Cd	17 5 (90°)	165 3	0 0343	1 742	
23	Bare	107 7	151 1	0 0354	6 792	0 832
24	Bare	138 2	151.1	0 0322	3 191	0.391

Run 1177

Foil Number	Foil Type	Location Radial (cm)	Location Axial (cm)	Foil Weight (g)	Specific Activity d/m-g x 10^{-6}	Local to Foil (X)
	Module 1, 90°					
1	Cd	4 0	163 3	0 0337	2 384	
2	Cd	15 4	163 3	0 0332	2 323	
	Module 3, 90°					
3	Cd	4 0	163 3	0 0325	1 685	
4	Cd	15 4	163 3	0 0335	1 666	
	Traverse from Module 1 to 3					
5	Cd	28 7	151 1	0 0335	2 533	
6	Cd	39 4	151 1	0 0336	2 201	
	Traverse Between Modules 5 & 6					
7	Cd	38 1	151 1	0 0334	2.248	
8	Cd	68 6	151 1	0 0334	1 818	
9	Cd	90 7	151 1	0 0335	0 706	

TABLE 6 5

(Continued)

Run 1177

Foil Number	Foil Type	Location Radial (cm)	Location Axial (cm)	Foil Weight (g)	Specific Activity d/m-g x 10^{-6}	Local to Foil (X)
	Inner Surface of CH in Module 1					
10	Cd	17 5 (270°)	165 3	0 0341	2 221	
11	Cd	17 5 (0°)	165 3	0 0341	2 262	
	Outer Surface of CH in Module 3					
12	Cd	22 4 (270°)	165 3	0 0341	1 797	
13	Cd	22 4 (90°)	165 3	0 0338	1 563	
	Traverse Tube Between Modules 5 & 6					
14	Bare	23 6	151 1	0 0385	10 763	1 319
15	Bare	22 4	151 1	0 0371	10 037	1 230
16	Bare	22 4	158 7	0 0379	9.990	1 224

TABLE 6 6

Gold Foil Cadmium Ratios

7-Module Cavity Reactor

0 72 Radius Ratio with Hydrogen

Location Radial (cm)	Location Axial (cm)	Module Number	Angle (°cw)	Infinitely Dilute Foil Activity d/m-g x 10^{-6} Bare Gold	Infinitely Dilute Foil Activity d/m-g x 10^{-6} Cd Gold	Cadmium Ratio
0	89 4			11 04	4 809	2 296
0	59 6			7 746	0 558	13 87
0	29 1			3 072	0 019	158 8
93 2	151 1			9 130	1 443	6 328
123 0	151 1			4 773	0 051	93 4
153 4	151 1			1 934	0 0077	252 8
4 0	136 3	1	90°	11 35	5 459	2 080
15 4	136 3	1	90°	12 09	5 287	2 287
4 0	136 3	3	90°	8 190	3 849	2 128
15 4	136 3	3	90°	8 532	3 806	2 242
4 0	136 3	3	270°	8 343	3 904	2 137
15 4	136 3	3	270°	9 240	4 049	2 282
23 6	151 1	Traverse from Module 1 to 3		14 14	5 777	2 447
28 7	151 1	Traverse from Module 1 to 3		16 24	5 786	2 807
34 0	151 1	Traverse from Module 1 to 3		16 25	5 290	3 071
39 4	151 1	Traverse from Module 1 to 3		14 73	5 034	2 927
44 4	151 1	Traverse from Module 1 to 3		11 25	4 031	2 790
23 6	151 1	Traverse from Module 1 Between Modules 5 & 6		14 38	5 798	2 481
38 1	151 1	Traverse from Module 1 Between Modules 5 & 6		16 89	5 129	3 294
53 3	151 1	Traverse from Module 1 Between Modules 5 & 6		15 01	5 011	2 995
68 6	151 1	Traverse from Module 1 Between Modules 5 & 6		13 49	4 148	3 252
83 8	151 1	Traverse from Module 1 Between Modules 5 & 6		11 06	2 294	4 822
90 7	151 1	Traverse from Module 1 Between Modules 5 & 6		9 597	1 613	5 951
22 4	166 8	1	0°	12 97	5 377	2 413
22 4	166 8	1	270°	13 00	5 350	2 431
17 5	166 8	1	0°	11 82	5 204	2 272
17 5	166 8	1	270°	11 54	5 110	2 258
22 4	166 8	3	90°	8 801	3 583	2 456
22 4	166 8	3	270°	10 37	4 135	2 507
17 5	166 8	3	90°	8 804	4 018	2 191
17 5	166 8	3	270°	8 930	3 755	2 378

TABLE 6 7

Thermal Neutron Flux

7-Module Reactor - Exhaust Nozzle Removed

0 72 Radius Ratio

Location				
Radial (cm)	Axial (cm)	Module Number	Angle (°cw)	Thermal Neutron Flux n/cm^2-sec-watt x 10^{-6}
0	89 4	End reflector		3.495
0	59 6	End reflector		4 031
0	29 1	End reflector		1 712
93 2	151 1	Radial reflector		4 311
123 0	151 1	Radial reflector		2.648
153 4	151 1	Radial reflector		1 080
4 0	136 3	1	90°	3 305
15 4	136 3	1	90°	3 816
4 0	136 3	3	90°	2 435
15 4	136 3	3	90°	2 650
4 0	136 3	3	270°	2 489
15 4	136 3	3	270°	2.911
23 6	151 1	Traverse from Module 1 to 3		4 679
28 7	151 1	Traverse from Module 1 to 3		5.863
34 0	151 1	Traverse from Module 1 to 3		6 146
39 4	151 1	Traverse from Module 1 to 3		5 440
44 4	151 1	Traverse from Module 1 to 3		4 046
23 6	151 1	Traverse between Modules 5 & 6		4 815
38 1	151 1	Traverse between Modules 5 & 6		6 598
53 3	151 1	Traverse between Modules 5 & 6		5 607
68 6	151 1	Traverse between Modules 5 & 6		5 240
83 8	151 1	Traverse between Modules 5 & 6		4 917
90 7	151 1	Traverse between Modules 5 & 6		4 478
22 4	151 1	1	0°	4 260
22 4	151 1	1	270°	4 293
17 5	151 1	1	0°	3.712
17 5	151 1	1	270°	3 605
22 4	151 1	3	90°	2 926
22 4	151 1	3	270°	3 495
17 5	151 1	3	90°	2 684
17 5	151 1	3	270°	2 902

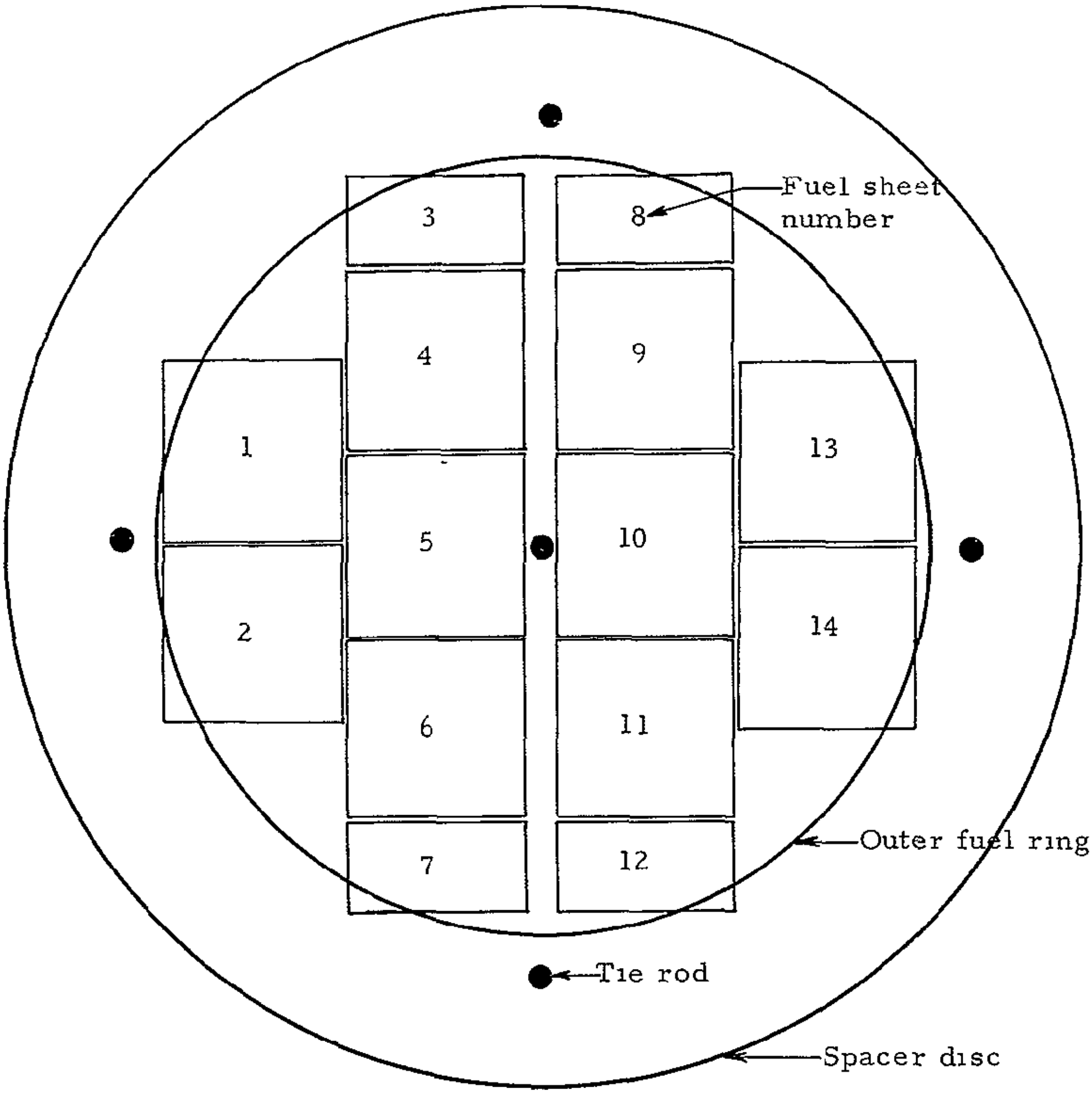

Figure 6.1 Layout of fuel sheets on fuel stage separation disc on the 7 module reactor fuel element with the 0 72 radius ratio loading (Note, for locations actually occupied by fuel, see Table 6 1)

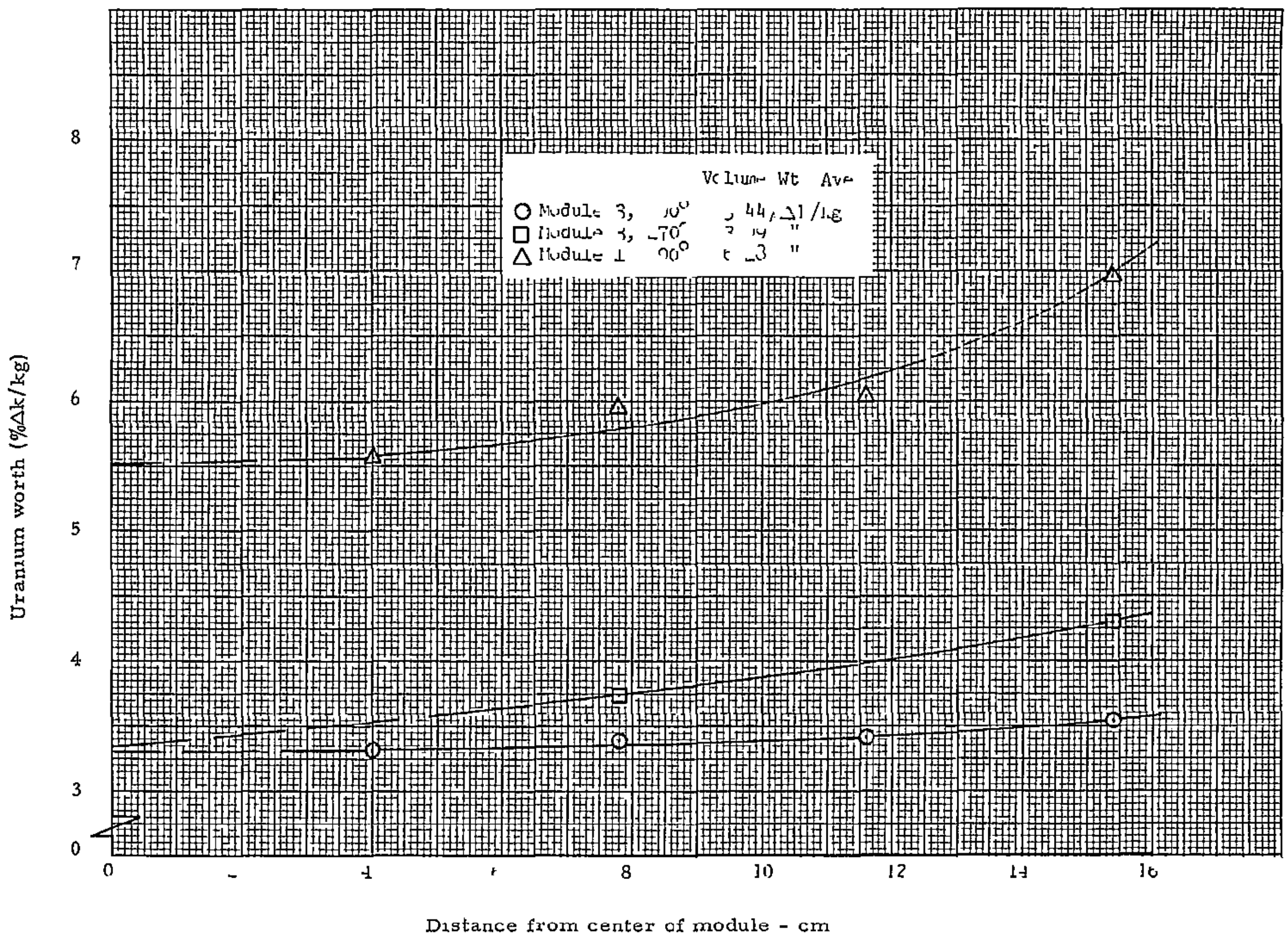

Figure 6 2 Uranium worth measurement, 7-module reactor with 0 72 fuel to module radius ratio

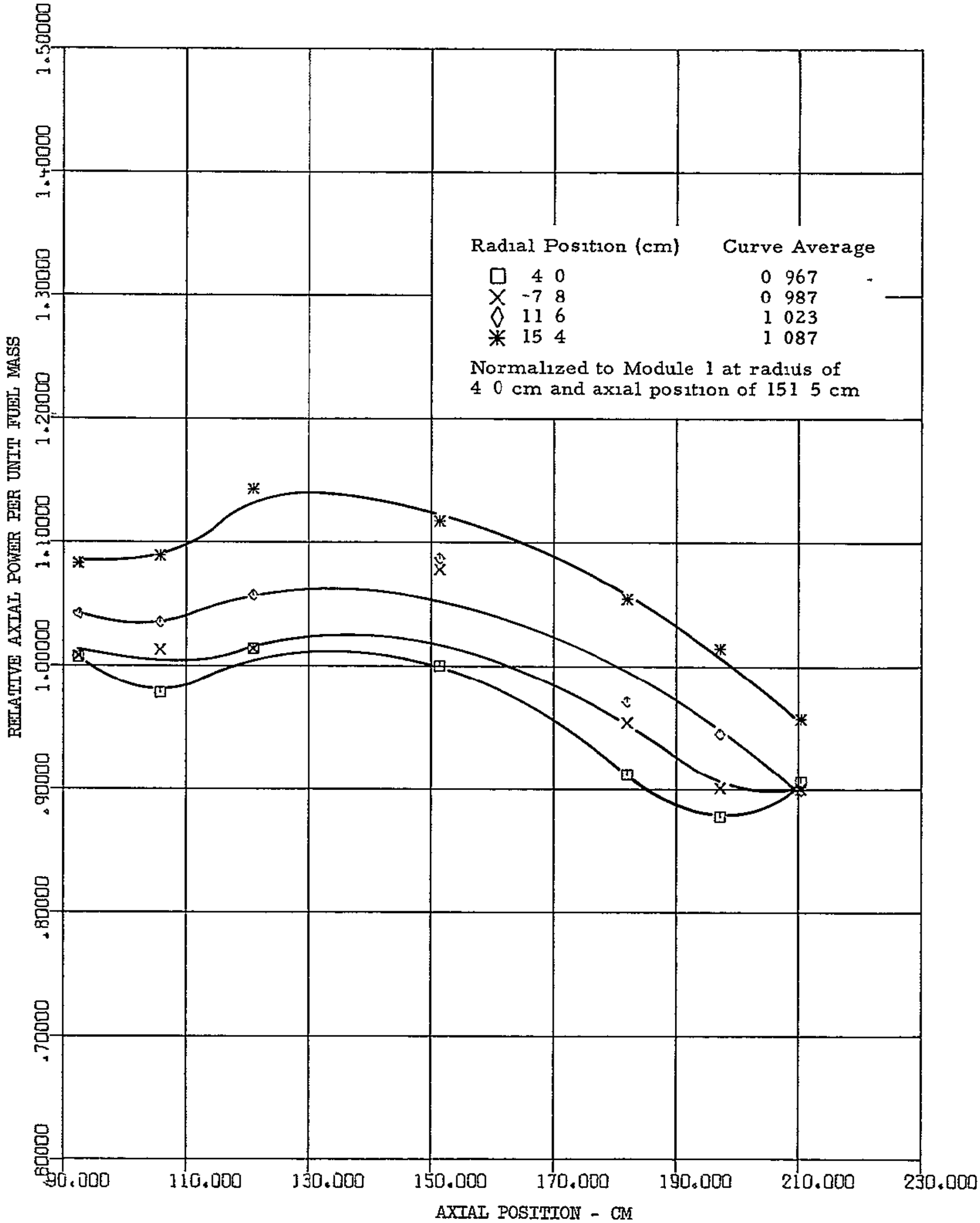

Figure 6 3 Relative axial power distribution in Module 1, 90° at the core centerline, 7-module reactor with 0 72 fuel to module radius ratio

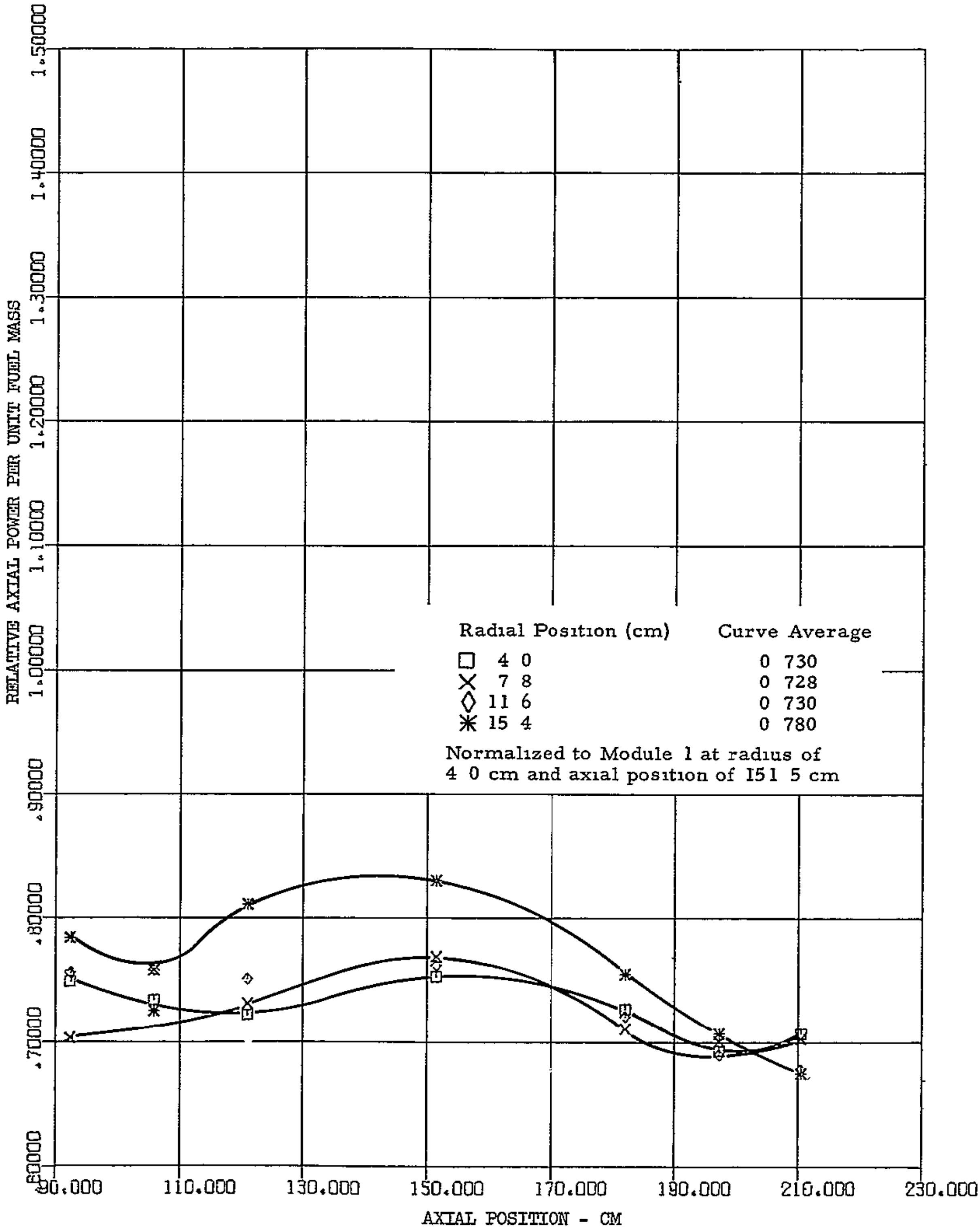

Figure 6 4 Relative axial power distribution in module 3, 90° at the core centerline, 7 module reactor with 0 72 fuel to module radius ratio

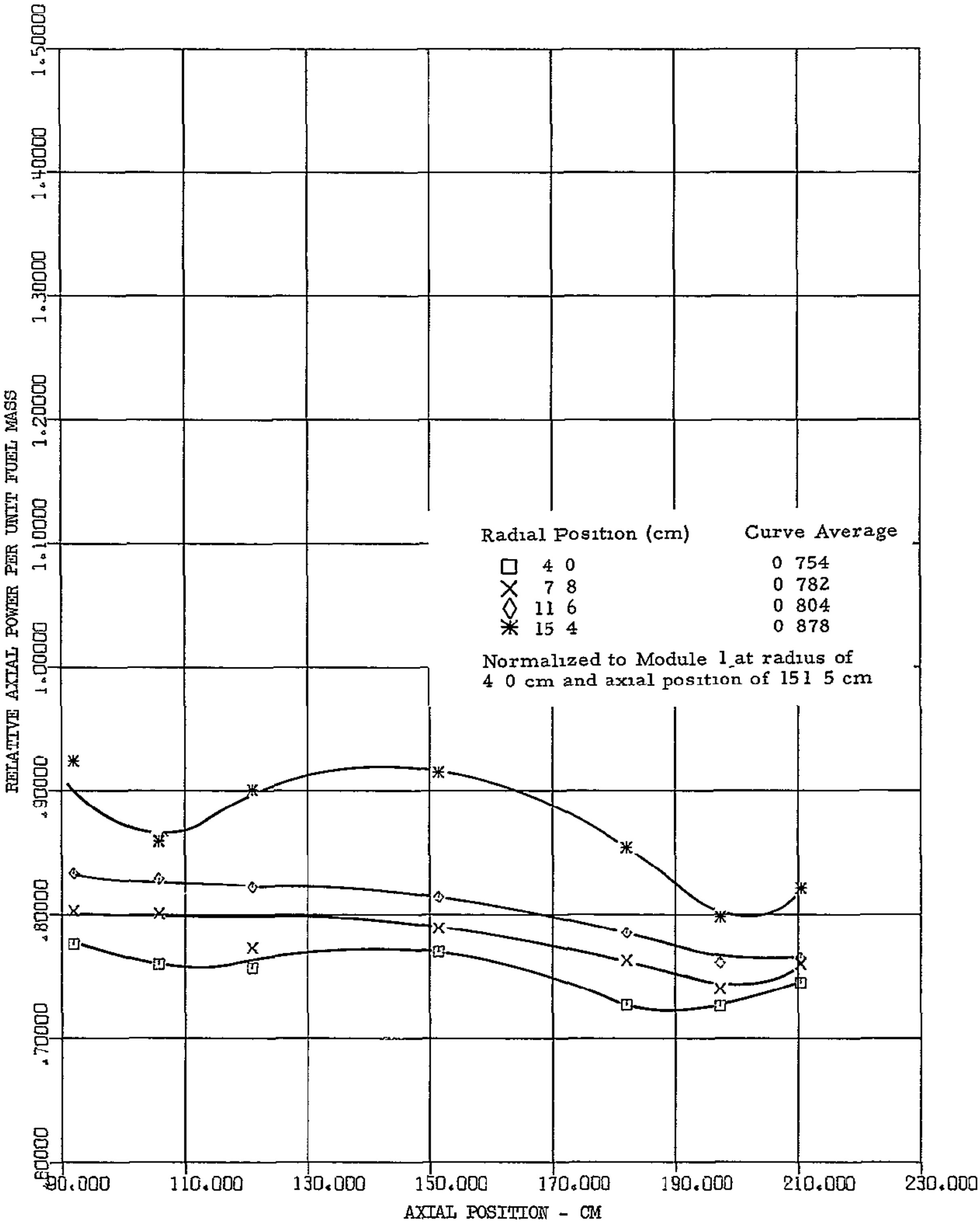

Figure 6 5 Relative axial power distribution in module 3, 270° at the core centerline, 7 module reactor with 0 72 fuel to module radius ratio

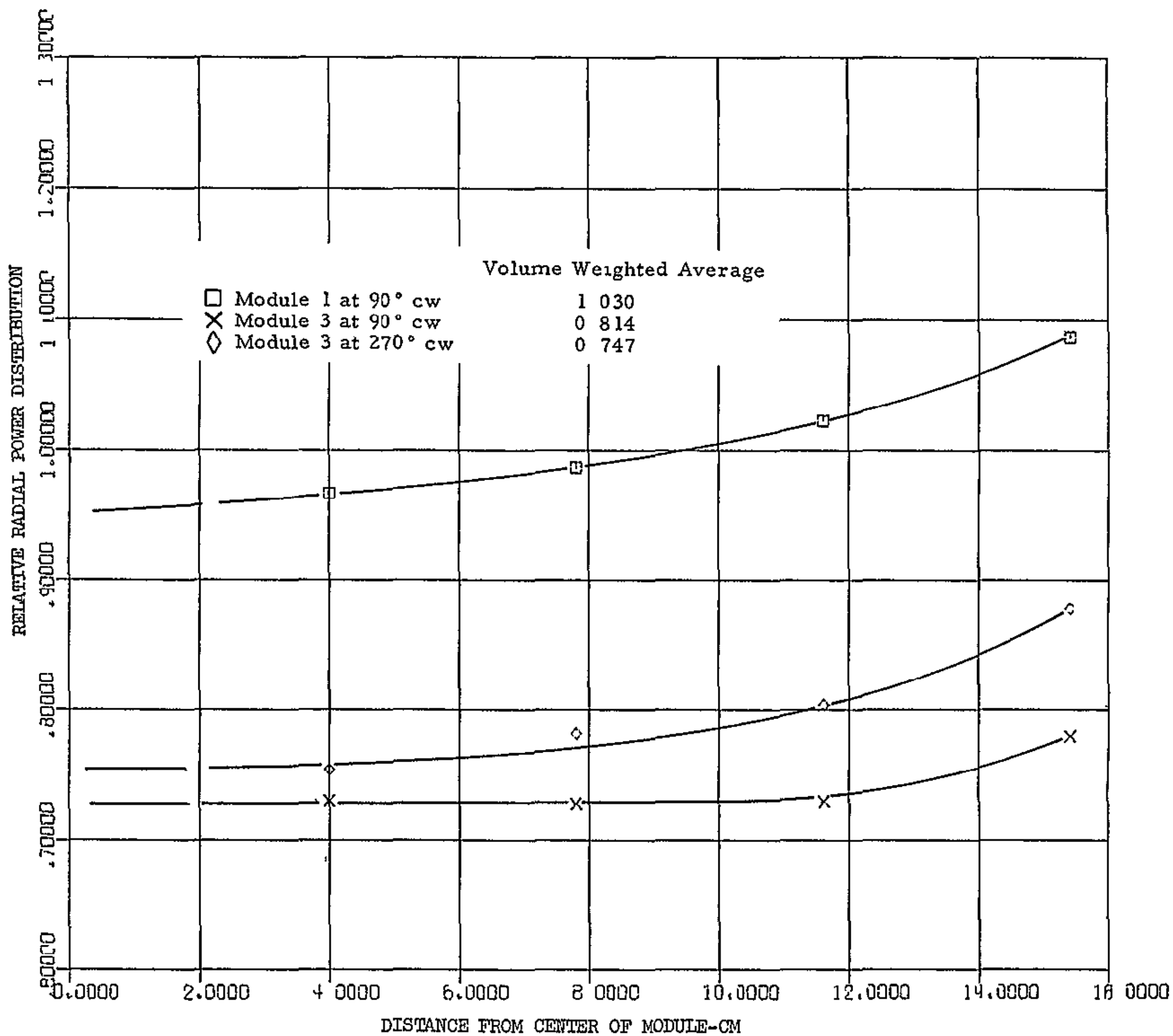

Figure 6.6 Relative radial power distribution in modules 1 and 3 based on axial average power distributions, 7-module reactor with 0 72 fuel to module radius ratio

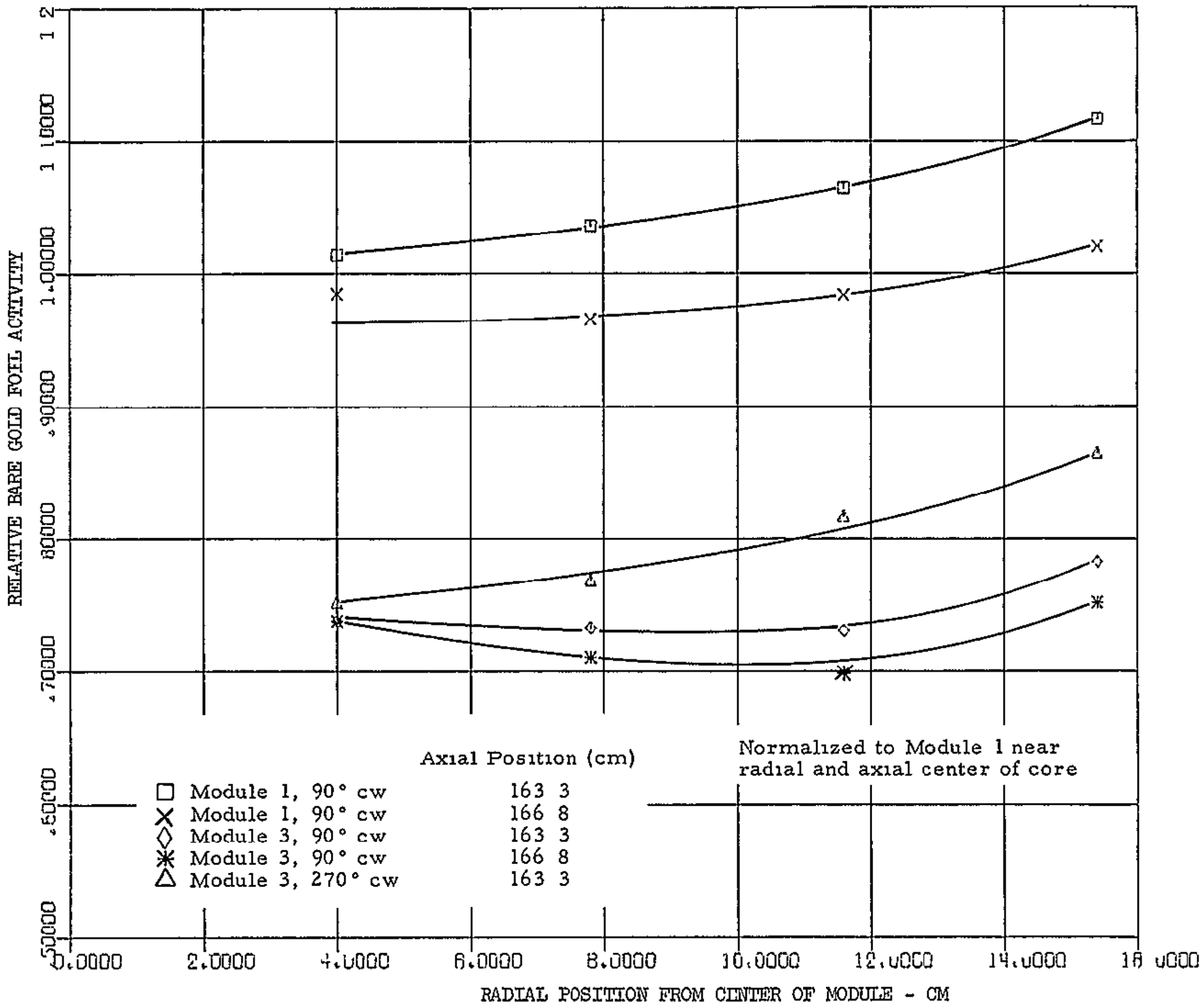

Figure 6.7 Relative radial bare gold foil activity in modules 1 and 3 at axial locations of 163 3 and 166 8 cm, 0 72 fuel to module radius ratio

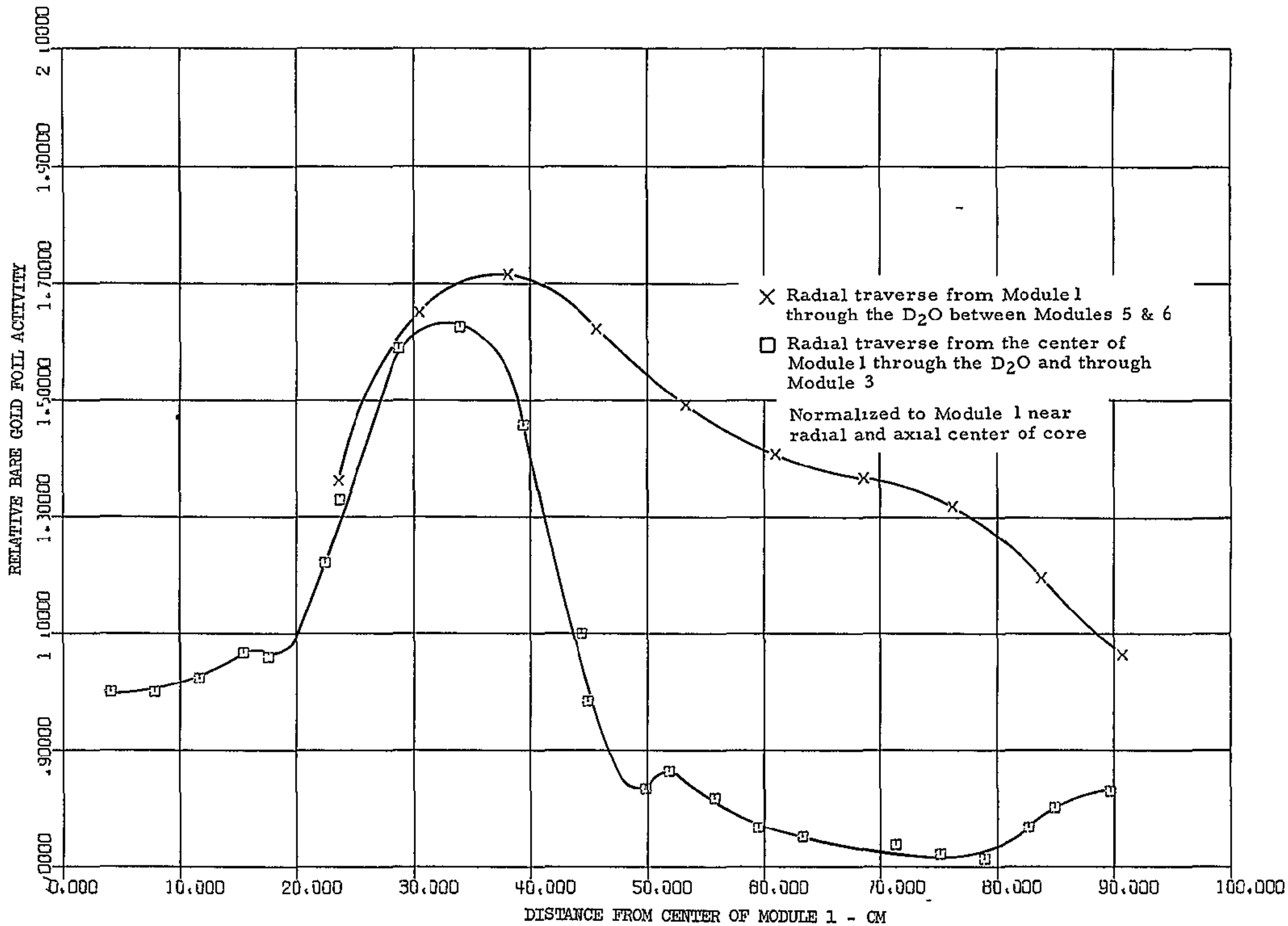

Figure 6.8 Relative bare gold foil activity distribution in the regions between modules, 0 72 fuel to module radius ratio

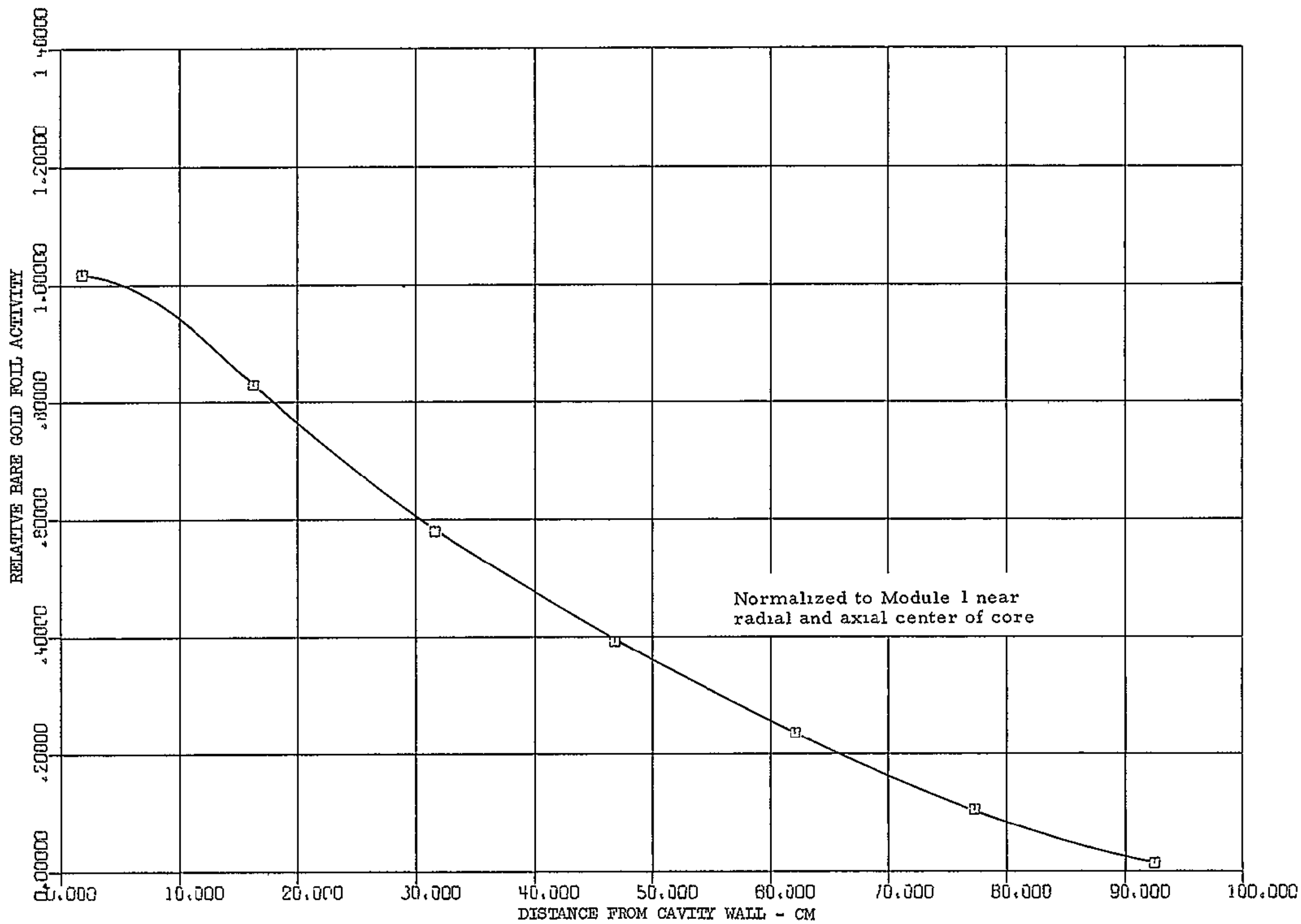

Figure 6 9 Gold foil activity in the radial reflector, 0 72 fuel to module radius ratio

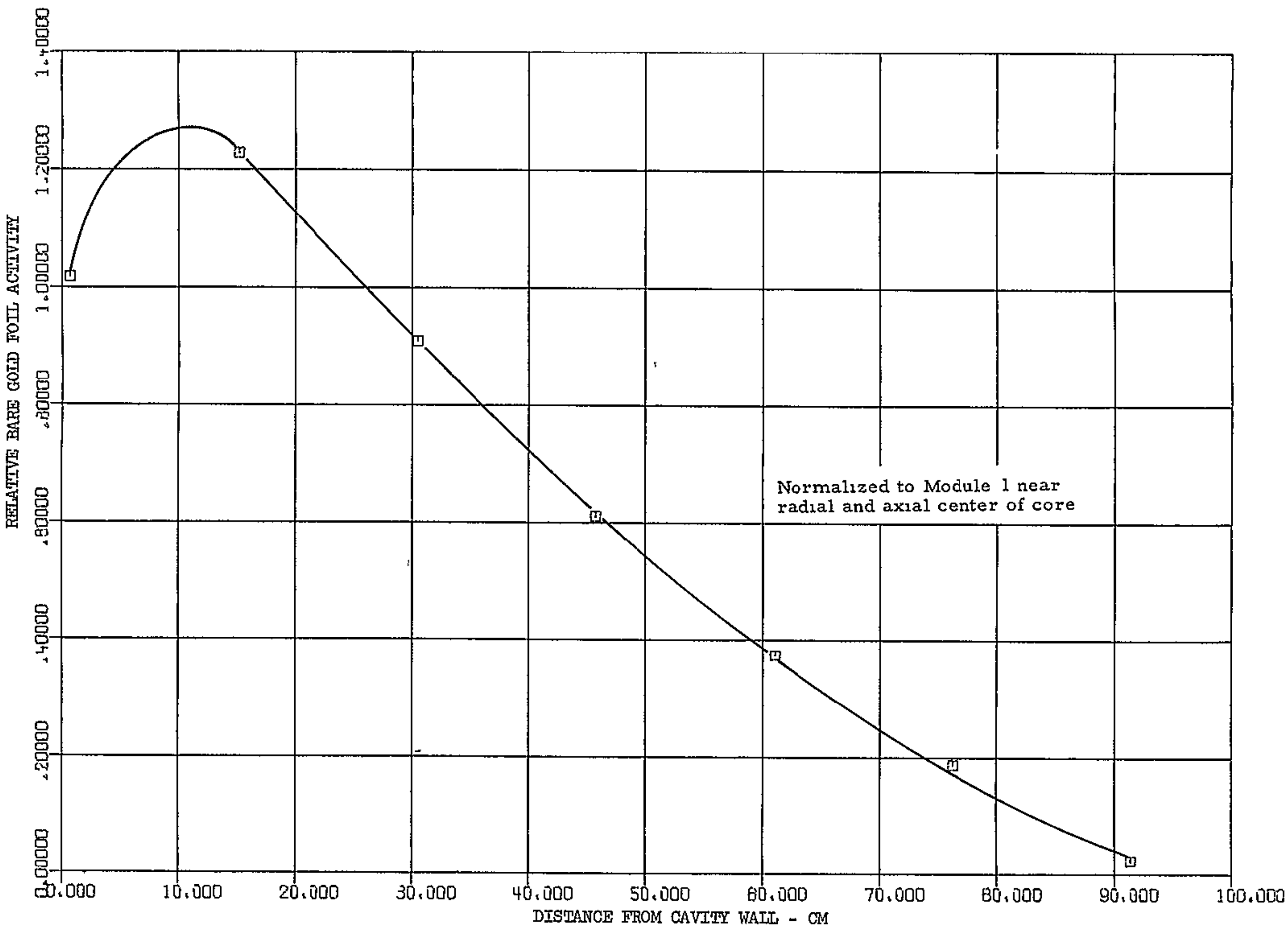

Figure 6 10 Gold foil activity in the end reflector, 0 72 fuel to module radius ratio

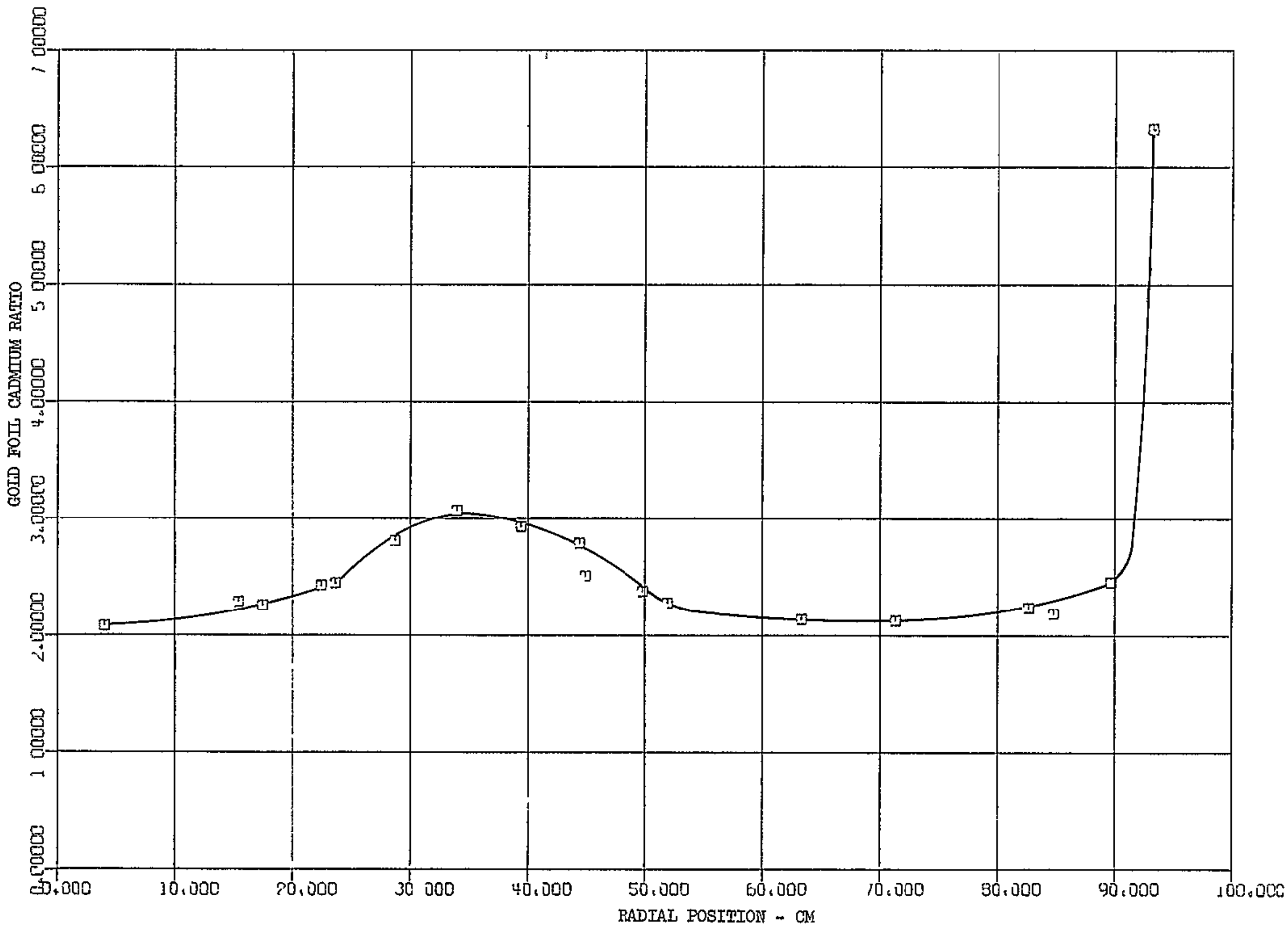

Figure 6 11 Gold Foil Cadmium Ratio - module 1 through module 3, 0 72 fuel to module radius ratio

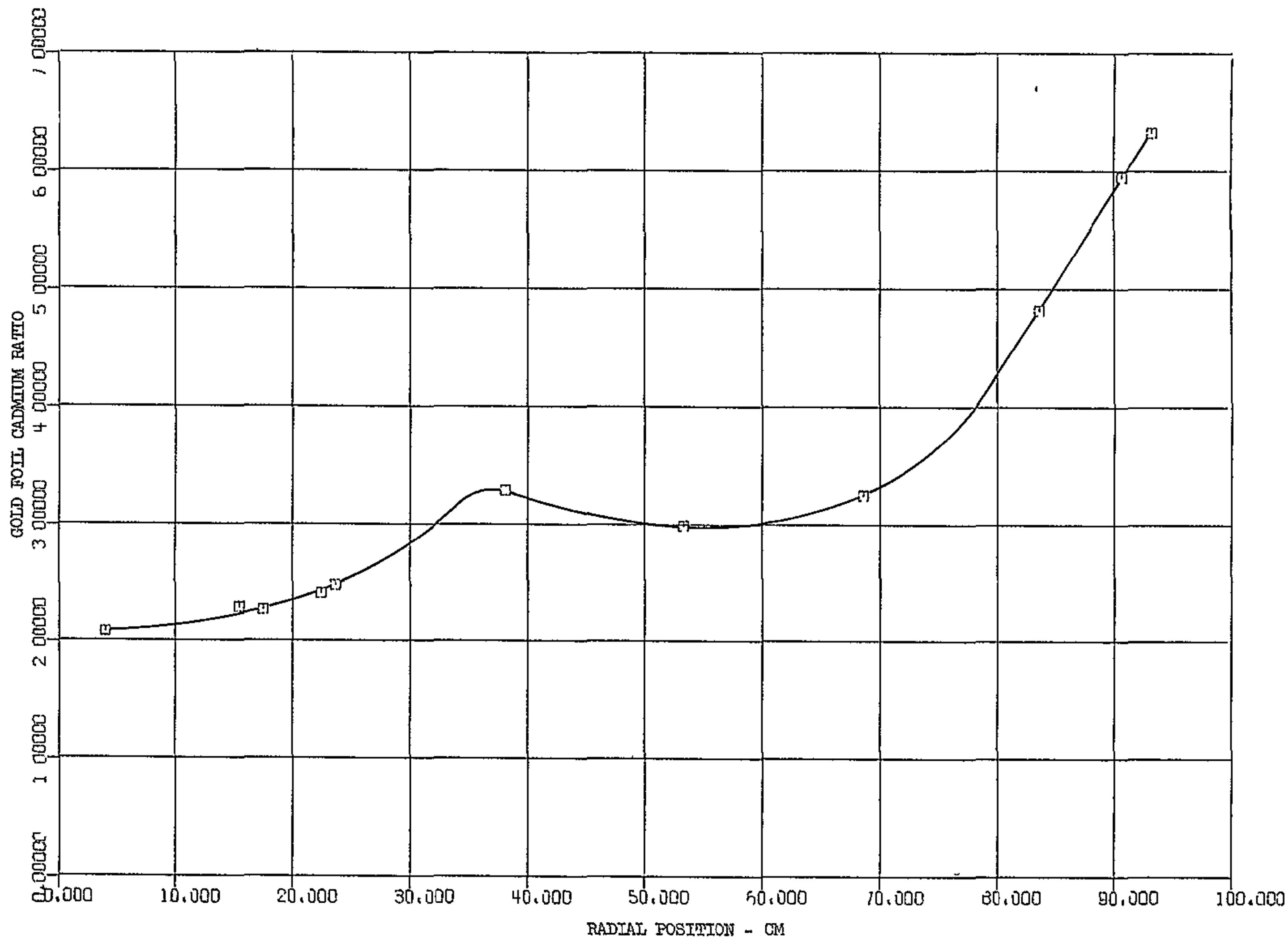

Figure 6 12 Gold Foil Cadmium Ratio - module 1 and between modules 5 & 6; 0 72 radius ratio

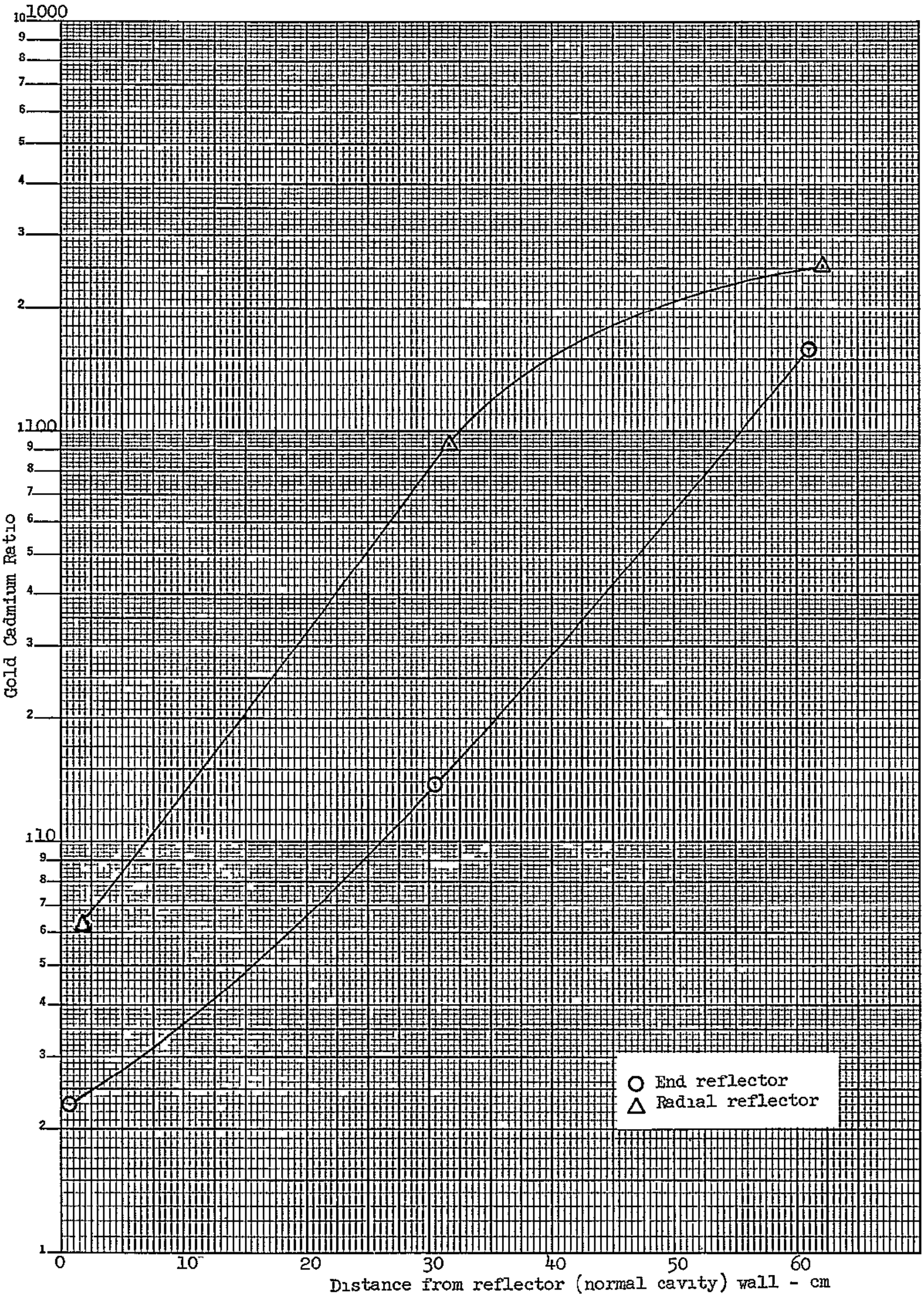

Figure 6 13 Infinite dilute gold cadmium ratios along centerlines of end and radial reflectors

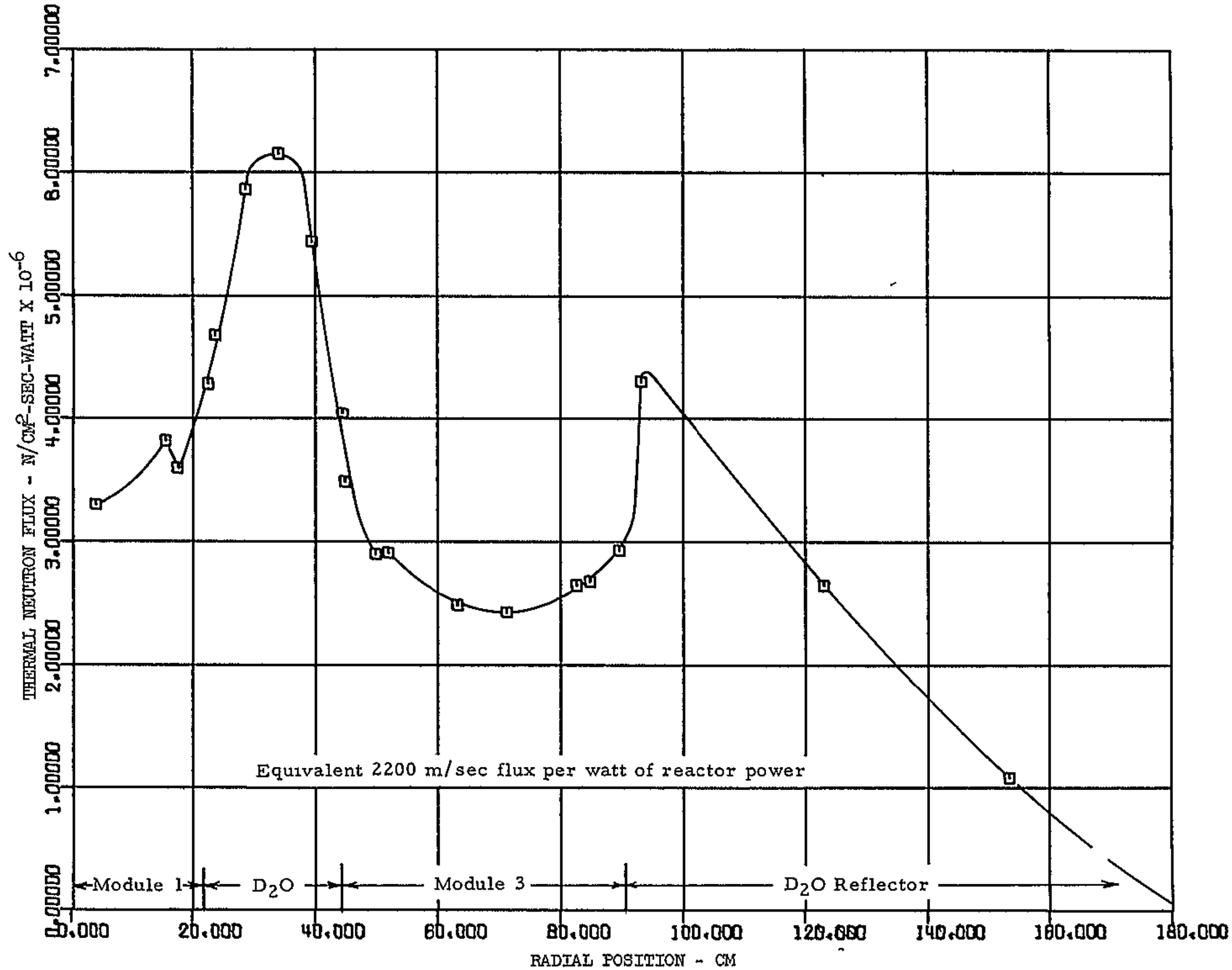

Figure 6 14 Radial distribution of thermal neutron flux from the center of the reactor across module 3 and into the radial reflector; 7 module reactor with 0 72 fuel to module radius ratio

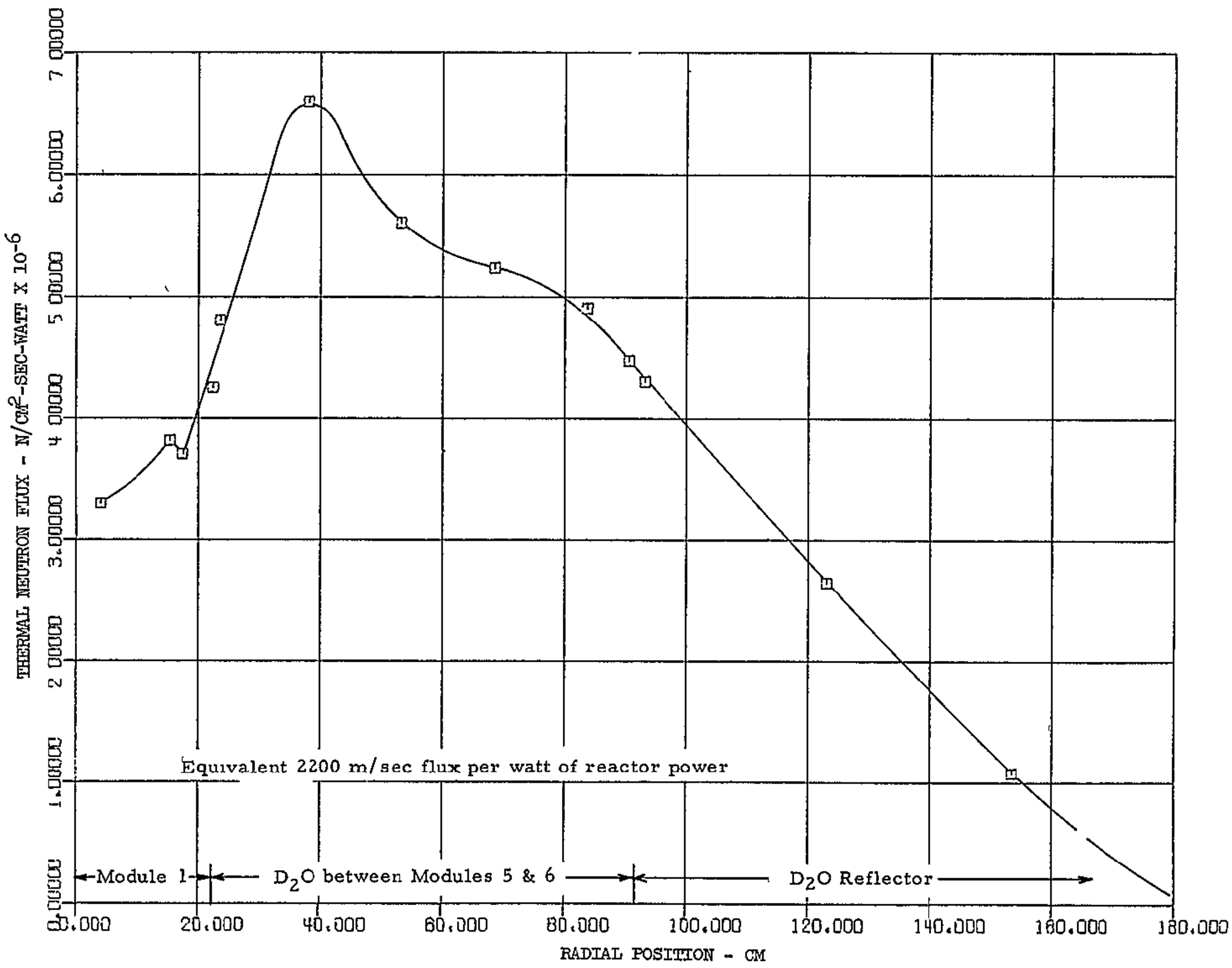

Figure 6.15 Radial distribution of thermal neutron flux from module 1 through the D_2O between modules 5 & 6 and into the radial reflector, 7-module reactor with 0 72 radius ratio

7.0 0 38 RADIUS RATIO CORE - 7 MODULE SYSTEM WITH HYDROGEN

A radius ratio of 0 388 for fuel to cavity dimensions was assembled in all seven of the modules The hydrogen simulation was still the same as for the 0.55 and 0.72 radius ratio systems, ie hydrogen began at the 0 72 R_0 position, or a diameter of 32 8 cm The 7 6 cm annular space from the outer ring of fuel, having a diameter of 17 5 cm, to the hydrogen contained no fuel, only a very dilute concentration of aluminum.

7 1 Initial Loading

The anticipated loading for criticality was 12 kg of uranium. The loading commenced from the 0.55 radius ratio without hydrogen, Section 8. One module at a time was changed by increasing its loading to 1.71 kg within four rings and the corresponding 0 38 radius ratio on the spacer disks and by simultaneously adding the hydrogen. The worth of the change in each of the outer modules was averaging approximately +0 3%Δk Therefore, after changing five of the six outer modules, it was decided that the fuel loading needed to be reduced below the predicted 12 kg so as to attain a final loading that was not excessively poisoned by control rods inserted into the end reflector.

The final loading consisted of 10 51 kg (1 50 kg per module), distributed on the four rings and spacer disks as shown in Table 7 1 and Figure 7.1 The excess reactivity was 1 00%Δk, without the end plug in the exhaust nozzle, ie. nozzle open

7 2 Reactivity Measurements

The worth of fuel was measured as a function of radius in the center module and of radius and angle in a typical peripheral module. These measurements were made with wands containing fuel uniformly distributed along the length of the reactor The results are given in Table 7.2, and are graphically presented in Figure 7 2 From these results, the integrated fuel worth throughout the seven modules was deduced, from which an overall "core" average worth of 2 87%Δk per kg of uranium was obtained. Note, the measurement results shown in Figure 7.2 and Table 7 2 give fuel worths out beyond the 8 75 cm radius of the fuel. However, the "core" average fuel worth of 2 87%Δk/kg refers only to the region out to the 0 38 radius ratio. The above fuel worth can be used to obtain an exactly critical mass (k=1 00.) of 10.16 kg of uranium, without the end plug in the exhaust nozzle

The average worth of aluminum in the center module from the center to the hydrogen (0.72 radius ratio) was measured to be 0 063%Δk/kg. This is about 80% of the value measured in the 0 55 radius ratio configuration, where a seven module core-average value of 0.030%Δk/kg was determined. Stainless steel, approximately 0 03 mean free absorption paths thick, was selectively placed on the module walls so as to give a representative measure of the average worth of stainless steel liner. The measurements gave 0.24%Δk/kg SS liner 0.12 cm thick (0.03 mean free paths) on all the walls, both radial and end, on all seven modules would create a 28%Δk penalty.

7.3 Power Distribution

The power distribution in the modules was measured using catcher foils. The same three typical radial traverses as employed for the fuel worth measurements were employed, but in each case detailed longitudinal traverses were made The average of the longitudinal, however, shows that the power distribution is a flatter function than the fuel worth function vs radius. The tabulated power distribution is given in Table 7.3, and is shown graphically in Figures 7 3 to 7 6 Total fission production rate in the reactor was computed from this data for referencing the thermal flux data of the next section.

7.4 Neutron Flux Distributions

Neutron fluxes were measured with gold foils, both bare and cadmium covered. The bare gold data is tabulated in Table 7 4, and presented graphically in Figures 7 7 and 7 8 These two figures also show the thermal (equivalent 2200 m/sec) per watt of reactor fission power Note, the traverse in the radial reflector starts along a line between two modules, and thus does not show the flux peak that usually occurs just outside the cavity region The thermal flux was obtained by subtracting the epi-cadmium activity from the bare activity The results of these measurements are given in Table 7 6, and are plotted in Figures 7 7 and 7 10 Note, all thermal flux values have been normalized to one watt of total reactor power The infinitely dilute gold cadmium ratios (Total activity/Epi-cadmium activity) are shown in Table 7 5 and Figures 7 11 and 7 12

TABLE 7 1

Fuel Element Loading Arrangement

0 38 Radius Ratio Configuration

Ring	Diameter (cm)		Number of Full Sized Sheets
1	6 1		3
2	9 9		6
3	13 7		9
4	17 5		12
		Total	30

Total on 16 stages = 480

Disks

Each of 17 disks contained

Single layers at positions 1, 3, 4, 6   See Figure 7 1
Double layers at positions 2,5

Full sized sheets 4
Half sized sheets 3

Total of 68 full size
Total of 51 half size

Module total - 573-1/2 full-sized equivalent sheets
or 1 501 kg

TABLE 7 2

Material Worth Measurements

7-Module Reactor – 0 38 Radius Ratio

Hydrogen in Reactor

	Location				
Module	Angle (°cw)	Radius (cm)	Material Mass (g)	Reactivity Change (%Δk)	Material Worth %Δk/kg
			Uranium Worth		
1	90	4 0	7 28	0 0268±0 003	3 68±0 41
1	90	7 8	7 28	0 0332±0 003	4 56±0 41
1	90	11 6	7 28	0 0570±0 003	7 83±0 41
3	90	4 0	7 28	0 0172±0 003	2 36±0 41
3	90	7 8	7 28	0 0208±0 003	2 86±0 41
3	90	11 6	7 28	0 0298±0 003	4 09±0 41
3	270	4 0	7 28	0 0158±0 003	2 17±0 41
3	270	11 6	7 28	0 0363±0 003	4 99±0 41
"Core" average fuel worth (7 modules, 0 cm to 8 75 cm) = 2 87 %Δk/kg					
			Aluminum Worth		
1	Module 1 Average		540	-0 0340±0 003	0 0630±0 0056
			Stainless Steel Worth		
1,2,3,4	Module Wall		850 5 g (4, 2 54 cm strips)	0 224±0 014	-0 263±0 016
5,6,7	Module Wall		637 0 g (3, 2 54 cm strips)	0 141±0 015	-0 221±0 024
Overall average = -0 245±0 014 %Δk/kg					

TABLE 7 3

Power Distribution

Catcher Foil Data

7-Module Reactor - 0 38 Radius Ratio

With Hydrogen

Run 1181

Foil Number	Foil Type	Module Number	Location			Normalized Counts	Local to Foil (X)
			Angle (°cw)	Radial (cm)	Axial (cm)		
1	Bare	1	90	4 0	92 5	183675	1 054
2	Bare	1	90	4 0	105 8	155738	0 893
3	Bare	1	90	4 0	121 0	152402	0 874
4	Bare	1	90	4 0	151 5	174285	1 000 (X)
5	Bare	1	90	4 0	166 8	170470	0 978
6	Bare	1	90	4 0	182 0	159598	0 916
7	Bare	1	90	4 0	197 2	156243	0 896
8	Bare	1	90	4 0	210 5	177867	1 020
9	Bare	1	90	7 8	92 5	209905	1 204
10	Bare	1	90	7 8	105 8	199126	1 142
11	Bare	1	90	7 8	121 0	200897	1 152
12	Bare	1	90	7 8	151 5	214323	1 230
13	Bare	1	90	7 8	166 8	206889	1 187
14	Bare	1	90	7 8	182 0	195432	1 121
15	Bare	1	90	7 8	197 2	184282	1 057
16	Bare	1	90	7 8	210 5	200583	1 151
17	Bare	1	90	11 6	92 5	254166	1 458
18	Bare	1	90	11 6	105 8	254442	1 460
19	Bare	1	90	11 6	121 0	259455	1 488
20	Bare	1	90	11 6	151 5	264577	1 518
21	Bare	1	90	11 6	166 8	268522	1 541
22	Bare	1	90	11 6	182 0	248947	1 428
23	Bare	1	90	11 6	197 2	236899	1 359
24	Bare	1	90	11 6	210 5	240696	1 381
25	Bare	1	90	15 4	92 5	263888	1 514
26	Bare	1	90	15 4	105 8	261593	1 501
27	Bare	1	90	15 4	121 0	----	---
28	Bare	1	90	15 4	151 5	282014	1 618
29	Bare	1	90	15 4	166 8	276615	1 587
30	Bare	1	90	15 4	182 0	268873	1 543
31	Bare	1	90	15 4	197 2	257799	1 479
32	Bare	1	90	15 4	210 5	240168	1 378
33	Bare	3	90	4 0	92 5	125735	0 721
34	Bare	3	90	4 0	105 8	113203	0 649
35	Bare	3	90	4 0	121 0	114747	0 658
36	Bare	3	90	4 0	151 5	117210	0 672
37	Bare	3	90	4 0	166 8	117378	0 673
38	Bare	3	90	4 0	182 0	113773	0 653

TABLE 7 3

(Continued)

Run 1181

Foil Number	Foil Type	Module Number	Angle (°cw)	Location Radial (cm)	Axial (cm)	Normalized Counts	Local to Foil (X)
39	Bare	3	90	4 0	197 2	107755	0 618
40	Bare	3	90	4 0	210 5	124437	0 714
41	Bare	3	90	7 8	92 5	142525	0 818
42	Bare	3	90	7 8	105 8	138566	0 795
43	Bare	3	90	7 8	121 0	137944	0 791
44	Bare	3	90	7 8	151 5	141301	0 811
45	Bare	3	90	7 8	166 8	140018	0 803
46	Bare	3	90	7 8	182 0	136823	0 785
47	Bare	3	90	7 8	197 2	131343	0 754
48	Bare	3	90	7 8	210 5	137438	0 788
49	Bare	3	90	11 6	92 5	166950	0 958
50	Bare	3	90	11 6	105 8	170026	0 975
51	Bare	3	90	11 6	121 0	173663	0 996
52	Bare	3	90	11 6	151 5	184274	1 057
53	Bare	3	90	11 6	166 8	174412	1 001
54	Bare	3	90	11 6	182 0	174438	1 001
55	Bare	3	90	11 6	197 2	163507	0 938
56	Bare	3	90	11 6	210 5	160273	0 919
57	Bare	3	90	15 4	92 5	181315	1 040
58	Bare	3	90	15 4	105 8	177698	1 019
59	Bare	3	90	15 4	121 0	190976	1 096
60	Bare	3	90	15 4	151 5	182421	1 047
61	Bare	3	90	15 4	166 8	189458	1 087
62	Bare	3	90	15 4	182 0	176452	1 012
63	Bare	3	90	15 4	197 2	171216	0 982
64	Bare	3	90	15 4	210 5	164896	0 946
Run 1182							
1	Bare	3	270	4 0	92 5	209446	1 202
2	Bare	3	270	4 0	105 8	208327	1 195
3	Bare	3	270	4 0	121 0	214298	1 229
4	Bare	3	270	4 0	151 5	211242	1 212
5	Bare	3	270	4 0	182 0	211733	1 215
6	Bare	3	270	4 0	197 2	203238	1 166
7	Bare	3	270	4 0	210 5	200561	1 151
8	Bare	3	270	7 8	92 5	194471	1 116
9	Bare	3	270	7 8	105 8	194029	1 113
10	Bare	3	270	7 8	121 0	205857	1 181
11	Bare	3	270	7 8	151 5	211503	1 213
12	Bare	3	270	7 8	182 0	189240	1 086
13	Bare	3	270	7 8	197 2	185085	1 062
14	Bare	3	270	7 8	210 5	192720	1 106

TABLE 7 3

(Continued)

Foil Number	Foil Type	Module Number	Angle (°cw)	Location Radial (cm)	Axial (cm)	Normalized Counts	Local Foil (X)
15	Bare	3	270	11 6	92 5	162716	0 934
16	Bare	3	270	11 6	105 8	153147	0 879
17	Bare	3	270	11 6	121 0	163614	0 939
18	Bare	3	270	11 6	151 5	158861	0 911
19	Bare	3	270	11 6	182 0	148729	0 853
20	Bare	3	270	11 6	197 2	143640	0 824
21	Bare	3	270	11 6	210 5	159290	0 914
22	Bare	3	270	15 4	92 5	130061	0 746
23	Bare	3	270	15 4	105 8	119911	0 688
24	Bare	3	270	15 4	121 0	121298	0 696
25	Bare	3	270	15 4	151 5	131828	0 756
26	Bare	3	270	15 4	182 0	117993	0 677
27	Bare	3	270	15 4	197 2	112231	0 644
28	Bare	3	270	15 4	210 5	133838	0 768
Run 1183							
1	Cd Cov	1	90	4 0	182 0	6301	25 3
2	Cd Cov	1	90	15 4	182 0	6349	42 3
3	Cd Cov	3	90	4 0	182 0	4349	26 2
4	Cd Cov	3	90	15 4	182 0	4407	40 0

TABLE 7 4

Bare Gold Foil Data

7-Module Cavity Reactor - 0 38 Radius Ratio

With Hydrogen

Run 1181

Foil Number	Foil Type	Location Radial (cm)	Location Axial (cm)	Foil Weight (g)	Specific Activity d/m-g $\times 10^{-6}$	Local to Foil (X)
1	Bare	0	89 4	0 0359	7 797	1 137
2	Bare	0	74 9	0 0396	10 233	1 492
3	Bare	0	59 6	0 0360	7 701	1 123
4	Bare	0	44 4	0 04006	5 090	0 742
5	Bare	0	29 1	0 04283	2 934	0 428
6	Bare	0	13 9	0 0357	1 508	0 220
7	Bare	0	0	-0 0360	0 199	0 029
8	Bare	93 2	151 1	0 0348	8 530	1 244
9	Bare	107 7	151 1	0 0343	6 830	0 996
10	Bare	123 0	151 1	0 0379	4 906	0 715
11	Bare	138 2	151 1	0 0374	3 254	0 474
12	Bare	153 4	151 1	0 0347	1 977	0 288
13	Bare	168 7	151 1	0 0352	0 893	0 130
14	Bare	183 7	151 1	0 0353	0 122	0 018
	Module 1, 90° cw					
15	Bare	4 0	136 3	0 0350	6 859	1 000(X)
16	Bare	7 8	136 3	0 0358	7 923	1 155
17	Bare	11 6	136 3	0 0344	11 022	1 607
18	Bare	15 4	136 3	0 0351	10 191	1 486
	Module 3, 90° cw					
19	Bare	4 0	136 3	0 0354	4 935	0 719
20	Bare	7 8	136 3	0 0350	5 786	0 844
21	Bare	11 6	136 3	0 0350	6 556	0 956
22	Bare	15 4	136.3	0.0361	6 856	1 000
	Traverse from Module 1 to Module 3					
23	Bare	23 6	151 1	0 0357	11 400	1 662
24	Bare	28 7	151 1	0 0350	13 078	1 907
25	Bare	34 0	151 1	0 0356	13 290	1 938
26	Bare	39 4	151 1	0 0354	11 832	1 725
27	Bare	44 4	151 1	0 0347	8 922	1 301
	Traverse Between Modules 5 & 6					
28	Bare	90 7	151 1	0 0349	8 638	1 259
29	Bare	83 8	151 1	0 0352	9 946	1 450
30	Bare	76 2	151 1	0 0347	9 838	1 434
31	Bare	68 6	151 1	0 0346	12 061	1 758
32	Bare	61 0	151 1	0 0355	11 586	1 689
33	Bare	53 3	151 1	0 0350	12 172	1 775
34	Bare	45 7	151 1	0 0367	13 065	1 905
35	Bare	38 1	151 1	0 0367	14 121	2 059

TABLE 7 4

(Continued)

Foil Number	Foil Type	Location Radial (cm)	Location Axial (cm)	Foil Weight (g)	Specific Activity d/m-g x 10^{-6}	Local to Foil (X)
Run 1181						
36	Bare	30 5	151 1	0 0369	13 937	2 032
37	Bare	23 6	151 1	0 0361	11 614	1 693
Run 1182						
1	Cd Cov	0	89 4	0 0349	2 029	
2	Cd Cov	0	59 6	0 0349	0 250	
3	Cd Cov	0	29 1	0 0349	0 007	
4	Cd Cov	93 2	151 1	0 0350	0 652	
5	Cd Cov	123 0	151 1	0 0350	0 025	
6	Cd Cov	153 4	151 1	0 0348	0 004	
	Module 3, 270° cw					
7	Bare	15 4	136 3	0 0349	7 693	1 122
8	Bare	11 6	136 3	0 0350	7 309	1 066
9	Bare	7 8	136 3	0 0350	6 155	0 897
10	Bare	4 0	136 3	0 0349	4 935	0 719
11	Cd Cov	4 0	166 8	0 0352	1 638	
12	Cd Cov	15 4	166 8	0 0354	1 597	
	Traverse from Module 1 to Module 3					
13	Cd Cov	23 6	151 1	0 0352	2 559	
14	Cd Cov	34 0	151 1	0 0351	2 411	
15	Cd Cov	44 4	151 1	0 0350	1 935	
	Traverse Between Modules 5 & 6					
16	Cd Cov	83 8	151 1	0 0348	0 982	
17	Cd Cov	53 3	151 1	0 0350	2 040	
18	Cd Cov	23 6	151 1	0 0353	2 563	
Run 1183						
1	Bare	0	82 5	0 0362	10 217	1 490
2	Bare	0	67.2	0 0353	10 289	1 500
3	Bare	0	52 0	0 0356	6 107	0 890
4	Bare	100 1	151 1	0 0351	7 638	1 114
5	Bare	115 4	151 1	0 0352	5 846	0 852
6	Bare	130 2	151 1	0 0358	4 057	0 591
	Module 1, 90°					
7	Cd Cov	4 0	136 3	0 0349	2 242	
8	Cd Cov	15 4	136 3	0 0351	2 392	
	Module 3, 90°					
9	Cd Cov	4 0	136 3	0 0351	1 526	
10	Cd Cov	15 4	136 3	0 0350	1 611	
	Traverse from Module 1 to Module 3					
11	Cd Cov	28 7	151 1	0 0350	2 601	
12	Cd Cov	39 4	151 1	0 0349	2 225	

TABLE 7 4

(Continued)

Run 1183

Foil Number	Foil Type	Location Radial (cm)	Location Axial (cm)	Foil Weight (g)	Specific Activity d/m-g x 10^{-6}	Local to Foil (X)
	Traverse Between Modules 5 & 6					
13	Cd Cov	90 7	151 1	0 0351	0 656	
14	Cd Cov	68 6	151 1	0 0425	1 674	
15	Cd Cov	38 1	151 1	0 0475	1 985	

TABLE 7 5

Gold Foil Cadmium Ratios

7-Module Cavity Reactor - 0 38 Radius Ratio

With Hydrogen

Location				Infinitely Dilute Foil Activity d/m-g x 10^{-6}		
Radial (cm)	Axial (cm)	Module Number	Angle (°cw)	Bare Gold	Cd Gold	Cadmium Ratio
0	89 4	End Reflector		10 504	4 713	2 229
0	59 6	End Reflector		8 035	0 581	13 838
0	29 1	End Reflector		2 944	0 016	180 855
93 2	151 1	Radial Reflector		9 393	1 516	6 195
123 0	151 1	Radial Reflector		4 940	0 058	84 976
153 4	151 1	Radial Reflector		1 982	0 009	213 616
4 0	136 3	1	90	9 827	5 207	1 887
15 4	136 3	1	90	13 368	5 569	2 400
4 0	136 3	3	90	6 967	3 553	1 961
15 4	136 3	3	90	9 011	3 746	2 406
4 0	136 3	3	270	7 109	3 818	1 862
15 4	136 3	3	270	9 818	3 731	2 631
	Traverse from Module 1 to Module 3					
23 6	151 1			14 820	5 964	2.485
28 7	151 1			16 525	6 048	2 732
34 0	151 1			16 506	5 613	2 941
39 4	151 1			14 788	5 168	2 861
44 4	151 1			11 480	4 500	2 551
	Traverse From Module 1 Between 5 & 6					
23 6	151 1			15 055	5 980	2 517
38 1	151 1			17 154	5 245	3 271
53 3	151 1			14 876	4 744	3 136
68 6	151 1			14 457	4 219	3 427
83 8	151 1			11 247	2 278	4 937
90 7	151 1			9 508	1 527	6 226

TABLE 7 6

Thermal Neutron Flux

7-Module Reactor - 0 38 Radius Ratio

With Hydrogen

Location Radial (cm)	Axial (cm)	Module Number	Angle (°cw)	Thermal Neutron Flux (n/cm^2-sec-watt x 10^{-6})
0	89 4	End Reflector		3 845
0	59 6	End Reflector		4 949
0	29 1	End Reflector		1 944
93 2	151 1	Radial Reflector		5 229
123 0	151 1	Radial Reflector		3 241
153 4	151 1	Radial Reflector		1 310
4 0	136 3	1	90	3 067
15 4	136 3	1	90	5 178
4 0	136 3	3	90	3 067
15 4	136 3	3	90	5 178
4 0	136 3	3	270	2 185
15 4	136 3	3	270	4 041
	Traverse from Module 1 Through Module 3			
23 6	151 1	3		5 879
28 7	151 1	3		6 956
34 0	151 1	3		7 232
39 4	151 1	3		6 386
44 4	151 1	3		4 634
	Traverse From Module 1 Between 5 & 6			
23 6	151 1	3		6 024
38 1	151 1	3		7 906
53 3	151 1	3		6 726
68 6	151 1	3		6 797
83 8	151 1	3		5 954
90 7	151 1	3		5 298

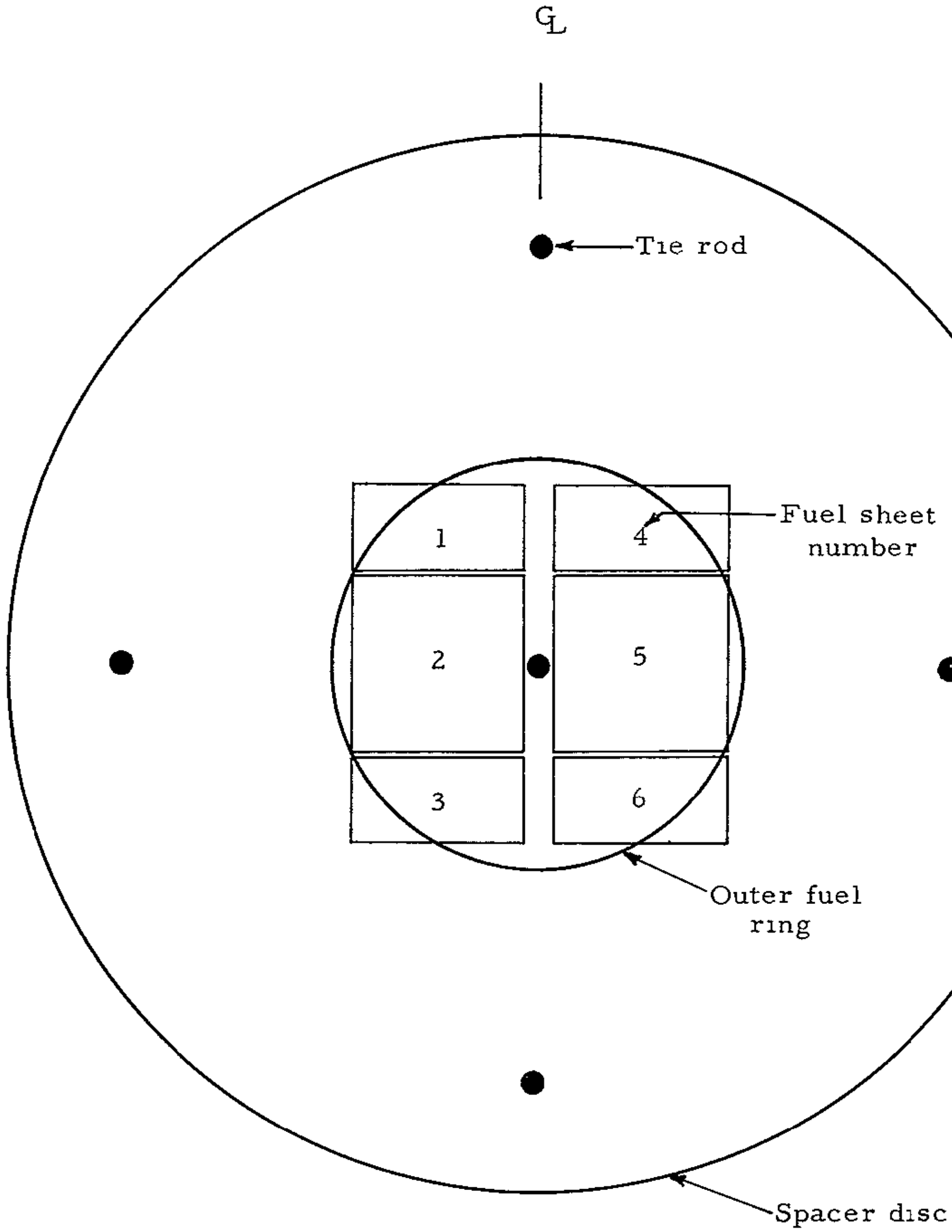

Figure 7 1 Fuel placement on disks Full sheets (2 and 5) will be double thickness Only three out of four half-size sheets (single thickness) will be on any given disk 7-module reactor with 0.388 radius ratio loading

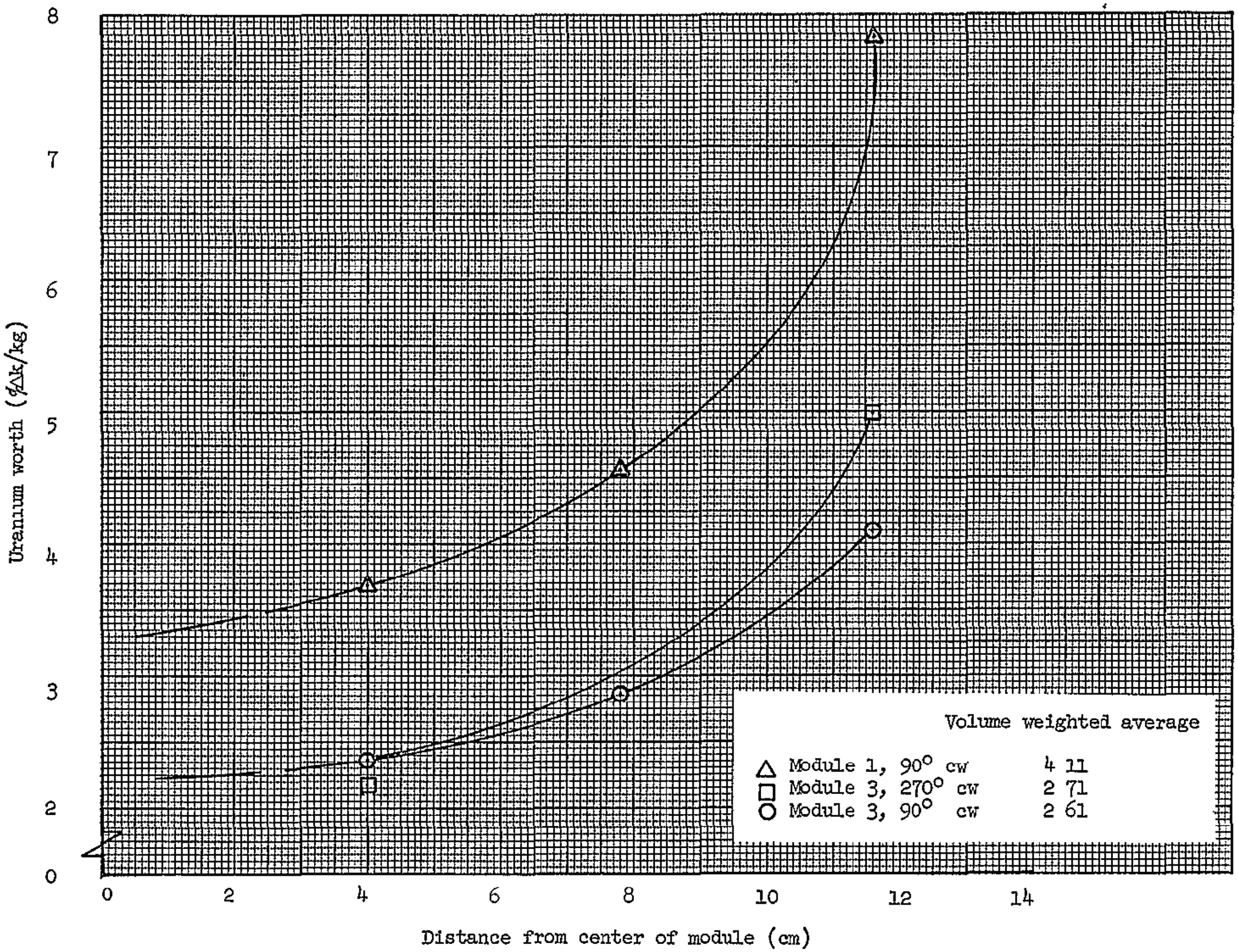

Figure 7.2 Uranium worth measurements, 7-module reactor with 0 38 fuel to module radius ratio

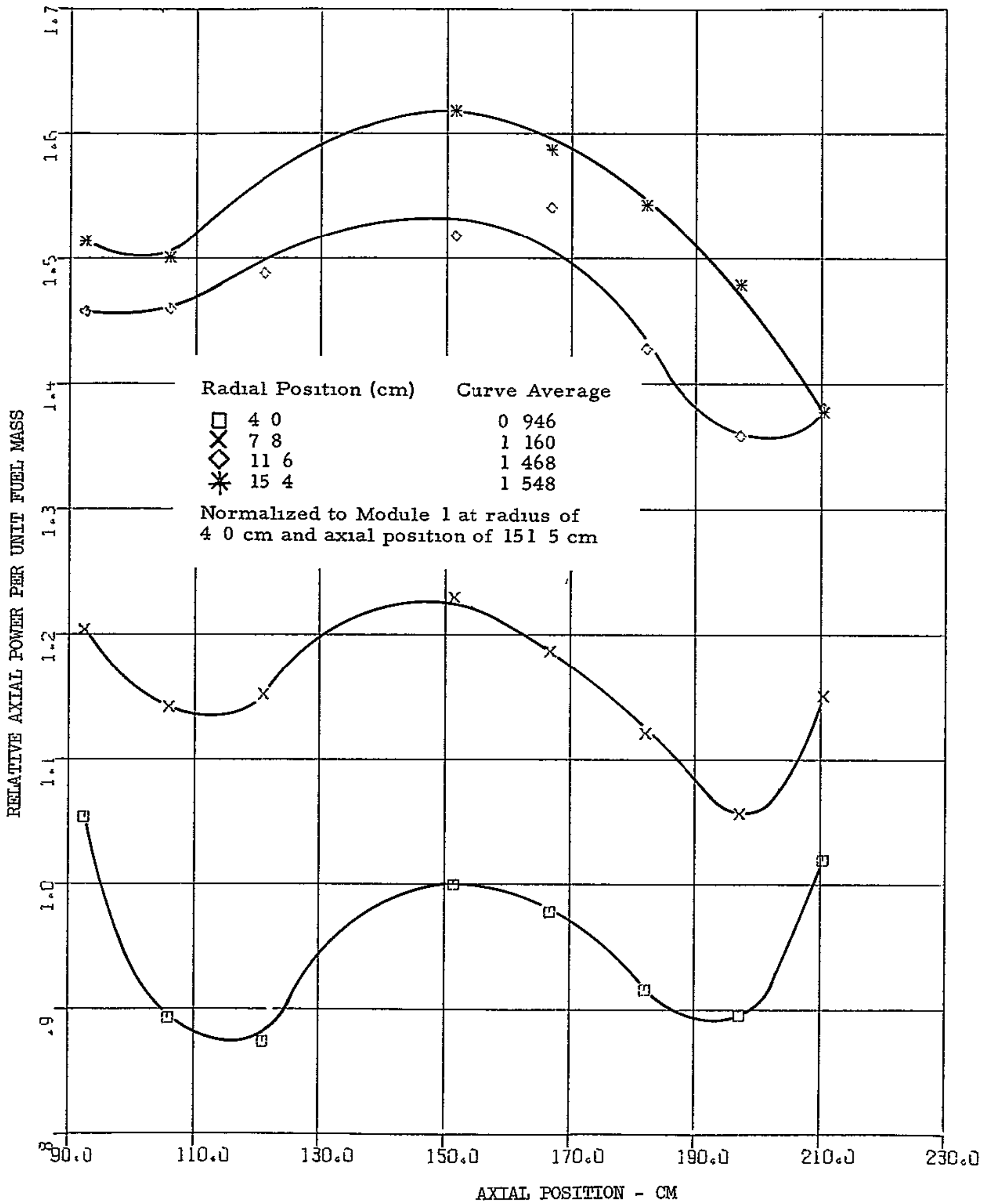

Figure 7 3 Relative axial power distribution in module 1, 90° at the core centerline, 7-module reactor with 0 38 fuel to module radius ratio

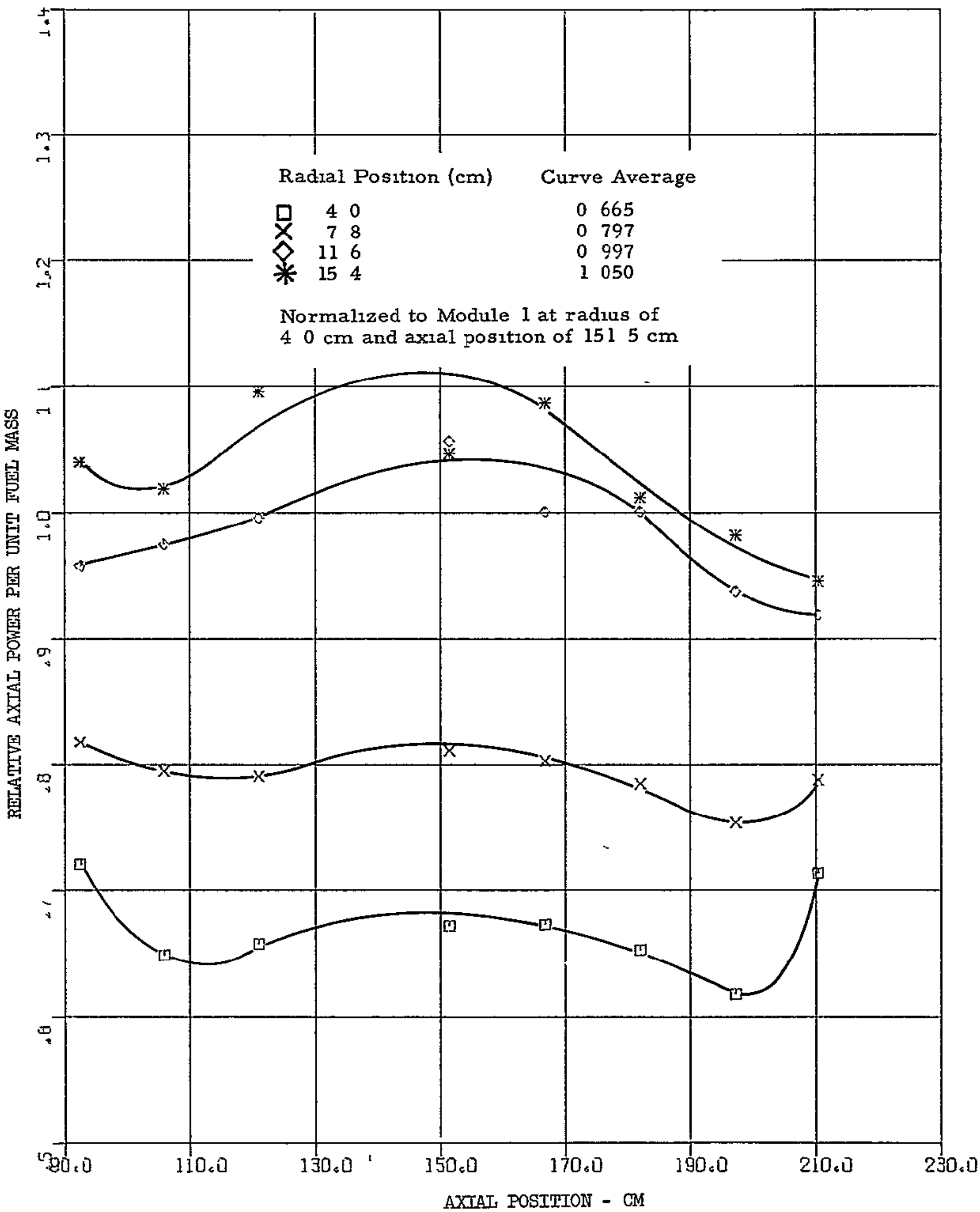

Figure 7.4 Relative axial power distribution in module 3, 90° at the core centerline, 7-module reactor with 0 38 fuel to module radius ratio

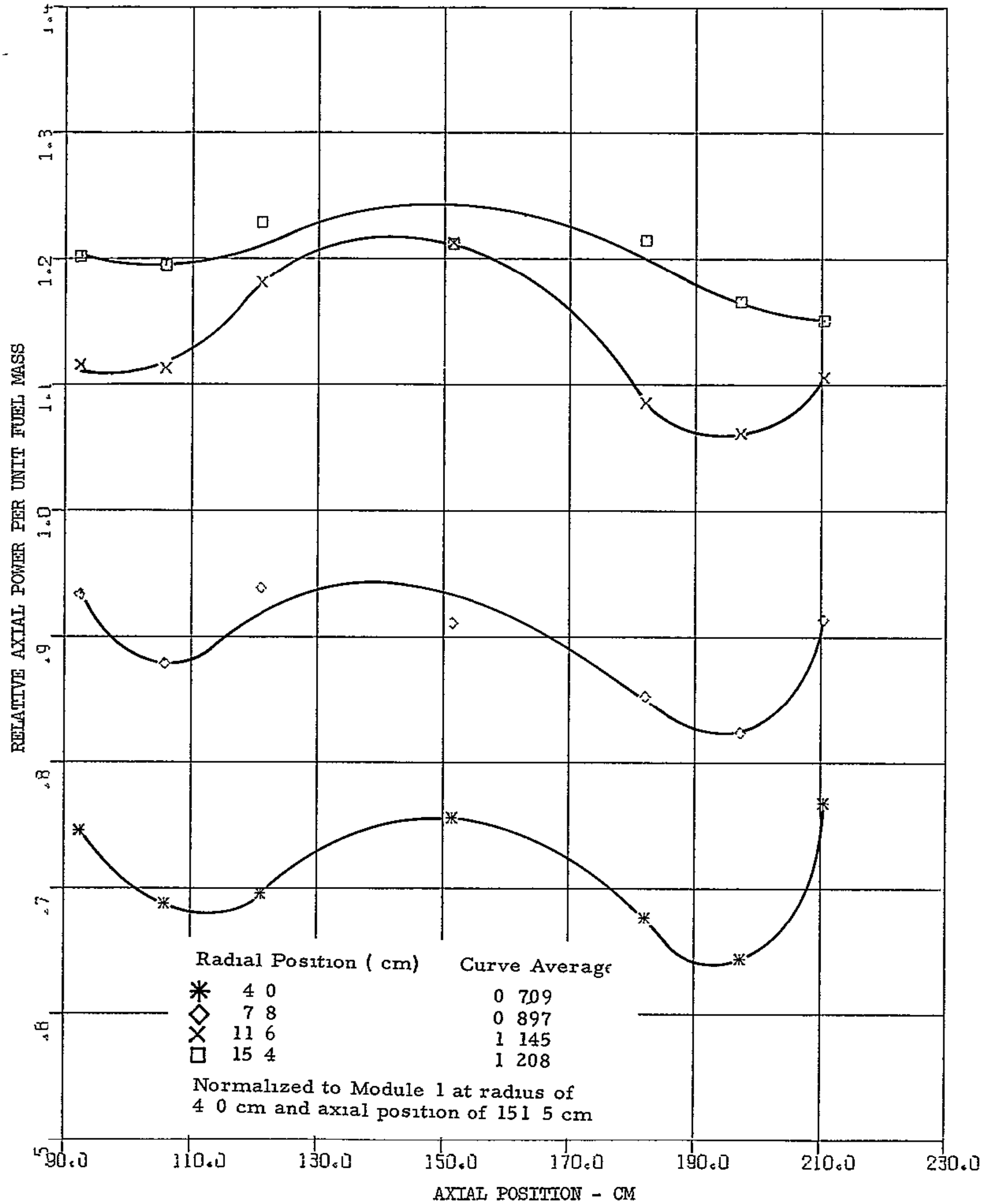

Figure 7 5 Relative axial power distribution in module 3, 270° at the core centerline, 7-module reactor with 0 38 fuel to module radius ratio

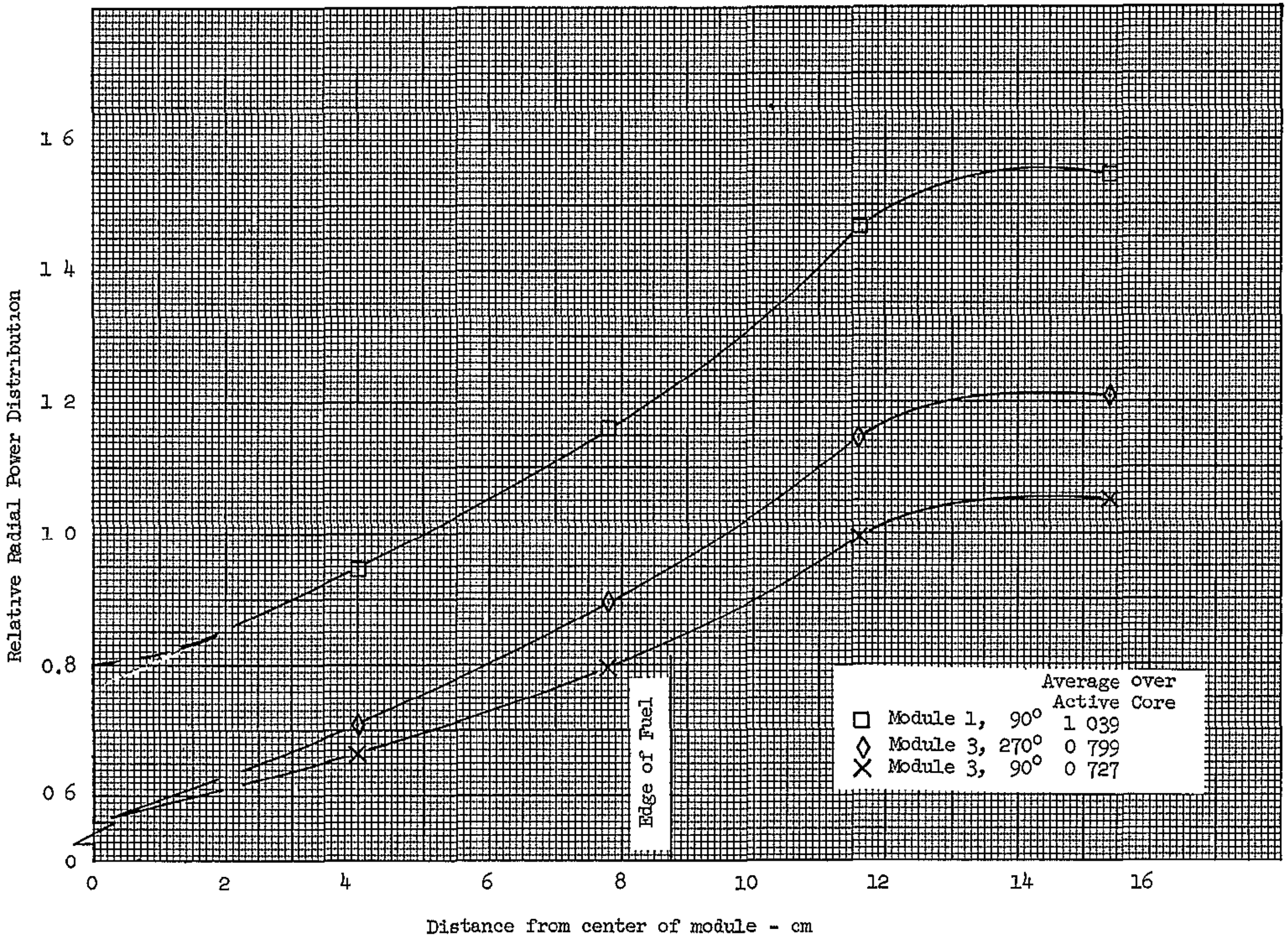

Figure 7 6 Normalized power distribution vs radius and angle, the plotted points are longitudinally averaged over core length

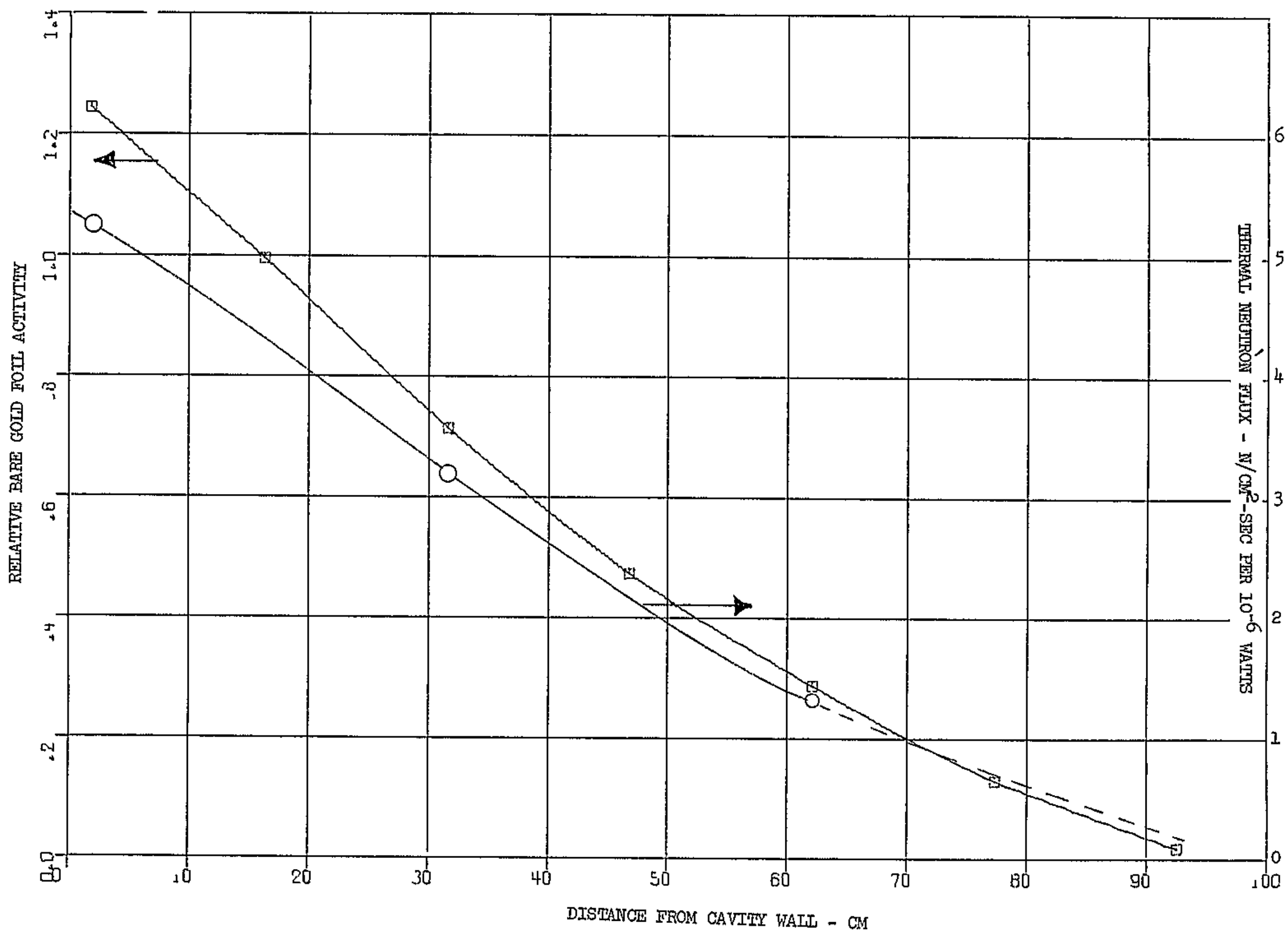

Figure 7.7 Bare gold activity and thermal flux in radial reflector, 7-module cavity reactor
0 38 radius ratio

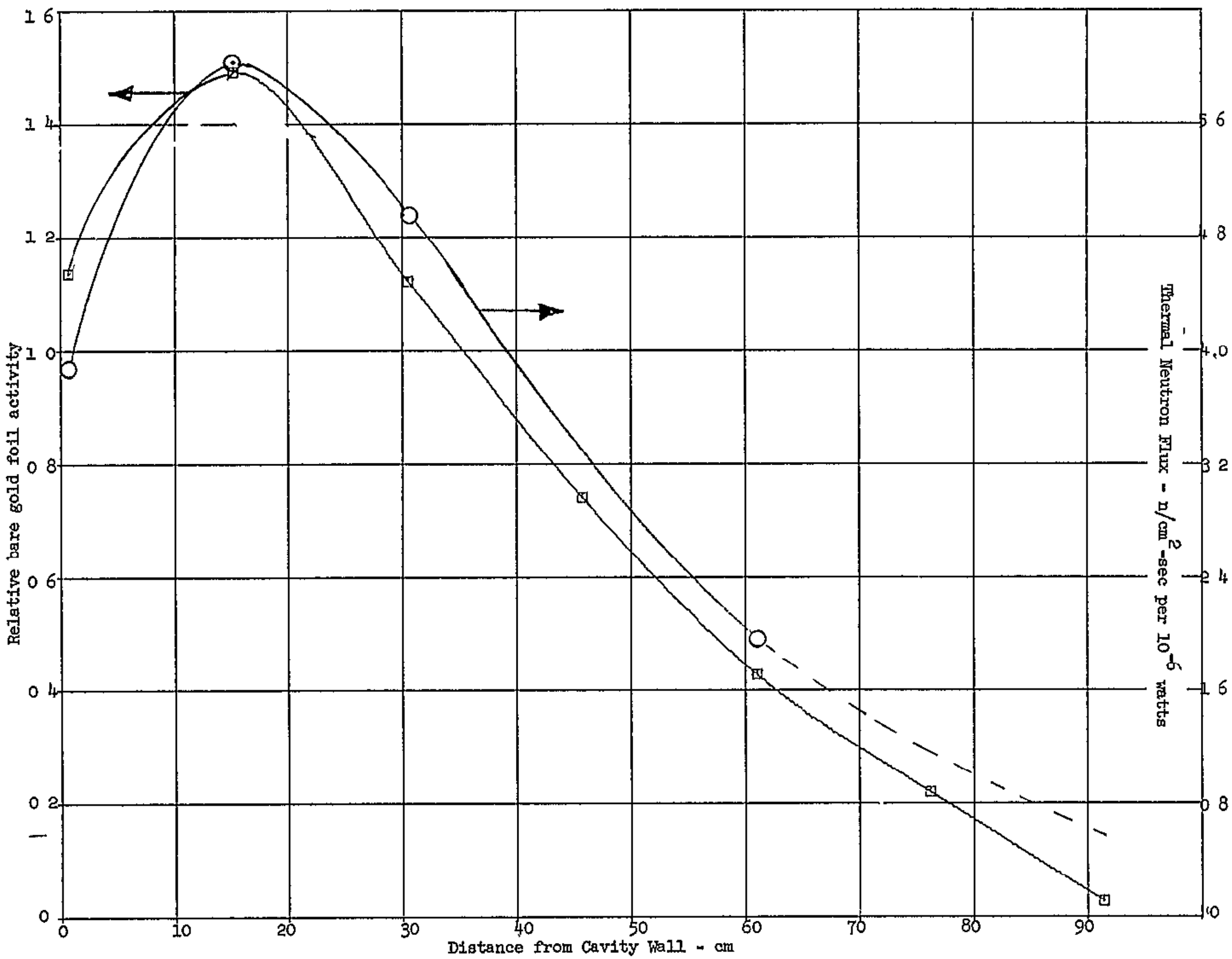

Figure 7.8 Bare gold activity and thermal flux in end reflector, 7-module cavity reactor 0.38 radius ratio

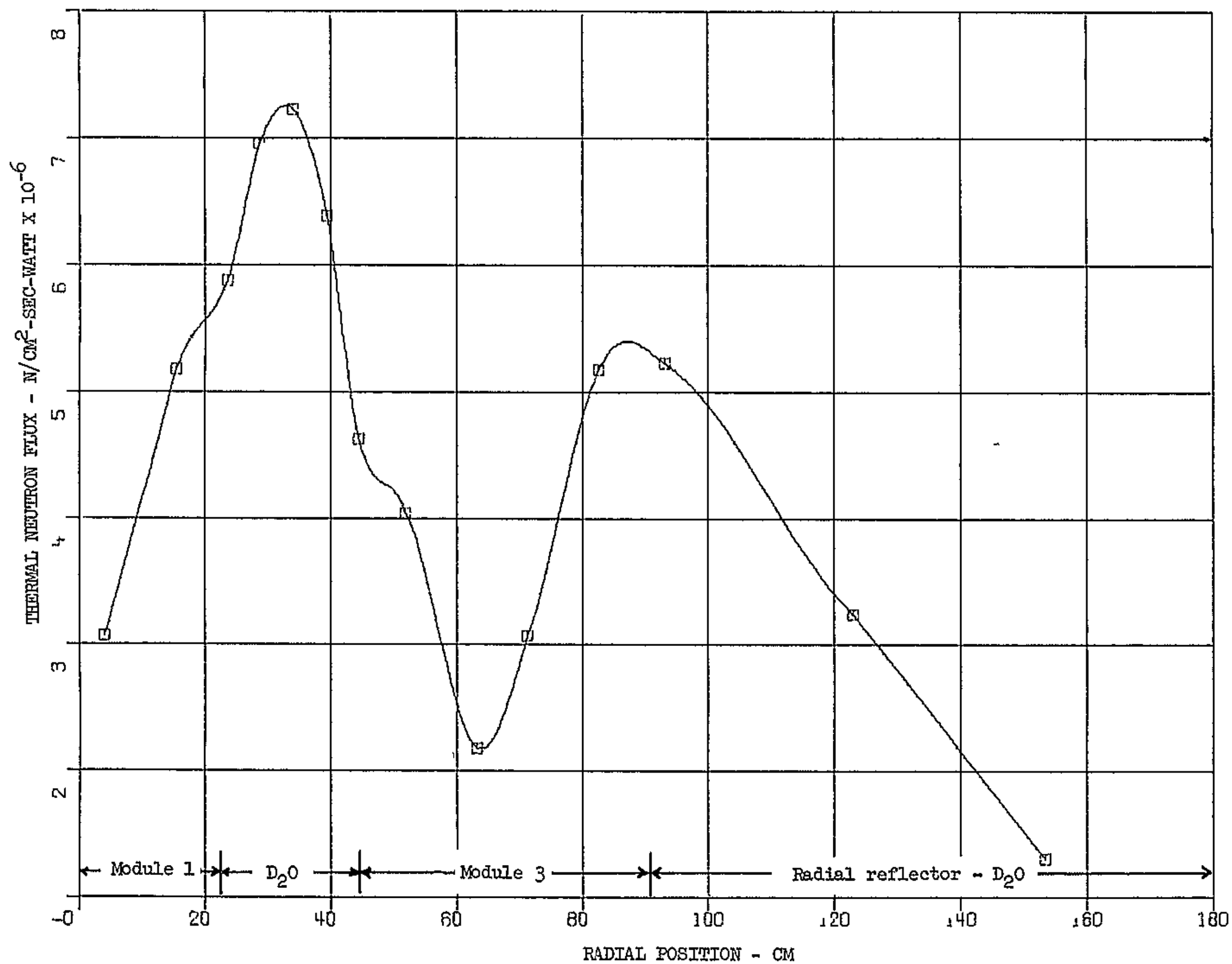

Figure 7.9 Radial distribution of thermal neutron flux from the center of the reactor across module 3 and into the radial reflector, 7-module reactor with 0 38 radius ratio

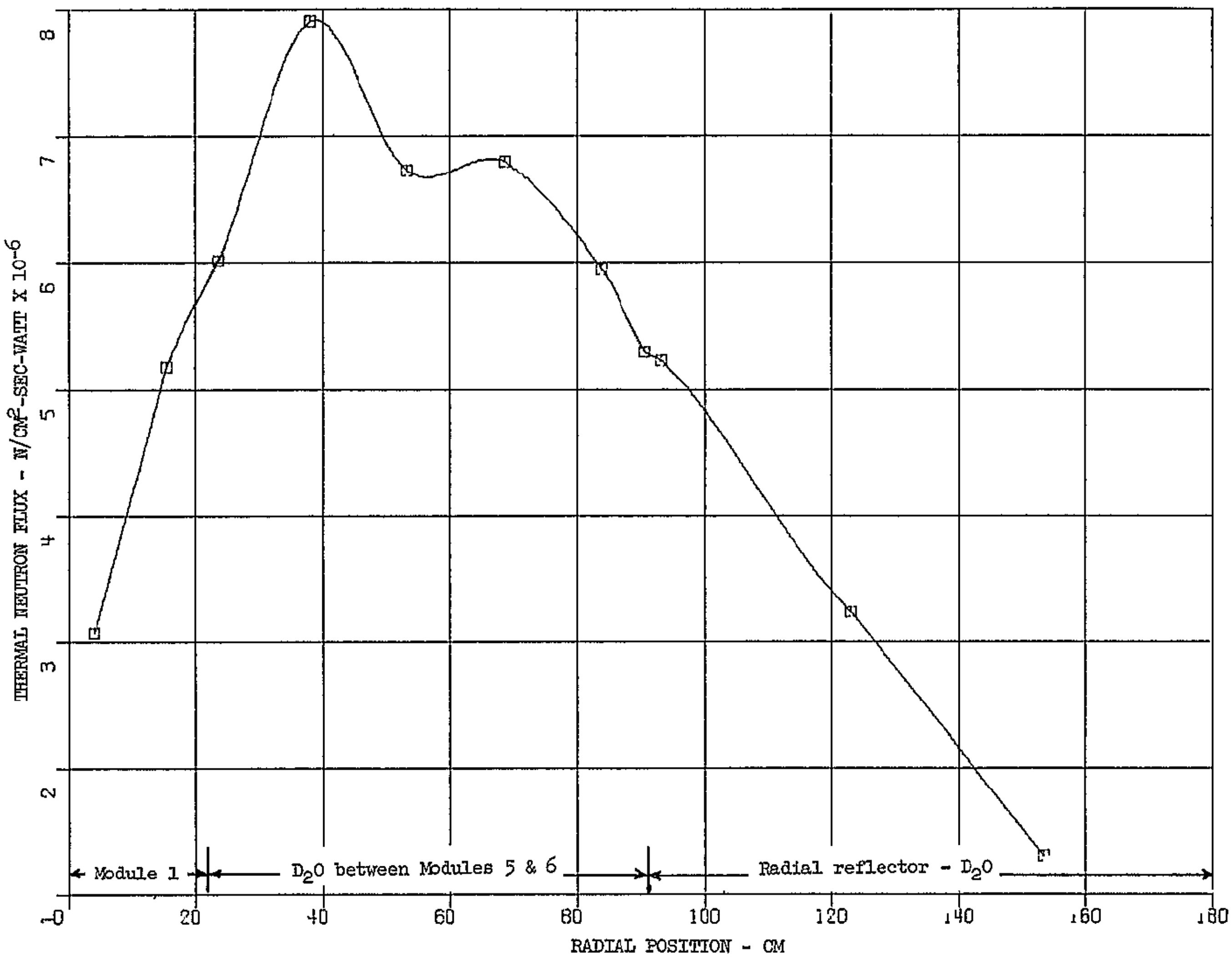

Figure 7.10 Radial distribution of thermal neutron flux from module 1 through the D_2O between modules 5 & 6 and into the radial reflector, 7-module reactor with 0.38 radius ratio

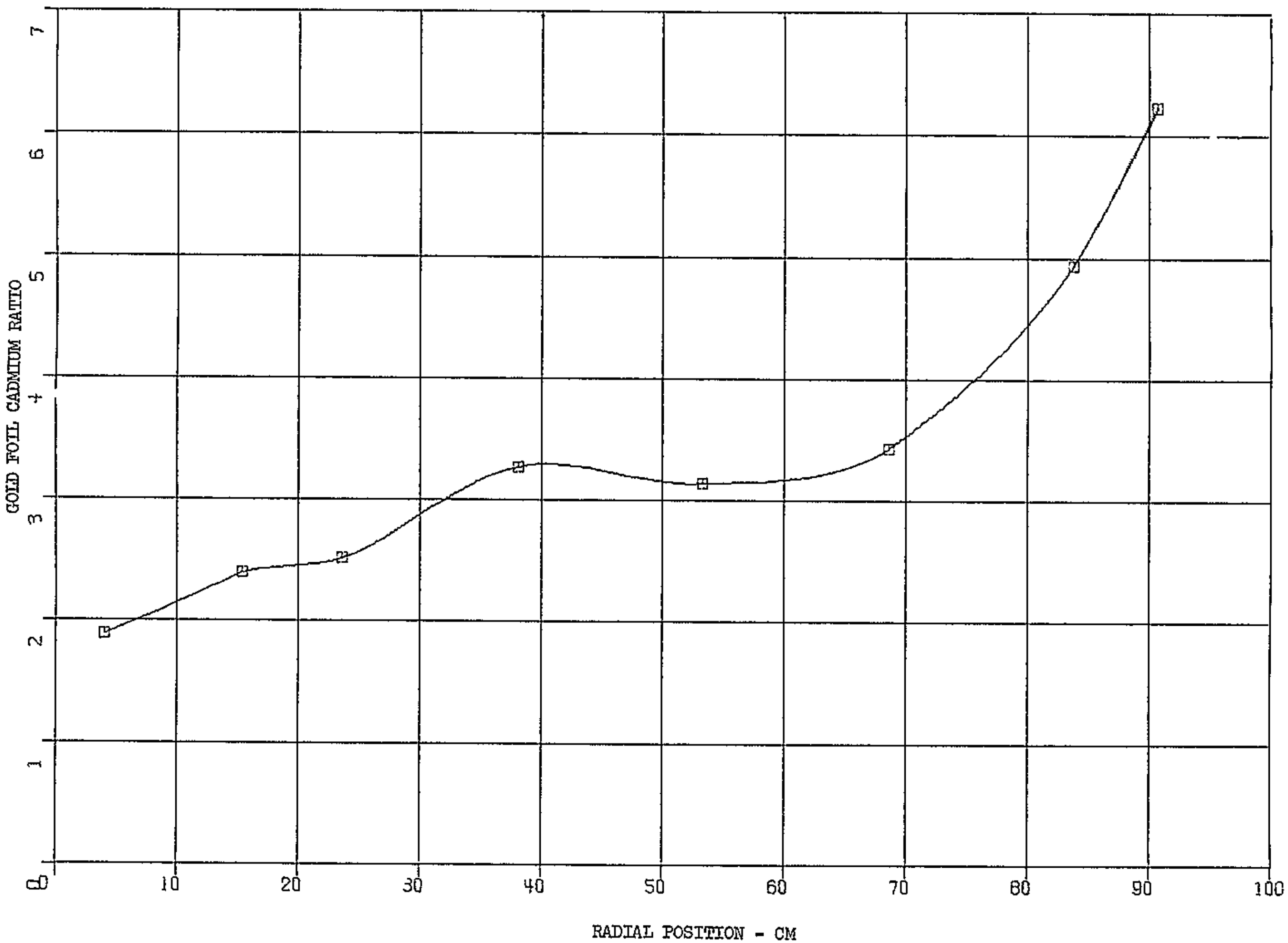

Figure 7.11 Infinitely dilute cadmium ratios from module 1 and between modules 5 & 6, 0.38 radius ratio

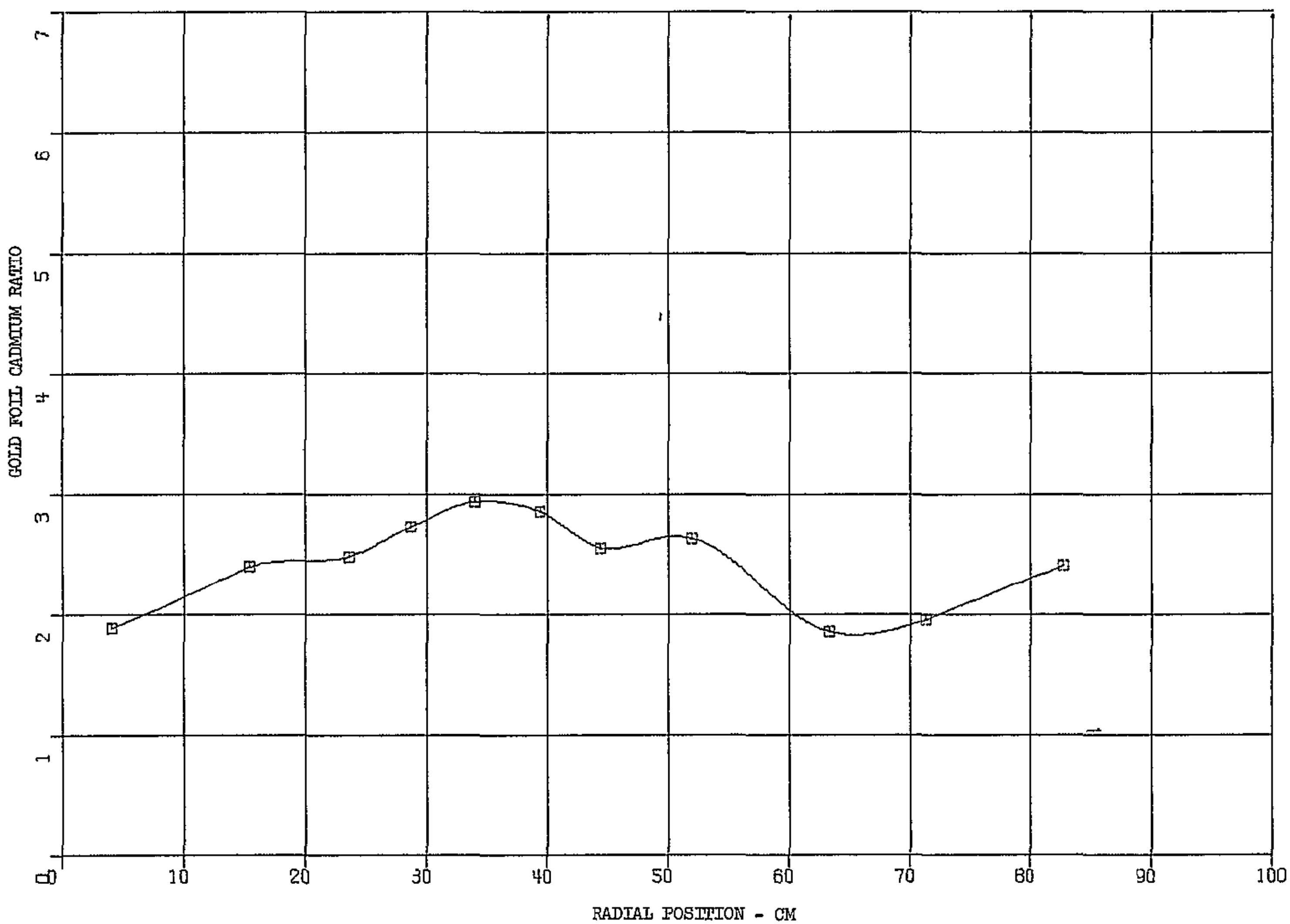

Figure 7.12 Gold foil cadmium ratio - module 1 through module 3, 0.38 fuel to module radius ratio

8.0 O 55 RADIUS RATIO WITHOUT HYDROGEN

Hydrogen coolant between the fuel regions and the heavy water reflector-moderator has a dual, deleterious effect on reactivity It both absorbs neutrons and acts as a diffusion barrier preventing the free migration of neutrons between the fuel and reflector Though the hydrogen does very effectively moderate the fast neutrons, this benefit is not very significant in a large reactor such as this, where fast leakage is not severe.

It is of value to know the reactivity penalty caused by the hydrogen, because there is some latitude available in engineering operating conditions of pressure, temperature, and annular thickness for this coolant. The hydrogen was removed from the 0 55 radius ratio configuration, which had a critical mass of 8 65 kg with hydrogen in the cavity.

8.1 Initial Loading

Loading of this configuration commenced with the 0.72 radius ratio configuration with hydrogen. One module at a time was converted by removing the hydrogen (styrofoam) and the outer two rings of fuel The net penalty was negative, averaging approximately -0 1%Δk per module In order to obtain the needed reactivity to remain critical, the nozzle plug was installed. The apparent worth of the plug was 0 96%Δk This plug was a complete cylinder, not the tank-inside-of-a-tank arrangement measured separately on the configuration with hydrogen and reported in Table 5.6. When the modification of all seven modules was completed, the mass of fuel in the reactor was 7.82 kg of uranium and

Kexcess was +0 36%Δk with the nozzle plug in
or -0.60%Δk with the plug out.

The fuel loading on each of the rings and disks is tabulated in Table 8 1, where a comparison tabulation of the 0 55 radius ratio configuration with hydrogen is also shown. The configuration without hydrogen had a small proportion of its fuel on the disks (16%) compared to the configuration with hydrogen (21%), but the difference should have negligible effect on the critical mass comparisons.

8 2 Reactivity Measurements

Fuel worth was measured in this configuration by the methods used on the three previous configurations Three major traverses of longitudinally averaged fuel worth were made The results are tabulated in Table 8.2 and shown graphically in Figure 8 1. The average fuel worth in the core region (to 0 55 radius ratio) was 3 95%Δk/kg This is essentially the same value as obtained on the 0 55 radius ratio core without hydrogen, ie, the difference in loading and removal of hydrogen in combinations did not create a statistically significant different value for the fuel worth. Aluminum worths were measured along three characteristic planes in the fuel region. These results are tabulated in Table 8 3, and are about 25% larger (averaged) than the corresponding aluminum worths measured in the 0 55 radius ratio core with hydrogen Using the fuel worth given above, the critical loading (k=1 00) without the nozzle plug would have been 7.97 kg (or 7.73 kg with the nozzle plug in place)

8.3 Power Distributions

Power distributions were determined along one major radial plane in the central module and along the two major planes in a typical outer module, as was done in the other three configurations. The relative fission power distributions are given in Table 8.4 and are graphically presented in Figures 8.2 to 8.4 as point values and in Figure 8.3 as the radial dependence of longitudinally averaged values

There are two different characteristics of the power distribution on this configuration compared to that on the similar configuration without hydrogen

1) The power near the outer edges of the fuel is slightly (2 to 5%) higher in the present configuration than in that with hydrogen. This is probably caused by the removal of the absorbing, diffusion barrier effect of hydrogen.
2) The power at the exit (nozzle) end of the center module is about 10% higher in this configuration This effect is simply because this reactor was power mapped with the nozzle plug inserted, and the hydrogen vs no hydrogen was not the cause of the power shift.

8 4 Flux Distribution

Gold, both bare and cadmium covered, was used to obtain cadmium ratios and hence thermal fluxes in various parts of the reactor. The direct gold data is given in Table 8 5 and Figures 8 6 to 8 9. The resulting thermal fluxes are in Table 8 6 and Figure 8.8 to 8.11.

Comparison of these thermal flux traverses with those on the 0.55 radius ratio configuration with hydrogen (Section 5 4) shows a slight indication of differences in the region where there was hydrogen. The flux shows slight peaking when the hydrogen is present. The anomalous dip in the flux between modules 5 and 6 as shown on Figure 5 32 has not appeared on any other configurations, and hence should not be considered relevant to the comparisons of the configurations with and without hydrogen.

TABLE 8 1

Comparison of Loading

With and Without Hydrogen

0 55 Radius Ratio

A) Loading of Fuel Rings - 0 55 Radius Ratio

Ring No.	Without Hydrogen No of Sheets	With Hydrogen (Section 5) No of Sheets
1	1	1
2	2	2
3	4	3
4	4	5
5	5	6
6	6 (on 4 elements) 7 (on 3 elements)	7
Total on rings of 7 elements	2512	2688

B) Loading of Fuel Disks (See Figure 5 4)

	Without Hydrogen	With Hydrogen
	56 full-size sheets 24 half-size sheets	72 full-size sheets 60 half-size sheets
Total equivalent full-size sheets	476	714

C) Total Fuel Loading in Reactor

Without Hydrogen	With Hydrogen
7 82 kg	8 91 kg

TABLE 8 2

Uranium Worth Measurements

7-Module Reactor - 0 55 Radius Ratio

No Hydrogen in Reactor

Module	Location Angle (°cw)	Location Radius (cm)	U Mass (g)	Reactivity Change (%Δk)	Uranium Worth %Δk/kg
1	90	4 0	7 28	0 0392±0 003	5 38±0 41
1	90	7 8	7 28	0 0444±0 003	6 10±0 41
1	90	11 6	7 28	0 0505±0 003	6 94±0 41
1	90	15 4	7 28	0 0637±0 003	8 75±0 41
3	90	4 0	7 28	0 0210±0 003	2 89±0 41
3	90	7 8	7 28	0 0240±0 003	3 30±0 41
3	90	11 6	7 28	0 0252±0 003	3 46±0 41
3	90	15 4	7 28	0 0320±0 003	4 40±0 41
	270	7 8		0 0272±0 003	3 74±0 41
	270	15 4		0 0404±0 003	5 55±0 41

Core average fuel worth = 3 95% Δk/kg

TABLE 8 3

Aluminum Worth Measurements

7-Module Reactor Without Hydrogen

Exhaust Nozzle in Reactor

	Location				
Module	Angle (°cw)	Radius (cm)	Mass (g)	Reactivity Change (%Δk)	Specific Worth %Δk/kg
1	90	Avg	540	-0 0337±0 003	$(6\ 24\pm0\ 56)\times10^{-2}$
4	150	Avg	540	-0 0087±0 003	$(1\ 61\pm0\ 56)\times10^{-2}$
4	330	Avg	540	-0 0217±0 003	$(4\ 02\pm0\ 56)\times10^{-2}$

TABLE 8 4

Catcher Foil Data

7-Module Reactor - 0 55 Radius Ratio

No Hydrogen

Run 1178

Foil Number	Foil Type	Module Number	Location: Angle (°cw)	Location: Radial (cm)	Location: Axial (cm)	Normalized Counts	Local to Foil (X)
1	Bare	1	90	4 0	92 5	219582	1 050
2	Bare	1	90	4 0	105 8	199585	0 954
3	Bare	1	90	4 0	121 0	216198	1 033
4	Bare	1	90	4 0	151 5	209032	1 000 (X)
5	Bare	1	90	4 0	182 0	205134	0 981
6	Bare	1	90	4 0	197 2	185945	0 889
7	Bare	1	90	4 0	210 5	217367	1 039
8	Bare	1	90	7 8	92 5	228872	1 094
9	Bare	1	90	7 8	105 8	214074	1 023
10	Bare	1	90	7 8	121 0	221946	1 061
11	Bare	1	90	7 8	151 5	226151	1 081
12	Bare	1	90	7 8	182 0	223993	1 071
13	Bare	1	90	7 8	197 2	204792	0 979
14	Bare	1	90	7 8	210 5	214152	1 024
15	Bare	1	90	11 6	92 5	231313	1 106
16	Bare	1	90	11 6	105 8	237738	1 136
17	Bare	1	90	11 6	121 0	244618	1 169
18	Bare	1	90	11 6	151 5	243123	1 162
19	Bare	1	90	11 6	182 0	236574	1 131
20	Bare	1	90	11 6	197 2	217682	1 041
21	Bare	1	90	11 6	210 5	235828	1 127
22	Bare	1	90	15 4	92 5	267116	1 277
23	Bare	1	90	15 4	105 8	272033	1 300
24	Bare	1	90	15 4	121 0	273704	1 308
25	Bare	1	90	15 4	151 5	282632	1 351
26	Bare	1	90	15 4	182 0	261306	1 249
27	Bare	1	90	15 4	197 2	254505	1 217
28	Bare	1	90	15 4	210 5	247991	1 185
29	Bare	3	90	4 0	92 5	163590	0 782
30	Bare	3	90	4 0	105 8	154273	0 737
31	Bare	3	90	4 0	121 0	156342	0 747
32	Bare	3	90	4 0	151 5	156155	0 746
33	Bare	3	90	4 0	182 0	147517	0 705
34	Bare	3	90	4 0	197 2	143137	0 684
35	Bare	3	90	4 0	210 5	156898	0 750

TABLE 8 4

(Continued)

Run 1178

Foil Number	Foil Type	Module Number	Angle (°cw)	Radial (cm)	Axial (cm)	Normalized Counts	Local to Foil (X)
36	Bare	3	90	7 8	92 5	167400	0 800
37	Bare	3	90	7 8	105 8	147212	0 704
38	Bare	3	90	7 8	121 0	158888	0 759
39	Bare	3	90	7 8	151 5	158791	0 759
40	Bare	3	90	7 8	182 0	158749	0 759
41	Bare	3	90	7 8	197 2	141050	0 674
42	Bare	3	90	7 8	210 5	153448	0 733
43	Bare	3	90	11 7	92 5	174279	0 833
44	Bare	3	90	11 7	105 8	165848	0 793
45	Bare	3	90	11 7	121 0	178521	0 853
46	Bare	3	90	11 7	151 5	170396	0 814
47	Bare	3	90	11 7	182 0	168103	0 804
48	Bare	3	90	11 7	197 2	153203	0 732
49	Bare	3	90	11 7	210 5	158697	0 759
50	Bare	3	90	15 4	92 5	184741	0 883
51	Bare	3	90	15 4	105 8	193376	0 924
52	Bare	3	90	15 4	121 0	195411	0 934
53	Bare	3	90	15 4	151 5	201681	0 964
54	Bare	3	90	15 4	182 0	187282	0 895
55	Bare	3	90	15 4	197 2	173724	0 830
56	Bare	3	90	15 4	210 5	162303	0 776

Run 1179

Foil Number	Foil Type	Module Number	Angle (°cw)	Radial (cm)	Axial (cm)	Normalized Counts	Local to Foil (X)
1	Bare	3	270	15 4	92 5	215956	1 032
2	Bare	3	270	15 4	105 8	209677	1 002
3	Bare	3	270	15 4	121 0	215892	1 032
4	Bare	3	270	15 4	151 5	217869	1 041
5	Bare	3	270	15 4	182 0	209922	1 003
6	Bare	3	270	15 4	197 2	205544	0 982
7	Bare	3	270	15 4	210 5	196548	0 939
8	Bare	3	270	11 6	92 5	188081	0 899
9	Bare	3	270	11 6	105 8	187744	0 897
10	Bare	3	270	11 6	121 0	196001	0 937
11	Bare	3	270	11 6	151 5	192690	0 921
12	Bare	3	270	11 6	182 0	179244	0 857
13	Bare	3	270	11 6	197 2	179932	0 860
14	Bare	3	270	11 6	210 5	182682	0 873
15	Bare	3	270	7.8	92 5	180514	0 863
16	Bare	3	270	7 8	105 8	167369	0 800
17	Bare	3	270	7 8	121 0	171830	0 821
18	Bare	3	270	7 8	151 5	167098	0 799
19	Bare	3	270	7 8	182 0	169964	0 812

TABLE 8 4

(Continued)

Run 1179

Foil Number	Foil Type	Module Number	Angle (°cw)	Location Radial (cm)	Location Axial (cm)	Normalized Counts	Local to Foil (X)
20	Bare	3	270	7 8	197 2	146735	0 701
21	Bare	3	270	7 8	210 5	161241	0 771
22	Bare	3	270	4 0	92 5	169292	0 809
23	Bare	3	270	4 0	105 8	159763	0 764
24	Bare	3	270	4 0	121 0	156902	0 750
25	Bare	3	270	4 0	151 5	158905	0 760
26	Bare	3	270	4 0	182 0	153068	0 732
27	Bare	3	270	4 0	197 2	147607	0 706
28	Bare	3	270	4 0	210 5	162630	0 777
Run 1180							
1	Cd	1	90	4 0	182 0	6040	34 0
2	Cd	1	90	15 4	182 0	6141	42 6
3	Cd	3	90	4 0	182 0	4238	34 8
4	Cd	3	90	15 4	182 0	4170	44 9

TABLE 8 5

Gold Foil Data

7-Module Cavity Reactor - 0 55 Radius Ratio

No Hydrogen

Run 1178

Number	Type	Location Radial (cm)	Location Axial (cm)	Foil Weight (g)	Specific Activity d/m-g x 10^{-6}	Local to Foil (X)*
1	Bare	0	89 4	0 0343	8 918	1 072
2	Bare	0	74 9	0 0363	10 691	1 285
3	Bare	0	59 6	0 0354	8 044	0 967
4	Bare	0	44 4	0 0381	5 385	0 647
5	Bare	0	29 1	0 0312	3 249	0 391
6	Bare	0	13 9	0 0380	1 579	0 190
7	Bare	0	0	0 0273	0 215	0 026
8	Bare	93 2	151 1	0 0410	8 577	1 031
9	Bare	107 7	151 1	0 0389	6 995	0 841
10	Bare	123 0	151 1	0 0399	5 140	0 618
11	Bare	138 2	151 1	0 0402	3 398	0 408
12	Bare	153 4	151 1	0 0333	1 992	0 239
13	Bare	168 7	151 1	0 0398	0 901	0 108
14	Bare	183 7	151 1	0 0408	0 126	0 015
	Module 1, 90° cw					
15	Bare	4 0	136 3	0 0330	8 415	1 011 (X)*
16	Bare	7 8	136 3	0 0415	8 609	1 035
17	Bare	11 6	136 3	0 0335	9 191	1 105
18	Bare	15 4	136 3	0 0322	10 199	1 226
19	Bare	4 0	166 8	0 0400	8 223	0 988 (X)*
20	Bare	7 8	166 8	0- 0366	8 589	1 032
21	Bare	11 6	166 8	0 0418	9 170	1 102
22	Bare	15 4	166 8	0 0392	9 995	1 201
	Module 3, 90° cw					
23	Bare	4 0	136 3	0 0385	6 211	0 747
24	Bare	7 8	136 3	0 0388	6 328	0 761
25	Bare	11 6	136 3	0 0374	6 676	0 802
26	Bare	15 4	136 3	0 0352	7 175	0 862
27	Bare	4 0	166 8	0 0373	6 023	0 724
28	Bare	7 8	166 8	0 0333	5 977	0 718
29	Bare	11 6	166 8	0 0385	6 326	0 760
30	Bare	15 4	166 8	0 0302	7 079	0 851
	Traverse from Module 1 to Module 3					
31	Bare	23 6	151 1	0 0364	10 786	1 296
32	Bare	28 7	151 1	0 0325	13 258	1 594
33	Bare	34 0	151 1	0 0319	13 146	1 580
34	Bare	39 4	151 1	0 0308	11 767	1 414
35	Bare	44 4	151 1	0 0348	8 608	1 035

*Note the standard normalizer position is at 4 0 cm radius, and 151.5 cm longitudinal position, midway between the two "Foil x's" shown

TABLE 8 5

(Continued)

Run 1178

Foil Number	Foil Type	Location Radial (cm)	Location Axial (cm)	Foil Weight (g)	Specific Activity d/m-g x 10^{-6}	Local to Foil (X)
	Traverse Between Modules 5 & 6					
36	Bare	90 7	151 1	0 0421	8 626	1 037
37	Bare	83 8	151 1	0 0345	9 876	1 187
38	Bare	76 2	151 1	0 0391	10 593	1 273
39	Bare	68 6	151 1	0 0390	11 019	1 324
40	Bare	61 0	151 1	0 0397	11 040	1 327
41	Bare	53 3	151 1	0 0410	11 584	1 392
42	Bare	45 7	151 1	0 0369	12 963	1 558
43	Bare	38 1	151 1	0 0338	13 837	1 663
44	Bare	30 5	151 1	0 0357	13 752	1 653
45	Bare	23 6	151 1	0 0338	11 147	1 340
	Module 1, Outer Surface of Module					
46	Bare	22 4 (270°)	151 1	0 0328	10 513	1 264
47	Bare	22 4 (315°)	151 1	0 0302	10 583	1 272
48	Bare	22 4 (0°)	151 1	0 0483	10 039	1 207
	Module 3, Outer Surface of Module					
49	Bare	22 4 (270°)	151 1	0 0409	8 125	0 977
50	Bare	22 4 (315°)	151 1	0 0426	7 821	0 940
51	Bare	22 4 (0°)	151 1	0 0404	7 560	0 909
52	Bare	22 4 (90°)	151 1	0 0381	7 195	0 865

Run 1179

Foil Number	Foil Type	Location Radial (cm)	Location Axial (cm)	Foil Weight (g)	Specific Activity d/m-g x 10^{-6}	Local to Foil (X)
1	Cd	0	89 4	0 0360	2 197	
2	Cd	0	59 6	0 0379	0 222	
3	Cd	0	29 1	0 0411	0 0089	
4	Cd	93 2	151 1	0 0357	0 694	
5	Cd	123 0	151 1	0 0402	0 0214	
6	Cd	153 4	151 1	0 0386	0 0046	
	Module 3, 270°					
7	Bare	15 4	136 3	0 0323	8 028	0 965
8	Bare	11 6	136 3	0 0425	7 314	0 879
9	Bare	7 8	136 3	0 0414	6 600	0 793
10	Bare	4 0	136 3	0 0417	6 165	0 741
11	Cd	4 0	166 8	0 0384	1 758	
12	Cd	15 4	166 8	0 0358	1 697	
	Traverse from Module 1 to Module 3					
13	Cd	23 6	151 1	0 0354	2 551	
14	Cd	34 0	151 1	0 0376	2 518	
15	Cd	44 4	151 1	0 0338	1 945	

TABLE 8 5

(Continued)

Run 1179

Foil Number	Foil Type	Location Radial (cm)	Location Axial (cm)	Foil Weight (g)	Specific Activity d/m-g x 10^{-6}	Local to Foil (X)
	Traverse Between Modules 5 & 6					
16	Cd	83 8	151 1	0 0384	0 927	
17	Cd	53 3	151 1	0 0341	2 148	
18	Cd	23 6	151 1	0 0335	2 678	
	Module 1, Outer Surface of Module					
19	Cd	22 4 (270°)	151 1	0 0418	2 388	
20	Cd	22 4 (0°)	151 1	0 0356	2 535	
Run 1180						
1	Bare	0	82 5	0 0339	10 876	1 307
2	Bare	0	67 2	0 0348	9 661	1 161
3	Bare	0	52 0	0 0416	6 811	0 819
4	Bare	100 1	151 1	0 0337	8 096	0 973
5	Bare	115 4	151 1	0 0361	6 088	0 732
6	Bare	130 2	151 1	0 0376	4 285	0 515
	Module 1, 90°					
7	Cd	4 0	136 3	0 0367	2 413	
8	Cd	15 4	136 3	0 0380	2 423	
	Module 3, 90°					
9	Cd	4 0	136 3	0 0368	1 567	
10	Cd	15 4	136 3	0 0414	1 564	
	Traverse from Module 1 to Module 3					
11	Cd	28 7	151 1	0 0392	4 110	
12	Cd	39 4	151 1	0 0399	1 785	
	Traverse Between Modules 5 & 6					
13	Cd	90 7	151 1	0 0350	0 671	
14	Cd	68 6	151 1	0 0335	1 811	
15	Cd	38 1	151 1	0 0421	2 052	
	Module 3					
16	Cd	22 4 (270°)	151 1	0 0318	2 518	
17	Cd	22 4 (0°)	151 1	0 0417	2 266	
18	Cd	22 4 (90°)	151 1	0 0307	2 609	

TABLE 8 6

Thermal Neutron Flux

7-Module Reactor - 0 55 Radius Ratio

No Hydrogen

Location				
Radial (cm)	Axial (cm)	Module Number	Angle (°cw)	Thermal Neutron Flux (n/cm^2-sec-watt x 10^{-6})
0	89 4	End Reflector		4 530
0	59 6	End Reflector		5 302
0	29 1	End Reflector		2 197
93 2	151 1	Radial Reflector		5 374
123 0	151 1	Radial Reflector		3 472
153 4	151 1	Radial Reflector		1 348
4 0	136 3	1	90	3 999
15 4	136 3	1	90	5 160
4 0	136 3	3	90	3 170
15 4	136 3	3	90	3 733
4 0	136 3	3	270	3 030
15 4	136 3	3	270	4 246
23 6	151 1	Traverse from Module 1 to 3		5 606
28 7	151 1	Traverse from Module 1 to 3		5 984
34 0	151 1	Traverse from Module 1 to 3		7 092
39 4	151 1	Traverse from Module 1 to 3		6 637
44 4	151 1	Traverse from Module 1 to 3		4 536
23 6	151 1	Traverse Between Modules 5 & 6		5 752
38 1	151 1	Traverse Between Modules 5 & 6		7 863
53 3	151 1	Traverse Between Modules 5 & 6		6 508
68 6	151 1	Traverse Between Modules 5 & 6		6 321
83 8	151 1	Traverse Between Modules 5 & 6		6 043
90 7	151 1	Traverse Between Modules 5 & 6		5 430
22 4	151 1	1	0	5 296
22 4	151 1	1	270	5 342
22 4	151 1	3	0	3 571
22 4	151 1	3	90	3 260
22 4	151 1	3	270	3 971

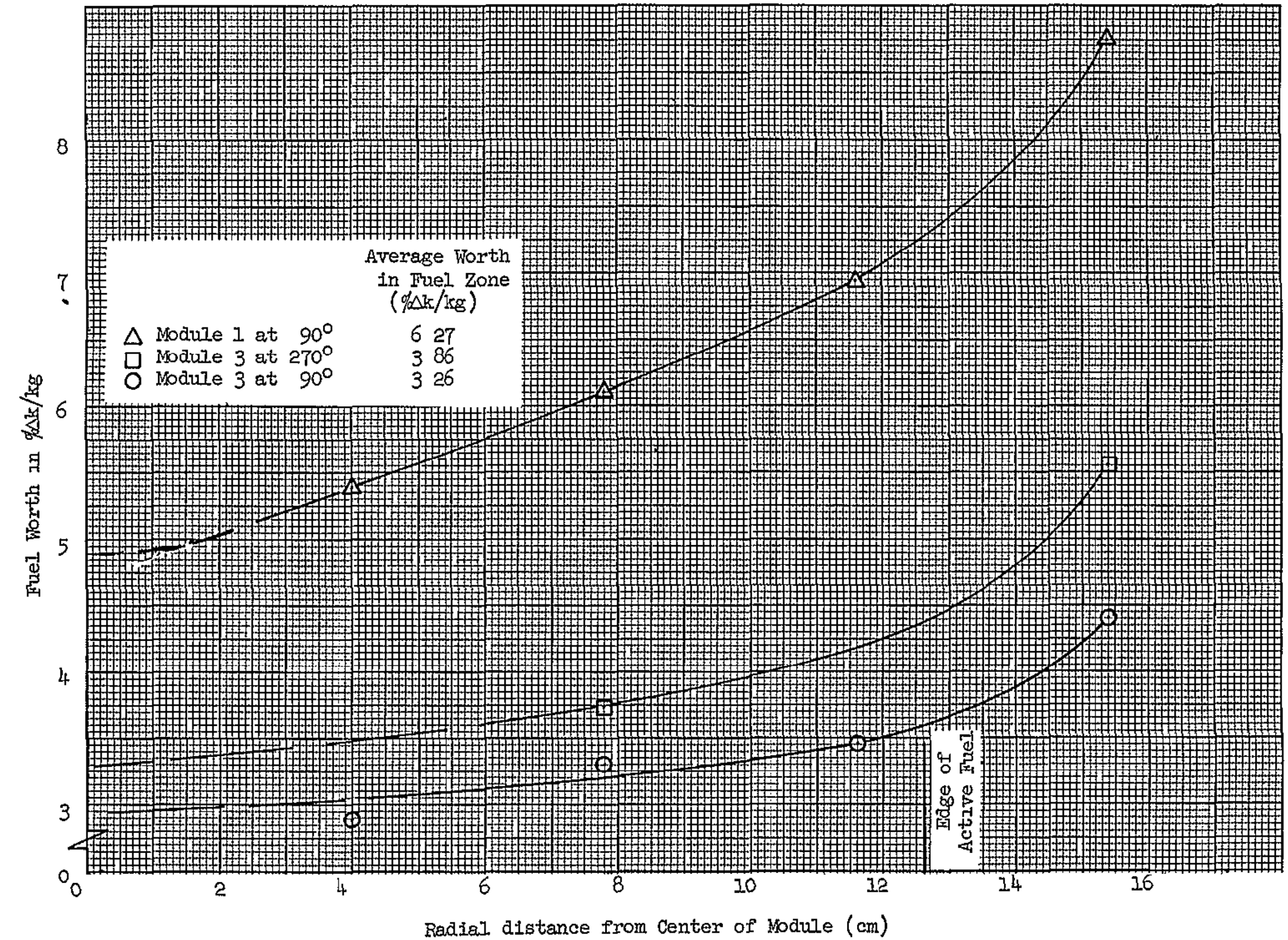

Figure 8.1 Fuel worth traverses (longitudinal averaged) in 0 55 radius ratio core without hydrogen

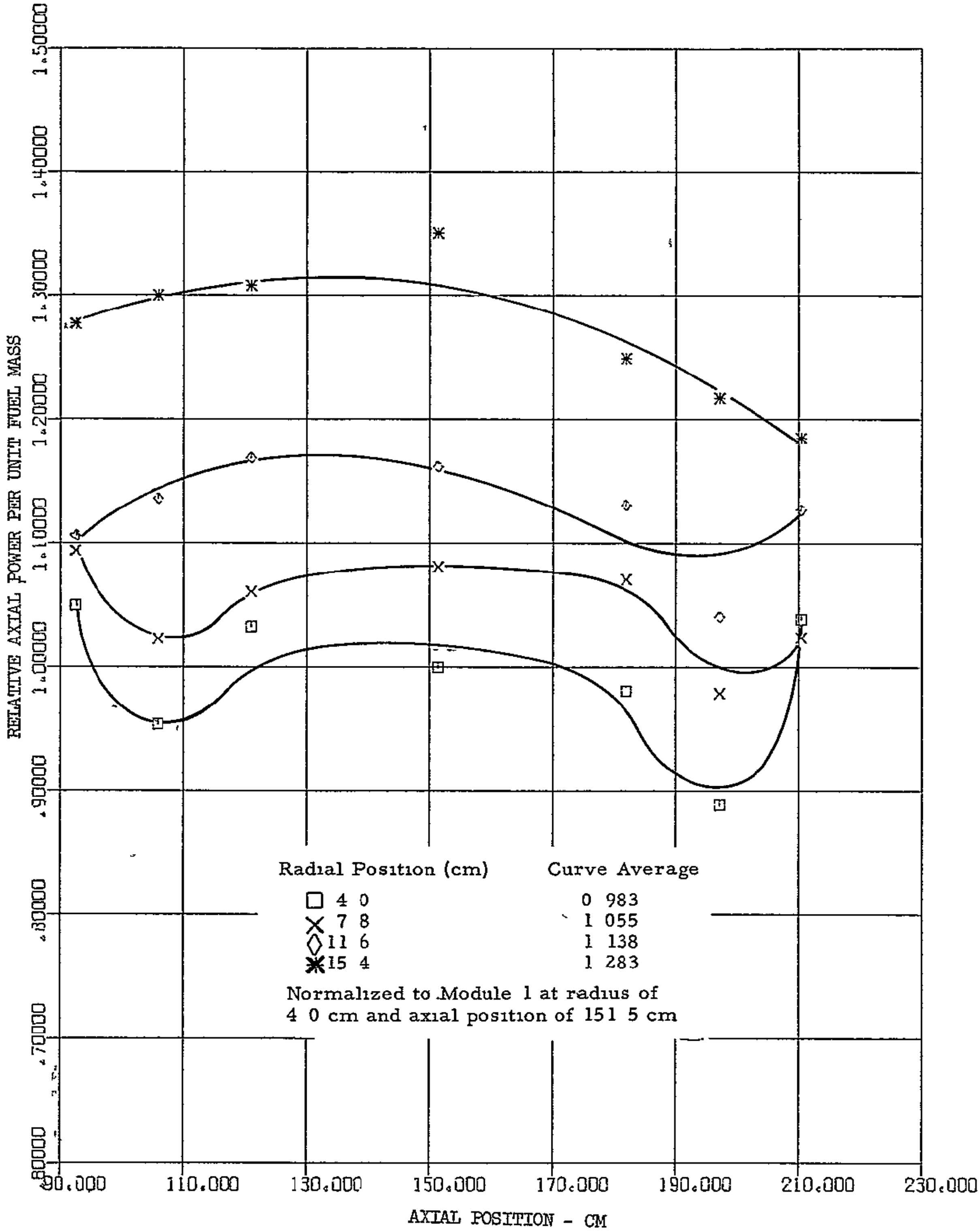

Figure 8.2 Relative axial power distribution in module 1, 90° at the core centerline, 7-module reactor with 0 55 fuel to module radius ratio without hydrogen

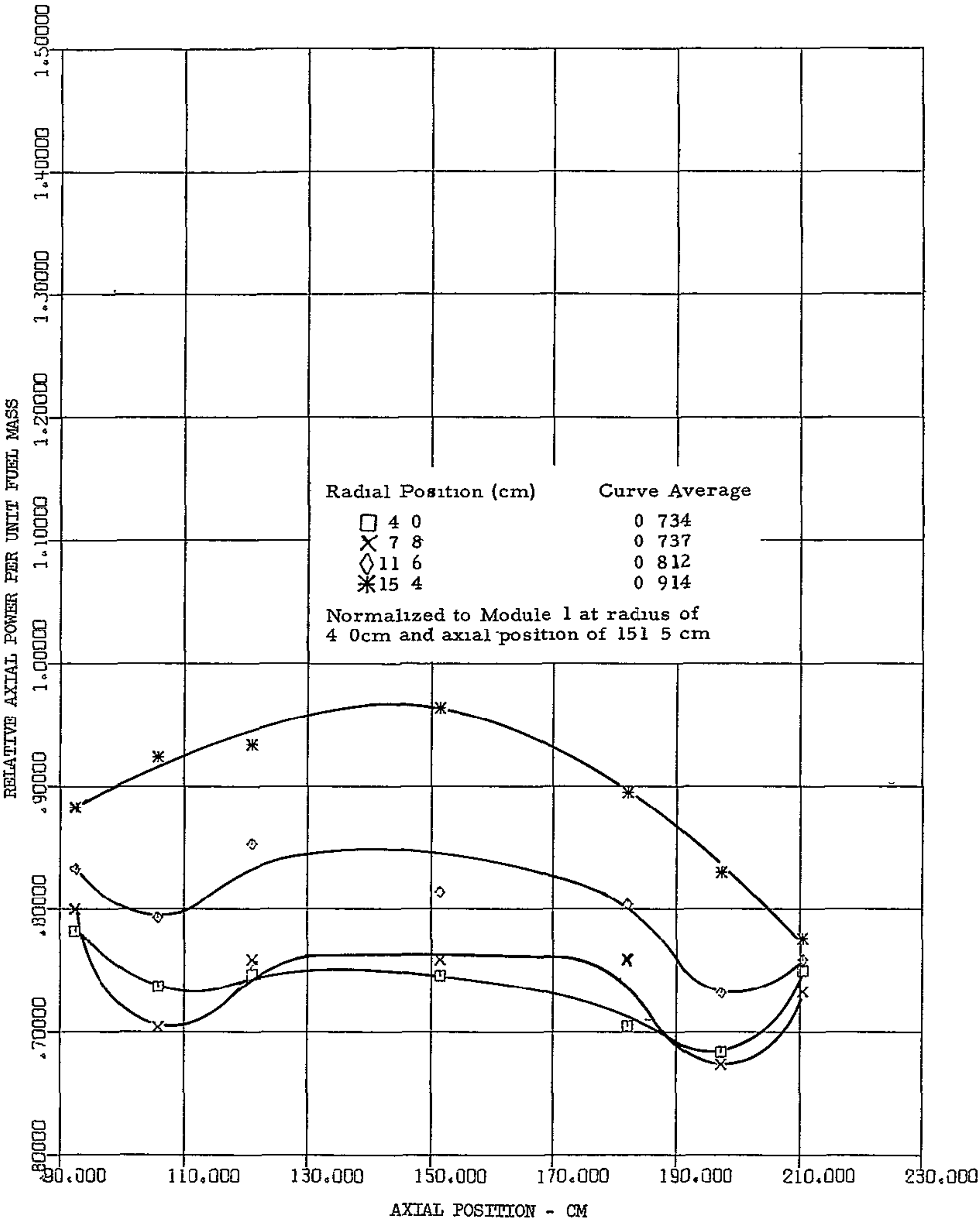

Figure 8 3 Relative axial power distribution in module 3, 90° at the core centerline, 7-module reactor with 0 55 fuel to module radius ratio without hydrogen

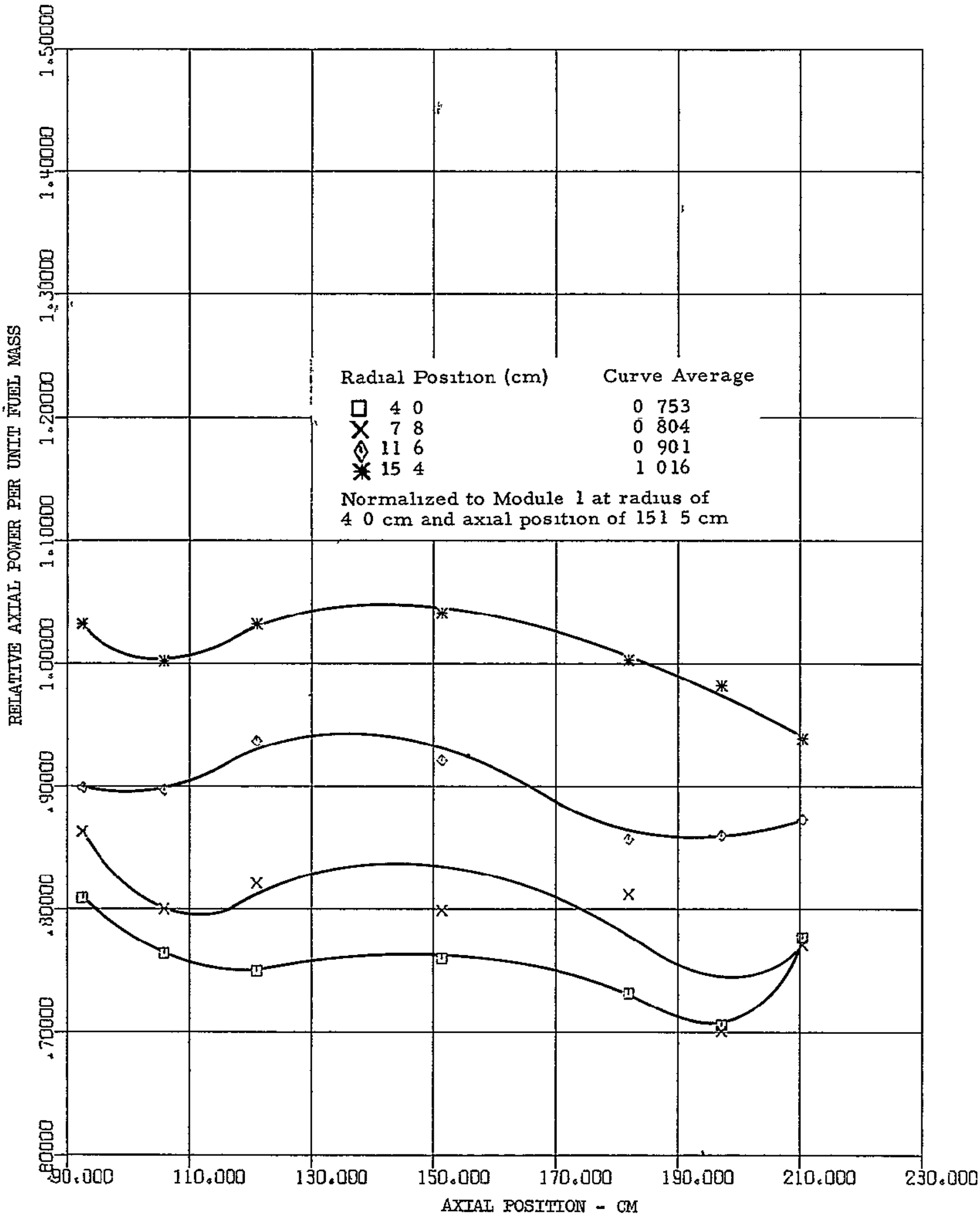

Figure 8.4 Relative axial power distribution in module 3, 270° at the core centerline, 7-module reactor with 0 55 fuel to module radius ratio without hydrogen

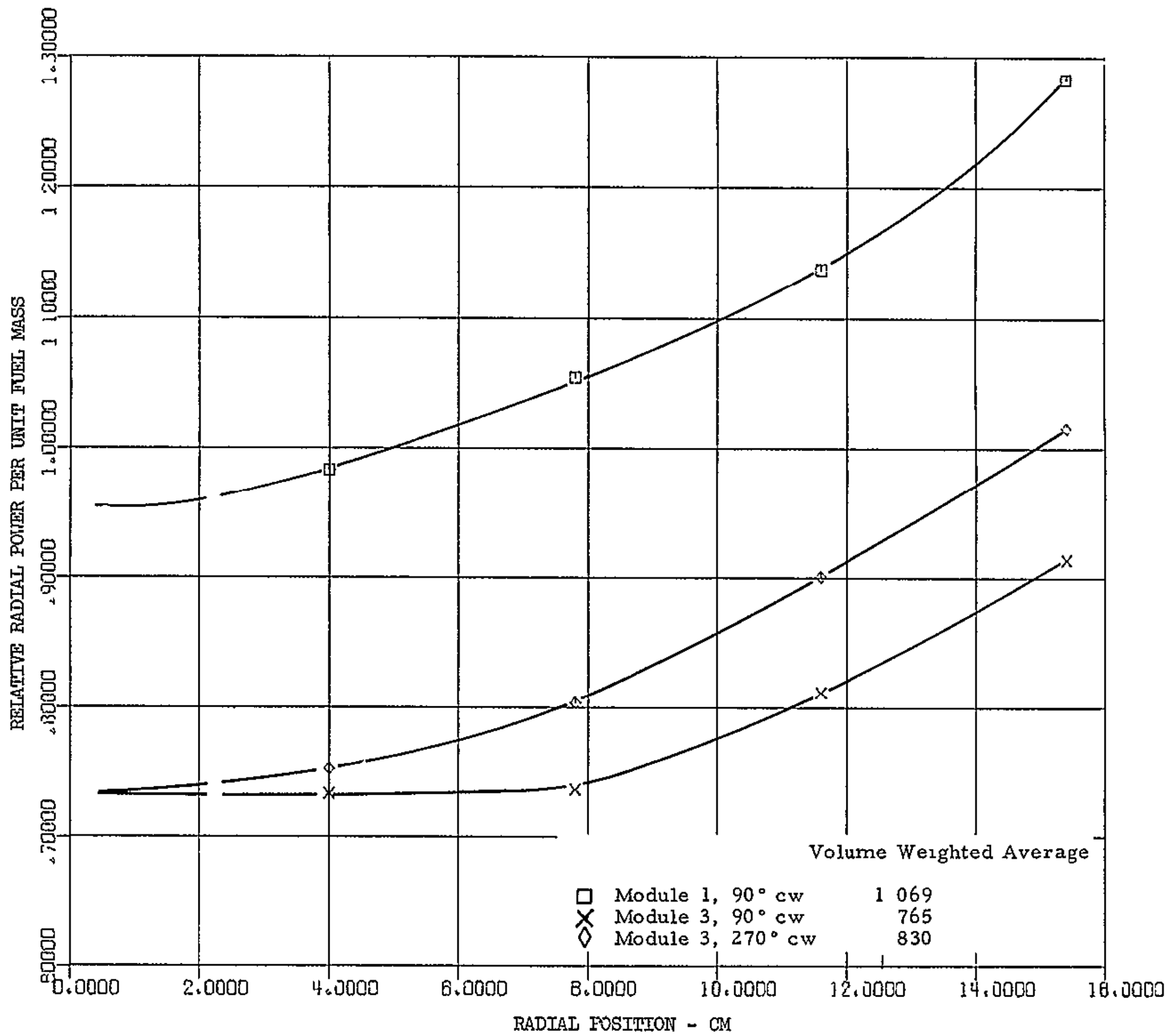

Figure 8.5 Relative radial power distribution in modules 1 and 3 based on axial average power distributions, 7-module reactor with 0 55 fuel to module radius ratio without hydrogen

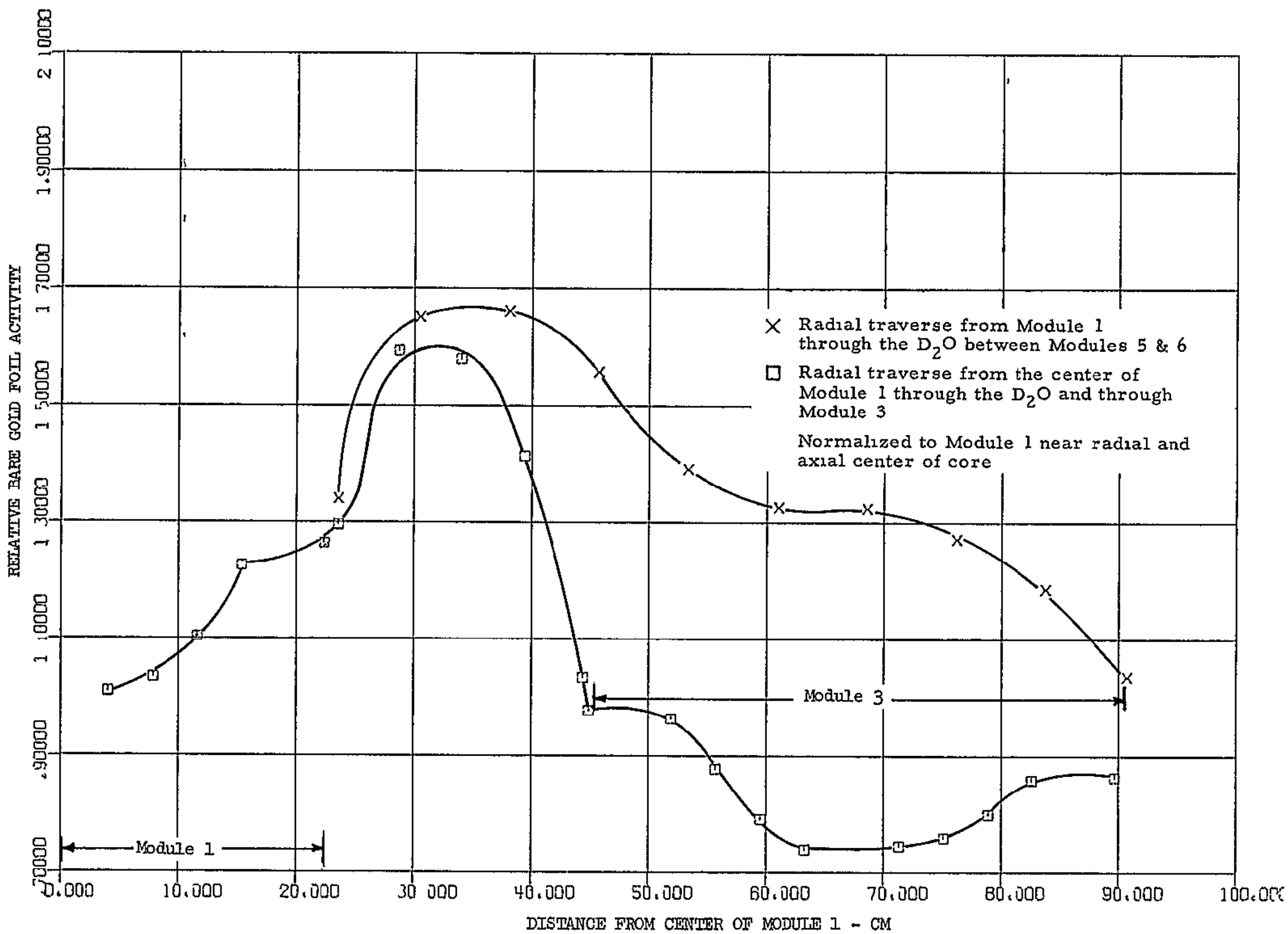

Figure 8.6 Relative bare gold foil activity distribution in the regions between modules, 0.55 fuel to module radius ratio without hydrogen

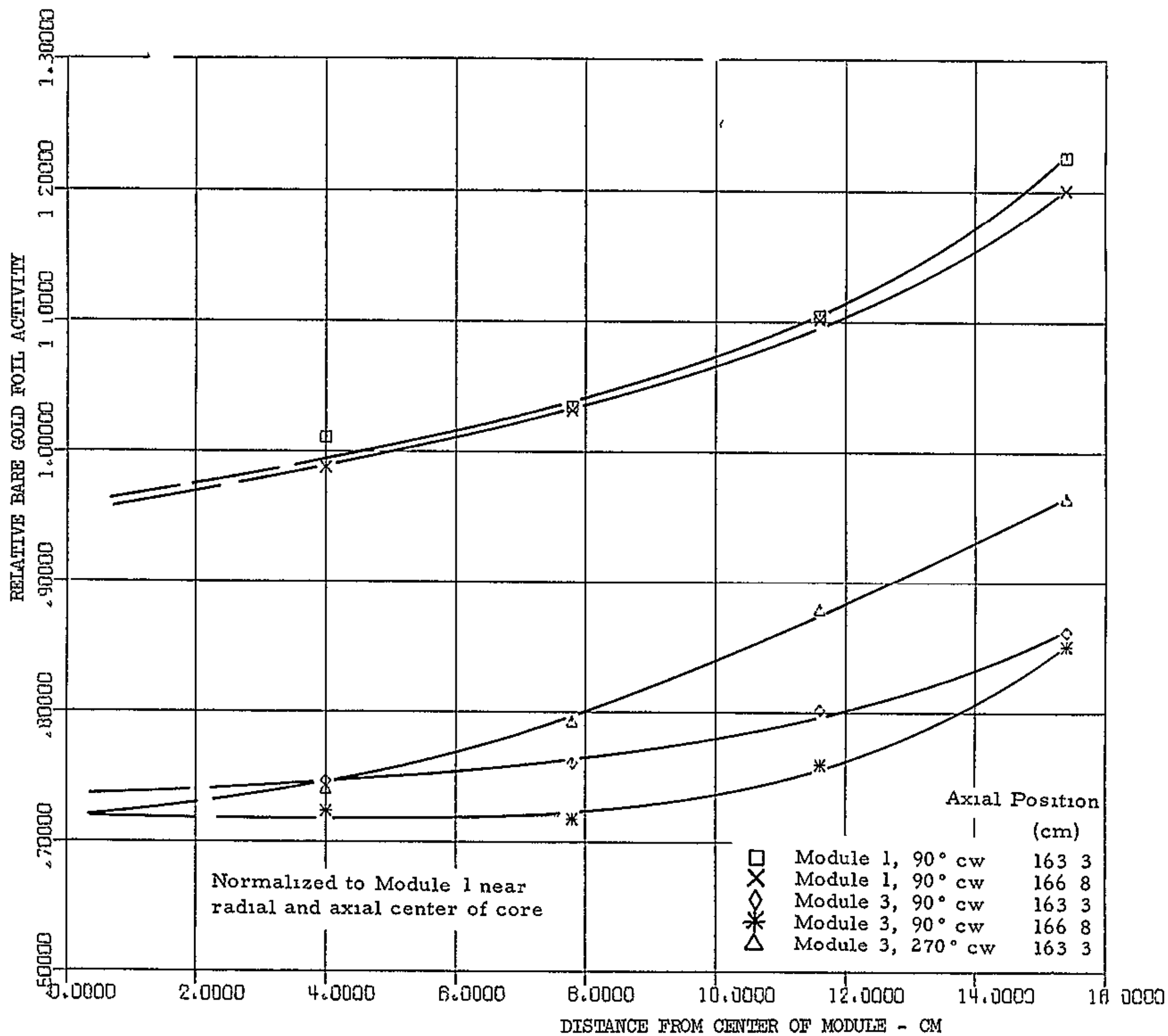

Figure 8.7 Relative radial bare gold foil activity in modules 1 and 3 at axial locations of 163 3 and 166.8 cm, 0 55 fuel to module radius ratio without hydrogen

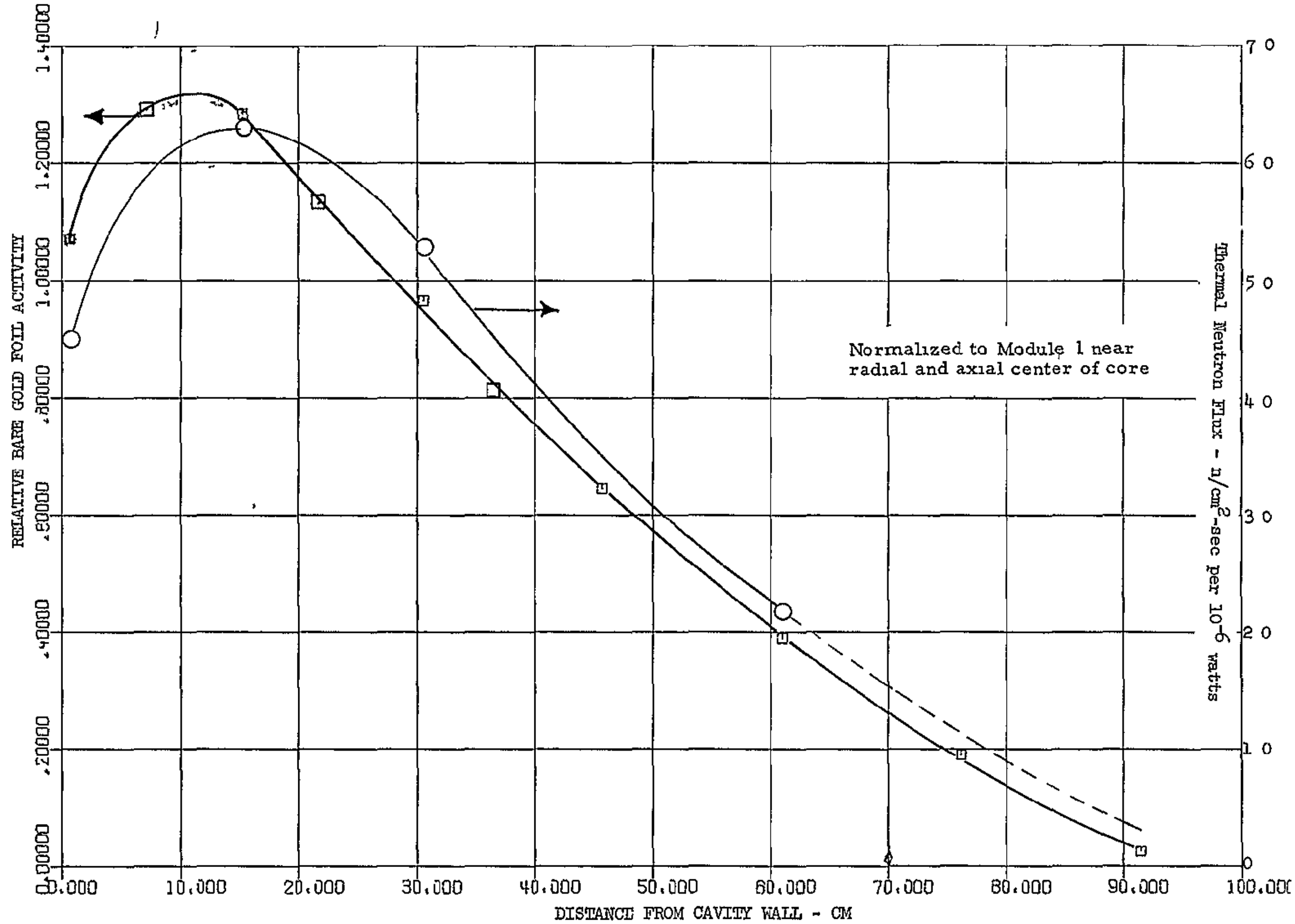

Figure 8.8 Bare gold activity and thermal flux in end reflector, 7-module cavity reactor, 0.55 radius ratio without hydrogen

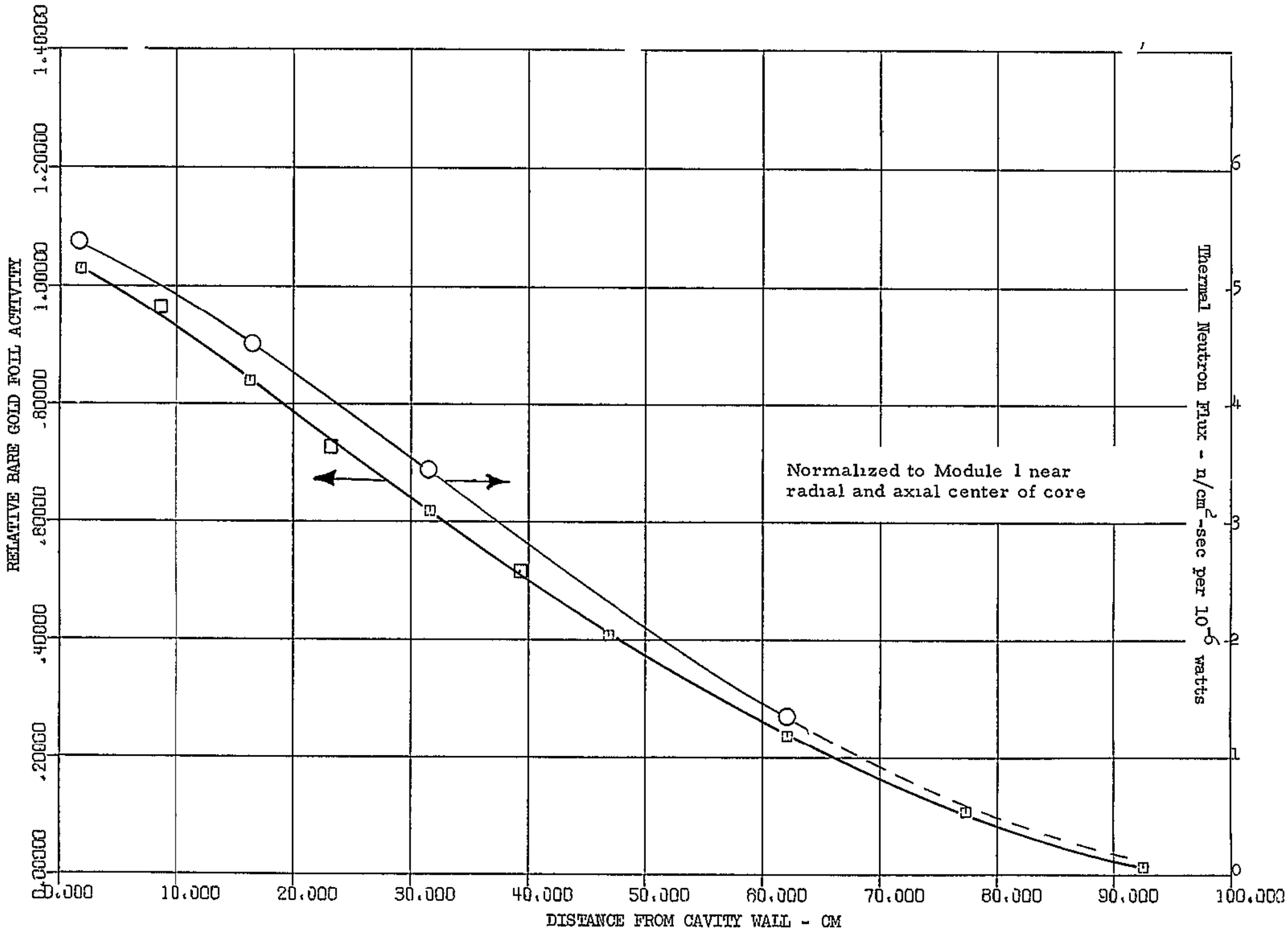

Figure 8.9 Bare gold activity and thermal flux in radial reflector, 7-module cavity reactor, 0.55 radius ratio

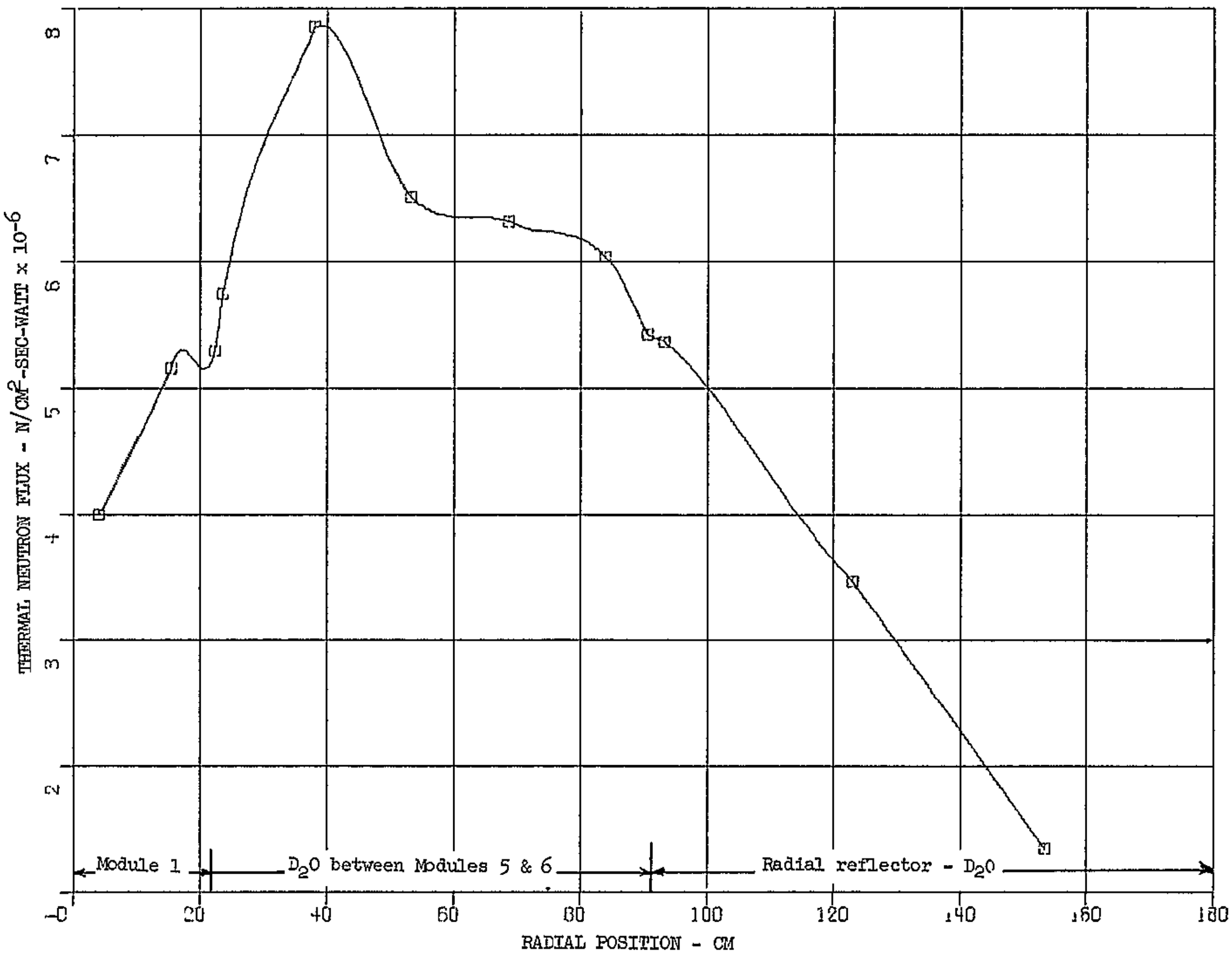

Figure 8 10 Radial distribution of thermal neutron flux from module 1 through D_2O between modules 5 & 6 and into the radial reflector, 7-module reactor with 0 55 fuel to module radius ratio

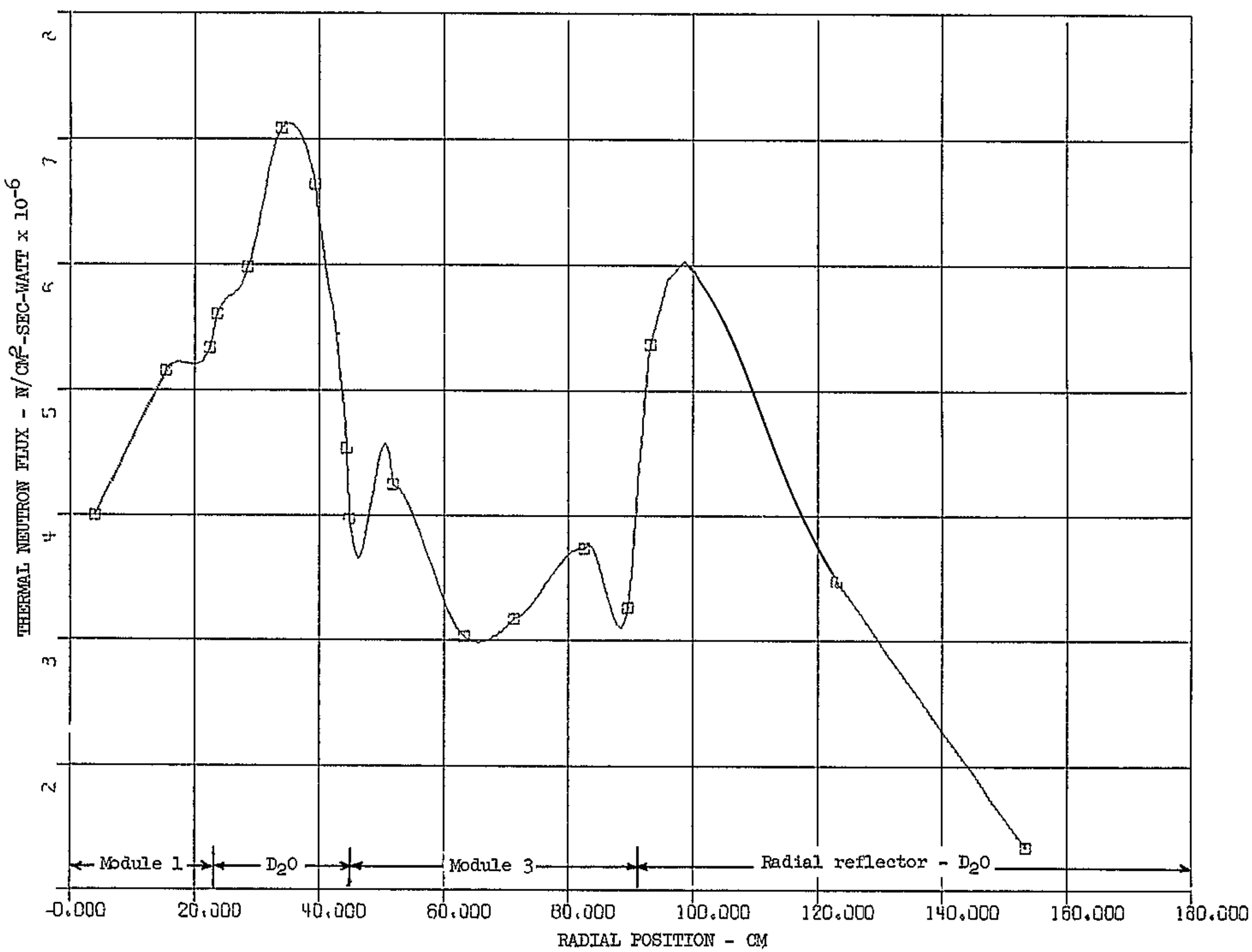

Figure 8.11 Radial distribution of thermal neutron flux from the center of the reactor across module 3 and into the radial reflector, 7-module reactor with 0 55 fuel to module radius ratio

9.0 THREE MODULE REACTOR - 0 55 RADIUS RATIO WITH HYDROGEN SIMULATION

A three module system, with the 70 5 cm O.D modules occupying the same region as that occupied by the seven modules, was assembled so as to furnish a measure of the advantage of having more and smaller modules. These advantages are exclusively neutronic, giving better utilization of the fuel, smaller critical mass, and quite likely smaller effective pressures for the gaseous fuel (The pressure, of course, depends on the total fuel volume as well as the fuel mass) Other considerations, such as thermodynamic, fluid dynamic, and fuel loss effects, generally favor the fewer and larger modules, best exemplified by the single cavity. Some discussion of the relative advantages and disadvantages pertaining to these various factors vs the number of modules is given in Section 10

A cross section view of the three module tank is shown in Figure 9.1 The fuel element structure with its 16 stages, 17 stage dividing disks, and eight fuel rings is shown in Figures 9 2 and 9 3 The tank was constructed from type 1100-H14 aluminum, 0 318 cm thick, except for the 0 635 cm thick end plates that were type 5052 aluminum The empty tank weighed 180 kg

9.1 Initial Loading

Pre-analysis of the three module experiment using the same techniques that were quite successful on the 7-module experiment (simple one-dimensional diffusion code utilizing cell calculations) predicted a loading of 14 kg of uranium with an estimated ±15% uncertainty (Unfortunately, as will be seen, the technique was not nearly as successful in this case; the measured critical mass was 11 5 kg.) Accordingly, each of the three modules was loaded with fuel to a radius ratio of 0 55 according to the description given in Table 9.1 and Figure 9.4. The fuel element design was similar to that used on the 7-module reactor The fuel on the stage separation disks was one layer thick on all 22 positions shown. The total loading was 1780 equivalent full size sheets per element, or 4 66 kg, for a total of 13 98 kg of uranium in the three modules of the reactor. The fuel element structure consisted of 16.2 kg of aluminum in each module, or 48 6 kg in the entire core.

Hydrogen was inserted in the form of foamed polystyrene and polyethylene sheet in an annulus between 0 69 radius ratio and the cavity wall, making an annulus that was 11 3 cm thick The annulus was loaded to a hydrogen atom density of 1 33 x 10^{21} atoms/cc These hydrogen values differ little from those used in the seven module experiment, which had 1.23 x 10^{21} atoms/cc between 0 72 radius ratio and the cavity wall.

Loading commenced by first loading the fuel elements one at a time, and then gradually increasing the water level in the modular tank until criticality was reached After 6 5 out of 8 2 barrels total capacity of heavy water was added, the reactor had a k-effective of 1 0064, with the nozzle plug in the nozzle It was obvious that the critical mass was overpredicted, and steps had to be taken to reduce k-excess in order to fill the module tank completely. These were as follows·

Nozzle plug removed	-0 46%Δk
12 fixed control rods added to end reflector	-2 18%Δk
Hydrogen atom density increased in two of the three modules from 1 33 to 1 $64x10^{21}$ (-0.26%Δk per module)	-0 52%Δk

The resulting k-excess was 0 73%Δk when the module tank was completely filled with 1884 kg of heavy water With 1 $33x10^{21}$ atoms of hydrogen/cc in the hydrogen annulus and 13 98 kg of fuel in the reactor, and with all control rods out,

k-effective = 1 0389 with nozzle plugged
= 1 0343 with nozzle open

Note the small worth (-0 46%Δk) of the nozzle plug in this reactor This is half of the value obtained on the 7-module configuration and the lowest value obtained on any of the cavity configurations measured with this basic 366 cm diameter by 305 cm long reflector tank

9 2 Reactivity Measurements

The control system in the 3-module reactor consisted of the standard 8 actuators, a total of 24 rods, but they were working in an end reflector that contained 12 fixed control rods The latter depressed the flux in the end reflector and reduced the movable control rod worth to 2 9%Δk The shape curve of this control system is given in Table 9 2, and shown graphically in Figure 9.5 Fuel worth was measured in one of the modules All three modules were considered equivalent, with the 20% difference in hydrogen density not considered significant enough to affect the fuel worth. The measurements were taken in module 3 (which had $1.33x10^{21}$ H/cc) in three different radial directions:

30°	a tangential traverse in the core tank
120°	toward the tank center, radially inward
300°	radially outward

All measurements were longitudinal averages at specific radial positions The results are shown graphically in Figure 9.6, and are tabulated in Table 9 3 The slot positions are indicated in Figure 9 3 Measurements on the outer ring of fuel were made both at the end and center of the module. All of this data was used to obtain a volume weighted average fuel worth of 1 65%Δk/kg of uranium Using the above fuel worth, the critical loading of the reactor with 1 33x10^{21} H/cc in the hydrogen annuli and no control rods in the end reflector is:

11.32 kg of U with the nozzle plugged or
11.70 kg of U with the nozzle open.

The aluminum worth measured in slot 4 (18.2 cm) was 0.030%Δk/kg This should nominally equal the cell average worth.

Hydrogen worth was evaluated when the density in the annulus in modules 1 and 2 was increased from 1 33 to 1 64x10^{21} H/cc This was done by adding polyethylene (CH_2) sheet, giving an average worth of 0 303%Δk/kg, or 0 26%Δk for the change per module (870 gm of CH_2 per module).

The effect of the gap between the aluminum tank walls of the fixed and movable tank was measured The gap was 1 89 cm on the 3-module configuration, 0.7 cm larger than the 1 2 cm gap of the 7-module configuration. A measurement was made over the next 1 40 cm and the gap worth was found to be essentially linear equal to 0 48%Δk/cm Thus, the full 1.89 cm gap cost 0 91%Δk, or approximately 0 55 kg of uranium The extra 0.7 cm gap compared to the seven module configuration cost 0.34%Δk, or 0.21 kg of uranium. The critical mass would have been

11 1 kg with the nozzle plugged or
11.5 kg with the nozzle open

with the same 1 2 cm gap that existed on the 7-module configurations.

9.3 Power Distribution - 3-Module Configuration

The fission power distribution (specific power) was measured throughout the reactor as well as the fueled core sections of the modules. The cadmium ratio was measured at selected points to obtain the ratio of epi-thermal to total fissions. The various data are listed in Table 9.4. Most of the radial traverses were taken with respect to the axis of module 3. However, traverses along the separation plane and in the radial reflector all use the reactor axis as the radial reference point.

Figures 9 7, 9 8, and 9.9 show the axial profiles in module 3. Note that the edge of the active fuel region occurs at 19 4 cm. All ordinates have suppressed zeros The power peaking at the separation plane end of the module is probably the result of thermal neutron streaming along the 1 89 cm wide gap Figure 9.10 shows the composite radial power distributions in the module. The values shown are longitudinal averages Note that it is fortuitous that the longitudinal average at 4 6 cm, 300° in module 3 is identical to the point normalization reference value These curve shapes are very similar to the fuel worth curve shapes in Figure 9 6 Figure 9.11 shows the circumferential power distribution on the outside of the fuel (19.4 cm) at the longitudinal center, and the U-235 fission response at the outside of the hydrogen around the module wall, also at the longitudinal center The cadmium ratio at these locations is shown in Figure 9 12. On the outside edge of the fuel, approximately 4 5% of the fissions are epi-thermal (above 0.43 ev cadmium cutoff), while at the outside of the module only 3% of the fission response is epi-thermal. The epi-thermal fractional response will drop even more as one penetrates into the reflector. Thus the fission response shown in the end and radial reflectors, Figure 9 13 and 9 14 respectively, are essentially relative thermal flux traverses A reflector peak was not observed in the radial flux traverse because the traverse originated from a radial line between modules 1 and 3. The end reflector peaking was much less than observed on the seven module system because on the latter a fuel element was situated on the axial centerline, whereas in this three module system the axial traverse originated from a region between modules Figure 9.15 is a traverse across the separation plane, the core face, and on a line through the end of module 1 The large flux peaking between the modules at the reactor center is apparent. Figure 9 16 shows the same type of traverse only going between the ends of modules 1 and 2 and on out through the reflector The peak flux occurs approximately at the circle of the module centerlines (54.6 cm), and a small dip occurs at 38 cm, the point of shortest chord length of moderator between modules

Cadmium ratios are shown in Figure 9.17 and 9 18 in the modules. These vary little axially. The 13 4 cm value of 20 (5% epithermal fissions) is probably characteristic of the average epithermal fission rate in the fuel

9.4 Thermal Flux and Gold Cadmium Ratios

Extensive gold foil measurements, both bare and cadmium covered, were taken throughout the 3-module assembly The foils were nominally 0 0013 cm thick, and the tabulated results are shown in Table 9.5.

A radial plot of the gold foil activity within a module is shown in Figure 9.19. The plotted values are point values from the axial midplane These bare gold foil curves are flatter than either the catcher foil (U-235) response or the fuel worth results. The difference is principally because of the high level of epithermal response to the foils, about 40% of the total at the edge of the fuel and 50% of the total at the center (The infinitely dilute response would be 60% epithermal at the edge and 70% epithermal at the center of the fuel) Other relative gold foil activity plots are shown in Figures 9.20 (circumferential on outside of fuel and at outside of hydrogen), 9.21 (traverse through moderator), 9.22 (traverse in reflectors), 9.23 and 9 24 (longitudinal traverses in the modules)

From the bare and cadmium data, thermal fluxes were obtained A plot of the flux across the reactor at the axial midplane is shown in Figure 9.25, in equivalent 2200 m/sec "thermal" flux per watt of reactor power. Unfortunately there is insufficient detail in this data to show if any flux peaking occurs in the hydrogen. However, the traverse through the moderator region between modules shows the same details of a dip at shortest moderator chord length, and a peak at about the circle of centers for the modules as was observed with the catcher foils (Figure 9 16) Note the catcher foil traverse was across the end of the core, at the core separation plane, whereas the thermal flux traverse is at the axial midplane The thermal flux data is tabulated in Table 9.16 In Table 9 7 the cadmium ratios for infinitely dilute gold are tabulated to show results from 1 4 at the center of the fuel (30% thermal response) to 630 near the outside of the reflector (essentially all thermal response)

TABLE 9 1

Distribution of Fuel Sheets on the Fuel Rings

3 Module Reactor - 0 55 Radius Ratio

Ring Number	Number of Fuel Sheets
1	3
2	5
3	8
4	10
5	12
6	15
7	17
8	20
	90
Total sheets on rings of 16 stages	1440
Sheets on disks -- 20 per disk	340
Total sheets per element	1780
Total sheets in reactor	5340
Total uranium mass	13 98 kg
Uranium mass inside module (fuel element)=	4 66 kg/module

TABLE 9 2

8 Actuator Tabular Rod Worth Curve

3-Module Reactor (12 Manual Rods in Reactor)

Position	00	100	200	300	400	500	600	700	800	900
00	100 00	100 00	97 20	93 30	89.45	85 70	82 02	78.44	74 97	71 61
1000	68 36	65 22	62 19	59 26	56 44	53 73	51 13	48 63	46 23	43 94
2000	41.75	39 66	37 67	35 78	33 99	32 29	30 67	29 12	27 64	26 22
3000	24 86	23 56	22 32	21 12	19 98	18 88	17 83	16 82	15 86	14 94
4000	14 06	13 22	12 42	11 64	10 92	10 23	9 58	8 96	8 38	7 83
5000	7 31	6 81	6 36	5 92	5 50	5.10	4.73	4 38	4 06	3 76
6000	3.47	3 20	2 95	2 71	2 49	2 28	2 08	1 90	1.73	1 57
7000	1 42	1 28	1 15	1 03	0.92	0 82	0 72	0 63	0 55	0 47
8000	0 39	0 32	0.25	0 19	0 14	0.10	0 06	0 03	0 02	0 01

Difference Table

Position	00	100	200	300	400	500	600	700	800	900
00	0 0	0.0	2 80	3 90	3 85	3 75	3 68	3 58	3 47	3 36
1000	3 25	3 14	3 03	2 93	2 82	2 71	2 60	2 50	2 40	2.29
2000	2 19	2 09	1 99	1 89	1 79	1 70	1.62	1 55	1 48	1 42
3000	1 36	1 30	1 24	1 20	1 14	1 10	1 05	1 01	0 96	0 92
4000	0 88	0 84	0 80	0 78	0 72	0 69	0 65	0 62	0 58	0 55
5000	0 52	0 50	0 45	0 44	0 42	0 40	0 37	0 35	0 32	0 30
6000	0 29	0 27	0 25	0 24	0 22	0 21	0.20	0 18	0 17	0 16
7000	0 15	0.14	0 13	0.12	0 11	0 10	0 10	0 09	0 08	0 08
8000	0 08	0 07	0 07	0 06	0 05	0.04	0 04	0 03	0 02	0 01

Position scale is a digital voltmeter reading

Units = 0 0155 cm/digit

TABLE 9 3

Fuel Worth, Longitudinally Averaged

Module # 3

Slot	Radial Position in Module	Circumferential Position in Module: 30° (tangential)	120° (radially inward)	300° (radially outward)
1	5 1 cm	---	1 40 %Δk/kg	---
2	---	---	---	---
3	13 8	---	2 23	1 54 %Δk/kg
4	18 2	2 06 %Δk/kg	2 28	---
5	22 6	---	3 41	2 86
	19 4	Outer ring of fuel		
		Stage 8 (longitudinal center)		2 27 %Δk/kg
		Stage 16 (nozzle end)		3 60 %Δk/kg

Average fuel worth = 1 65 %Δk/kg

TABLE 9 4

Catcher Foil Data

3-Module Reactor

All Radial Locations are with Respect to the Module Axis Except as Noted

All Values are Normalized to Power Level of Run 1186

Run 1185

Foil Number	Foil Type	Module Number	Angle (°cw)	Location Radial (cm)	Location Axial (cm)	Normalized Counts	Local to Foil (X)
1	Bare	3	300	4 6	92 5	95438	1 159
2	Bare	3	300	4 6	105 8	80763	0 980
3	Bare	3	300	4 6	121 5	78941	0 958
4	Bare	3	300	4 6	136 3	77323	0 938
5	Bare	3	300	4 6	151 5	82378	1 000 (X)
6	Bare	3	300	4 6	166 8	77873	0 946
7	Bare	3	300	4 6	182 0	78339	0 950
8	Bare	3	300	4 6	197 2	83260	1 001
9	Bare	3	300	4 6	210 5	110061	1 335
10	Bare	3	300	9 0	92 5	99145	1 203
11	Bare	3	300	9 0	105 8	84727	1 028
12	Bare	3	300	9 0	121 5	80203	0 973
13	Bare	3	300	9 0	136 3	82025	0 995
14	Bare	3	300	9 0	151 5	80432	0 976
15	Bare	3	300	9 0	166 8	79572	0 965
16	Bare	3	300	9 0	182 0	81007	0 983
17	Bare	3	300	9 0	197 2	80314	0 974
18	Bare	3	300	9 0	210 5	112167	1 361
19	Bare	3	300	13 4	92 5	105171	1 276
20	Bare	3	300	13 4	105 8	94673	1 148
21	Bare	3	300	13 4	121 5	86957	1 055
22	Bare	3	300	13 4	136 3	87004	1 055
23	Bare	3	300	13 4	151 5	92357	1 120
24	Bare	3	300	13 4	166 8	91152	1 106
25	Bare	3	300	13 4	182 0	91057	1 105
26	Bare	3	300	13 4	197 2	89270	1 083
27	Bare	3	300	13 4	210 5	119800	1 453
28	Bare	3	300	17 8	92 5	125427	1 521
29	Bare	3	300	17 8	105 8	118012	1 431
30	Bare	3	300	17 8	121 5	112559	1 365
31	Bare	3	300	17 8	136 3	109808	1 332
32	Bare	3	300	17 8	151 5	109960	1 334
33	Bare	3	300	17 8	166 8	112516	1 365
34	Bare	3	300	17 8	182 0	110550	1 341
35	Bare	3	300	17 8	197 2	119680	1 452
36	Bare	3	300	17 8	210 5	132787	1 611

TABLE 9 4

(Continued)

Run 1185

Foil Number	Foil Type	Module Number	Location: Angle (°cw)	Location: Radial (cm)	Location: Axial (cm)	Normalized Counts	Local to Foil (X)
37	Bare	3	300	22 2	92 5	153205	1 858
38	Bare	3	300	22 2	105 8	136691	1 658
39	Bare	3	300	22 2	121 5	139716	1 695
40	Bare	3	300	22 2	136 3	137386	1 666
41	Bare	3	300	22 2	151 5	141899	1 721
42	Bare	3	300	22 2	166 8	135418	1 643
43	Bare	3	300	22 2	182 0	135140	1 639
44	Bare	3	300	22 2	197 2	132054	1 602
45	Bare	3	300	22 2	210 5	149857	1 818

Foil Number	Foil Type	Module Number	Stage	Location: Radial From Center (cm)	Location: Degrees cw	Normalized Counts	Local to Foil (X)
46	Bare	3	8	19 4	0	113063	1 371
47	Bare	3	8	19 4	22 5	116115	1 408
48	Bare	3	8	19 4	45 0	121596	1 475
49	Bare	3	8	19 4	67 5	127937	1 552
50	Bare	3	8	19 4	90 0	136821	1 660
51	Bare	3	8	19 4	112 5	139115	1 687
52	Bare	3	8	19 4	135 0	142253	1 726
53	Bare	3	8	19 4	157 5	144806	1 756
54	Bare	3	8	19 4	180 0	134031	1 626
55	Bare	3	8	19 4	202 5	137056	1 662
56	Bare	3	8	19 4	225 0	124467	1 510
57	Bare	3	8	19 4	247 5	118043	1 432
58	Bare	3	8	19 4	270 0	118007	1 431
59	Bare	3	8	19 4	292 5	120373	1 460
60	Bare	3	8	19 4	315 0	117655	1 427
61	Bare	3	8	19 4	337 5	103584	1 256

TABLE 9 4

(Continued)

Run 1186

				Location			
Foil Number	Foil Type	Module Number	Angle (°cw)	Radial (cm)	Axial (cm)	Normalized Counts	Cadmium Ratio
1	Cad Cov	3	300	13 4	92 5	5462	19 255
2	Cad Cov	3	300	13 4	151 5	5252	17 585
3	Cad Cov	3	300	13 4	210 5	5356	22 367
4	Cad Cov	3	300	22 2	92 5	5233	29 277
5	Cad Cov	3	300	22 2	151 5	5578	25 439
6	Cad Cov	3	300	22 2	210 5	5009	29 917

Foil Number	Foil Type	Module Number	Stage	Radial (cm)	Degrees cw	Normalized Counts	Cadmium Ratio
7	Cad Cov	3	8	19 4	0	5455	20 726
8	Cad Cov	3	8	19 4	90	5549	24 657
9	Cad Cov	3	8	19 4	180	5631	23 802
10	Cad Cov	3	8	19 4	270	5498	21 463

Run 1187

Foil Number	Foil Type	Module Number	Stage	Radial (cm)	Degrees cw	Normalized Counts	Local to Foil (X)
1	Bare	3	8	35 2	0	184228	2 235
2	Bare	3	8	35 2	22 5	188391	2 285
3	Bare	3	8	35 2	45 0	203109	2 464
4	Bare	3	8	35 2	67 5	216157	2 622
5	Bare	3	8	35 2	90 0	228701	2 774
6	Bare	3	8	35 2	112 5	225596	2 736
7	Bare	3	8	35 2	135 0	233208	2 829
8	Bare	3	8	35 2	157 5	224540	2 724
9	Bare	3	8	35 2	180 0	217375	2 637
10	Bare	3	8	35 2	202 5	218397	2 649
11	Bare	3	8	35 2	225 0	199628	2 421
12	Bare	3	8	35 2	247 5	192808	2 339
13	Bare	3	8	35 2	270 0	179469	2 177
14	Bare	3	8	35 2	292 5	177880	2 158
15	Bare	3	8	35 2	315 0	178387	2 164
16	Bare	3	8	35 2	337 5	177692	2 155

TABLE 9 4

(Continued)

Run 1188

Foil Number	Foil Type	Module Number	Location: Angle (°cw)	Location: Radial (cm)	Location: Axial (cm)	Normalized Counts	Local to Foil (X)
1	Bare	3	120	4 6	92 5	99760	1 210
2	Bare	3	120	4 6	105 8	84414	1.024
3	Bare	3	120	4 6	121 5	83250	1 010
4	Bare	3	120	4 6	136 3	82762	1 004
5	Bare	3	120	4 6	151 5	81460	0 988
6	Bare	3	120	4 6	166 8	80208	0 973
7	Bare	3	120	4 6	182 0	81312	0 986
8	Bare	3	120	4 6	197 2	86528	1 050
9	Bare	3	120	4 6	210 5	116108	1 408
10	Bare	3	120	9 0	92 5	----	---
11	Bare	3	120	9 0	105 8	90898	1 103
12	Bare	3	120	9 0	121 5	90156	1 094
13	Bare	3	120	9 0	136 3	90303	1 095
14	Bare	3	120	9 0	151 5	87433	1 061
15	Bare	3	120	9 0	166 8	89371	1 084
16	Bare	3	120	9 0	182 0	88661	1 075
17	Bare	3	120	9 0	197 2	93260	1 131
18	Bare	3	120	9 0	210 5	121791	1 477
19	Bare	3	120	13 4	92 5	117345	1 423
20	Bare	3	120	13 4	105 8	104779	1 271
21	Bare	3	120	13 4	121 5	100503	1 219
22	Bare	3	120	13 4	136 3	97991	1 189
23	Bare	3	120	13 4	151 5	104424	1 267
24	Bare	3	120	13 4	166 8	104203	1 264
25	Bare	3	120	13 4	182 0	99200	1 203
26	Bare	3	120	13 4	197 2	101041	1 226
27	Bare	3	120	13 4	210 5	119531	1 450
28	Bare	3	120	17 8	92 5	149763	1 817
29	Bare	3	120	17 8	105 8	138200	1 676
30	Bare	3	120	17 8	121 5	134442	1 631
31	Bare	3	120	17.8	136 3	129930	1 576
32	Bare	3	120	17 8	151 5	126930	1 540
33	Bare	3	120	17 8	166 8	130152	1 579
34	Bare	3	120	17 8	182 0	130456	1 582
35	Bare	3	120	17 8	197 2	125648	1 524
36	Bare	3	120	17 8	210 5	153695	1 864
37	Bare	3	120	22 2	92 5	180388	2 188
38	Bare	3	120	22 2	105 8	160374	1 945
39	Bare	3	120	22 2	121 5	165243	2 004
40	Bare	3	120	22 2	136 3	163781	1 987
41	Bare	3	120	22 2	151 5	169323	2 054

TABLE 9 4

(Continued)

Run 1188

Foil Number	Foil Type	Module Number	Location Angle (°cw)	Location Radial (cm)	Location Axial (cm)	Normalized Counts	Local to Foil (X)
42	Bare	3	120	22 2	166 8	165588	2 009
43	Bare	3	120	22 2	182 0	166522	2 020
44	Bare	3	120	22 2	197 2	159356	1 933
45	Bare	3	120	22 2	210 5	170104	2 063

Run 1190

Foil Number	Foil Type	Module Number	Angle (°cw)	Radial (cm)	Axial (cm)	Normalized Counts	Cadmium Ratio
1	Cad Cov	3	120	13 4	92 5	5584	21 015
2	Cad Cov	3	120	13 4	151 5	5209	20 047
3	Cad Cov	3	120	13 4	210 5	5384	22 201
4	Cad Cov	3	120	22 5	92 5	5488	32 870
5	Cad Cov	3	120	22 5	151 5	6109	27 717
6	Cad Cov	3	120	22 5	210 5	5642	30 150

Run 1190

Foil Number	Foil Type	Module Number	Stage	Radial (cm)	Degrees cw	Normalized Counts	Cadmium Ratio
7	Cad Cov	3	8	19 4	45 0	5517	22 040
8	Cad Cov	3	8	19 4	135 0	5803	24 514
9	Cad Cov	3	8	19 4	225 0	5926	21 004
10	Cad Cov	3	8	19 4	315 0	5664	20 772

Run 1190

Foil Number	Foil Type	Module Number	Stage	Radial From Reactor Center Through Module 1	Axial (cm)	Normalized Counts	Local to Foil (X)
11	Bare			0 0	212 0	222988	2 705
12	Bare			7 6	212 0	222339	2 697
13	Bare			15 2	212 0	206680	2 507
14	Bare			22 8	212 0	191842	2 327
15	Bare			30 5	212 0	161160	1 955
16	Bare			38 1	212 0	139914	1 697
17	Bare			45 7	212 0	119847	1 454
18	Bare			53 3	212 0	111464	1 352
19	Bare			61 0	212 0	112442	1 364
20	Bare			68 6	212 0	120887	1 466
21	Bare			76 2	212 0	141204	1 713
22	Bare			83 8	212 0	147984	1 795
23	Bare			91 4	212 0	150031	1 820

TABLE 9 4

(Continued)

Run 1190

Foil Number	Foil Type	Module Number	Stage	Radial From Center of Module	Degrees cw	Normalized Counts	Local to Foil (X)
24	Cad Cov	3	9	35 2	0 0	6094	30 231
25	Cad Cov	3	9	35 2	90 0	6113	37 412
26	Cad Cov	3	9	35 2	180 0	6234	34 869
27	Cad Cov	3	9	35 2	270 0	5853	30 663

Run 1191

Foil Number	Foil Type	Module Number	Location: Angle (°cw)	Location: Radial (cm)	Location: Axial (cm)	Normalized Counts	Local to Foil (X)
1	Bare	3	30	4 6	92 5	93878	1 139
2	Bare	3	30	4 6	121 5	80225	0.973
3	Bare	3	30	4 6	151 5	79978	0 970
4	Bare	3	30	4 6	182 0	82691	1 003
5	Bare	3	30	4 6	210 5	114555	1 390
6	Bare	3	30	9 0	92 5	99468	1 207
7	Bare	3	30	9 0	121 5	85136	1 033
8	Bare	3	30	9 0	151 5	86548	1 050
9	Bare	3	30	9 0	182 0	86111	1 045
10	Bare	3	30	9 0	210 5	114011	1 383
11	Bare	3	30	13 4	92 5	107610	1 305
12	Bare	3	30	13 4	121 5	96285	1 168
13	Bare	3	30	13 4	151 5	97513	1 183
14	Bare	3	30	13 4	182 0	94780	1 150
15	Bare	3	30	13 4	210 5	126112	1 530
16	Bare	3	30	17 8	92 5	127799	1 550
17	Bare	3	30	17 8	121 5	121939	1 479
18	Bare	3	30	17 8	151 5	123158	1 494
19	Bare	3	30	17 8	182 0	114308	1 387
20	Bare	3	30	17 8	210 5	138584	1.681
21	Bare	3	30	22 2	92 5	152954	1 855
22	Bare	3	30	22 2	121 5	151053	1 832
23	Bare	3	30	22 2	151 5	144102	1 748
24	Bare	3	30	22 2	182 0	146436	1 776
25	Bare	3	30	22 2	210 5	161265	1 956

TABLE 9 4

(Continued)

Run 1191

Foil Number	Foil Type	Module Number	Angle (°cw)	Radial From Reactor Center 120° Between Modules 1 & 2	Axial (cm)	Normalized Counts	Local to Foil (X)
26	Bare			0 0	212 0	221884	2 691
27	Bare			7 6	212 0	226369	2 746
28	Bare			15 2	212 0	224470	2 723
29	Bare			22 8	212.0	238862	2 897
30	Bare			30 5	212.0	244019	2 960
31	Bare			38 1	212 0	219551	2 663
32	Bare			45 7	212 0	249887	3.031
33	Bare			53 3	212 0	245591	2 979
34	Bare			61 0	212 0	225012	2 729
35	Bare			68 6	212 0	203410	2 467
36	Bare			76 2	212 0	170000	2 062
37	Bare			83 8	212 0	147966	1 795
38	Bare			91 4	212 0	119341	1.448
39	Bare			99 0	212 0	95875	1 163
40	Bare			106 6	212 0	81926	0.994
41	Bare			114 3	212 0	69747	0 846
42	Bare			121 9	212 0	58198	0 706
43	Bare			137 1	212 0	38445	0.466
44	Bare			152 4	212 0	23824	0 289
45	Bare			167 5	212 0	12397	0 150
46	Bare			182 9	212 0	2704	0 033
47	Bare			0 0	89 4	300691	3 647
48	Bare			0 0	74 9	314211	3 811
49	Bare			0 0	59 6	249079	3 021
50	Bare			0 0	44 4	157391	1 909
51	Bare			0 0	29 1	95971	1 164
52	Bare			0 0	13 9	48690	0 591
53	Bare			0 0	0	7359	0 089

Run 1191

Foil Number	Foil Type	Module Number	Angle (°cw)	Location Radial (cm)	Location Axial (cm)	Normalized Counts	Local to Foil (X)
54	Bare			93 2	151 5	226323	2 745
55	Bare			107 7	151 5	169309	2 054
56	Bare			123 0	151 5	123644	1 500
57	Bare			138 2	151 5	83317	1 011
58	Bare			153.4	151 5	50480	0 612
59	Bare			168 7	151.5	23425	0.284
60	Bare			183 7	151 5	3266	0 040

TABLE 9 4

(Continued)

Run 1191

Foil Number	Foil Type	Module Number	Angle (°cw)	Radial From Center of Element	Axial (cm)	Normalized Counts	Local to Foil (X)
61	Bare	1		0 0	212 0	111704	1 355
62	Bare	1		0 0	212 0	108279	1 313
63	Bare	2		0 0	212 0	115520	1 401
64	Bare	2		0 0	212 0	107092	1 299
65	Bare	3		0 0	212 0	116124	1 409
66	Bare	3		0 0	212 0	117216	1 422

TABLE 9 5

Gold Foil Data

3-Module Cavity Reactor

(All Normalized to Power Level of Run 1186)

Run 1185

Foil Number	Foil Type	Location Radial (cm)	Location Axial (cm)	Foil Weight (gm)	Specific Activity d/m/gm x 10^{-6}	Local to Foil (X)
1	Bare	0 0	89.4	0 0362	10 774	2 535
2	Bare	0 0	74 9	0 0360	10 461	2 461
3	Bare	0 0	59 6	0 0336	7 634	1 796
4	Bare	0 0	44 4	0 0359	5 021	1 181
5	Bare	0 0	29 1	0 0357	2 989	0 703
6	Bare	0 0	13 9	0 0349	1 478	0 348
7	Bare	0 0	0	0.0367	0 250	0 059
8	Bare	93 2	151 5	0.0366	6 887	1 620
9	Bare	107 7	151 5	0 0364	5 267	1 239
10	Bare	123 0	151 5	0 0373	3 677	0 865
11	Bare	138 2	151 5	0 0353	2 493	0 587
12	Bare	153 4	151 5	0 0356	1 521	0 357
13	Bare	168 7	151 5	0 0367	0 643	0 151
14	Bare	183.7	151 5	0 0370	0 098	0 023

Foil Number	Foil Type	Module Number	Stage	Radial Distance From Center	Degrees cw	Foil Weight (gm)	Specific Activity d/m/gm x 10^{-6}	Local to Foil (X)
15	Bare	3	9	19 4	0	0 0362	5 670	1 334
16	Bare	3	9	19 4	22 5	0 0360	5 746	1 352
17	Bare	3	9	19 4	45 0	0 0372	6 200	1 459
18	Bare	3	9	19 4	67 5	0 0358	6 443	1 516
19	Bare	3	9	19 4	90 0	0 0357	6 929	1 630
20	Bare	3	9	19 4	112 5	0 0357	6 445	1 516
21	Bare	3	9	19 4	135 0	0 0377	6 331	1 490
22	Bare	3	9	19 4	157 5	0 0359	6 329	1 489
23	Bare	3	9	19 4	180 0	0 0353	6 500	1 529
24	Bare	3	9	19 4	202 5	0 0364	6 344	1 493
25	Bare	3	9	19 4	225 0	0 0364	5 998	1 411
26	Bare	3	9	19 4	247 5	0 0364	5 690	1 339
27	Bare	3	9	19 4	270 0	0 0353	5 612	1 320
28	Bare	3	9	19 4	292 5	0 0368	5 713	1 344
29	Bare	3	9	19 4	315 0	0 0359	5 679	1 336
30	Bare	3	9	19 4	337 5	0 0353	5 691	1 339

TABLE 9 5

(Continued)

Run 1185

Foil Number	Foil Type	Radial Traverse Distance From Module Center	Foil Weight (gm)	Specific Activity d/m/gm x 10^{-6}
31	Cad Cov	35 3	0 0358	3 493
32	Cad Cov	57 4	0 0360	2 942
33	Cad Cov	79 5	0 0364	3 545
34	Cad Cov	101 6	0 0361	2 575
35	Cad Cov	123 7	0 0346	0 759
36	Cad Cov	145 8	0 0356	0 119

Run 1186

Foil Number	Foil Type	Location Radial (cm)	Location Axial (cm)	Foil Weight (gm)	Specific Activity d/m/gm x 10^{-6}	Local to Foil (X)
1	Cad Cov	0 0	74 9	0 0365	0 726	
2	Cad Cov	0 0	44 4	0 0358	0 034	
3	Cad Cov	107 7	151 5	0 0351	0 044	
4	Cad Cov	138 2	151 5	0 0367	0 002	

Foil Number	Foil Type	Module Number	Stage	Radial Distance From Center	Degrees cw	Foil Weight (gm)	Specific Activity d/m/gm x 10^{-6}	Local to Foil (X)
5	Bare	3	9	35 2	0	0 0369	7 718	1 816
6	Bare	3	9	35 2	22 5	0 0353	8 057	1 896
7	Bare	3	9	35 2	45 0	0 0359	8 524	2 006
8	Bare	3	9	35 2	67 5	0 0368	8 905	2 095
9	Bare	3	9	35 2	90 0	0 0353	9 322	2 193
10	Bare	3	9	35 2	112 5	0 0337	9 459	2 226
11	Bare	3	9	35 2	135 0	0 0371	9 270	2 181
12	Bare	3	9	35 2	157 5	0 0355	8 995	2 116
13	Bare	3	9	35 2	180 0	0 0345	8 533	2 008
14	Bare	3	9	35 2	202 5	0 0363	8 175	1 923
15	Bare	3	9	35 2	225 0	0 0359	7 828	1 842
16	Bare	3	9	35 2	247 5	0 0363	7 550	1 776
17	Bare	3	9	35 2	270 0	0 0355	7 413	1 744
18	Bare	3	9	35 2	292 5	0 0369	7 322	1 723
19	Bare	3	9	35 2	315 0	0 0372	7 468	1 757
20	Bare	3	9	35 2	337 5	0 0349	7 557	1 778

TABLE 9 5

(Continued)

Run 1187

Foil Number	Foil Type	Location Radial (cm)	Location Axial (cm)	Foil Weight (gm)	Specific Activity d/m/gm x 10^{-6}	Local to Foil (X)
1	Cad Cov	0 0	89 4	0 0348	1 619	
2	Cad Cov	0 0	59 6	0 0364	0 168	
3	Cad Cov	0 0	29 1	0 0350	0 006	
4	Cad Cov	93 2	151 5	0 0360	0 070	
5	Cad Cov	123 0		0 0357	0 006	
6	Cad Cov	153 4		0 0360	0 0001	
7	Bare	4 6	92 5	0 0357	4 823	1 135
8	Bare	4 6	121 5	0 0369	4 339	1 021
9	Cad Cov	4 6	136 3	0 0371	2 064	
10	Bare	4 6	151 5	0 0348	4.250	1 000 (X)
11	Cad Cov	4 6	166 8	0 0354	2 108	
12	Bare	4 6	182 0	0 0359	4 324	1 017
13	Bare	4 6	210 5	0 0365	5 338	1 256
14	Bare	9 0	92 5	0 0350	4 956	1 166
15	Bare	9 0	121 5	0 0359	4 398	1 035
16	Bare	9 0	151 5	0 0350	4 477	1 053
17	Bare	9.0	182 0	0 0355	4 444	1 046
18	Bare	9 0	210 5	0 0360	5 229	1 230
19	Bare	13 4	92 5	0 0359	4 988	1 174
20	Bare	13 4	121 5	0 0368	4 618	1 087
21	Bare	13 4	151 5	0 0364	4 764	1 121
22	Bare	13 4	182 0	0 0358	4 670	1 099
23	Bare	13 4	210 5	0.0351	5 565	1 309
24	Bare	17 8	92 5	0 0357	5 644	1 328
25	Bare	17 8	121 5	0 0363	5 288	1 244
26	Cad Cov	22 2	136 3	0 0359	2 212	
27	Bare	17 8	151 5	---	---	---
28	Cad Cov	22 2	166 8	0 0353	2 249	
29	Bare	17 8	182 0	0 0359	5 244	1 234
30	Bare	17 8	210 5	0.0356	6 002	1 412
31	Bare	22 2	92 5	0 0360	6 495	1 528
32	Bare	22 2	121 5	0 0365	6 211	1 461
33	Bare	22 2	151 5	0 0352	6 418	1 510
34	Bare	22 2	182 0	0 0365	6 066	1 427
35	Bare	22 2	210 5	0 0360	6 450	1 518

Foil Number	Foil Type	Radial Traverse Distance From Module Center	Foil Weight (gm)	Specific Activity d/m/gm x 10^{-6}	Local to Foil (X)
36	Bare	35 3	0 0359	6 647	1 564
37	Bare	46 3	0 0361	9 305	2 189
38	Bare	57 4	0 0350	11 744	2 763

TABLE 9 5

(Continued)

Run 1187

Foil Number	Foil Type	Radial Traverse Distance From Module Center	Foil Weight (gm)	Specific Activity d/m/gm x 10^{-6}	Local to Foil (X)
39	Bare	68 4	0 0364	13 705	3 225
40	Bare	79 5	0 0365	14 287	3 362
41	Bare	90 5	0 0354	14 371	3 381
42	Bare	101 6	0 0361	14 585	3 432
43	Bare	112 6	0 0374	15 569	3 663
44	Bare	123 7	0 0364	16 675	3 923
45	Bare	134 7	0 0369	15 616	3 674
46	Bare	145 8	0 0356	10 327	2 430

Run 1187

Foil Number	Foil Type	Module Number	Stage	Radial Distance From Center	Degrees cw	Foil Weight (gm)	Specific Activity d/m/gm x 10^{-6}
47	Cad Cov	3	9	19 4	0	0 0365	2 149
48	Cad Cov	3	9	19 4	90	0 0356	2 357
49	Cad Cov	3	9	19 4	180	0 0359	2 256
50	Cad Cov	3	9	19 4	270	0 0368	2 179

Run 1188

Foil Number	Foil Type	Location Radial (cm)	Location Axial (cm)	Foil Weight (cm)	Specific Activity d/m/gm x 10^{-6}	Local to Foil (X)
1	Bare	0 0	82 5	0 0356	11 654	2 742
2	Bare	0 0	67 2	0 0372	9 294	2 187
3	Bare	0 0	52 0	0 0363	6 249	1 470
4	Bare	100 1	151 5	0 0367	6 387	1 503
5	Bare	115 4	151 5	0 0354	4 610	1 085
6	Bare	130 6	151 5	0 0365	3 230	0 760

Run 1188

Foil Number	Foil Type	Module Number	Stage	Radial Distance From Center	Degrees cw	Foil Weight (gm)	Specific Activity d/m/gm x 10^{-6}
7	Cad Cov	3	9	35 2	0	0 0363	2 496
8	Cad Cov	3	9	35 2	90	0 0359	2 672
9	Cad Cov	3	9	35 2	180	0 0362	2 554
10	Cad Cov	3	9	35 2	270	0 0360	2 387

TABLE 9 5

(Continued)

Run 1188

Foil Number	Foil Type	Distance From Module Center	Foil Weight (gm)	Specific Activity d/m/gm x 10^{-6}
11	Cad Cov	46 3	0 0363	2 323
12	Cad Cov	68 4	0 0363	2 883
13	Cad Cov	90 5	0 0350	2 102
14	Cad Cov	112 6	0 0346	0 591

Run 1190

Foil Number	Foil Type	Radial Traverse Distance From Module Center	Foil Weight (gm)	Specific Activity d/m/gm x 10^{-6}	Local to Foil (X)
1	Bare	57 4	0 0356	17 242	4 057
2	Bare	79 5	0 0348	15 088	3 550
3	Bare	101 6	0 0375	14 948	3 517
4	Bare	123 7	0 0364	12 208	2 872

Run 1190

Foil Number	Foil Type	Location Radial (cm)	Location Axial (cm)	Foil Weight (gm)	Specific Activity d/m/gm x 10^{-6}	Local to Foil (X)
5	Cad Cov	0 0	74 9	0 0359	0 738	
6	Cad Cov	0 0	44 4	0 0361	0 032	
7	Cad Cov	0 0	13 9	0 0360	0 001	
8	Bare	93 2	151 5	0 0366	6 569	1 546
9	Bare	107 7	151 5	0 0358	5 183	1 220
10	Bare	123 0	151 5	0 0351	---	
11	Bare	138 2	151 5	0 0376	---	
12	Bare	153 4	151 5	0 0365	---	
13	Bare	168 7	151 5	0 0370	---	
14	Bare	183 7	151 5	0 0345	---	
15	Bare	99 0	212 0	0 0368	5 574	1 312
16	Bare	107 7	212 0	0 0364	4 886	1 150
17	Bare	115 3	212 0	0 0369	4 211	0 991
18	Bare	130 5	212 0	0 0361	2 718	0 640
19	Bare	145 7	212 0	0 0344	1 640	0 386
20	Bare	160 9	212 0	0 0370	0 890	0 209
Run 1191						
1	Bare	0 0	212 0	0 0351	7 744	1 822
Run 1192						
1	Bare	4 6	92 5	0 0356	5 245	1 234
2	Bare	4 6	121 5	0 0358	4 537	1 068

TABLE 9 5

(Continued)

Run 1192

Foil Number	Foil Type	Location Radial (cm)	Location Axial (cm)	Foil Weight (gm)	Specific Activity d/m/gm x 10^{-6}	Local to Foil (X)
3	Cad Cov	4 6	136 3	0 0360	2 264	
4	Bare	4 6	151 5	0 0361	4 644	1 093
5	Cad Cov	4 6	166 8	0 0346	2 259	
6	Bare	4 6	182 0	0 0363	4 526	1 065
7	Bare	4 6	210 5	0 0352	5 528	1 301
8	Bare	9 0	92 5	0 0357	5 318	1 251
9	Bare	9 0	121 5	0 0351	4 727	1 112
10	Bare	9 0	151 5	0 0362	4 860	1 144
11	Bare	9 0	182 0	0 0372	4 604	1 083
12	Bare	9 0	210 5	0 0363	5 731	1 348
13	Bare	13 4	92 5	0 0363	5 551	1 306
14	Bare	13.4	121 5	0 0354	5 096	1 199
15	Bare	13 4	151 5	0 0358	5 259	1 237
16	Bare	13 4	182 0	0 0369	5 037	1 185
17	Bare	13.4	210 5	0 0360	5 979	1 407
18	Bare	17 8	92 5	0 0350	6 699	1 576
19	Bare	17 8	121 5	0 0352	6 173	1 452
20	Bare	17 8	151 5	0 0363	6 244	1 469
21	Bare	17 8	182 0	0 0365	6 196	1 458
22	Bare	17 8	210 5	0 0358	6 529	1 536
23	Bare	22 2	92 5	0 0366	7 470	1 758
24	Bare	22 2	121 5	0 0350	7 345	1 728
25	Cad Cov	22 2	136 3	0 0346	2 433	
26	Bare	22 2	151 5	0 0363	7 264	1 709
27	Cad Cov	22 2	166 8	0 0375	2 388	
28	Bare	22 2	182 0	0 0358	7 149	1 682
29	Bare	22 2	210 5	0 0346	7 374	1 735
30	Cad Cov	107 7	151 5	0 0351	0 018	
31	Cad Cov	138 2	151 5	0 0379	0 003	
32	Cad Cov	168 7	151 5	0 0359	0 002	
33	Bare	0 0	89 4	0 0353	10 875	2 559
34	Bare	0 0	74 9	0 0363	10 325	2 429
35	Bare	0 0	59 6	0 0365	7 644	1 799
36	Bare	0 0	44 4	0 0328	4 915	1 156
37	Bare	0 0	29 1	0 0358	3 063	0 721
38	Bare	0 0	13 9	0 0359	1 499	0 353
39	Bare	0 0	0 0	0 0355	0 209	0 049

TABLE 9 5

(Continued)

Run 1192

Foil Number	Foil Type	Module Number	Stage	Radial Distance From Center	Degrees cw	Foil Weight (gm)	Specific Activity d/m/gm x 10^{-6}
40	Cad Cov	3	8	35 2	45	0 0360	2 391
41	Cad Cov	3	8	35 2	135	0 0370	2 583
42	Cad Cov	3	8	35 2	225	0 0365	2 368
43	Cad Cov	3	8	35 2	315	0 0368	2 246
44	Cad Cov	3	9	19 4	45	0 0365	2 295
45	Cad Cov	3	9	19 4	135	0 0365	2 314
46	Cad Cov	3	9	19 4	225	0 0375	2 300
47	Cad Cov	3	9	19 4	315	0 0338	2 293

Run 1192

Foil Number	Foil Type	Radial	Axial	Radial Traverse Distance From Module Center	Degrees cw	Foil Weight (gm)	Specific Activity d/m/gm x 10^{-6}
48	Cad Cov			57 4		0 0369	2 35
49	Cad Cov			79 5		0 0342	2 878
50	Cad Cov			101 6		0 0363	2 124
51	Cad Cov			123 7		0 0367	0 586
52	Cad Cov			145 7		0 0367	0 092
53	Cad Cov	100 1	210 5			0 0367	1 023
54	Cad Cov	115 3	210 5			0 0370	0 340
55	Cad Cov	130 5	210 5			0 0355	0 093

TABLE 9 6

Thermal Neutron Flux

3-Module Reactor

Location		
Radial (cm)	Axial (cm)	Thermal Neutron Flux (n/cm^2-sec-watt x 10^{-6})
0	89 4	5 528
0	74 9	5 855
0	59 6	4 492
0	44 4	3 004
0	29 1	1 796
0	13 9	0 889
93 2	151 5	4 046
107 7	151 5	3 161
123 0	151 5	2 210
138 2	151 5	1 499
153 4	151 5	0 916
168 7	151 5	0 386

Radial Across Core Distance From Module Center (cm)	Thermal Neutron Flux (n/cm^2-sec-watt x 10^{-6})
35 3	---
46 3	4 201
57 4	5 279
68 4	6 518
79 5	6 470
90 5	7 393
101 6	7 231
112 6	9 030
123 7	9 593
145 8	6 146

Circumferential - Module 3, Stage 9

Distance From Module Center (cm)	Degrees cw	Thermal Neutron Flux (n/cm^2-sec-watt x 10^{-6})
19 4	0	2 116
19 4	45	2 362
19 4	90	2 755
19 4	135	2 437
19 4	180	2 546
19 4	225	2 210
19 4	270	2 045
19 4	315	2 072

TABLE 9 6

(Continued)

Circumferential - Module 3, Stage 9

Distance From Module Center (cm)	Degrees cw	Thermal Neutron Flux (n/cm^2-sec-watt x 10^{-6})
35 2	0	3 154
35 2	45	3 876
35 2	90	3 993
35.2	135	4 028
35 2	180	3 570
35 2	225	3 278
35 2	270	3 018
35 2	315	3 150

Location Radial (cm)	Axial (cm)	Module Number	Degrees	Thermal Neutron Flux (n/cm^2-sec-watt x 10^{-6})
4 6	151 5	3	300	1 286
22 6	151 5	3	300	2 515
4 6	151 5	3	120	1 450
22 6	151 5	3	120	2 919
19 4	151 5	3	120	2 716
35 2	151 5	3	120	4 058
19 4	151 5	3	300	2 071
35 2	151 5	3	300	3 044
		Across Face at Separation Plane		
99 1	212 0			2 741
114 3	212 0			2 331
144 8	212 0			1 581

TABLE 9 7

Infinitely Dilute

Gold Foil Cadmium Ratios

3-Module Cavity Reactor

Location: Radial (cm)	Location: Axial (cm)	Infinitely Dilute Foil Activity d/m/gm x 10^{-6}: Bare Gold	Infinitely Dilute Foil Activity d/m/gm x 10^{-6}: Cd Gold	Cadmium Ratio
0	89 4	12 937	3 756	3 444
0	74 9	11 458	1 734	6 608
0	59 6	7 857	0 397	19 793
0	44 4	5 064	0 075	67 203
0	29 1	2 997	0 014	214 808
0	13 9	1 479	0 002	628 904
93 2	151 5	6 884	0 165	41 807
107 7	151 5	5 291	0 042	126 267
123 0	151 5	3 685	0 014	262 006
138 2	151 5	2 497	0 007	346 452
153 4	151 5	1 521	---	---
168 7	151 5	0 646	0 005	137 412

Radial Across Core Distance From Module Center	Bare Gold	Cd Gold	Cadmium Ratio
35 3	11 356	---	---
46 3	12 460	5 483	2 272
57 4	15 688	6 920	2 267
68 4	17 630	6 805	2 591
79 5	19 123	8 377	2 283
90 5	17 167	4 888	3 512
101 6	18 074	6 064	2 981
112 6	16 364	1 368	11 964
123 7	17 688	1 757	10 069
145 8	10 487	0 279	37 635

Circumferential - Module 3, Stage 9

Distance From Module Center (cm)	Degrees cw	Infinitely Dilute Foil Activity d/m/gm x 10^{-6}: Bare Gold	Infinitely Dilute Foil Activity d/m/gm x 10^{-6}: Cd Gold	Cadmium Ratio
19 4	0	8 597	5 084	1 691
19 4	45	9 352	5 429	1 723
19 4	90	10 094	5 519	1 829
19 4	135	9 522	5 474	1 739
19 4	180	9 529	5 301	1 798
19 4	225	9 171	5 502	1 667

TABLE 9 7

(Continued)

Circumferential - Module 3, Stage 9

Distance From Module Center (cm)	Degrees cw	Infinitely Dilute Foil Activity d/m/gm x 10^{-6} Bare Gold	Cd Gold	Cadmium Ratio
19 4	270	8 567	5 172	1 657
19 4	315	8 699	5 257	1 655
35 2	0	11 130	5.891	1 889
35.2	45	11 755	5 624	2 090
35 2	90	12 910	6 278	2 056
35 2	135	12.835	6 145	2 089
35 2	180	11 950	6 021	1 985
35 2	225	11 046	5 602	1 971
35 2	270	10 627	5 615	1 893
35 2	315	10 563	5 331	1 981

Location Radial (cm)	Axial (cm)	Module Number	Degrees cw	Infinitely Dilute Foil Activity d/m/gm x 10^{-6} Bare Gold	Cd Gold	Cadmium Ratio
4 6	151 5	3	300	7 050	4 920	1 433
22 6	151 5	3	300	9 400	5 223	1 800
4 6	151 5	3	120	7 674	5 267	1 457
22 6	151 5	3	120	10 551	5 703	1 850
19 4	151 5	3	120	10 021	5 511	1 818
35 2	151 5	3	120	13 004	6 264	2 076
19 4	151 5	3	300	8 527	5 086	1 676
35 2	151 5	3	300	10 695	5 640	1 896
		Across Face at Separation Plane				
99 1	212 0			6 978	2 425	2 877
114 3	212 0			4 679	0 809	5 786
144 8	212 0			2 843	0 218	13 071

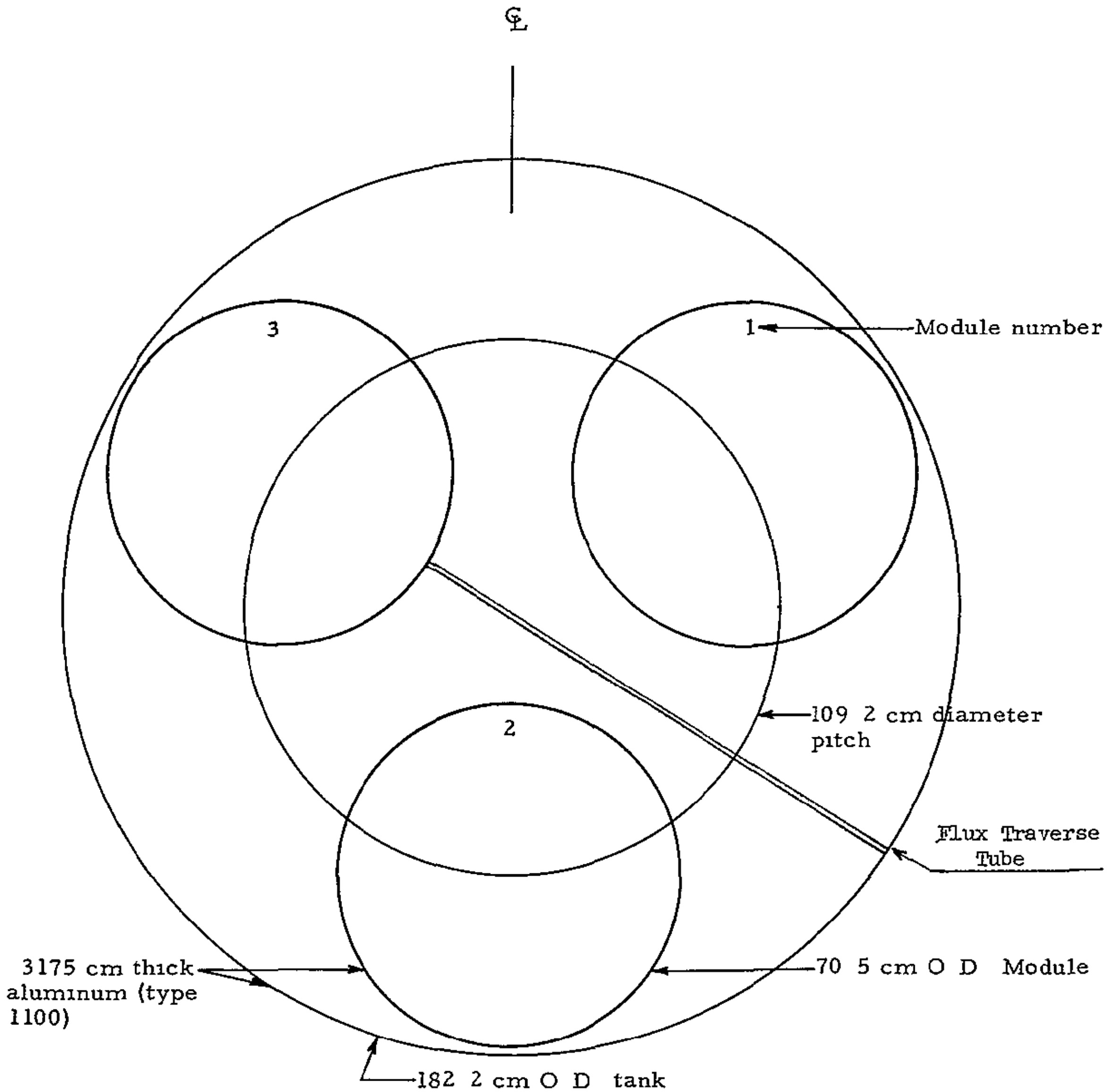

Figure 9 1 Cross section view at separation plane of 3 module tank insert

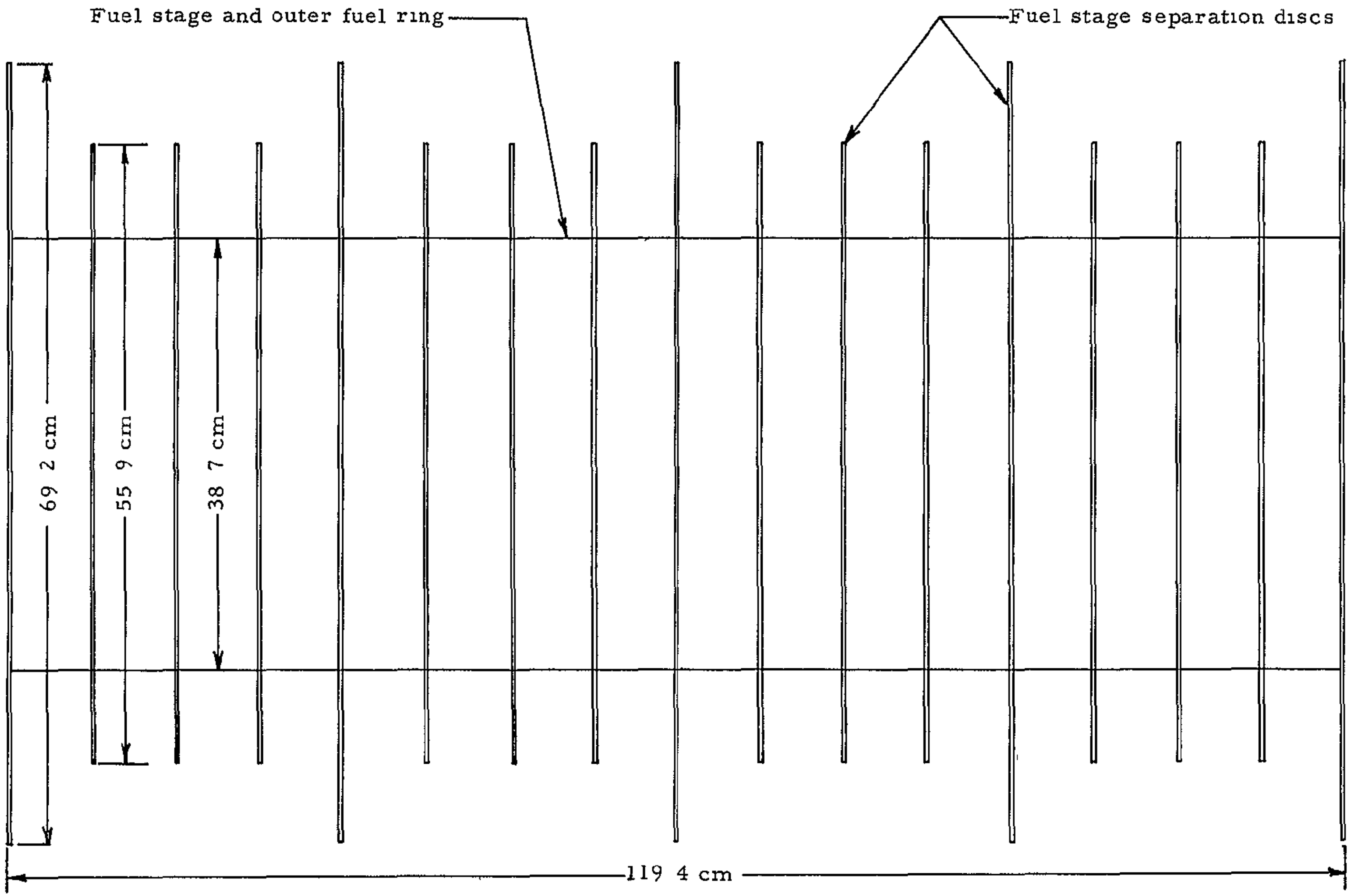

Figure 9.2 Side view of fuel element for 3 module reactor

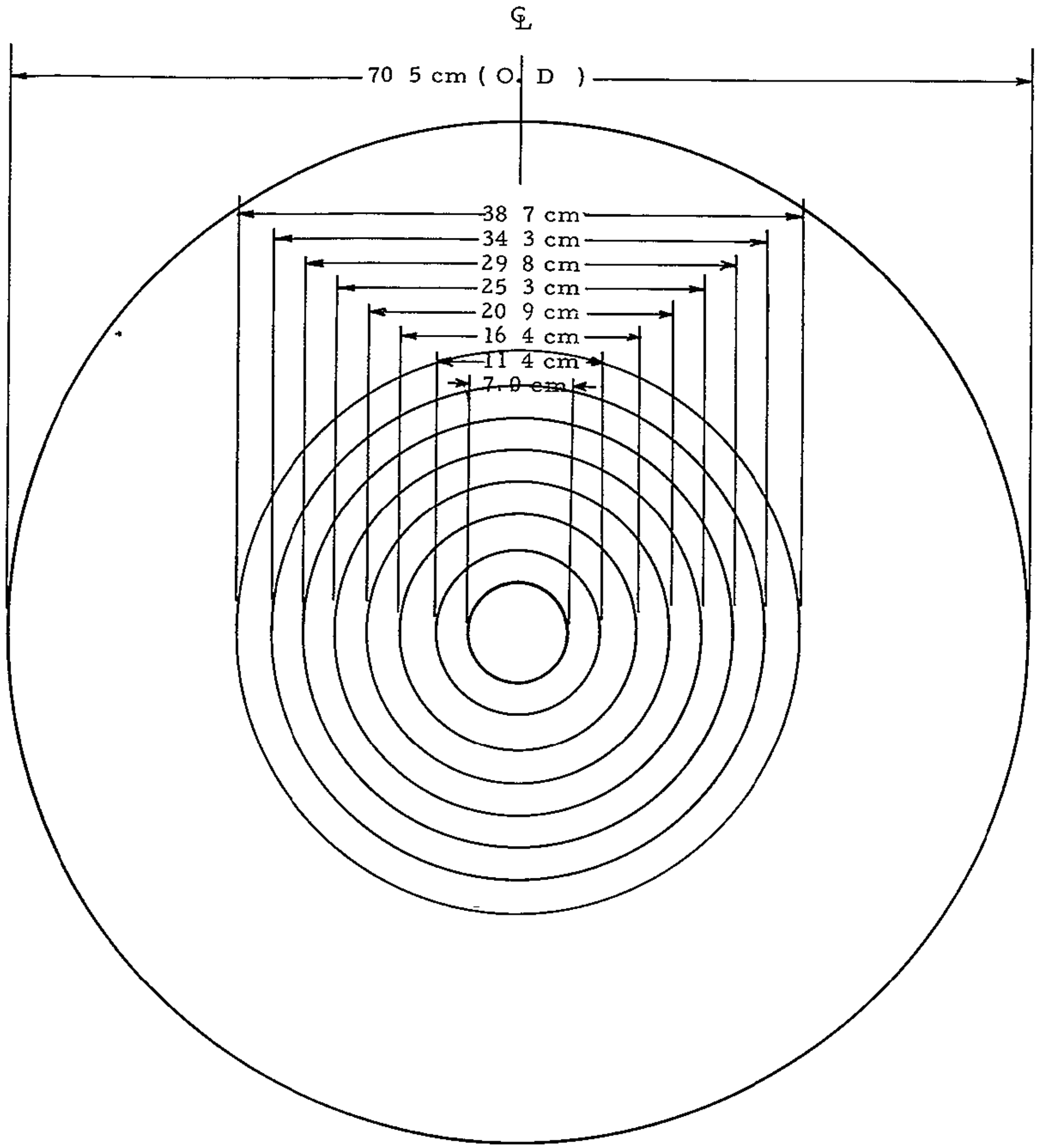

Figure 9 3 Layout of fuel rings for 3 module reactor fuel element

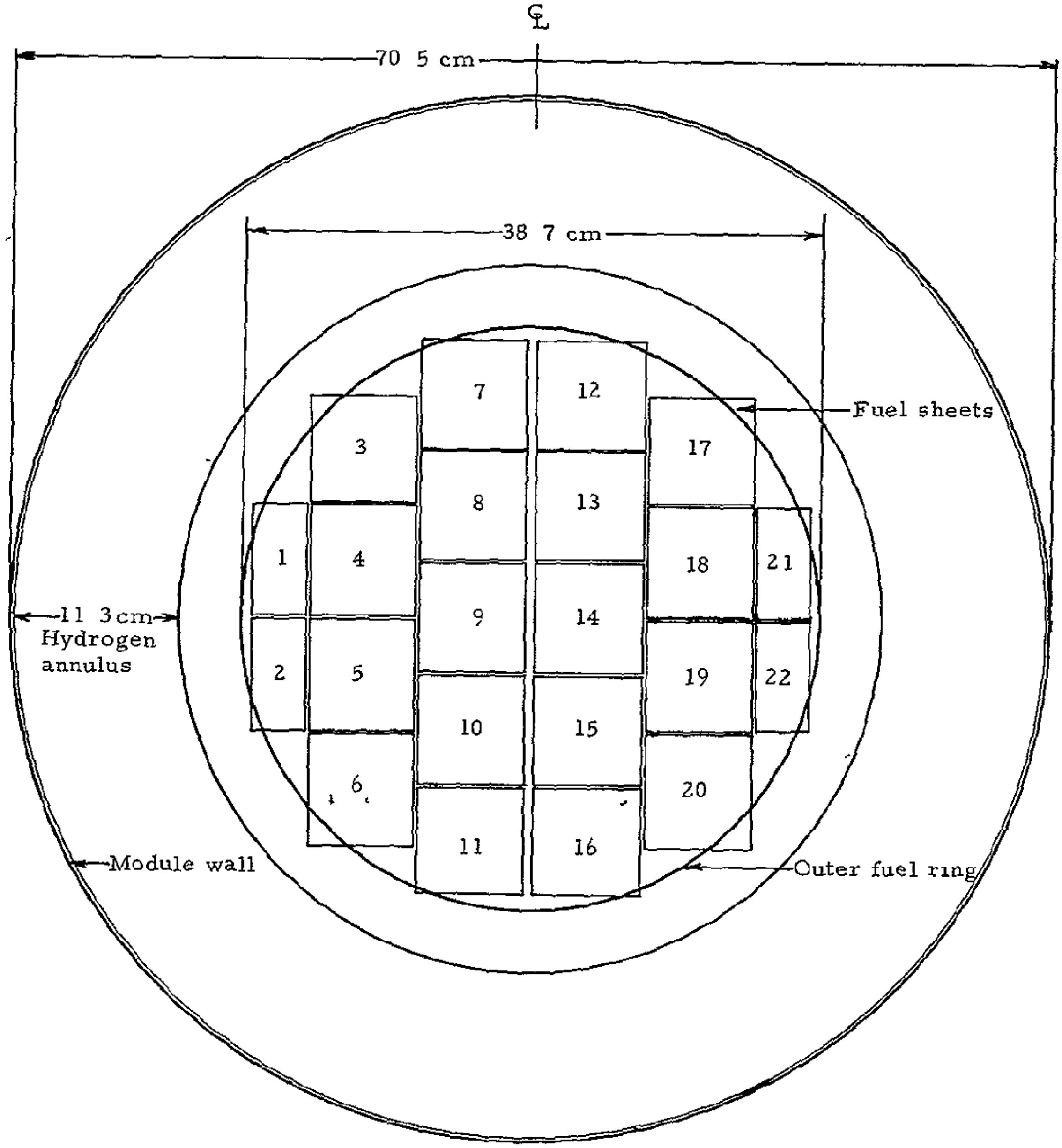

Figure 9.4 Layout of fuel sheets on fuel stage separation discs of 3 module reactor fuel element

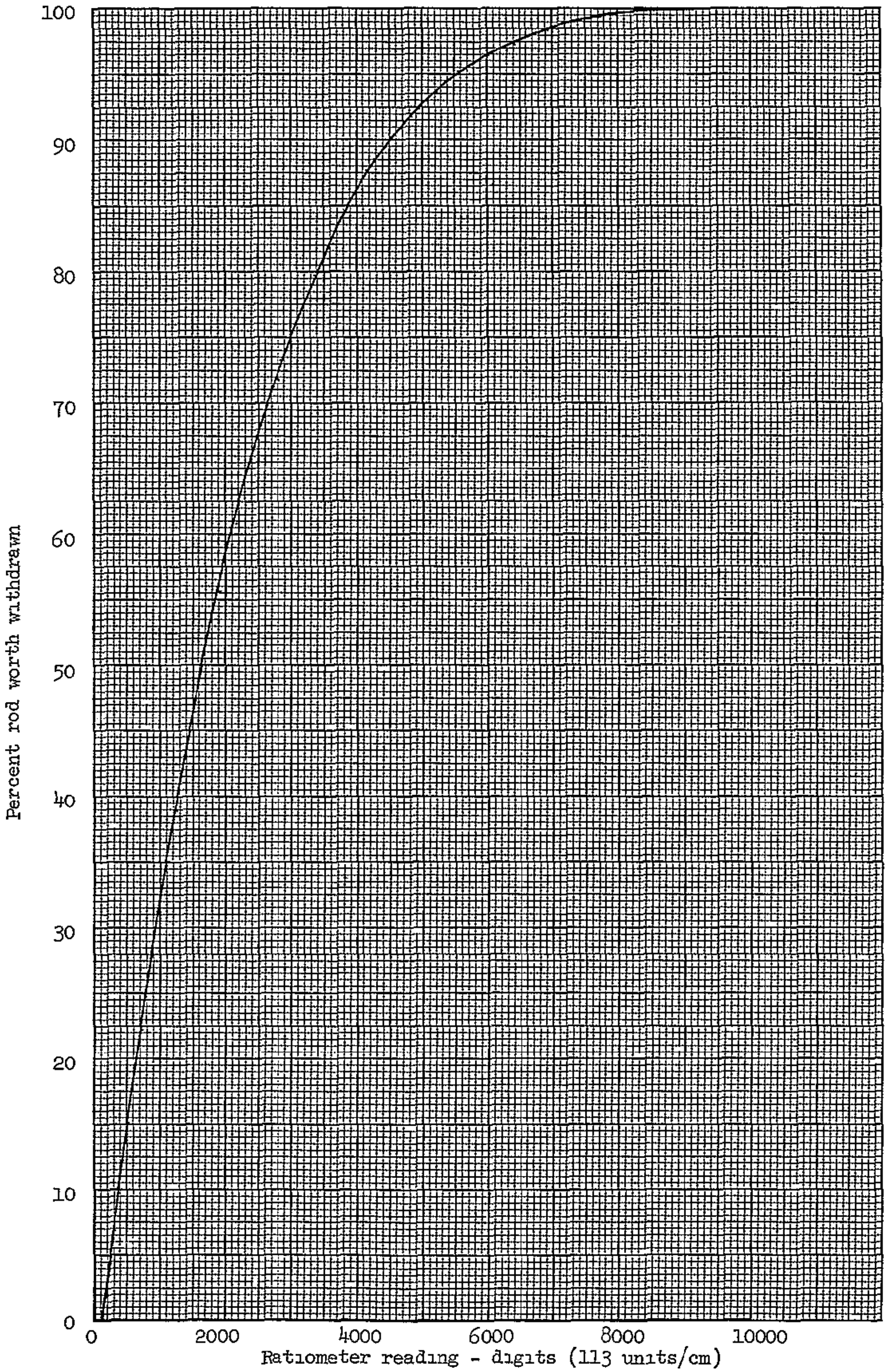

Figure 9 5 Control rod shape curve - eight actuators

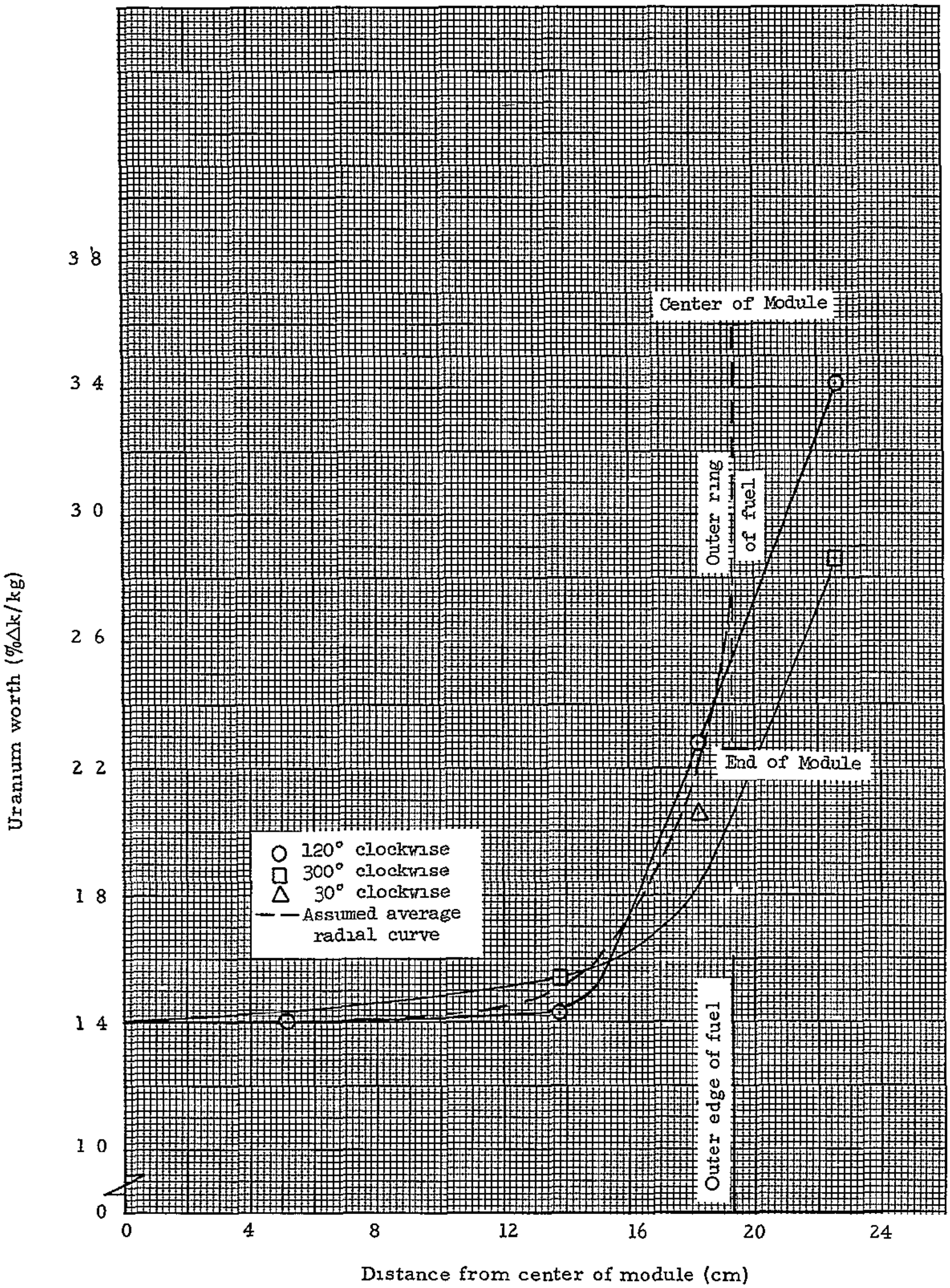

Figure 9.6 Fuel worth measurements from module 3 of the 3 module cavity reactor

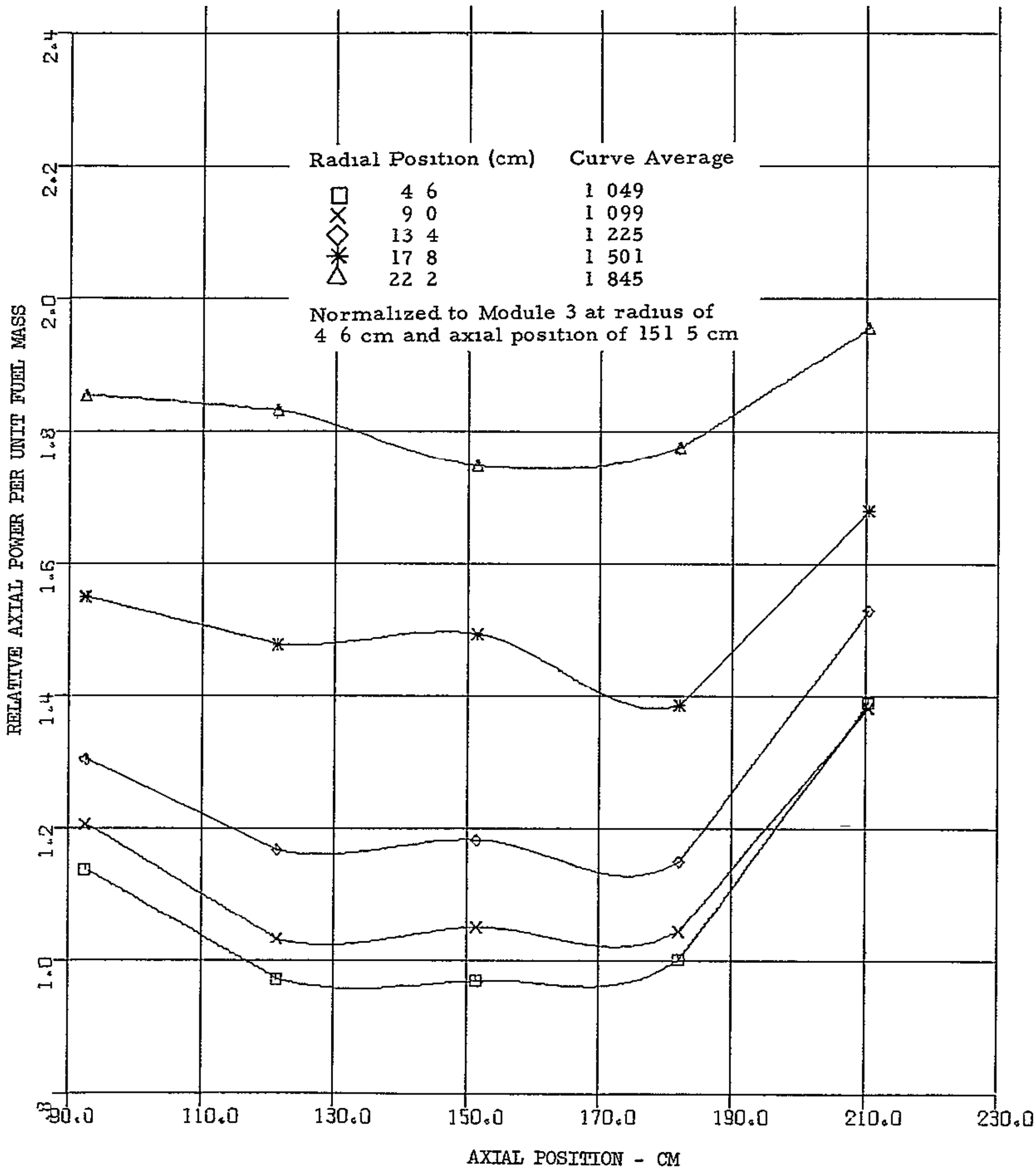

Figure 9.7 Relative axial power distribution in module 3, 30° at the core centerline, 3 module reactor with 0 55 fuel to module radius ratio

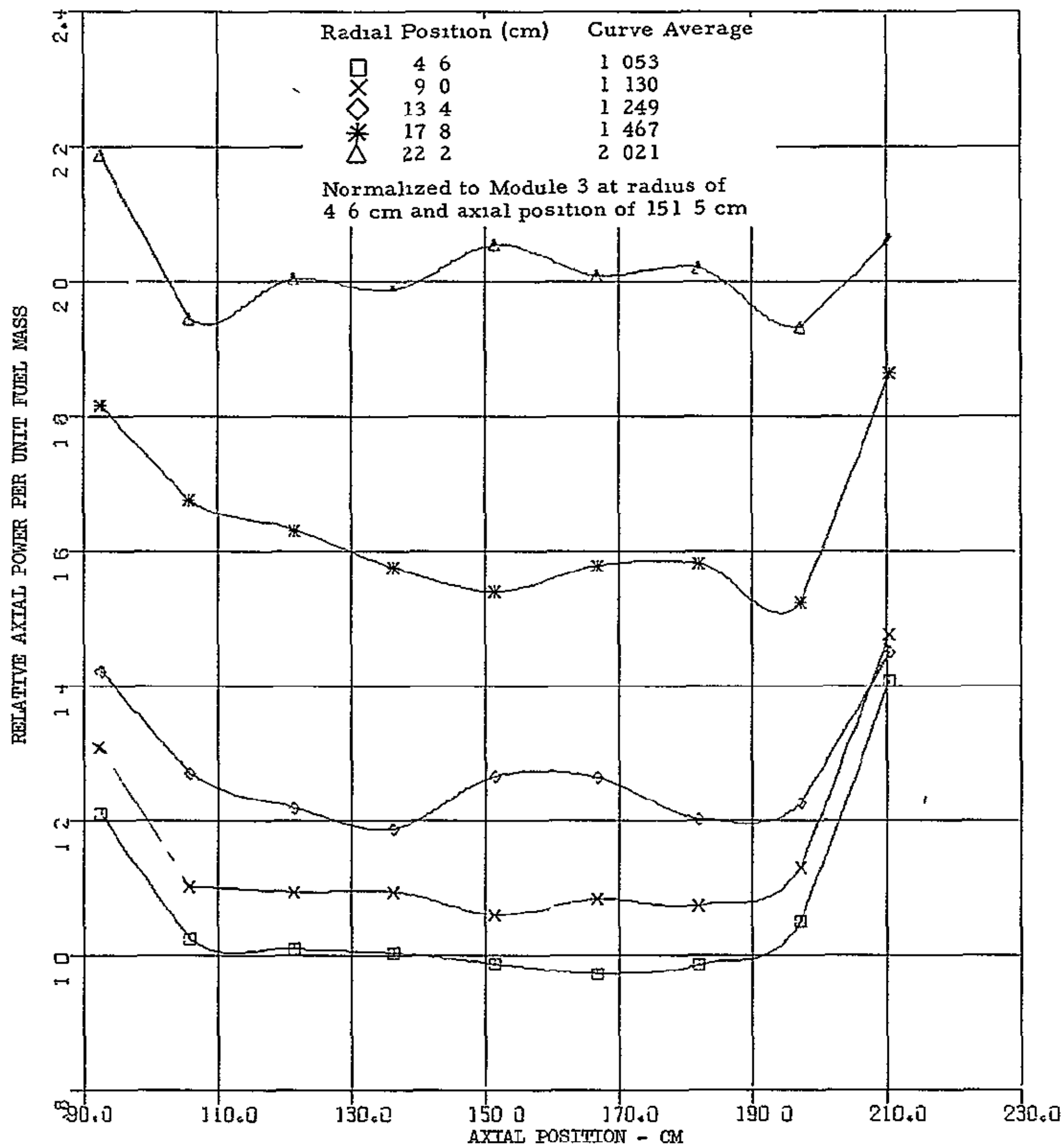

Figure 9 8 Relative axial power distribution in module 3, 120° at the core centerline, 3 module reactor with 0.55 fuel to module radius ratio

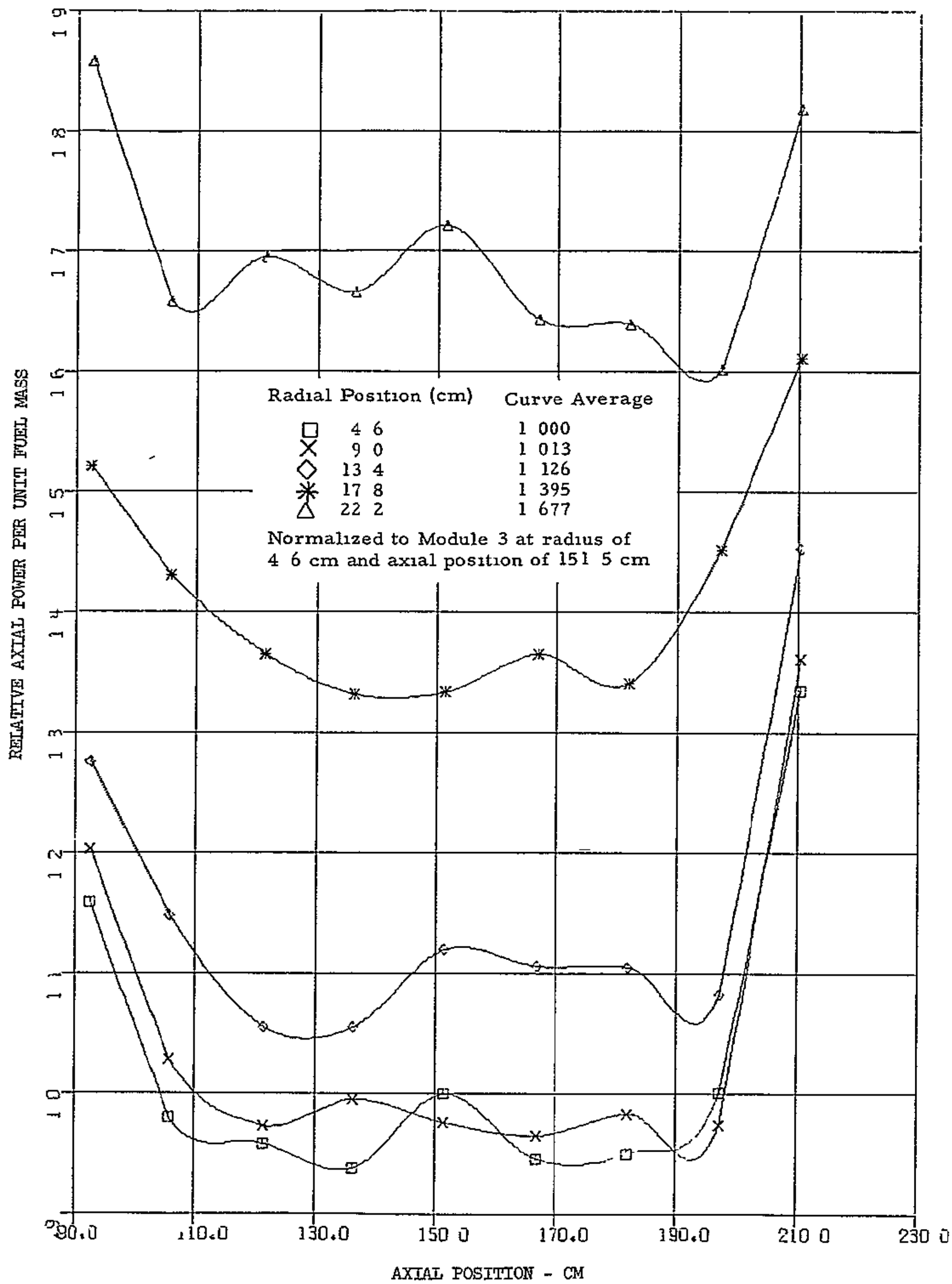

Figure 9 9 Relative axial power distribution in module 3, 300° at the core centerline, 3 module reactor with 0 55 fuel to module radius ratio

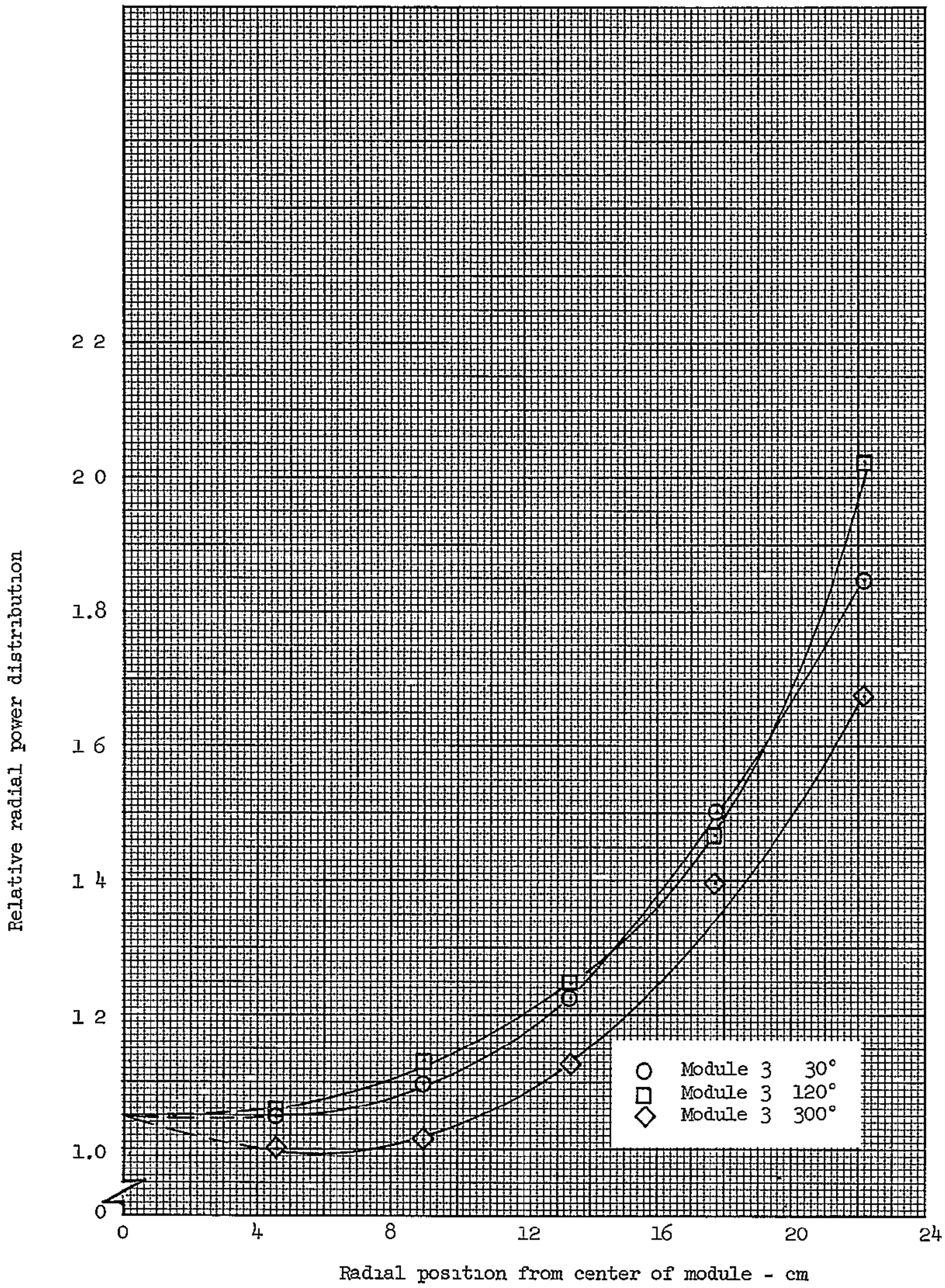

Figure 9 10 Relative radial power distribution in module 3 based on axial average power distributions - 3 module reactor with 0.55 fuel to module radius ratio

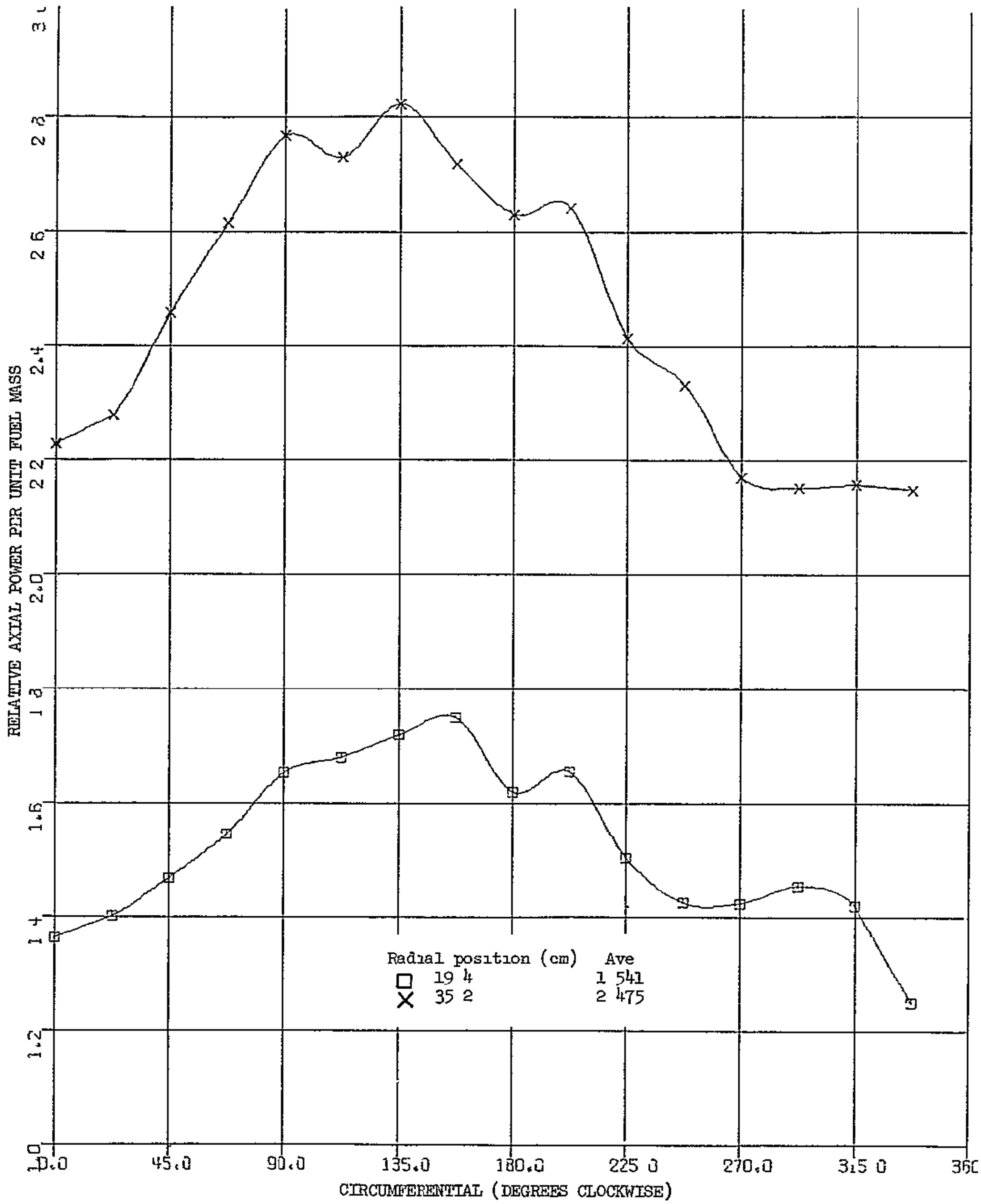

Figure 9 11 Circumferential power distribution on outside fuel ring, stage 8, 3 module reactor with 0 55 fuel to module radius ratio

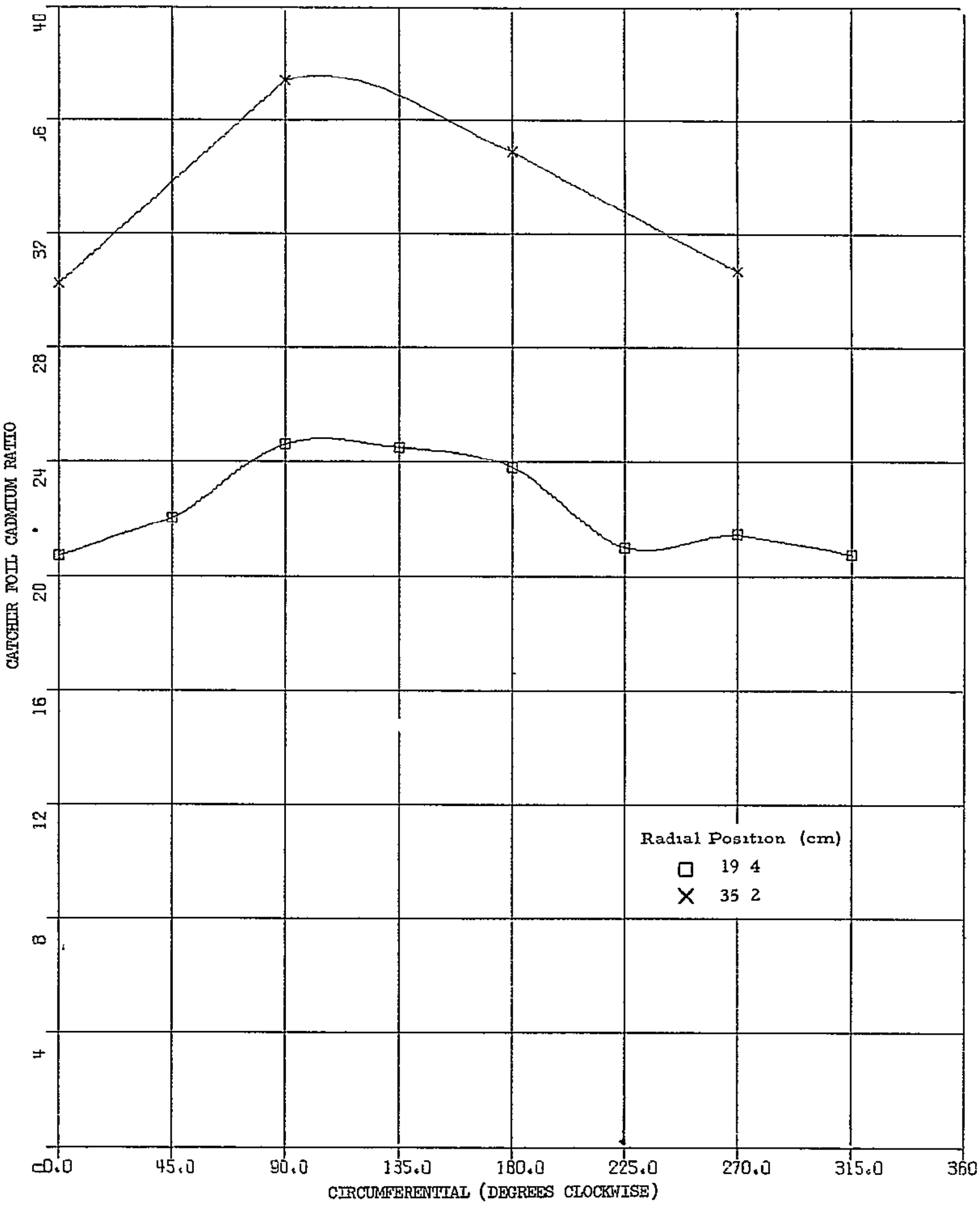

Figure 9.12 Circumferential catcher foil cadmium ratio on outside fuel ring, stage 8, 3 module reactor with 0 55 fuel to module radius ratio

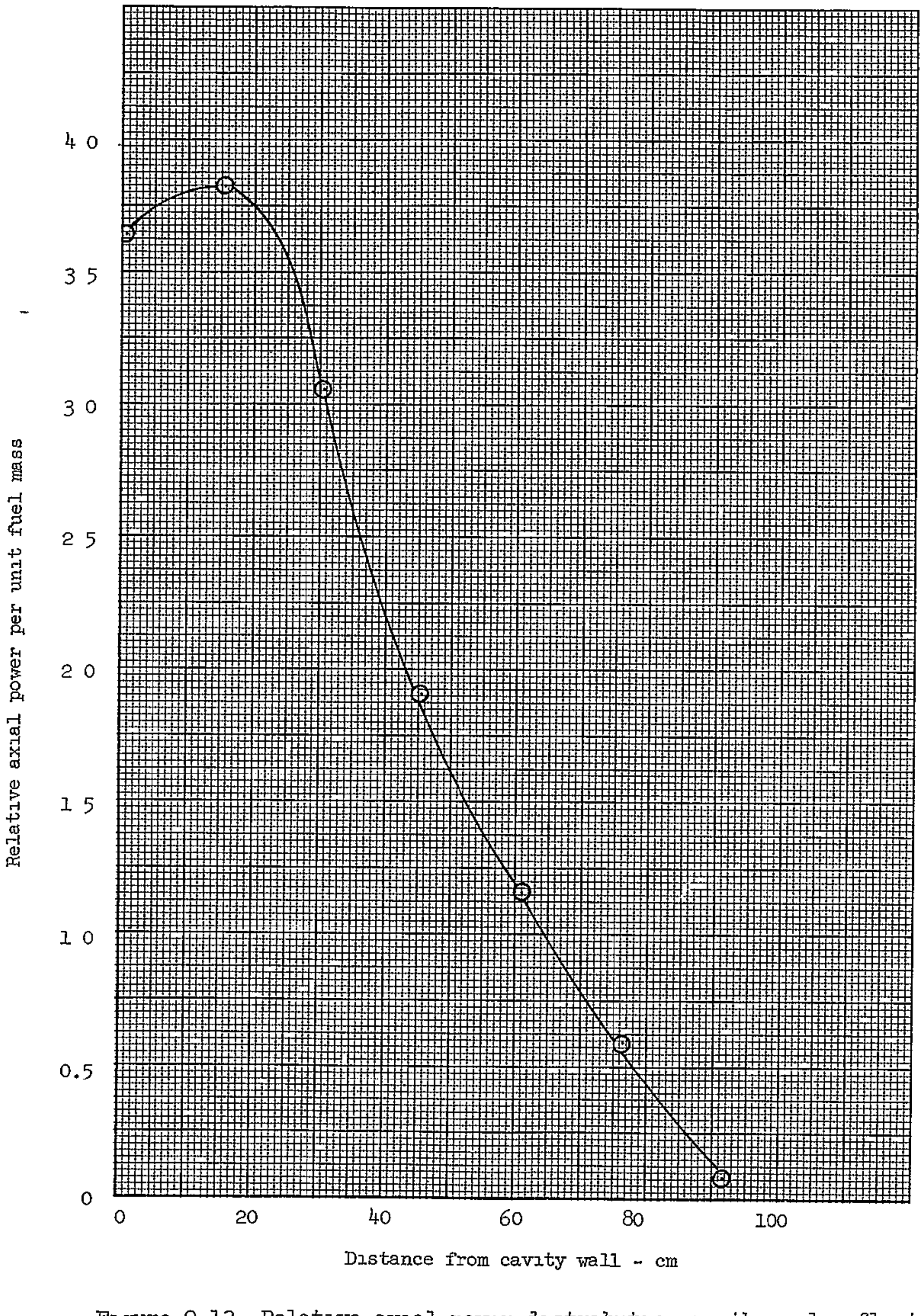

Figure 9 13 Relative axial power distribution in the end reflector, 3 module reactor with 0 55 fuel to module radius ratio

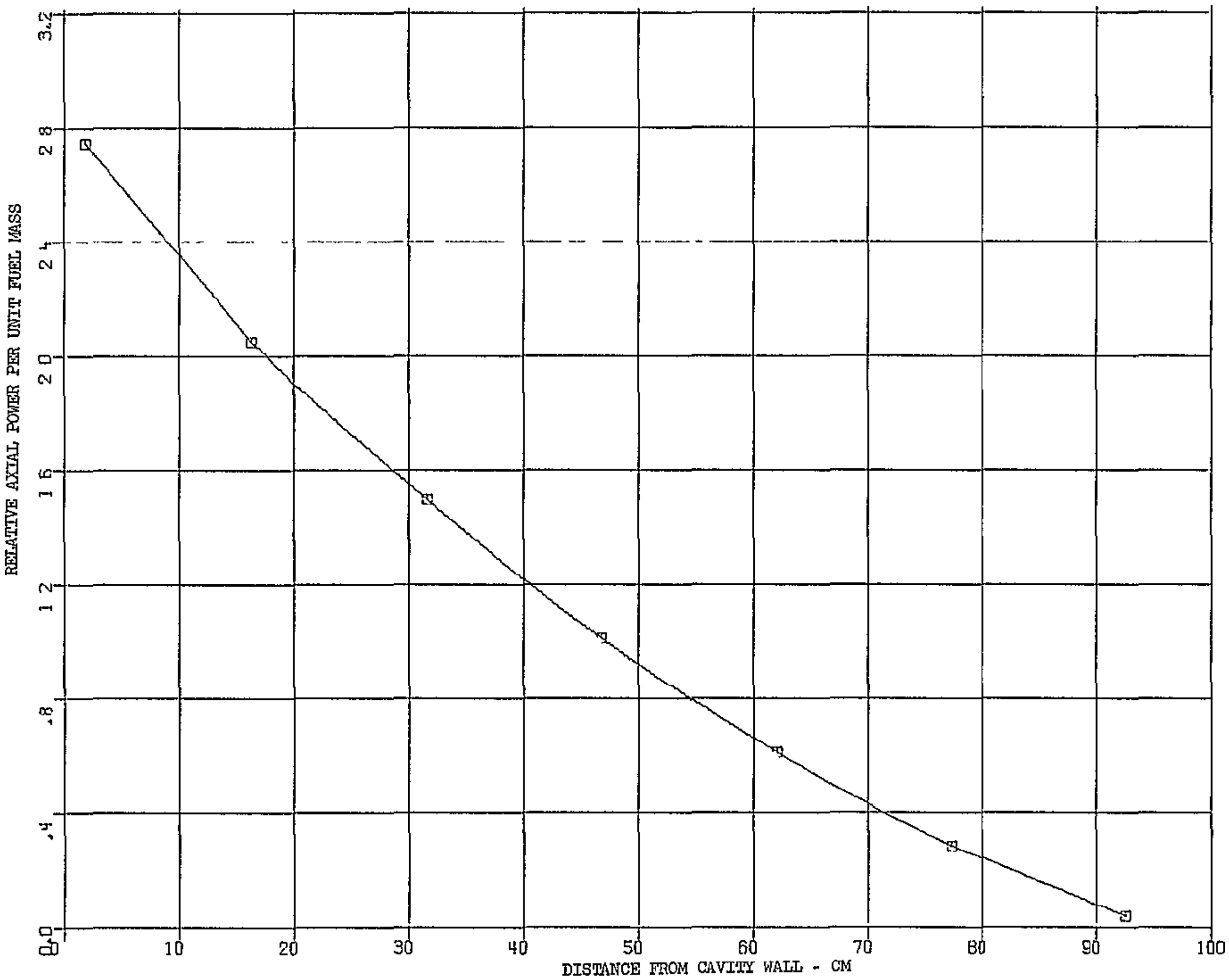

Figure 9.14 Relative axial power distribution in the radial reflector, 3 module reactor with 0.55 fuel to module radius ratio

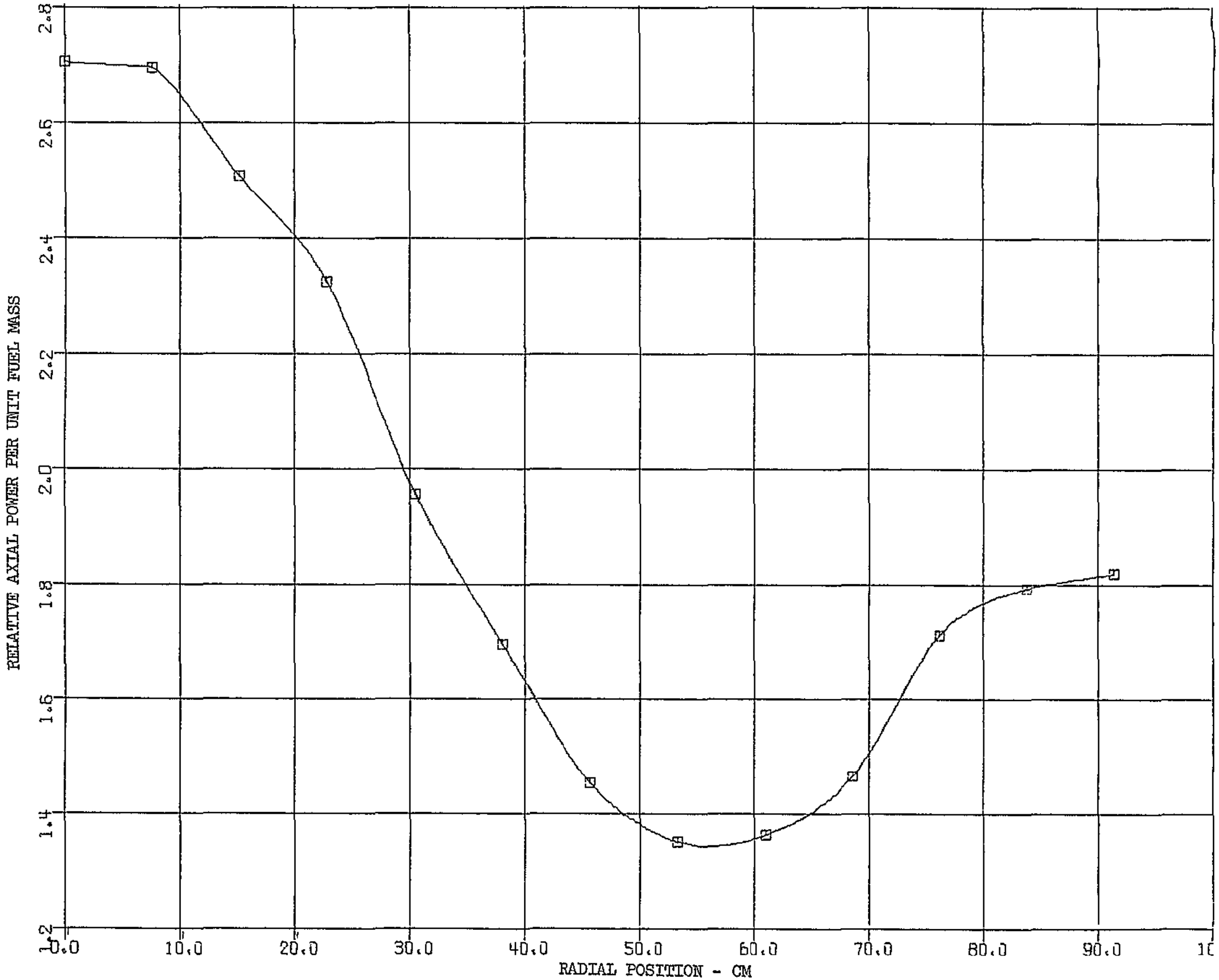

Figure 9.15 Relative axial power distribution across face of the core through module 1 axis, 3 module reactor with 0 55 fuel to module radius ratio

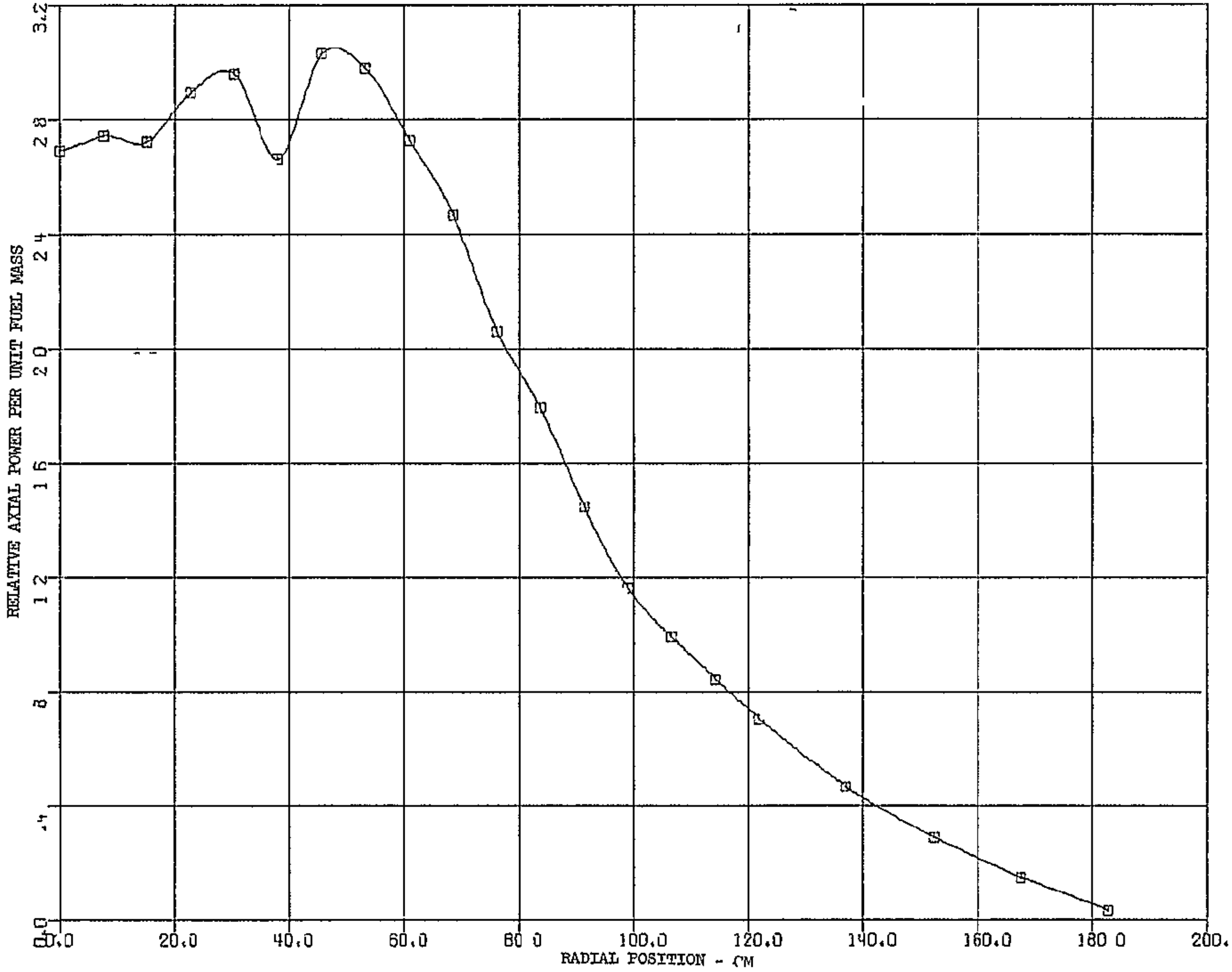

Figure 9.16 Relative axial power distribution across face of core with traverse between modules 1 and 2

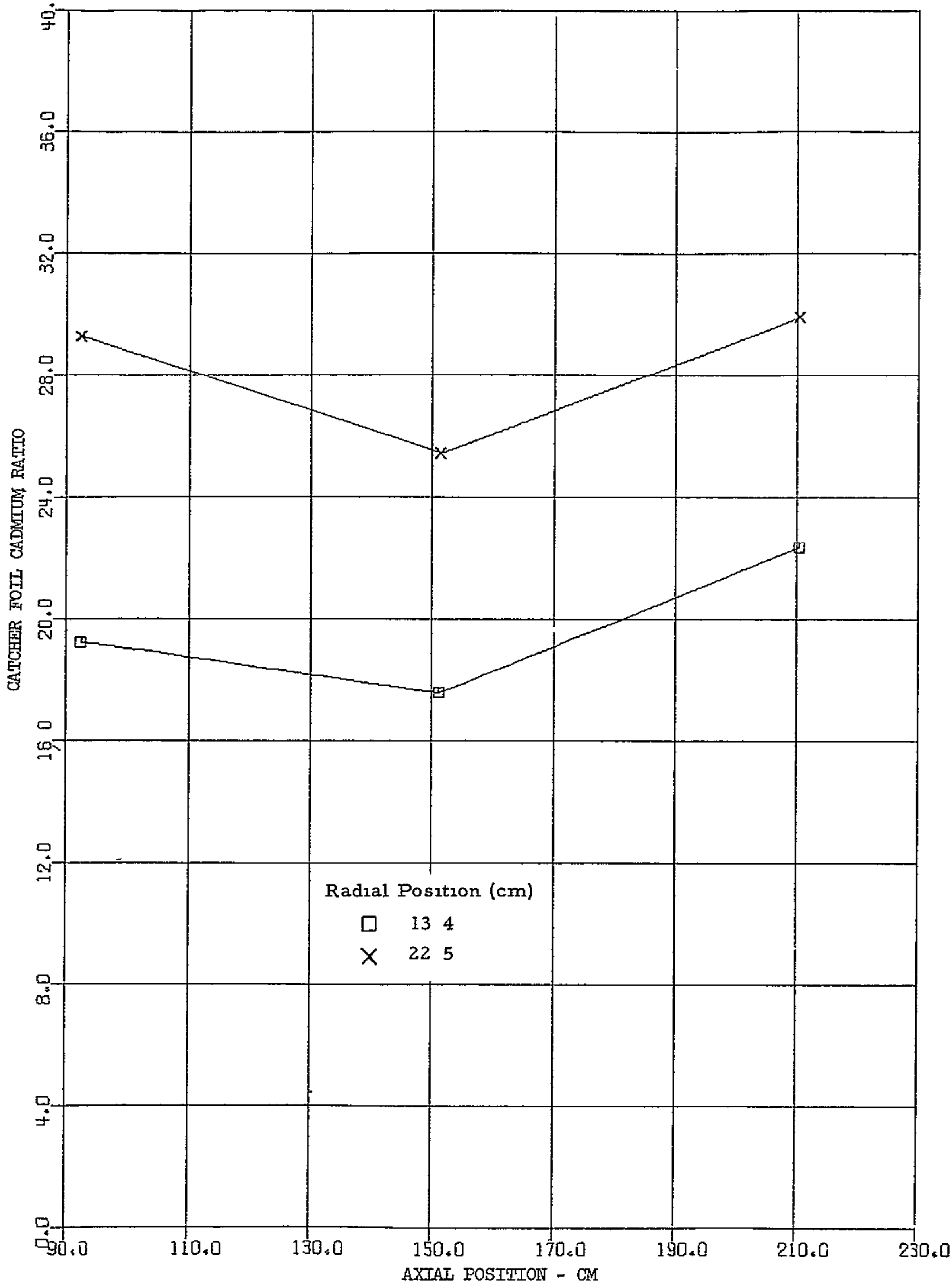

Figure 9.17 Axial distribution of catcher foil cadmium ratios through module 3, 300°, 3 module reactor with 0 55 fuel to module radius ratio

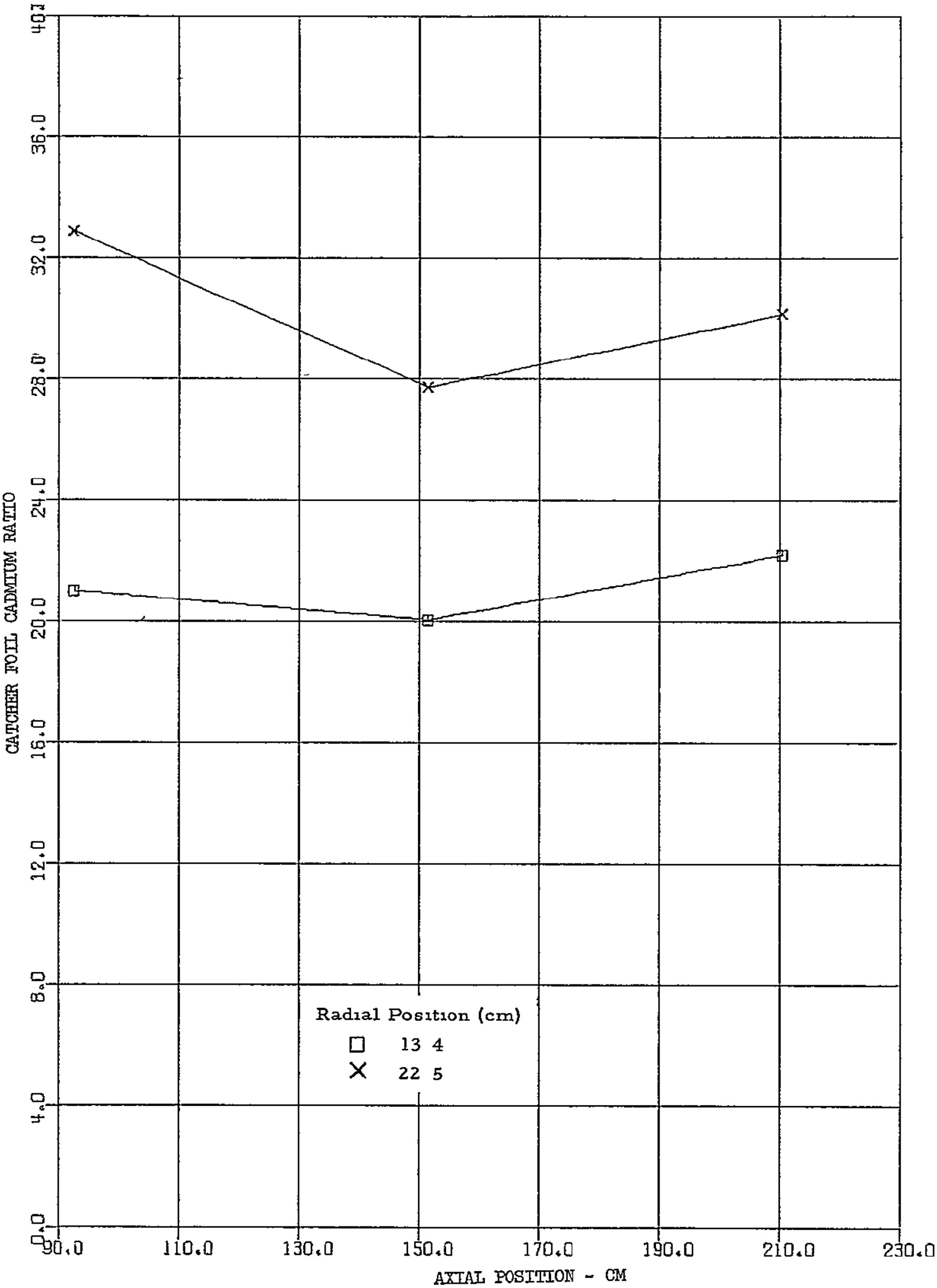

Figure 9 18 Axial distribution of catcher foil cadmium ratios through module 3, 120°, 3 module reactor with 0 55 fuel to module radius ratio

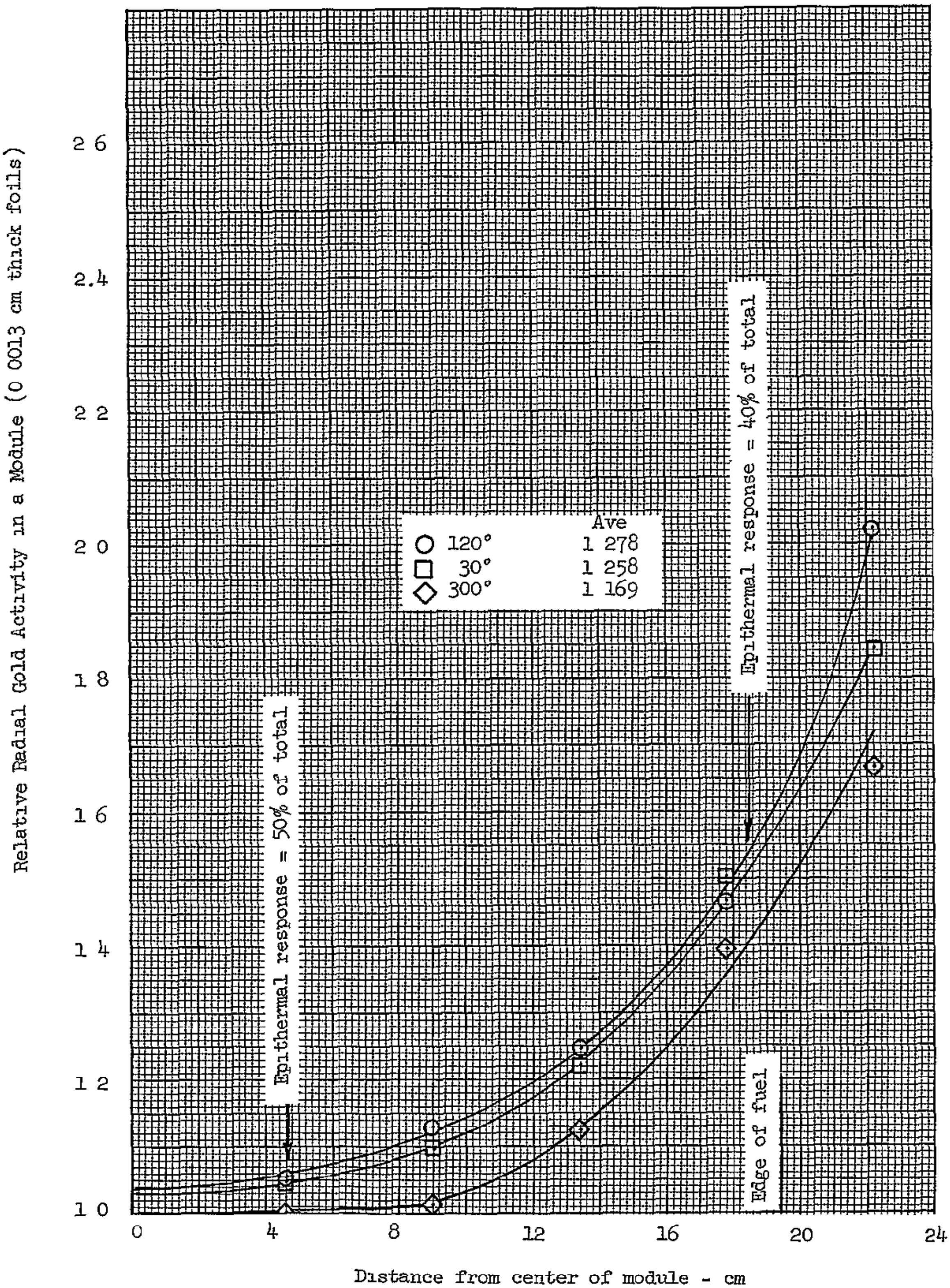

Figure 9 19 Relative radial gold foil activity in a module, 3 module reactor with 0 55 fuel to module radius ratio

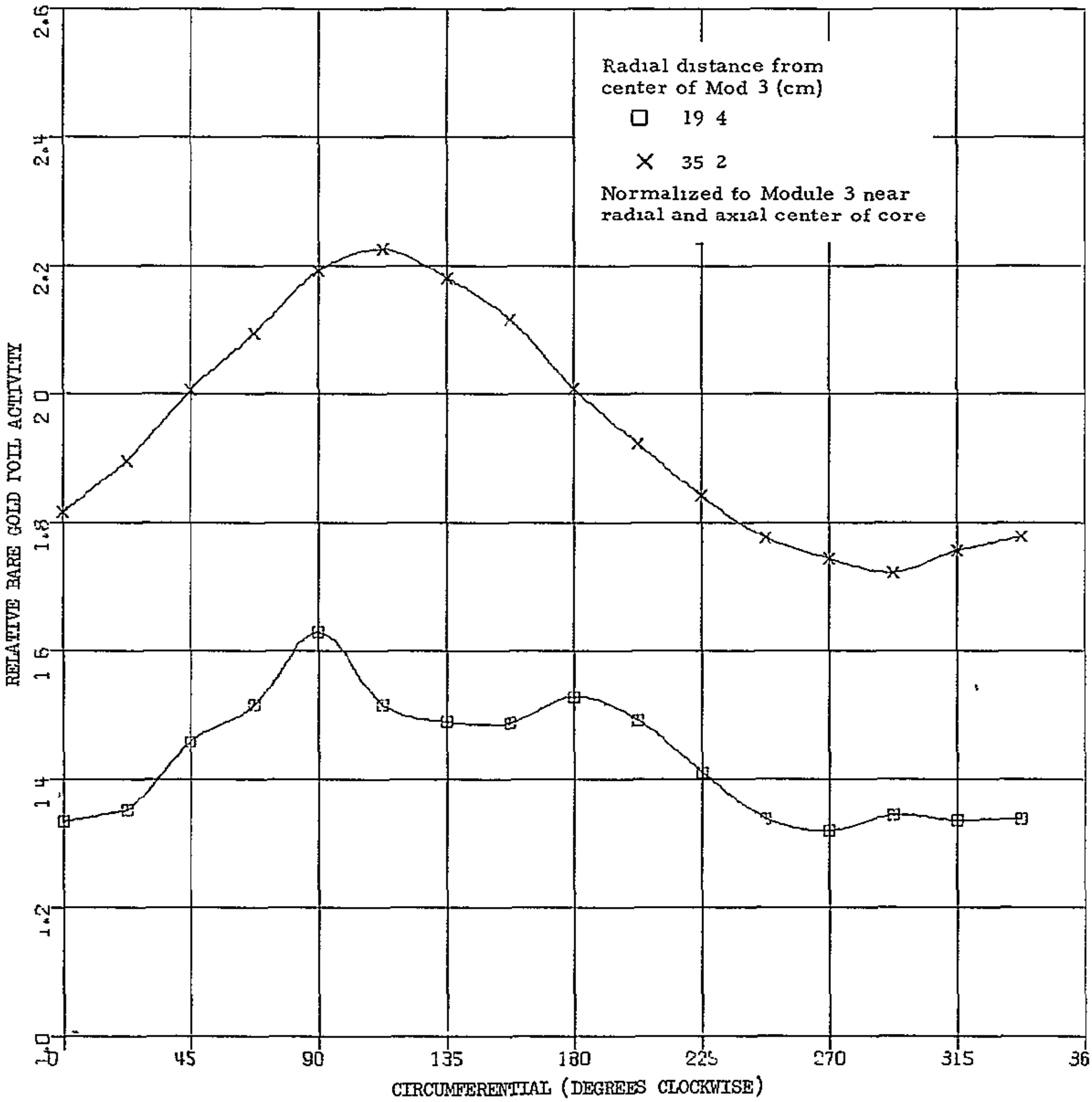

Figure 9 20 Circumferential relative gold foil activity on outside fuel ring, stage 9, 3-module reactor with 0 55 fuel to module radius ratio

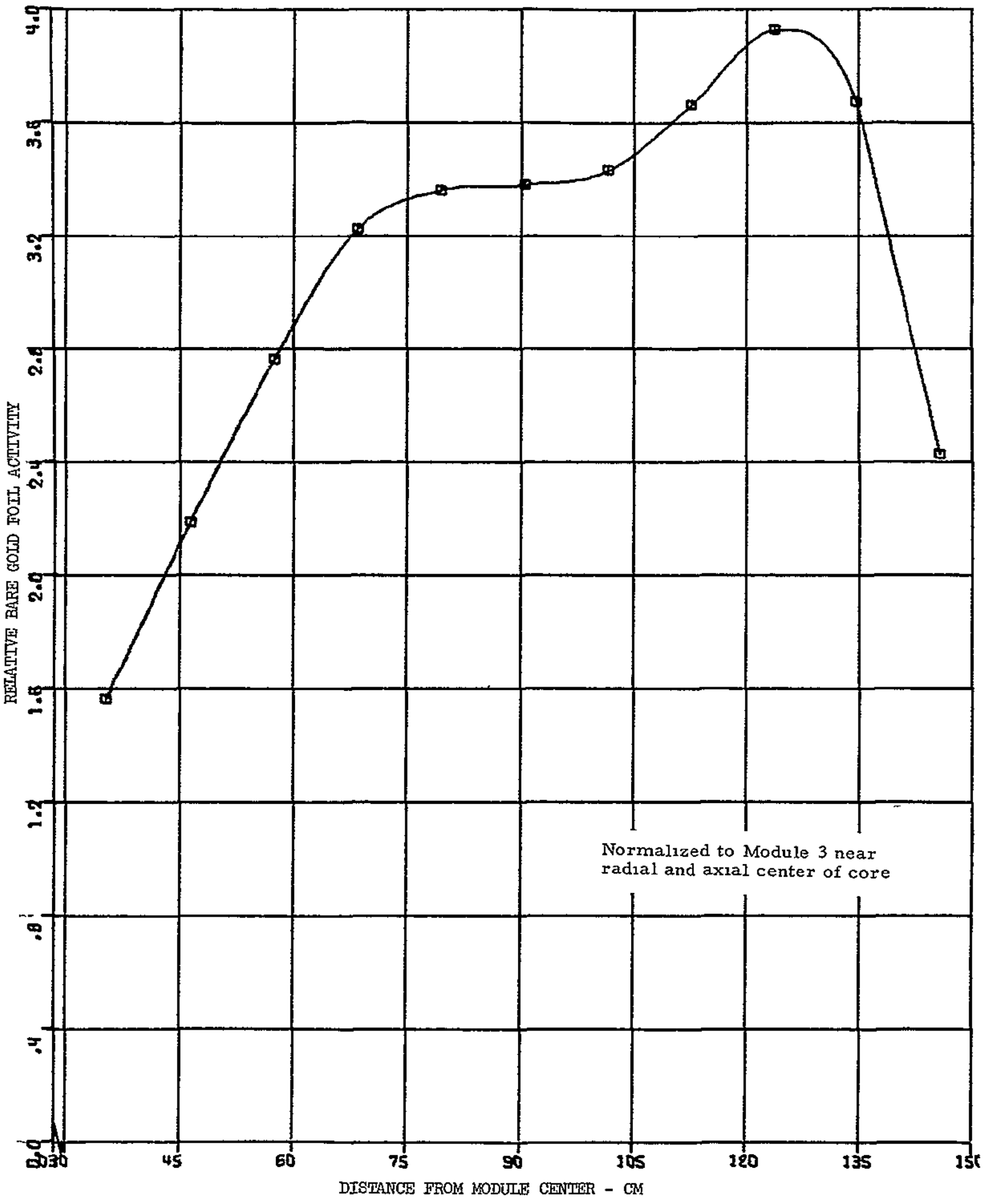

Figure 9 21 Relative radial bare gold foil activity traverse out through D_2O between modules 1 and 2, 3 module reactor with 0.55 fuel to module radius ratio

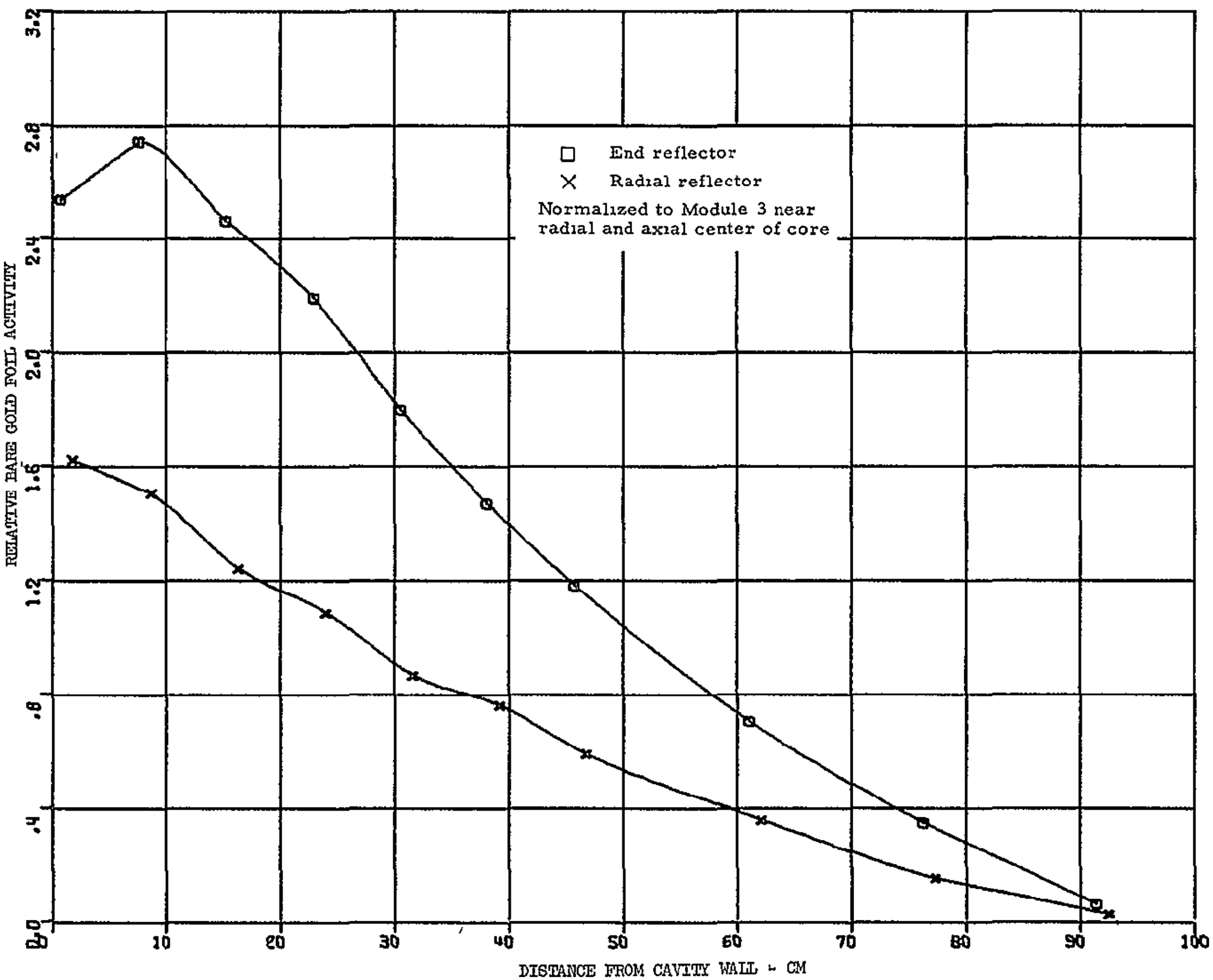

Figure 9.22 Relative bare gold foil activity in the end and radial reflectors, 3 module reactor with 0 55 fuel to module radius ratio

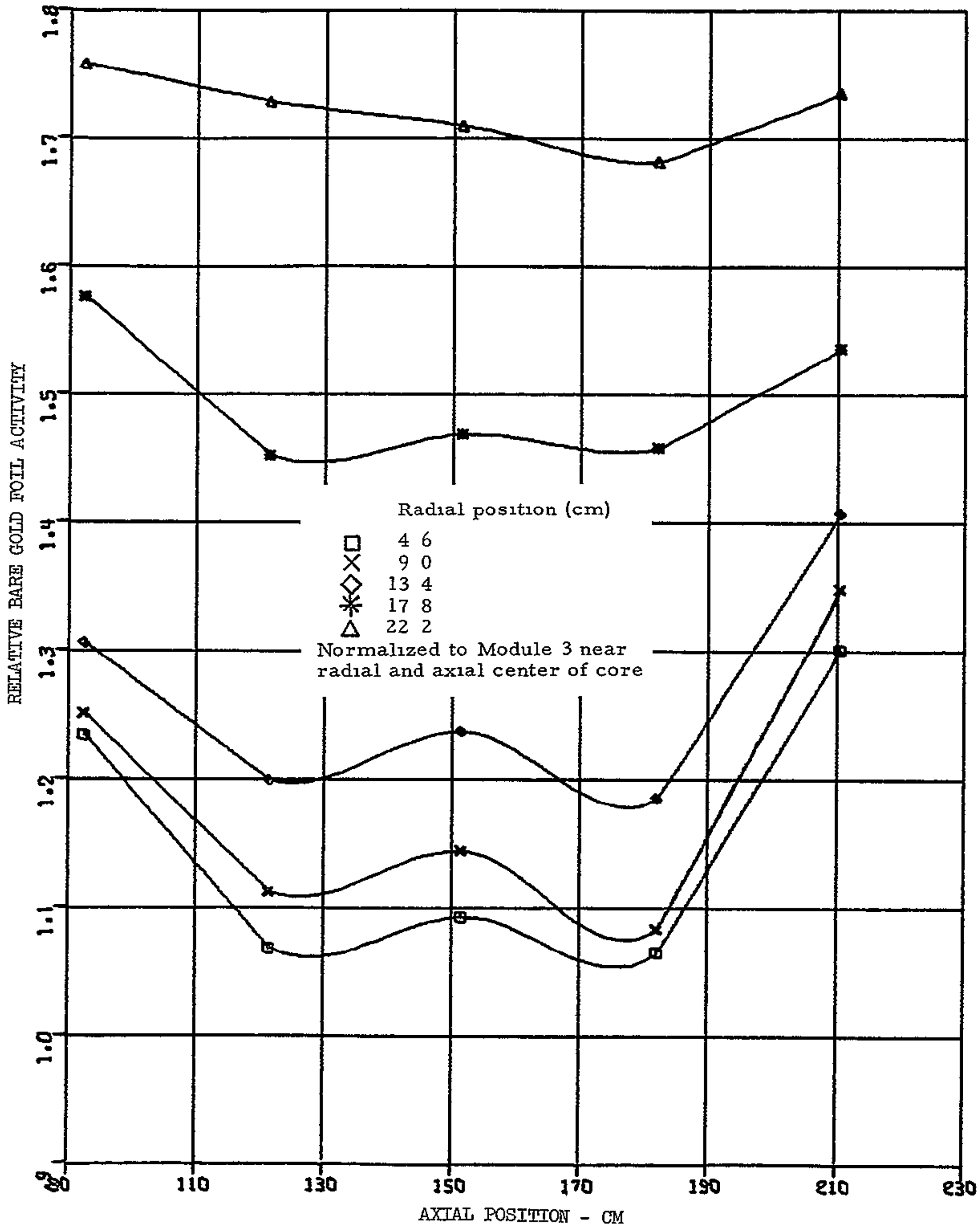

Figure 9.23 Relative bare gold foil activity in module 3, 120°, 3 module reactor with 0.55 fuel to module radius ratio

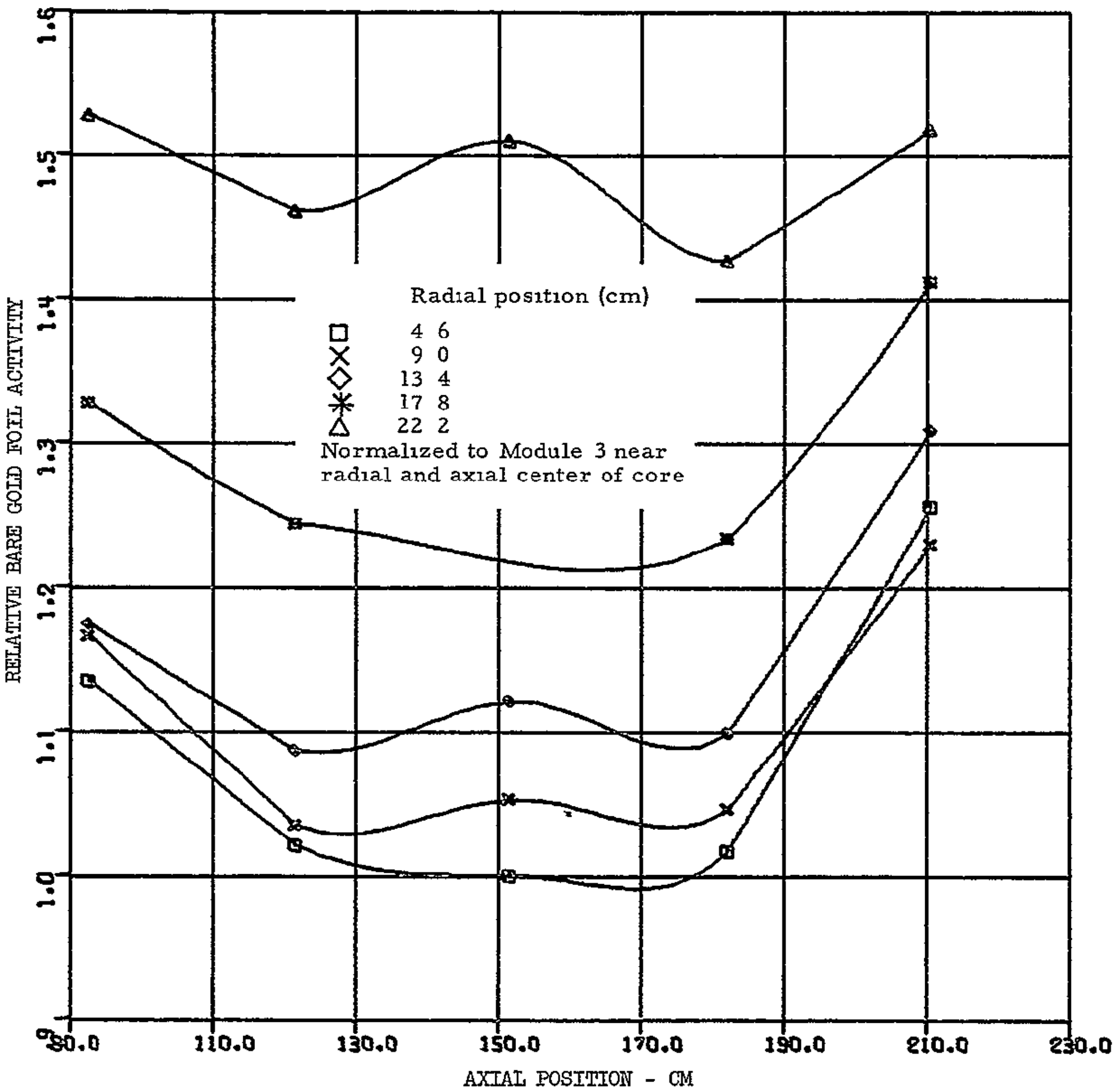

Figure 9 24 Relative bare gold foil activity in module 3, 300°, 3 module reactor with 0 55 fuel to module radius ratio

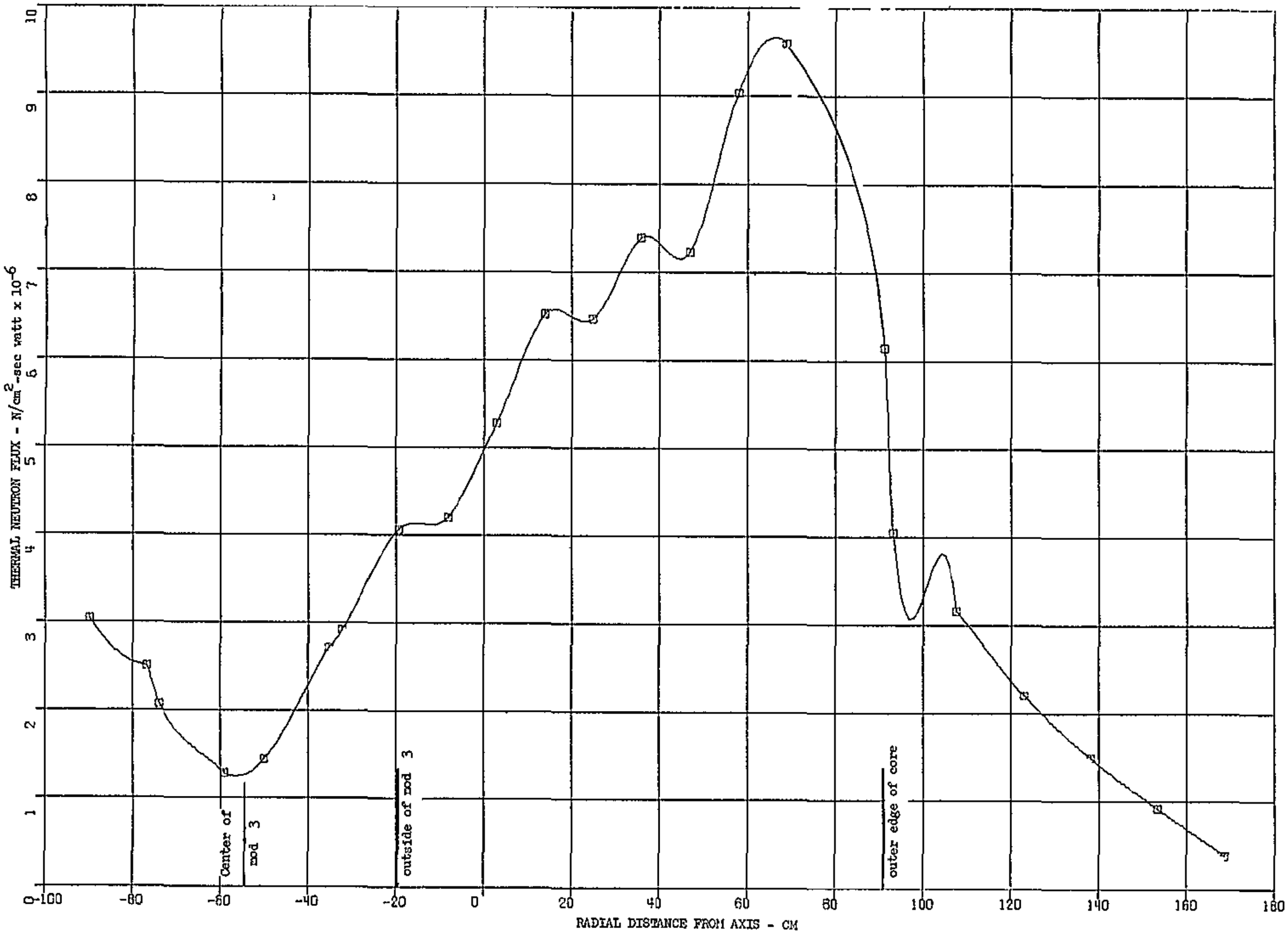

Figure 9.25 Radial distribution of thermal neutron flux through core and radial reflector, 3-module reactor with 0 55 fuel to module radius ratio

10 0 DISCUSSION OF RESULTS

The critical mass variations for the four different seven-module configurations were unexpectedly relatively insensitive to the radius ratio of the fuel within the modules These and other major results are summarized in Table 10 1. It is especially interesting to note the critical mass vs radius effects of these module configurations compared to that of a single large cavity. Figure 10 1 shows this variation for the three experimental cylindrical cavity reactors that have been measured:

(1) this module experiment
(2) the six foot single cavity experiment in Idaho, the reflector tank from which was used in the module experiment
(3) the Los Alamos 40-inch cavity, measurements made about 1960 (9)

These curves show a striking difference between the limiting conditions for the two principal types of reactors, single and multiple cavities The minimum radius ratio for which the critical mass becomes excessive is lower for the module or multiple cavity system The flatter curve of the module reactor is in part caused by the presence of hydrogen, which was not included in the two sets of single cavity experimental results shown.

The fuel worth of uniform changes in fuel density was measured on all configurations In Figure 10 2 these results are plotted vs fuel mass in the reactor and compared with the results obtained with the single large cavity configurations The results all lie virtually on the same curve Note the solid curve (Ref 4, page 50), actually has a spread of ±10% for some reactor configurations But the general applicability and hence usefulness of this curve on all cavity reactors of the same general overall size is readily apparent

The penalty for hydrogen in these modular systems is not significantly different from the penalty measured in the single cavity concept (Reference 2, p 252 and Reference 4) The hydrogen penalty is approximately 2 1%Δk/kg of hydrogen, averaged throughout the void region In the large single cavity experiments, hydrogen nearer the fuel had a worse penalty (factor of 2.5) than that near the cavity wall (Reference 2, p 252 and 358) The same variation of worth in the cavity might be anticipated in this module experiment The measurement was not made because the hydrogen thickness was so small as to make a reliable measurement very difficult if not impossible The variation is believed to be caused by molecular binding effects which allows the hydrogen to scatter isotropically at thermal energies, thus effectively scatter-returning those neutron traveling from the core to the reflector At operating temperatures of 4 or 5000°K, molecular binding would not exist, and such a position dependence is not expected to be as strong an effect as in this low temperature experiment.

The simulation of hydrogen with polyethylene and polystyrene is realistic, since the carbon content represents only about 10% of the total worth of CH_2 and 20% of CH (p 251 of Ref. 2) The materials used had adequate purity, containing no high cross section impurities in concentrations greater than a few ppm. A chlorine compound gas is used in some processes for expanding styrofoam, but the material was analyzed for residual trapped chlorine and none was found

The penalty of the exhaust nozzle opening was worse on the seven module configuration than on any of the other configurations, including the single large cavities The highly effective fuel of the center module was directly affected by this nozzle hole However, this penalty of 1 15%Δk for the seven module configuration was not severe compared to the penalty of hydrogen or cavity wall lining material Therefore, the nozzle design need not be considered especially important for the nuclear characteristics provided the same considerations are given to material selections as are done for the cavity wall

The walls of the cavities present one of the most difficult design problems for the cavity reactor The walls must be able to withstand ultra-high temperatures, very high pressures, and also be nuclearly thin. The walls in the present module experiments are exceedingly thin, 0 32 cm of aluminum, only 0 005 thermal absorption mean free paths Such walls are quite unrealistic for the actual high temperature application For this reason the effect of thicker walls was evaluated on the 0 38 radius ratio, 7-module configuration. Stainless steel 0 125 cm thick, representing 0 038 thermal mean free paths was added to the aluminum walls Extrapolated to all seven modules, the penalty was 28%Δk With the use of Figure 10.2, it can readily be seen that this penalty would have required quadrupling the critical mass from 10 2 to 43 kg of uranium Stainless steel 0.125 cm thick is equivalent to 4 5 cm thickness of zircalloy, so this value of nuclear thickness (0 038 plus 0 005=0.043 mean free paths) is probably a pessimistic estimate of what would be required Nevertheless, the severe penalties paid for neutron absorption on the walls of the cavity show that the wall is one of the most important and sensitive areas of the reactor design.

Flux and power distributions were extensively measured on all configurations Very large thermal flux peaking occurs in the regions between modules and in the reflector surrounding the modules If structural supports are needed in the reactor, these areas should be avoided However, a thorough analysis of the optimum location for structural members requires knowledge of the adjoint flux Calculated shapes for the adjoint flux and statistical weight may be found in Ref. 5, page 61

Power distributions on the module reactors did not show a self-shielding effect large enough to be of great significance to thermodynamic considerations on any but the 0 38 radius ratio configurations. The peak to minimum radial power ratio for the configurations is listed below:

	7-Module Configurations				3-Module
R/R_o	0.55 with H	0.72 with H	0.38 with H	0 38 no H	0 55 with H
Edge/Center Power	1 20	1 13	1 50	1 24	1 17

The measured flux distributions on some of the configurations showed unusual dips at the cavity walls and at the outer wall of the module tank These were assumed to be the result of flux perturbation in the moderator by the aluminum Since adequate detail (resolution) was not obtained in these experiments, a supplementary flux perturbation experiment was performed later in an equivalent environment (heavy water reflector of a gas core reactor) The results are shown in Figure 10 3 Approximately a 10% flux perturbation resulted from 1/2-inch thick aluminum, which was the net thickness of the outer wall of the module tank plus the inner wall of the reflector tank The same magnitude of flux perturbation would have shown on Figures 5 32, 6 15, 7 10 and 8 10 if sufficient detail had been obtained on the curves.

10.1 Effects on Cavity Reactor Operating Characteristics at Power

The principal fuel loading and reactivity results measured on the five configurations of the module concept are summarized in the foregoing discussion Though critical mass results themselves are ostensibly the most significant piece of data, it should be cautioned that an even more important parameter to the cavity reactor concept is the cavity pressure. Thus low critical masses will have little merit if they are confined in so small a volume that the gas pressure would be excessive under operating conditions.

In order to view the relative advantages of the various module arrangements, it is appropriate to adjust them all to equivalent structural and hydrogen coolant configurations, and then to compare the results in terms of the relative cavity pressures created by that critical mass at operating temperatures of the order of 80,000°R for the fuel

In Table 10 2 are shown comparisons between the directly measured characteristics of the three principal configurations of this experiment, two 7-module cases and one 3-module case, and the nearest applicable single large cavity configuration, that performed with UF_6 fuel in a radius ratio core of 0 67 (Reference 3, page 119) To this configuration was added the effect of hydrogen (Reference 2, p 251 and Reference 4, p 76). All configurations were then corrected to the same amounts of structural aluminum within the core region, which, in the case of the module configurations included the mass of module tank as well as that of the fuel elements. The corrected critical masses for these configurations is then given at the bottom of Table 10.2. Note, this is with 1.23×10^{21} atoms/cc of hydrogen in the hydrogen regions of each configuration. However, the total quantities of hydrogen in these configurations differ significantly, amounting to a factor of 2.5 times more hydrogen in a single module configuration than is in the 7-module configuration.

In order to make a better comparison, the 0.67 radius ratio of the single module configuration should be converted to 0.55 and 0.72 radius ratio. This can be done using Figure 10.1, and yielding the following results:

	0.55 radius ratio		0.72 radius ratio	
	Critical mass (kg)	U/cc	Critical mass (kg)	U/cc
Single module	27	8.2×10^{19}	21	3.8×10^{19}
3-module	12.2	7.3×10^{19}	--	--
7-module	8.6	5.3×10^{19}	8.2	2.9×10^{19}

In the above configurations, for convenience the hydrogen in each was taken as occupying the volume from 0.72 to 1.0 radius ratio. If the hydrogen filled out the rest of the volume at 1.23×10^{21} H/cc in the 0.55 radius ratio cases, the critical masses would increase for these configurations. The changes would be approximately a 0.3 kg increase for the 7 module configuration and a 6 kg increase for the single module configuration. So as to provide approximate calibration points for the atom densities discussed above, atomic hydrogen at 5500°K, assumed not to be ionized and at an atom density of 1.23×10^{21} H/cc, is at approximately 900 atmospheres of pressure. Uranium gas at a temperature of 45,000°K is at 900 atmospheres when its atom density is approximately 4.5×10^{19} (10). Thus it appears that at 900 atmospheres, the stable operating configuration for either the single, 3-module, or 7-module systems is with a fuel radius ratio in the 0.60 to 0.70 range.

The above comparisons of the sheet fuel module configurations with the UF_6 gas-core single cavity configurations raises the question of how well the sheet fuel simulated a gas? The arrangement of the foils essentially eliminated all streaming paths that could not encounter fuel. It is felt that the arrangement utilized in these module experiments was at least as valid a simulation of a gas as was Mockup #2 of the single cavity experiments (3). This latter sheet fuel configuration had a measured bias of a 4% higher critical mass than existed in the all-gas cores. The same bias might be used as an expected bias value for the module experiments.

10.2 Calculations

The difficulty of doing reliable calculations on the modular configurations limited the amount of analytical correlation performed with this experiment. Major compromises are required to even reduce the reactor configuration problem to two dimensions. Because of these complexities, a synthesis approach was used to predict the critical mass so that the fuel elements could be preloaded to a value that would, hopefully, not require complete disassembly and reloading to complete the experiment.

A 19-energy group one dimensional diffusion code was used It had been extensively calibrated for bias using the single large cavity experiments Preliminary calculations were made using the mean-chord-length concept ($\frac{4V}{S}$) to obtain estimated thermal flux depression factors in the fuel modules. Then several calculations were performed to obtain an expected range for the critical loading Over this range, a number of cell calculations were performed, taking the radius of the 7-module cell as 38 cm and the 3-module cell as 50 cm These cell radii were chosen as the approximate mean radius at which the gradient of the flux was zero.

Using the cell calculations, the "cell correction factors" for fuel absorption relative to moderator flux were obtained and used in the overall reactor calculation. The critical masses predicted by this method were as follows and are compared with the measured critical masses with the exhaust nozzle plugged:

	7-Module 0.55 Radius Ratio with Hydrogen	3-Module 0.55 Radius Ratio with Hydrogen
Predicted	7.7 kg	13 kg
Measured	8 3 kg	11 kg

This method of calculating these reactors was more successful on the 7-module configuration, principally because it was more realistic to define a "cell" for this configuration than for the 3-module configuration No calculations were performed on the other configurations since pre-analysis was obtained by extrapolation of measurements on the previous configuration(s).

TABLE 10 1

Principal Results from the Five Different Modular Configurations

	7-Modules 0 55 R/R_o No Hydrogen	7-Modules 0 55 R/R_o With Hydrogen	7-Modules 0 72 R/R_o With Hydrogen	7-Modules 0 38 R/R_o With Hydrogen	3-Modules 0 55 R/R_o With Hydrogen
Critical Mass (nozzle plug out) kg of U	7 97	8 64	8 01	10 16	11 5
Worth of Fuel (core average) % Δk/kg	3 95	3 93	4 08	2 87	1 65
Nozzle Plug Worth	----	-1 15 $\pm$ 0 09 % Δk	----	----	-0 46 $\pm$ 0 03 % Δk
H Atom Density	1 23 x 10^{21} atoms/cc from 0 72 R/R_o				1 33 x 10^{21}
CH_2 Worth % Δk/kg	----	-0 41 $\pm$ 0 10	----	----	----
CH Worth (Complete Removal)	----	-0 11 $\pm$ 0 02	----	----	----
Stainless Steel Liner Worth		-0 096 $\pm$ 0 011 (0 125 cm thick)		-0 24% Δk/kg	
Aluminum Worth		-0 03 % Δk/kg in cores of all configurations			
Control Rod Worth		-2 80% Δk in 21 rods -3 93% Δk in 30 rods			

TABLE 10 2

Comparisons of 1-, 3- and 7-Module Configurations
(All Use Same Reflector Bank)

	7-Module 0 55 R/R_o	7-Module 0 72 R/R_o	3-Module 0 55 R/R_o	1-Module 0 67 R/R_o
Measured Critical Mass (kg of U)	8 64	8 01	11 5	16 21
Uranium Atom Density U/cc	5.27×10^{19}	$2\ 84 \times 10^{19}$	$6\ 84 \times 10^{19}$	$3\ 27 \times 10^{19}$
Volume Occupied by Hydrogen (cm^3) (From 0 72 to 1 0 R/R_o)	$6\ 37 \times 10^5$	$6\ 37 \times 10^5$	$8\ 18 \times 10^5$	$15\ 44 \times 10^5$
H Atom Density	$1\ 23 \times 10^{21}$	$1\ 23 \times 10^{21}$	$1\ 33 \times 10^{21}$	0
Total H Atoms	$7\ 83 \times 10^{26}$	$7\ 83 \times 10^{26}$	$10\ 88 \times 10^{26}$	0
Correction to $1\ 23 \times 10^{21}$ H/cc	0	0	+0 29% Δk	-5 4% Δk
Aluminum Mass Inside Reflector (kg)	271 6	291 8	216 8	245
Correction to 272 kg	0	-0 60% Δk	+1 7% Δk	-0 8% Δk
Total Correction (% Δk) (kg of U)	0	-0 60% Δk +0 15 kg	+2 0% Δk -0 69 kg	-6 2% Δk +6 2 kg
Corrected Critical Mass*	8 64 kg	8 24 kg	12 2 kg	22 4 kg
Corrected U Density/cc	$5\ 3 \times 10^{19}$	$2\ 9 \times 10^{19}$	$7\ 3 \times 10^{19}$	$4\ 5 \times 10^{19}$
Total Atoms of Hydrogen	$7\ 8 \times 10^{26}$	$7\ 8 \times 10^{26}$	$10\ 1 \times 10^{26}$	19×10^{26}

*Corrected to 271 6 kg of aluminum and $1\ 23 \times 10^{21}$ H/cc

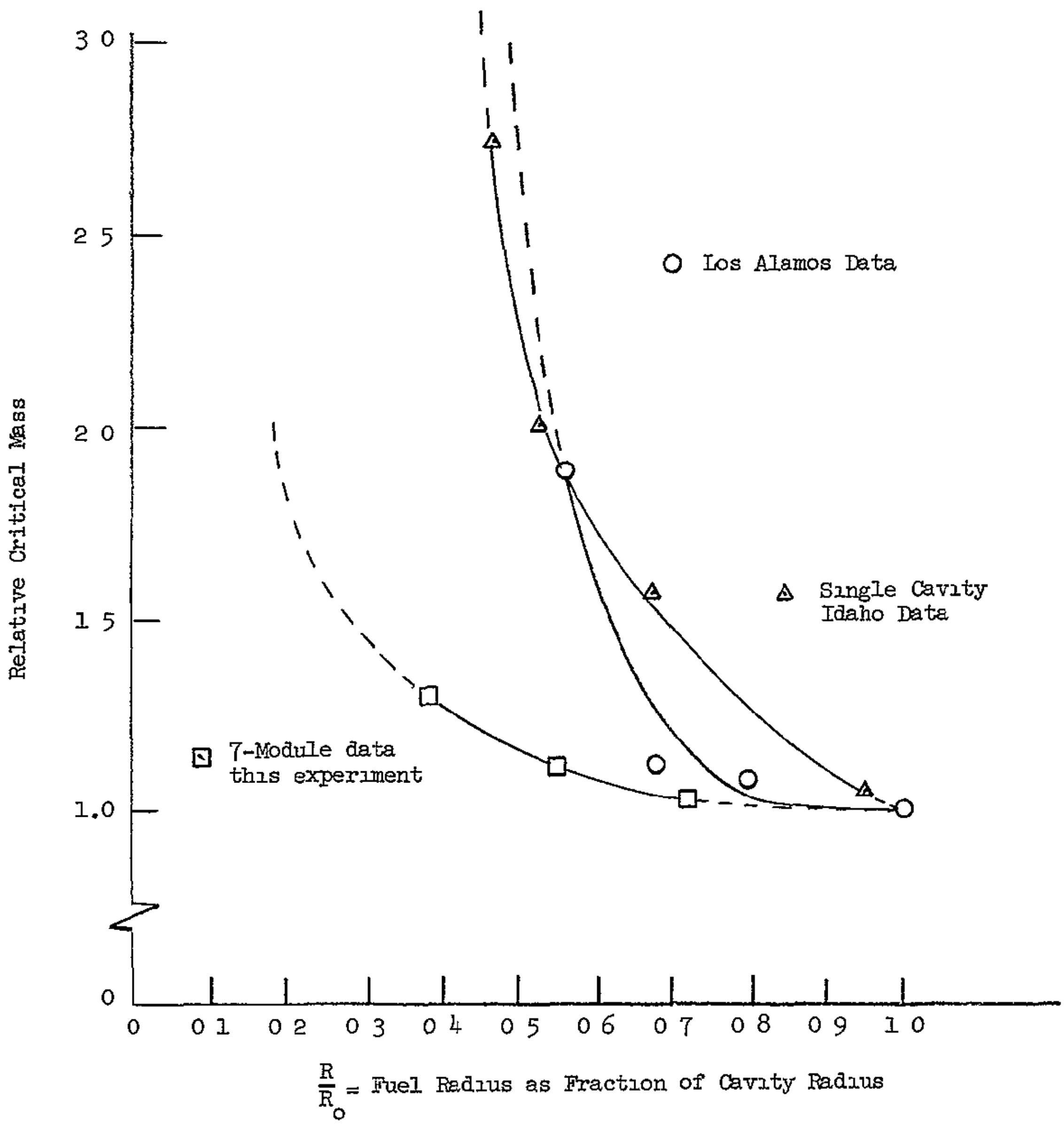

Figure 10 1 Experimental Relationship between Fuel Mass and Fuel Radius as Fraction of Cavity Radius

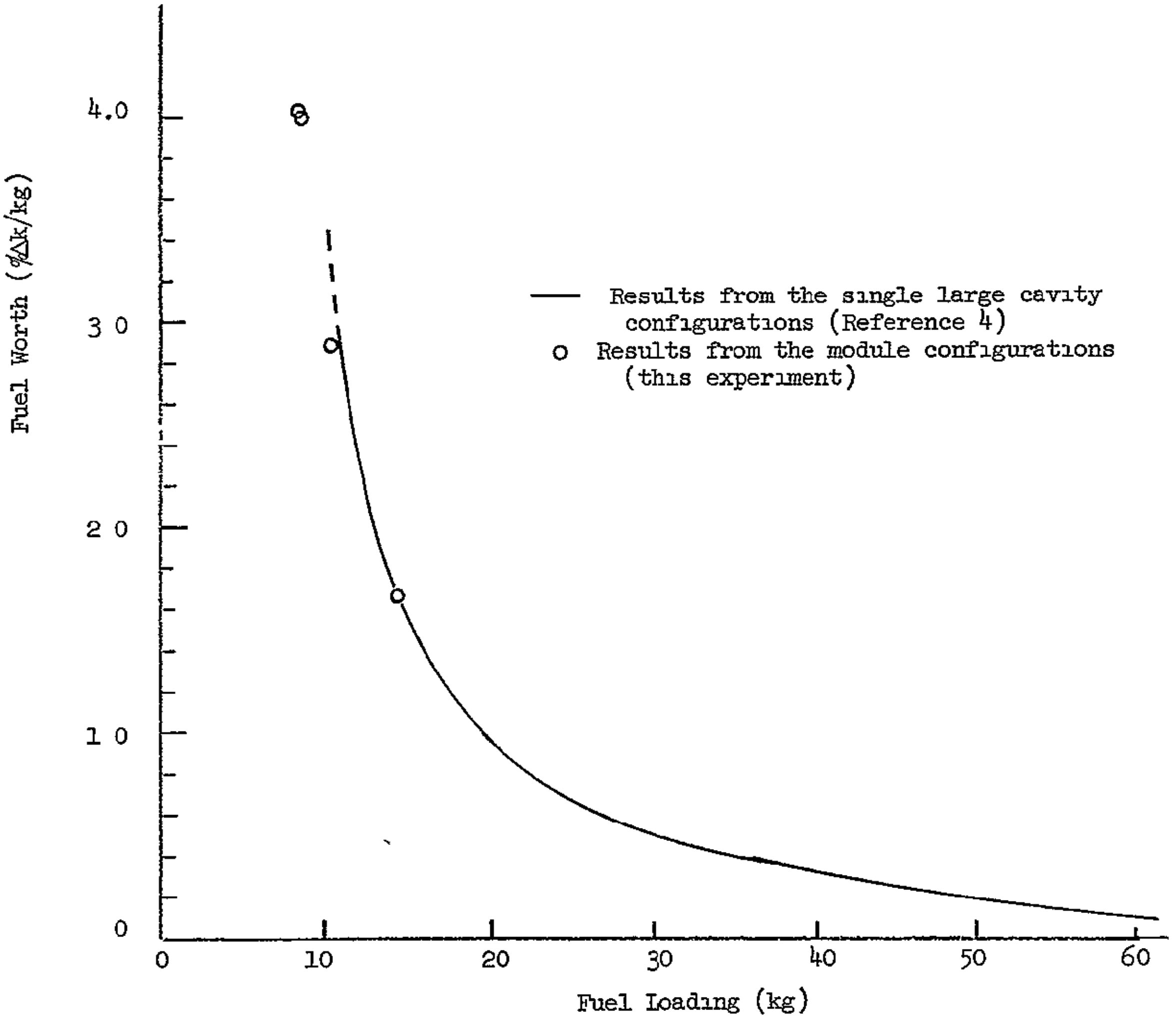

Figure 10 2 Comparison of Fuel Worth vs Fuel Loading for Two Configurations

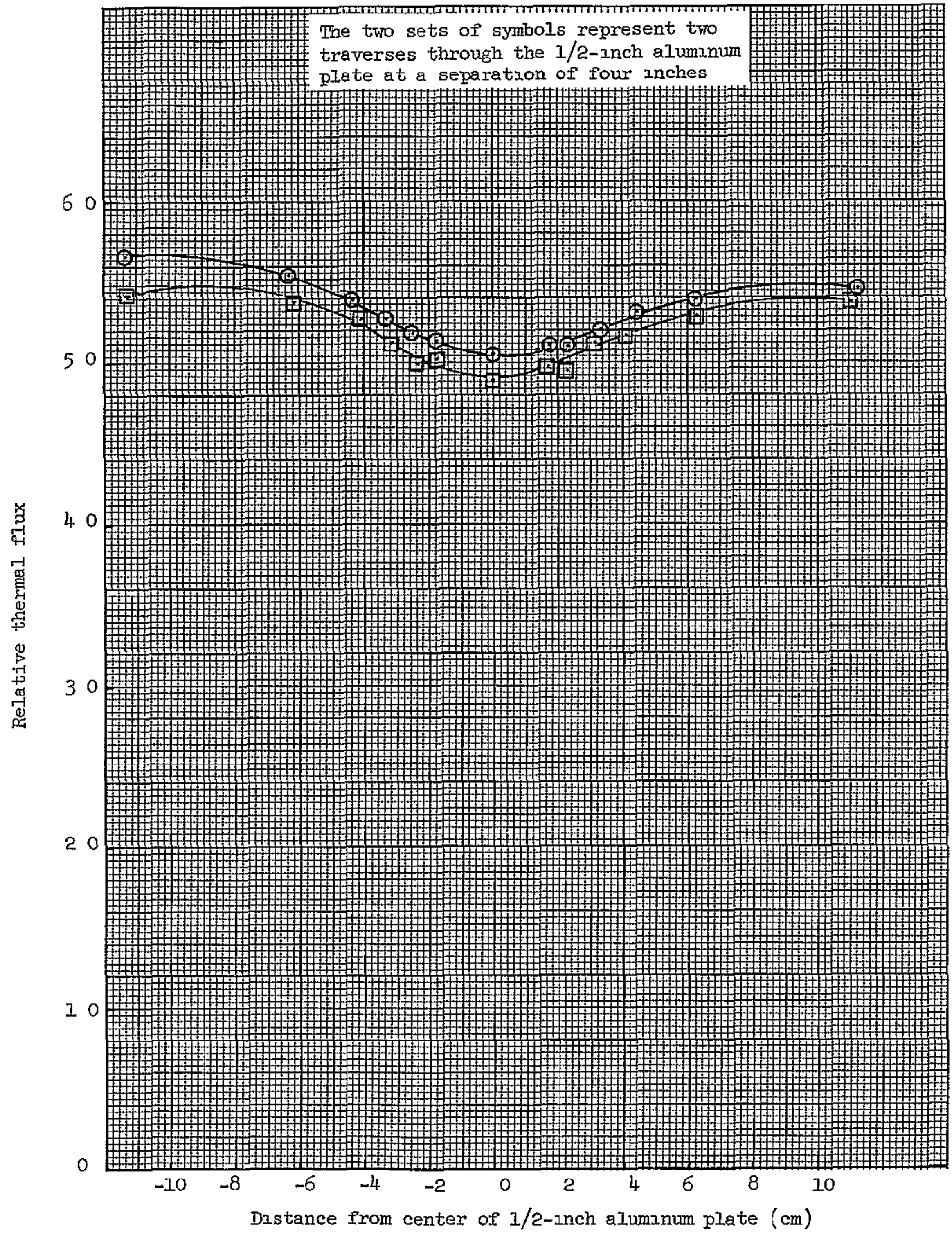

Figure 10 3 Flux-Perturbation Effect of 1/2-inch thick Aluminum Plate in D_2O Reflector of Cavity Reactor

11 0 CONCLUSIONS

The modular cavity reactor critical experiments showed substantially lower critical masses than obtained with single cavities built within the same sized reflector systems However, this "equivalent" single cavity contained 2 1/2 times as much propellant and had only a 35 to 50% higher plasma pressure (uranium atom density)* The various conclusions are summarized below·

1 Critical masses of 7-module configurations were approximately 1/3 to 1/2 of the critical masses of the "equivalent" single cavity system

2 Cavity pressures (uranium atom densities), however, did not show as large a difference They were only 2/3 to 3/4 of that of the equivalent single cavity system.

3 The 3-module results fell relatively uniformly between the results of the 7-module and single cavity systems

4. The 7-module system could be operated (as a thermal reactor) down to lower fuel to cavity radius ratios than could the single cavity system However, the lower limit of the radius ratio would be the practical limit of cavity pressure

5. The penalty paid for neutron absorption in the cavity walls is somewhat more severe in the seven module system than in the single module system, but then the smaller cavity size would not require as thick a wall to contain the pressure in the 7-module system

6 Except in the low fuel/cavity radius ratios (0 38), the module systems had very little fuel self shielding, and peak to minimum flux ratios (radially only) were usually 1 25 or less

7 The penalty paid per kg of hydrogen coolant appears to be essentially the same in the 7-module and the single cavity configurations.

8. The exhaust nozzle was worth the most when directly along the axis of one of the cavities Still, its reactivity penalty was not severe ($\sim 1\% \Delta k$).

---

* As shown in Ref 10, the pressure of the uranium plasma is directly proportional to the density of the uranium in the range of interest and for constant temperature This implies a constant compressibility factor

These experiments did not investigate the effect of variations in interstitial moderator between modules, and thus it is not known if a more optimum module spacing can be achieved Neither was there an experiment on a single cavity of a size that would have nominally the same fuel and hydrogen volumes as that of the 7 and 3-module configurations The single cavity system used for comparison was the one that fit into the same sized external reflector It had 2 1/2 times the hydrogen volume and three times the fuel volume of the modular configurations The comparisons thus made are open to questions of interpretation The aluminum structure, though corrected to the same mass for all configurations, was generally in a slightly higher worth location in the modular configurations However, it is believed that the above listed conclusions are valid even when considering such uncertainties as these Future investigations should probably be concerned with optimizing the module size and spacing and obtaining data to make a comparison with a single cavity system of the same small hydrogen (and fuel) volumes

REFERENCES

1. Latham, T S., "Nuclear Studies of the Nuclear Light Bulb Rocket Engine," NASA Contractor Report G-910375-3, United Aircraft Corp , September, 1968.

2 Pincock, G D , Kunze, J F , "Cavity Reactor Critical Experiment, Volume I," General Electric Company, NMPO-ITS, September 6, 1967, (NASA-CR-72234)

3 Pincock, G D., Kunze, J F , "Cavity Reactor Critical Experiment, Volume II," General Electric Company, NSP-ITS, May 31, 1968, (NASA-CR-72415).

4 Pincock, G. D., Kunze, J F , "Cavity Reactor Critical Experiment, Volume III," General Electric Company, NSP-ITS, September, 1968, (NASA-CR-72384).

5 Henderson, W B , and Kunze, J F , "Analysis of Cavity Reactor Experiments," General Electric Company, NSP-ITS, January, 1969 (NASA-CR-72484)

6 Kelber, C. N , "Resonance Integrals for Gold and Indium Foils", Nucleonics, August 1962, p 162

7. Dalton, G. R. and Osborne, R K , "Flux Perturbations by Thermal Neutron Detectors", Nuclear Science and Engineering, Vol 9, p 198 (February, 1961).

8. Brown, H L and Connolly, T J., "Cadmium Cutoff Energies", Nuclear Science and Engineering, Volume 24, p 6, (January 1966).

9 Mills, C. B., "Reflector Moderated Reactors", Nuclear Science and Engineering, Volume 13, p. 301, (1962)

10. Parks, D E., et al, "Optical Constants of Uranium Plasma", Gulf General Atomic, NASA-CR-72348, February, 1968
For a condensation of pertinent operating parameters for a gas core, see R G. Ragsdale, "Relationship Between Engine Parameters and the Fuel Mass Contained in an Open-Cycle Gas-Core Reactor," NASA TM X-52733, January, 1970

11. Pincock, G. D., Kunze, J. F., "Cavity Reactor Critical Experiment, Volume IV," Idaho Nuclear Corporation, October, 1969 (NASA-CR-72550)

12. Pincock, G. D., Chase, P. L., "Cavity Reactor Critical Experiment, Volume V," Idaho Nuclear Corporation, November, 1969 (NASA-CR-72577)

INDEX